Ion-exchange based processes in hybrid water treatment

Marjolein Vanoppen

UNIVERSITEIT GENT

FACULTY OF BIOSCIENCE ENGINEERING

"Sometimes shifting your perspective is more powerful than being smart."

Astro Teller

Supervisor

Prof. dr. ir. Arne R. D. Verliefde

Particle and Interfacial Technology Group (PaInT)

Faculty of Bioscience Engineering, Ghent University

Board of Examiners

Prof. dr. ir. Korneel Rabaey (Chairman)

Centre for Microbial Ecology and Technology (CMET)

Faculty of Bioscience Engineering, Ghent University

Prof. dr. ir. Kitty Nijmeijer

Department of Chemical Engineering and Chemistry

Technische Universiteit Eindhoven

dr. ir. Jan Post

Wetsus

dr. ir. Peter Cauwenberg

VITO nv

Prof. dr. ir. Bart De Gusseme

Centre for Microbial Ecology and Technology (CMET)

Faculty of Bioscience Engineering, Ghent University

dr. ing. Wim Audenaert

Centre for Microbial Ecology and Technology (CMET)

Faculty of Bioscience Engineering, Ghent University

Dean of the faculty of Bioscience Engineering, Ghent University

Prof. dr. ir. Marc Van Meirvenne

Rector of Ghent University

Prof. dr. Anne De Paepe

ION-EXCHANGE BASED PROCESSES IN HYBRID WATER TREATMENT

Marjolein Vanoppen

Thesis submitted in fulfilment of the requirements for the degree of Doctor (PhD) in Applied Biological Sciences: Environmental Technology

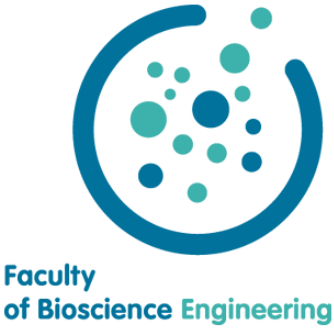

Dutch translation of the title:

Processen gebaseerd op ion-uitwisseling in hybride waterbehandeling

Citing this PhD

Vanoppen, M. (2016) Ion-exchange based processes for hybrid water treatment. PhD thesis, Ghent University, Belgium

Cover design

Photo courtesy of Manu Claes

ISBN 978-90-5989-895-0

Acknowledgements

In the past 4 years I have learned more than ever before. Doing a PhD is an exciting journey that would not have been the same without some important people joining me on my path.

First of all I really want to thank Arne, who has always believed in me more than I did, and continues to do so. You gave me the opportunity to start this research based on my enthusiasm and passion for the environment and for research. I have grown a lot, both personally and professionally, under your never failing guidance and support. You always challenged me, joined in my enthusiasm when things were going well and supported me through the rougher patches. I am sure the little group we started with will continue to grow and flourish, driven by your passion.

Of course I couldn't have finished this work without the help of my colleagues. Arnout DH, you seem to be a walking encyclopaedia sometimes, and although you needed a reminder every once in a while, you were always there to help me with practical stuff, for a little brainstorm and for DIY advice. Klaas, thank you for answering my endless questions on organic micropollutants and for doing a million analysis. By lighting samples on fire, covering part of the lab in acid and regular trips to the Coupure river, you have certainly made working in the lab more adventurous. Seba, you can be a real rock when times get tough, but are equally ready for a smile and a joke. Thank you for all the hugs and support (and a little less for the demi-water showers and piss odour). You guys have really made the lab a second home for me. To all of my other present and former PaInT colleagues, Lingshan, Mathieu, Evelyn, Lien V, Lorenz, Arima, Wahyu, Ali, Arnout DC and of course Oranso, Machawe and Gaetan, and to my ISOFYS colleagues, thank you for all the fun moments in the lab!

Of course I would like to thank all of the supporting staff. Katja, Quenten, Saskia, Stijn, John and Erik, my years in de lab would not have been the same without you. Thank you for all the practical help, but also the talks and jokes that always lightened my day. Katja, I am looking forward to many more cooking nights (with matching wines, of course) and Quenten, we should urgently organise a board game night with the colleagues!

To all of my thesisstudents; thank you for all the hard work and devotion, and of course for the parties! Annelies, Annelise, Nick, Dorien, Ella, Griet S., Griet W., Jolien and Sérafine, I

wish you all the best in all of your future endeavours. My PhD years would not have been the same without you.

Also to the colleagues of the Blue Circle, Paul, Luc, Peter, Charlotte, Dirk and An, a very warm thank you. I would also like to extend my thanks to some industrial partners; Tom and Stijn from Eurowater, Bart, Bart and Stijn from Farys and Induss, Martine from Monks. Thank you for helping me with my work and making this thesis possible.

I must also not forget my friends, who helped me relax with the necessary food, drinks and entertainment. Timothy, Magali, Robin and Caroline, we graduated together and started this adventure together, good luck with finishing your own PhD journey. The crazy loveable CMET people, especially Cristina, Stephen and Antonin, not only for the professional brainstorming sessions, but especially for the laughs and jokes (and Kevin and Chairman Meow of course, can't forget about those guys!). "De Antwerpenaren" for all the memorable times and "De SULlies" for over 15 years of fun and games. And last but not least Geert, for mentoring me and believing in me, I'm looking forward to our future endeavours! Thank you all!

I would also love to thank my family, that has always supported me in everything I wanted to do. Mom and dad, thank you for believing in me and supporting me to become the person I am today. You always stood by me when I needed advice or just a hug. Also a big thanks to Peter and Ann, for making my parents the happy people they now are. And of course thank you to my brother, Jeroen. I know you have no idea what the hell I do all day, but I hope I will someday be able to make it clear to you. Although our journey has not always been an easy one, I am proud of the man you have become.

Last but not least I want to thank the love of my life and my soulmate, Thomas. Thooms, you've always had faith in me, listened to all my worries and insecurities every night, and accepted the times I didn't want to talk. Despite your own crappy job, I can't count the times you told me 'Je bent goed bezig schatje!'. We have made it through these four years together and I can't wait to spend the rest of our life side by side.

Summary

Water and energy are two major challenges facing our world today and are two important drivers in the search for alternative water sources and more energy-efficient treatment systems. Industrial and domestic water use, at 20% and 10% of the total water withdrawal respectively, are two major contributors in this regard. Membrane technology is one of the key-players in future treatment schemes, as membranes can provide energy-efficient, sustainable and economic ways for treatment. However, as sources of fresh water become scarcer, new water sources such as impaired water, brackish water or groundwater will become more interesting. These will require different treatment strategies. Often, multiple treatment steps are needed to achieve the desired water quality, and different technologies are combined in so-called hybrid systems.

These hybrid systems are the focus in this research. Furthermore, the focus is on the incorporation of ion-exchange technologies into the hybrid systems. Unique about ion-exchange technologies is that they specifically target ions instead of water. This is of great value in combination with more established pressure driven processes, that target water. Indeed, ion-exchange technologies, although developed in the 1950's, are less wide-spread and developed than classic pressure-driven processes such as nanofiltration (NF) and reverse osmosis (RO). In this thesis, the value of ion-exchange technologies in hybrid water treatment schemes is explored and demonstrated.

The first part discusses the hybridisation of ion-exchange and RO. RO is an established technique for the production of high-quality (process) water from different sources. However, the water recovery of RO in these cases is often hampered by the presence of salts with a limited solubility. These can cause scaling of the RO membranes at high recoveries and require the addition of expensive and environmentally harmful anti-scalants. Ion-exchange (IEX) and Donnan dialysis (DD) are techniques which can selectively remove multivalent cations from the RO feed, limiting scaling on the membranes. As multivalent cations (e.g. Ca^{2+} and Mg^{2+}) are removed prior to RO, the water recovery can be increased and the RO concentrate, now containing high concentrations of monovalent cations (e.g. Na^{+} and K^{+}), can be used for the regeneration of the IEX or as a concentrated source of ions in DD. In a first, lab-scale study, two different RO feed streams (treated industrial wastewater and simple tap water) were tested in the envisioned IEX-RO and DD-RO

hybrids including recycling of the RO concentrate to the first step. The efficiency of the multivalent cation removal depends mainly on the ratio of monovalent to multivalent cations (monovalent:multivalent cation ratio or MMR) in the feed stream. This ratio determines the ion-exchange efficiency in both IEX and DD. Since the MMR is very high in the wastewater (±25), the RO recovery can be increased from 72 to 92%. For the tap water, these high RO recoveries can only be reached by adding additional NaCl to the RO concentrate, because of the low initial MMR in the feed. In an economic analyses, the IEX-RO hybrid proves to be most cost-efficient, due to the high current cost of the membranes used in DD. The membrane cost would have to decrease to 10-30 €/m², similar to current RO membranes, to achieve a comparable cost.

Because of the higher current economic viability of IEX-RO, it was decided to test this hybrid at pilot-scale. The pilot tests were carried out on brackish surface water in the harbour of Ghent at a process-water production facility. The tests were carried out over several months, during which the feed water composition changed, allowing to assess the effect of feed water composition on the hybrid's efficiency. Furthermore, the effect of changing RO recoveries was studied. The recovery can easily be increased to 85% without the addition of anti-scalants, while in normal stand-alone operation the recovery is only 70% including anti-scalant dosing. The achieved recovery is only limited by the pilot's capabilities and can probably be increased further in real life operations. An increase in recovery does however not influence the efficiency of the IEX regeneration with the RO concentrate, which shows that not the RO concentrate volume but only the total amount of cations present for regeneration is important at the recoveries tested. In other words, the MMR is the only factor that determines the viability of the system. Although in this study the MMR was not high enough to ensure 100% regeneration efficiency in the IEX, this was solved by the addition of NaCl to the RO concentrate prior to regeneration. An operational parameter, called CNK, was developed to predict the amount of NaCl to add in the concentrate during operation based on the feed water composition, so excess dosage of chemicals is avoided. In this particular case, the implementation of the IEX-RO hybrid system instead of the stand-alone hybrid system is expected to increase product water revenues by ±30%.

This research shows that combining IEX and RO in a hybrid system is both technologically and economically interesting. The system leads to a decrease in waste discharge (due to the increased water recovery) and completely avoids the use of harmful, expensive anti-scalants. However, not all RO systems are limited by the scaling potential of the feed water. In

seawater RO for example, the water recovery is limited to about 50% by the hydraulic pressure limitations of the equipment. The main concern in these systems is the high energy demand due to the high pressures needed. Therefore, a second part of this study focussed on increasing the energy efficiency of seawater RO.

State-of-the-art RO installations for seawater desalination require 2-3 kWh/m³ of energy. Salinity gradient power (SGP) technologies can generate energy from the salinity gradient, generated for example between seawater and a low salinity water source (e.g. river water or impaired water). These technologies are pressure retarded osmosis (PRO, where water transport from the impaired water to the seawater drives a turbine) and reverse electrodialysis (RED, where ion transport from the seawater to the impaired water generates electricity). The hybridisation between these technologies and seawater RO has two big advantages: SGP technologies produce energy from seawater that can be used in the RO system and they reduce the seawater salinity, further reducing the energy demand in RO. Based on thermodynamic calculations, the SGP-RO hybrids can even be energy-neutral or energy-producing. However, the main drawback of SGP technologies is their slow kinetics of desalination, resulting in a high required membrane area and thus a high investment cost. This is why 'assisted' versions of the technologies were developed, in which a small additional driving force is applied to increase the rate of desalination and decrease the required membrane area. These are pressure assisted osmosis (PAO) and assisted reverse electrodialysis (ARED). Modelling shows that the overall energy demand of a hybrid including these technologies is still significantly lower than that of stand-alone RO, at around 1.2 kWh/m³. Although the hybrid systems are theoretically promising, some practical questions remain. First of all, the transport of contaminants from the low salinity source to the seawater should be carefully investigated. In the case of impaired water for example, organic micropollutants such as pharmaceuticals and pesticides could potentially contaminate the seawater and thus potentially the produced water. Secondly, the influence of these contaminants and the reduced salinity of the seawater on RO fouling should be looked into.

Although research had already looked into PAO and its behaviour on lab-scale, ARED had not been thoroughly looked into. First lab-scale experiments carried out in this study show great promise. Because of the faster desalination rate compared to RED, the resistances caused by the low salinity compartment and the membranes can be easily overcome. At higher concentrations (> 0.1M) of the low salinity stream, this benefit disappears due to the lower resistance. This indicates that ARED is especially useful in the first stages of the

mixing process. When the initial high resistances of the solution and membranes is overcome, energy production in RED can be started. More research is needed to further optimise the hybrid process including both ARED and RED before RO.

As mentioned before, transport of pollutants through ion-exchange membranes (IEM) can cause issues in hybrids with ion-exchange technologies. Although fouling of IEM has been intensively studied in literature, transport mechanisms of organic pollutants are largely unknown. That is why a final part of this thesis focuses on transport of organics through IEM. At first, transport of trace organic contaminants (TOrCs) are studied under different conditions as a model for a wide variety of organic compounds. It was found that in the absence of salt and external potential difference, the electrochemical equilibrium across the membranes is the main driver for TOrC transport, resulting in the transport of mainly charged TOrCs. When salt is present, the transport of TOrCs is hampered in favour of the NaCl transport, which shows a preferential interaction with the membranes due to its small size, high mobility and concentration. Further experiments were carried out at different current densities. The external potential difference seems to have only a small effect on the TOrC transport. It is only when the salt becomes nearly completely depleted that the TOrCs are transported as carriers of the applied charge. This shows that transport of organics is mainly driven by diffusion as long as salt is present.

These results were confirmed in experiments with different salts ($MgCl_2$ and Na_2SO_4). In the presence of multivalent ions, transport of TOrCs is slightly higher, due to the lower diffusion coefficient of these ions. When Mg^{2+} is present, especially the transport of positively charged TOrCs is higher, while the presence of SO_4^{2-} results in a higher transport of both negatively and positively charged TOrCs. As in ARED, the transport direction of the organics is not always the same as that of the salt. Tests with TOrC transport opposite to the dominant salt transport direction were carried out as well. These show that Donnan dialysis plays an important role. As the high salt concentration causes a high electrochemical potential difference across the membranes, transport is not only caused by the electroneutral transport of both negative and positive ions across the membranes, but also by the exchange of salt ions for TOrCs with the same charge.

To confirm the observations with TOrCs and further look into the diffusive nature of the organics transport, experiments with organic acids were carried out. The main advantage of these acids is that their solubility is much higher than that of the TOrCs. However, even at these higher concentrations, the salt transport greatly dominates the transport of the organic

acids. It is only when no salt is present that a significant amount of the applied current is carried by the acids. This again clearly proves that transport of organics is mainly driven by diffusion in the presence of salts. To limit the transport of organics in favour of their selective separation from the salts, it is important to look at the membranes properties and not at the operational parameters.

Samenvatting

Water en energie zijn twee grote uitdagingen waar onze wereld vandaag voor staat en zijn een belangrijke motivatie in de zoektocht naar alternatieve bronnen voor water en meer energie-efficiënte behandelingssystemen. Industrieel en huishoudelijk waterverbruik, goed voor respectievelijk 20% en 10% van het totale wereldwijde waterverbruik, zijn hierin twee belangrijke bijdragen. Membraantechnologie is één van de hoofdrolspelers in de behandelingssystemen van de toekomst, omdat hiermee energie-efficiënte, duurzame en economisch interessante manieren van behandeling voorzien kunnen worden. Aangezien traditionele bronnen van zoet water schaarser worden, zullen nieuwe bronnen zoals verontreinigd water, brak water of grondwater interessanter worden, maar deze zullen andere behandelingsstrategieën vereisen. Vaak zijn verschillende behandelingsstappen nodig om de gewenste waterkwaliteit te behalen, en worden verschillende technologieën gecombineerd in zogenaamde hybride systemen.

Hybride systemen zijn het onderwerp van dit onderzoek. Daarenboven ligt de focus op de implementatie van ion-uitwisselingstechnologieën in deze hybride systemen. Deze technieken zijn uniek omdat ze zich specifiek richten op ionen in plaats van water. Dit is een groot voordeel in combinatie met de meer bekende druk-gedreven membraanprocessen, die zich richten op water. Hoewel ion-uitwisselingstechnieken ontwikkeld werden in de jaren 1950 zijn deze nog minder bekend en ontwikkeld dan klassieke druk-gedreven processen zoals nanofiltratie (NF) en omgekeerde osmose (RO). In deze thesis wordt de waarde van ion-uitwisselingstechnologieën in hybride watersystemen onderzocht en aangetoond.

Het eerste deel bespreekt de hybridisatie van ion-uitwisseling met RO. RO is een gevestigde technologie voor de productie van (proces)water van hoge kwaliteit vanuit verschillende bronnen. De wateropbrengst van RO wordt in deze gevallen vaak gelimiteerd door de aanwezigheid van zouten met een beperkte oplosbaarheid. Deze veroorzaken scaling op de RO membranen bij een hoge wateropbrengst en vereisen het gebruik van (vaak dure en/of milieu-schadelijke) anti-scalants. Ion-uitwisselingsharsen (IEX) en Donnan dialyse (DD) zijn technieken die selectief multivalente kationen kunnen verwijderen uit de voeding van de RO en daarmee scaling van de membranen vermijden. Wanneer multivalente kationen (zoals Ca^{2+} en Mg^{2+}) verwijderd worden voor RO kan de wateropbrengst verhoogd worden en kan het RO concentraat, dat dan een hoge concentratie monovalente kationen (zoals Na^{+} en K^{+})

bevat, gebruikt worden voor de regeneratie van de IEX of als geconcentreerde bron van ionen in DD. In een eerste studie op laboschaal werden twee verschillende voedingsstromen van RO (secundair behandeld afvalwater en kraanwater) getest in de IEX-RO en DD-RO hybride systemen inclusief recyclage van het RO concentraat naar de eerste stap. De efficiëntie van de verwijdering van multivalente kationen hangt vooral af van de ratio van monovalente kationen ten opzichte van multivalente kationen (monovalent:multivalent cation ratio of MMR) in de voeding. Deze ratio bepaalt de ion-uitwisselingsefficiëntie in zowel IEX als DD. Aangezien de MMR hoog is in het afvalwater (±25), kan de RO wateropbrengst verhoogd worden van 72 naar 92%. Voor kraanwater kan deze hoge opbrengst enkel bereikt worden als NaCl toegevoegd wordt aan het concentraat, omwille van de lage initiële MMR in de voeding. In een economische analyse komt IEX-RO naar voor als de meest kostenefficiënte technologie, door de hoge huidige kost van de membranen die gebruikt worden in DD. De membraankost zou moeten dalen tot 10-30 €/m², vergelijkbaar met de huidige RO membranen, om een economisch interessante kost te behalen.

Omwille van de hogere economische haalbaarheid van IEX-RO, werd beslist deze hybride uit te testen op pilootschaal. De piloottesten werden uitgevoerd op brak oppervlaktewater in de haven van Gent op een proceswaterproductie-site over verschillende maanden. Gedurende deze tijd varieerde de samenstelling van de voeding significant, waardoor het effect van deze samenstelling op de efficiëntie van de hybride nagegaan kon worden. Daarnaast werd ook het effect van een veranderende RO opbrengst bestudeerd. Deze opbrengst kan makkelijk verhoogd worden tot 85% zonder anti-scalants toe te voegen, in vergelijking met een opbrengst van 70% bij de huidige stand-alone RO installatie waarbij wél anti-scalants gedoseerd worden. De bereikte wateropbrengst wordt gelimiteerd door de capaciteit van de pilootinstallatie zelf en kan waarschijnlijk nog verhoogd worden bij implementatie op grote schaal. Een verhoogde wateropbrengst heeft echter geen invloed op de efficiëntie van de regeneratie van de IEX met het concentraat van de RO, wat aantoont dat niet het volume RO concentraat maar enkel de totale hoeveelheid kationen aanwezig voor regeneratie belangrijk is bij de geteste omstandigheden. Met andere woorden, de MMR is de enige factor die de haalbaarheid van het systeem bepaalt. Hoewel de MMR hier niet hoog genoeg was om een regeneratie-efficiëntie van 100% te behalen in de IEX, wordt dit makkelijk opgelost door een kleine hoeveelheid NaCl toe te voegen aan het RO concentraat. De operationele parameter CNK werd ontwikkeld om de exacte hoeveelheid NaCl die toegevoegd moet worden aan het RO concentraat tijdens de werking te bepalen, gebaseerd op de samenstelling van het voedingswater. Zo wordt vermeden dat te veel chemicaliën

toegevoegd worden. In het onderzochte geval wordt verwacht dat de implementatie van de IEX-RO hybride in plaats van de huidige stand-alone RO installatie de opbrengst van het geproduceerde water met ±30% zal verhogen.

Dit onderzoek toont dat de combinatie van IEX met RO in een hybride systeem technologisch en economisch interessant is. Het systeem leidt tot een vermindering in het volume te lozen water (door de verhoogde wateropbrengst) en vermijdt het gebruik van schadelijke, dure anti-scalants. Niet alle RO systemen zijn echter gelimiteerd door de aanwezigheid van slecht oplosbare zouten in de voeding. RO systemen voor zeewaterontzouting bijvoorbeeld zijn gelimiteerd tot een wateropbrengst van ongeveer 50% door de beperkingen in hydraulische druk die de apparatuur kan weerstaan. Door de hoge drukken die in deze systemen gebruikt worden, is de belangrijkste zorg hier eerder het hoge energieverbruik. Een tweede deel van deze studie focuste daarom op het verhogen van de energie-efficiëntie van zeewater RO.

State-of-the-art RO installaties voor zeewaterontzouting hebben 2-3 kWh/m³ energie nodig. Recent werden echter systemen ontwikkeld waarmee energie gewonnen kan worden uit zoutgradiënten (SGP of salinity gradient power), zoals bijvoorbeeld tussen zeewater en rivierwater of gecontamineerd water. Deze technologieën zijn pressure retarded osmosis (PRO, waar watertransport van het gecontamineerde water naar het zeewater een turbine aandrijft) en reverse electrodialysis (RED, waar het ionentransport van het zeewater naar het gecontamineerde water elektriciteit genereert). De hybridisatie tussen deze technologieën en zeewater RO heeft twee grote voordelen: SGP technologieën produceren energie uit het zeewater die gebruikt kan worden in het RO systeem en ze verminderen de zoutconcentratie van het zeewater, waardoor de energievraag van de RO verder gereduceerd wordt. Thermodynamische berekeningen wijzen uit dat de SGP-RO hybrides zelfs energie-neutraal of energie-producerend kunnen zijn. Het grootste nadeel bij SGP technologieën is echter dat de kinetiek van ontzouting zeer traag is, wat resulteert in een hoge benodigde membraanoppervlakte en dus een hoge investeringskost. Daarom werden 'assisted' versies van deze technologieën ontwikkeld, waarbij een kleine extra drijvende kracht aangelegd wordt om de snelheid van ontzouting te verhogen en de benodigde hoeveelheid membraan te verlangen: pressure assisted osmosis (PAO) en assisted reverse electrodialsis (ARED). Modelleerresultaten tonen aan dat de algemene energievraag van een hybride systeem met deze technologieën nog steeds significant lager is dan die van een stand-alone RO systeem, rond 1.2 kWh/m³. Hoewel deze hybride systemen veelbelovend zijn, blijven nog enkele

praktische vragen over. Om te beginnen moet het transport van verontreinigingen vanuit het water met een lage zoutconcentratie naar het zeewater grondig onderzocht worden. Als bijvoorbeeld gezuiverd afvalwater gebruikt wordt, zouden organische micropolluenten zoals farmaceutica en pesticiden het zeewater, en dus ook het geproduceerde water, kunnen verontreinigen. Verder moet ook de invloed van verontreinigingen en van de gereduceerde zoutconcentratie van het zeewater op vervuiling van het RO systeem onderzocht worden.

Hoewel PAO al op laboschaal onderzocht werd, werd ARED nog niet grondig bekeken. De eerste experimenten op laboschaal uitgevoerd in deze studie waren veelbelovend. Omwille van de snellere ontzouting in vergelijking met RED kan de weerstand veroorzaakt door het compartiment met lage concentratie en de membraanweerstand makkelijk overwonnen worden. Bij hogere concentraties (> 0.1M) in het lage saliniteitscompartiment verdwijnt dit voordeel omwille van de lagere weerstand. Vooral in het begin van de menging van zeewater met gecontamineerd water kan ARED dus nuttig zijn om de initiële weerstand van de oplossingen en membranen te verlagen, waarna overgegaan kan worden op energieproductie met RED. Veel meer onderzoek is echter nodig om het hybride proces, met ARED en RED voor RO, verder te optimaliseren.

Zoals vroeger al besproken kan het transport van organische micropolluenten (OMP) door ion-uitwisselingsmembranen (IEM) problemen veroorzaken in hybrides met ion-uitwisselingstechnieken. Hoewel vervuiling van IEM reeds grondig bestudeerd werd in de literatuur, zijn de exacte transportmechanismen van OMP nog grotendeels onbekend. Daarom focust het laatste gedeelte van deze thesis op het transport van organica door IEM. Allereerst werd het transport van OMP bestudeerd bij verschillende operationele condities, als een model voor diverse organische verbindingen. Hieruit bleek dat in de afwezigheid van zout en zonder extern potentiaalverschil het elektrochemisch potentiaalverschil over de membranen de belangrijkste drijvende kracht is voor OMP transport, wat resulteert in het transport van voornamelijk geladen OMP. Wanneer zout aanwezig is, wordt het transport van OMP gehinderd ten gunste van het transport van het de zoutionen, die preferentieel interageren met de membranen door hun beperkte grootte en hoge mobiliteit en concentratie. Verdere experimenten werden uitgevoerd bij verschillende stroomdichtheden. Het externe potentiaalverschil blijkt maar een klein effect te hebben op het OMP transport. De OMP gedragen zich pas als dragers van de stroom wanneer het zout bijna volledig verwijderd is. Dit toont aan dat het transport van organica vooral diffusie-gedreven is zolang zout aanwezig is.

De resultaten werden bevestigd door experimenten met verschillende zouten ($MgCl_2$ en Na_2SO_4). In de aanwezigheid van multivalente ionen is het transport van OMP licht hoger, omwille van de lagere diffusie coëfficiënt van deze ionen. Wanneer Mg^{2+} aanwezig is, is vooral het transport van positief geladen OMP hoger, terwijl de aanwezigheid van SO_4^{2-} het transport van zowel negatief als positief geladen OMP stimuleert. Het transport van OMP gebeurt niet altijd in dezelfde richting als het zouttransport, zoals in ARED bijvoorbeeld. Daarom werden testen uitgevoerd met verschillende richtingen van het OMP transport ten opzichte van het transport van zout. Deze tonen aan dat Donnan dialyse hier een belangrijke rol speelt. Omdat de hoge zoutconcentratie een hoge elektrochemische potentiaal over de membranen veroorzaakt, zal het transport van zout niet enkel veroorzaakt worden door het elektroneutrale transport van negatieve en positieve ionen doorheen de membranen, maar ook door uitwisseling van de zoutionen voor OMP met dezelfde lading.

Om de resultaten met OMP te bevestigen en het diffusief karakter van het transport van organica verder te bekijken, werden experimenten uitgevoerd met organische zuren. Het grote voordeel van deze zuren is dat hun oplosbaarheid veel hoger ligt dan die van de OMP. Zelfs bij hogere concentraties domineert het zouttransport echter over het OMP transport. Enkel wanneer geen zout aanwezig is, wordt een significante hoeveelheid stroom gedragen door de zuren. Dit toont weer duidelijk aan dat het transport van organica vooral diffusie gedreven is in de aanwezigheid van zout. Om het transport van organica te limiteren ten gunste van de selectieve scheiding tussen zouten en organica, moet dus naar de membraaneigenschappen gekeken worden en niet naar de operationele condities.

List of abbreviations

AEM	Anion exchange membranes
ARED	Assisted reverse electrodialysis
BV	Bed volumes
CAPEX	Capital expenses
CEM	Cation exchange membranes
CP	Concentration polarisation
DD	Donnan dialysis
DI	Deionised
ED	Electrodialysis
EDR	Electrodialysis reversal
FO	Forward osmosis
ICP-OES	Inductively coupled plasma optical emission spectroscopy
IEM	Ion-exchange membranes
IEX	Ion-exchange resins
MCDI	Membrane capacitive deionisation
ME	Membrane electrolysis
MES	Microbial electrosynthesis
MFC	Microbial fuel cell
MMR	Monovalent:multivalent cation ratio
NF	Nanofiltration
OA	Organic acids
PAO	Pressure assisted osmosis
PRO	Pressure retarded osmosis
RED	Reverse electrodialysis
RO	Reverse osmosis
RSD	Reverse salt diffusion
SAC	Strong acid cation
SBA	Strong base anion
scRED	Short-circuited reverse electrodialysis
SD	Swelling degree
SEC	Specific energy consumption
SGP	Salinity gradient power
SV	Space velocity
TDS	Total dissolved solids
TOC	Total organic carbon
TOrC(s)	Trace organic contaminant(s)
UHPLC-HR-MS	Ultra high pressure liquid chromatography – high resolution – mass spectrometry
WAC	Weak acid cation
WBA	Weak base anion

Nomenclature

a	Activity coefficient	(-)
A_m	Active membrane area	m^2
C	Concentration	mol/m^3 - mol/l - mg/l - µg/l
Cap	Capacity	eq/l
D	Diffusion coefficient	m^2/h
E	Potential difference	V
F	Faraday constant	C/mol
h	Compartment thickness	m
J_s	Solute flux	$mol/(m^2.h)$
K_d	Relative concentration	(-)
k	Boltzmann constant	$m^2.kg/(s^2.K)$
MMR	Monovalent:multivalent cation ratio	(-)
MR	Mixing ratio	(-)
MW	Molecular weight	g/mol
n	Molar amount	mol
N	Cell pairs	(-)
Q	Flow rate	m^3/h
R	Recovery	(-)
r	Pore radius	m
R_g	Gasconstant	J/(mol.K)
R_Ω	Resistance	$\Omega.cm^2$ - $\Omega.m^2$
SD	Swelling degree	(-)
T	Temperature	K
V	Volume	l - m^3
W	Weight	g
x	Mole fraction	(-)
z	Ionic valence	(-)
α	Permselectivity	(-)
β	Shadow factor	(-)
ΔG	Gibbs free energy	J
Δn	Molar flow rate	mol/h
ΔS	Entropy	J/K
Δx	Membrane thickness	m
ε	Porosity	(-)
ϰ	Conductivity	S/m
λ	Ratio solute/pore radius	(-)
ϱ	Density	kg/m^3
ϕ	Partition coefficient	(-)

Table of contents

Chapter 1: Introduction to ion-exchange and hybrid technologies

There is no doubt that water and energy are two of the major challenges our world is facing today. It is well known that regions such as North-Africa, the Middle East, India and Australia (among many others) suffer from severe water stress. In Figure 1.1, the projected water stress in 2020 (if business as usual is considered) shows that water stress will increase in many regions and will also spread more north, affecting major parts of the United States, Europe and Asia. With water stresses achieving alarming levels, a reduction in and increased efficiency of water use is urgently called for. This pushes the search for alternative water sources, such as (secondary treated) wastewater, polluted or brackish surface water and seawater.

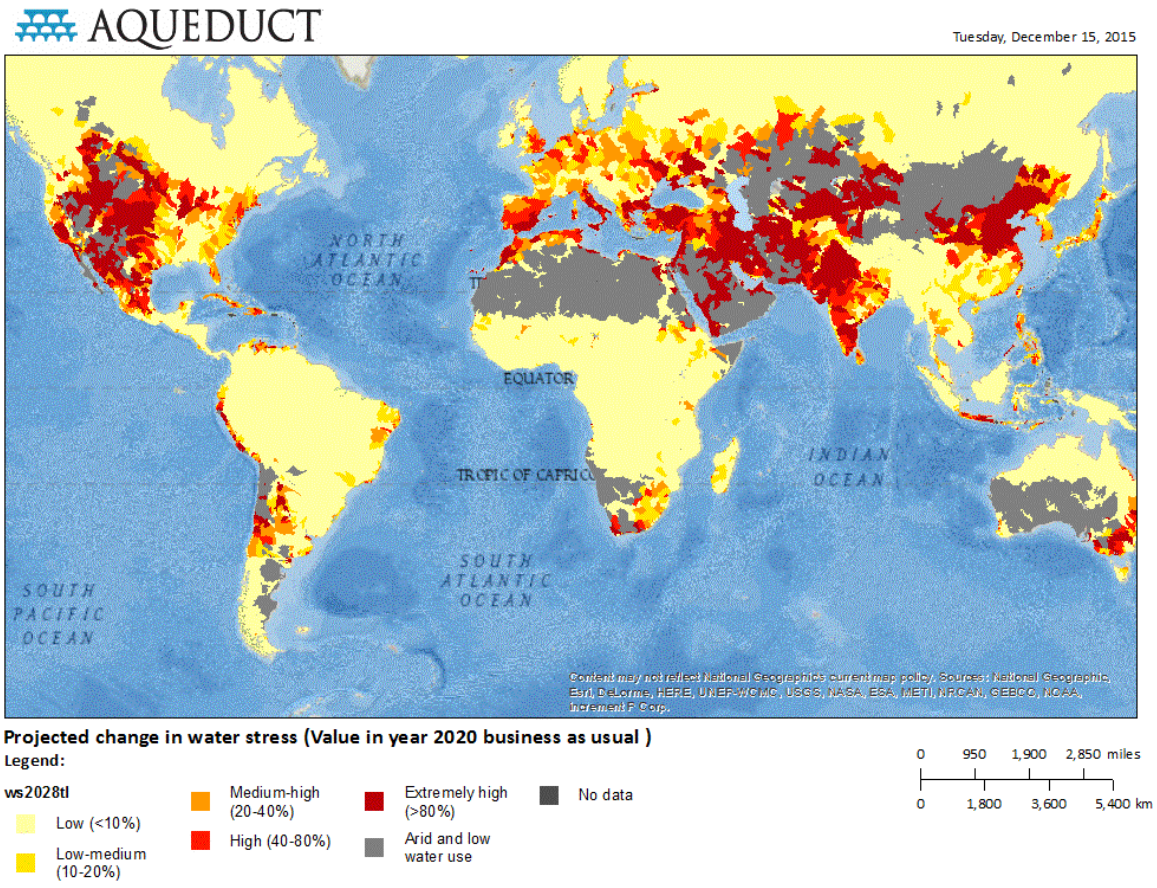

Figure 1.1 Projected worldwide water stress in 2020 if nothing changes [1].

However, these alternative water sources come with their own set of challenges. Before they can be used, extensive treatment is needed for the removal of hardness, pollutants and/or dissolved salts (typically so for brackish water and seawater). This treatment can involve biological treatment steps, such as classic activated sludge treatments or more recent membrane bioreactors, and/or physico-chemical treatment steps, such as coagulation/flocculation, activated carbon treatment, precipitation, ion-exchange or

(membrane) filtration. A polishing (such as ion-exchange polishing) and/or disinfection (such as chlorination or ozonation) step might be included as well. Many of these treatment steps require large amounts of energy, such as for example aeration in biological treatments or pressure in membrane filtration. As feed waters become more complex, more extensive treatment is necessary, which entails a higher energy demand. However, to produce this energy, water is needed as well, for example as ultrapure steam or cooling water. This cycle of energy needed for water purification and water needed for energy production is called the water-energy nexus, as shown in Figure 1.2.

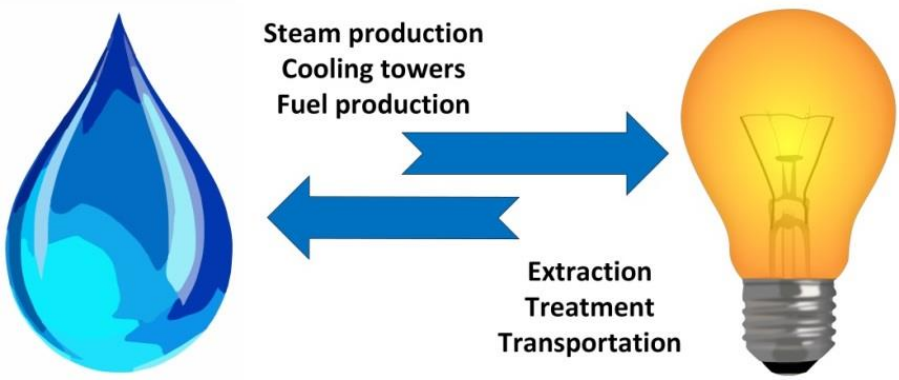

Figure 1.2 Schematic illustration of the water-energy nexus (adapted from [2]).

With about 20% of the global water withdrawal [3] and 50% of the total energy use [4] being attributed to industrial activities, industry is one of the main players in the water-energy nexus. Furthermore, increasing domestic demands for fresh water, accounting for about 10% of the worldwide water withdrawal at this moment [3], should be met in such a way that the vicious energy-water nexus cycle can be broken. This means the development of environmentally, energetically and economically sustainable water treatment systems.

Membrane processes always have been and will remain one of the key technologies in the development of these sustainable systems. By combining membrane technologies and other technologies in so-called hybrid schemes, the strengths of the technologies together can lead to more efficient treatment processes. Hybrid processes are the main focus in this PhD dissertation. Furthermore, the focus will be on the implementation of ion-exchange technologies in these hybrids. Ion-exchange processes are unique in that they selectively target the transport of ions. As such, they can be a valuable addition, complementing more established membrane systems that focus on water transport instead. In this thesis, the value and viability of hybrid water treatment systems incorporating ion-exchange technologies and membrane processes are investigated and demonstrated.

1 Development and current applications of ion-exchange technologies

One of the first mentions of ion-exchange applications was by Aristotle, who noticed that some types of sand could be used to clean seawater and impure water [5]. The development of these processes has come a long way since then, and many comprehensive review papers exist giving a good overview of the development and general working principals of ion-exchange processes [6–9]. In this part, such a review will thus not be given, but rather a short description of the ion-exchange process itself and of the ion-exchange technologies used in this dissertation will be given, to help the reader understand the rationale behind this work. More details on the processes themselves and relevant recent developments are discussed in the appropriate chapters.

1.1 Ion-exchange: basic principles

Ion-exchange processes in this dissertation are defined as any type of processes that remove ions from a water stream by exchanging them for other ions - be it in a direct way such as in ion-exchange resins (where counter-ions associated with the functional groups on the resin are exchanged for ions in the solution that are either higher in concentration or have a higher affinity for the resin); or indirectly such as is the case for ion-exchange membranes (where ions from the solution are transported through a membrane and are exchanged between different solutions, whereby charge neutrality needs to be maintained). Kumar and Jain (2013) define an 'ion-exchanger' as 'a water-insoluble substance which can exchange some of its ions for similarly charged ions contained in a medium with which it is in contact' [9]. Generally, ion-exchange materials consist of a backbone that is functionalised with fixed charged functional groups. These functional groups are paired with mobile ions of the opposite charge, called counter-ions. It is these counter-ions that are exchanged for ions of the same charge in the treated solution. A schematic overview of this exchange process is shown in Figure 1.3.

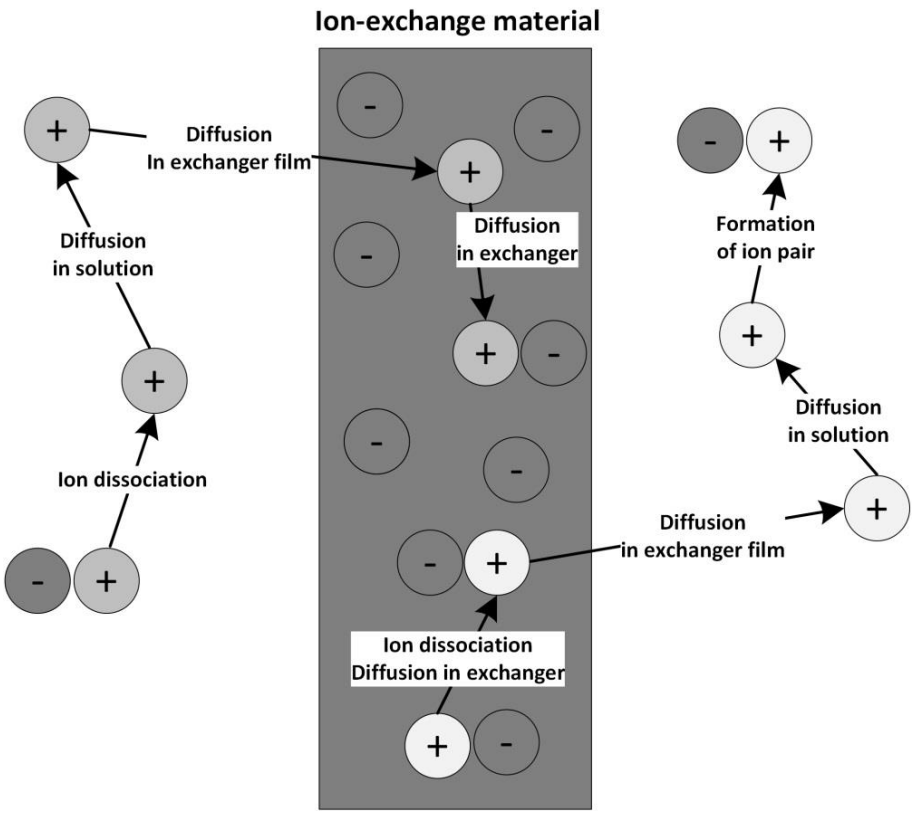

Figure 1.3 Different types of technologies for ion-exchange exist, but all are based on the same basic processes, schematically shown here (adapted from [9]).

1.2 Ion-exchange resins (IEX)

Ion exchange resins were one of the first ion-exchange materials to be developed. In the beginning of the 20th century, Rober Gans, a German chemist, prepared resins from sodium aluminate and sodium silicate for water softening and sugar refining [9,10]. In the 1940's, resins as we know them today were developed by copolymerisation of styrene crosslinked with divinylbenzene (as shown in Figure 1.4). This backbone is functionalised with functional groups of a particular charge to facilitate ion-exchange. The polymerisation determines whether the final resins has a gel or macroporous structure. Gel-based resins have a greater capacity and better regeneration efficiency, which is why they are the most common resins used in standard water treatment applications, while macroporous (or macroreticular) resins are more resistant in case of chemically aggressive feeds or high temperatures. The typical appearance of gel-based IEX resins is shown in Figure 1.5.

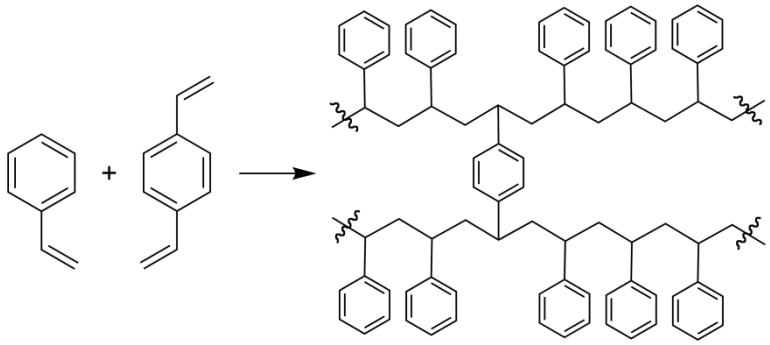

Figure 1.4 Polymerisation of styrene cross-linked with divinylbenzene.

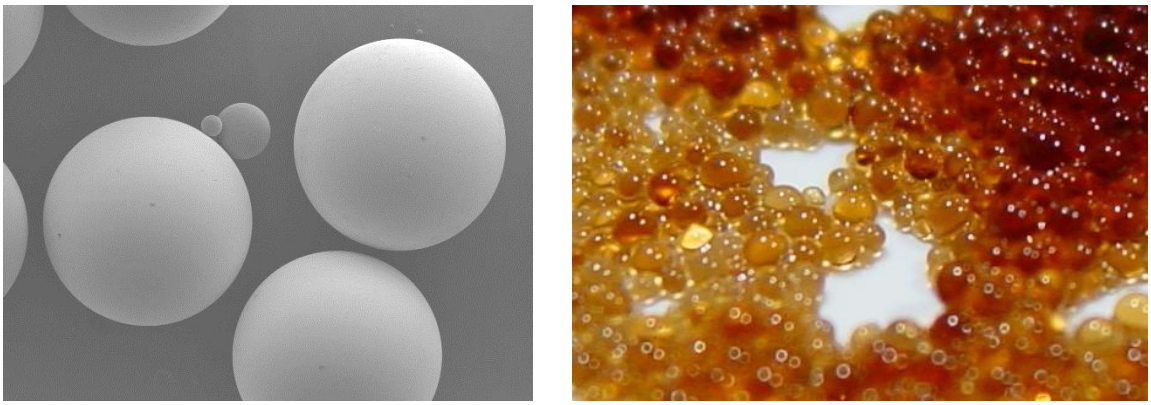

Figure 1.5 Scanning electron microscope image of IEX beads at 100x magnification (left) and typical appearance of the IEX beads (right).

IEX resins are typically divided into four groups depending on their functional groups [11]; strong acid cation (SAC), weak acid cation (WAC), strong base anion (SBA) and weak base anion (WBA). They mainly differ in functionalisation of the backbone. In SAC resins, the functional groups are mostly formed through sulfonation (resulting in $–SO_3^-$ functional groups), while in WAC resins, the exchange capacity mostly comes from carboxylic groups ($-COO^-$). SBA resins typically contain quaternary ammonia functional groups ($-NR_3^+$, with R usually three methyl groups), while WBA resins contain primary ($-NH_2$), secondary (-NHR) or tertiary amine ($-NR_2$) groups. SAC and SBA resins are able to exchange almost all cations/anions from a given water stream with their mobile counter-ion, while their weak counterparts will only exchange part of the ions present. The latter have the benefit of greater regeneration efficiency, because of their weaker bond with the counter-ions, resulting in a lower need for regeneration chemicals. Regeneration is necessary to bring the functional groups back to their original form (with original counter-ion) after saturation of the resin. This way, the resins can be re-used in a next treatment cycle. Regeneration usually requires a strong acid or base or a highly concentrated NaCl solution (6-10 wt.%), depending on the application.

When a resin is fully regenerated, the mobile counter-ions are available for the ion-exchange process. This process can be represented by the following simplified equation for a cation exchange resin (and similarly for an anion exchange resin) [9]:

$$X^-A^+ + B^+ + C^- \rightarrow X^-B^+ + A^+ + C^-$$

where X is the functional group and A is the counter-ion. This counter-ion is exchanged for the cations in solution (B) with a higher affinity for the resin, whereby the own counter-ion of B (C) now pairs with the mobilized counter-ion A. Typically, the affinity of cationic exchange resins is $Ca^{2+} > Mg^{2+} > Na^+ > H^+$ and that for anionic exchange resins is $SO_4^{2-} > NO_3^- > Cl^- > HCO_3^- > OH^-$ [12]. After saturation, the exchange capacity is restored by a regeneration step as discussed before. During regeneration, the affinity of the resin for the original counter-ion A is increased by using a high concentration and/or volume.

Two typical applications for IEX are complete demineralisation and water softening. Complete demineralisation is required for e.g. high-pressure boiler feed waters and is used to remove all dissolved solids. To achieve this, a combination of SAC and SBA resins is used in their H^+/OH^- form respectively. The SAC exchanges the cations in solutions for H^+ while the SBA does the same with OH- and anions, resulting in complete demineralisation of the feed stream. These are often combined with WAC and WBA resins, to protect the SAC and SBA resins (e.g. by removing organic material) and to partially demineralise the feed water. After saturation, the resins are typically regenerated with HCl and NaOH respectively. For softening of for example tap water, cations that can easily precipitate because of their nature to form insoluble salts (e.g. calcium, magnesium, barium…) are removed with a SAC resin. This is desired for low pressure boilers, washing procedures and RO operations, for example. To avoid pH changes, the cations here are exchanged for sodium, which forms very soluble salts. After saturation the resin is thus regenerated with a concentrated NaCl solution.

Recent research on ion-exchange has focussed for example on the integration of IEX with NF or RO to protect the membranes and to increase the process efficiency. New resins, such as the Puralite® Shallow Shell Technology™ resins, are being developed with a higher fouling resistance and lower demand for regeneration chemicals and rinsing water. More details on recent developments will be discussed in the relevant chapters and the general discussion.

1.3 Electrodialysis (ED)

The principles of ion-exchange membranes (IEM) were first postulated as early as the end of the 19th century, when Ostwald and Donnan described ion-selective membranes and Donnan exclusion. However, it took until 1952 for the first commercial ED plant to start operations [7,13,14]. At present, ED is mostly used for the desalination of brackish water, the production of industrial process water and the demineralisation of food products [8,15].

In ED, IEM are used to (selectively) remove charged species from a feed stream. These IEM are very similar to IEX resins, with most commercially available membranes containing a poly(styrene divinylbenzene) backbone and sulfonic or carboxylic functional groups for cation exchange membranes (CEM) and quaternary ammonia groups for anion exchange membranes (AEM). These functional groups ensure the membranes are selective for a certain charge, i.e. CEM only allow cations to pass, while AEM only allow anions to pass. The IEM are placed alternately between an anode and cathode, creating diluate and concentrate compartments. A potential difference or current is applied over the membrane stack, drawing the ions to the electrodes and thus achieving desalination of the diluate. Every electron delivered to the system will ideally cause the transport of one ionic charge and its counter-ion in every cell pair from diluate to concentrate. One cell pair consists of a diluate compartment, a CEM, a concentrate compartment and an AEM. By alternating the membranes in this way, the ions are retained in the concentrate. This process is illustrated schematically in Figure 1.6.

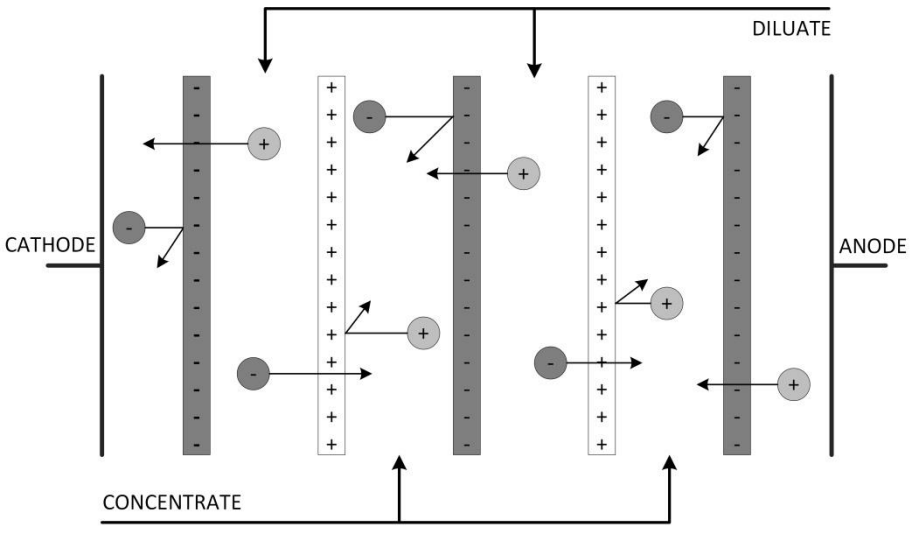

Figure 1.6 Schematic representation of the ED process.

As in all membrane processes, fouling and scaling can be a problem in ED. To avoid these phenomena, electrodialysis reversal (EDR) is often applied, in which the polarity of the electrodes is periodically switched.

1.4 Reverse electrodialysis (RED)

In ED, energy is consumed to transport ions, often against their concentration gradient, as such selectively removing (certain) ions from the feed stream and concentrating them in a concentrate stream. In RED, the opposite is achieved. By contacting a high and low salinity feed source through IEM, a spontaneous flow of ions will occur. This ion flow can be harvested as an electric current by implementing an external resistance into the system. This type of sustainable energy is known as Blue Energy or Salinity Gradient Power (SGP). Although the possibilities of this technology were already recognized in the 1950's and 70's [16,17], it was only thoroughly investigated in 2005 at Wetsus (the Netherlands) and is currently under pilot scale testing at the Afsluitdijk in the Netherlands. Although the main focus for RED is on the controlled mixing of seawater and river water for energy production, other applications are also possible. The REAPower project operated a pilot plant for 12 months on brackish water and saturated brine (coming from the production of sea salt) without significant performance losses [18].

As in ED, in RED a number of cell pairs are placed between two electrodes, forming high and low salinity compartments. The alternating high and low salinity compartments create a salinity gradient across the membranes, which results in the build-up of an electrochemical potential difference. This causes the spontaneous transport of ions from the high salinity compartments to the low salinity compartments. The resulting potential build-up can be harvested as electrical energy in two ways: (1) the potential difference drives redox-reactions at the anode and cathode, through the recirculation of an electrode rinse solution (e.g. $K_4Fe(CN)_6/K_3Fe(CN_6)$ or NaCl) in the electrode compartments, which in turn create an electron flow from the anode to the cathode that can be harvested through an external load or (2) capacitive electrodes are used which act as a capacitor, converting ionic current into electric current without the need for redox reactions but requiring a periodical flow switch to regenerate the electrode [19].

1.5 Donnan dialysis (DD)

Donnan dialysis was named after Donnan, who in 1924 described the equilibrium across an ion exchange membrane that develops when the membrane separates two different electrolyte solutions [20].

Figure 1.7 shows the DD process for the exchange of cations. Cations from the feed (e.g. Ca^{2+}) on one side of the membrane are exchanged with cations from the concentrate (e.g. Na^{+}) on the other side of the membrane. This exchange is driven by a concentration difference across the membrane, resulting in transport of the concentrate cations to the feed and vice versa. When CEM are used, anions can not cross the membrane, and an equal amount of charge is transported in both directions (e.g. 1 Ca^{2+} from feed to concentrate for 2 Na^{+} from concentrate to feed). The same is true for anions in case AEM are used. The exchange across the membranes continues until the electrochemical potential difference across the membrane is equal to the Donnan potential of the membrane, and the solutions are in equilibrium. Due to a difference in electrochemical potential for different ionic species, this can drive transport of some species against their concentration gradient, resulting in high removal efficiencies.

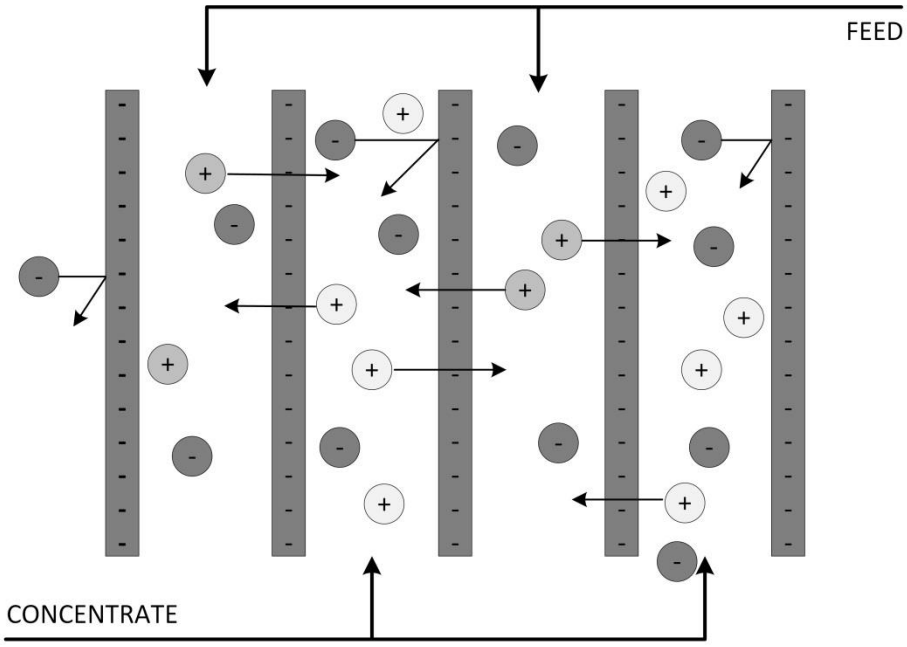

Figure 1.7 Schematic representation of the DD process.

Application of DD today is limited, mainly because of competition of the technology with conventional IEX. Indeed, DD resembles IEX in that ions of the same charge are exchanged between two solutions. In DD however, this exchange takes place continuously across an IEM. Contrary to in ED, only one type of IEM is used, depending on the charge of the target ion. As such, DD can be used for the removal of hardness [21], but it is more often applied for selective removal of certain metals, such as boron [22,23], fluoride [24–26] or arsenate [27]. Although the technology is in direct competition with IEX for several

applications, it has some major advantages; the process is continuous and no interruption for regeneration is needed and in some cases, a significant reduction in waste salt is achieved [28].

2 Hybrid treatment schemes

The water-energy nexus forces research to focus on trying to find sustainable, energy efficient technologies to cope with alternative water sources such as brackish water, wastewater and seawater. To overcome the challenges that come with these water sources (e.g. pollution, high salinity, …), a combination of different treatment techniques is often required. Such a combination of different treatment steps, of which the overall performance is better than any of the component parts, is called a hybrid system [29]. In such hybrid schemes, the strengths of the different technologies involved can be combined into the optimal treatment, both technologically and economically. Often, different pressure driven membrane techniques are combined with each other or with other unit processes (e.g. coagulation or activated carbon). With ion-exchange processes, different technologies can be integrated into one single process in continuous electrodeionisation, a combination of ED and IEX for the production of high-purity water [30–32]. However, the hybridisation of pressure driven and electrochemically driven processes (as the ones discussed before) is a more recent development.

In this thesis, focus will be on the hybridisation of ion-exchange technologies with RO. Although RO has many benefits and is currently the worldwide leading technology in terms of seawater desalination [33,34], it also has its drawbacks. RO recovery is often limited either by pressure limitations (seawater desalination typically is not carried out above 50% recovery, due to the high osmotic pressure of the concentrate) or by fouling and scaling. The latter can affect all RO systems, for example in wastewater reuse schemes, seawater desalination and water production from ground- or surface water, resulting in overall RO recoveries of typically 40-70%). This thus typically results in 30-60% of the incoming water to be discharged as waste (concentrate).

In practice, in order to obtain decent feed water recoveries, often anti-scalants are added to the feed water to avoid scaling at the concentrate side. However, these anti-scalants (which eventually end up in the concentrate) not only entail significant additional costs, but can also result in discharge issues. Classically, many anti-scalants contain phosphorus, which can entail operational issues by stimulating biological growth in the system, which in turn requires the addition of biocides [35]. Although phosphate-free anti-scalants are now

available, their cost and dosing can be significantly higher. Furthermore, energy requirements in RO are often high, in the range of 2-3 kWh/m³ for seawater desalination [33,36] and 1.5-1.7 kWh/m³ in applications aimed at (in)direct reuse of wastewater [37,38]. To overcome the limitations of RO in terms of recovery, fouling, chemical use and energy demand, some hybrid systems have already been suggested in recent literature. IEX resins for example can be used to treat the RO feed to avoid scaling (by the removal of multivalent cations by cationic IEX) and/or biofouling (by the removal of organics by anionic IEX) [7,39]. By replacing chloride ions in the feed by sulphate ions in IEX, the RO system can be replaced by a less energy-consuming NF system [40,41]. In seawater RO, energy demand can also be reduced by incorporating SGP techniques to harvest energy from the seawater and reduce the seawater energy demand prior to RO operations [42,43]. Details of the appropriate systems, their strengths and drawbacks, will be discussed with the separate chapters.

3 This thesis

This thesis explores the application of novel hybrid treatment schemes of ion exchange processes and pressure driven membranes, focussing both on improving resource (water and solute) recovery and on energy efficiency. Throughout the thesis, the evolution of ion-exchange technologies and their application in hybrid water treatment schemes is the main thread, going from novel arrangements of existing commercial technologies, over emerging applications, all the way to fundamental studies of solute-IEM interactions.

The thesis is divided into three distinct, but inter-related parts (as shown in Figure 1.8).

In **Part 1**, the combination of state-of-the-art IEX and the more novel DD process with RO for improved process water production are investigated and compared. **Chapter 2** compares the technological and economic viability of classic IEX softening, compared to DD for the removal of multivalent cations prior to RO to decrease scaling on the RO membranes and increase the RO recovery. In both cases, and this is the novelty of this research, the RO concentrate is recycled to the ion-exchange process as a high concentration source of monovalent cations. As IEX-RO showed the greatest promise based on these results, a pilot-test for the IEX-RO hybrid was conducted, as discussed in **Chapter 3**. This pilot study includes the recycling of the RO concentrate for the regeneration of the IEX column. The influence of the feed water composition, RO recovery and addition of NaCl to the RO concentrate on the IEX regeneration efficiency were investigated and the results were used for a more detailed economic analysis of the system.

Another application of RO is the production of potable water from seawater. Although RO is approaching the thermodynamic limit of desalination in terms of energy demand, this energy demand is still relatively high due to the typical RO configuration with a single feed pump. Furthermore, RO recovery is often limited by the osmotic pressure of the concentrate, resulting in the pressure reaching the physical limits of the installation. In **Part 2**, the hybridisation of RO for seawater desalination with emerging and new electrochemical membrane processes is therefore discussed, to assess if the energy efficiency and/or recovery for seawater desalination can be increased. **Chapter 4** introduces the possible hybridisation options of SGP (e.g. reverse electrodialysis) and osmotic dilution technologies with RO. In all mentioned technologies, the seawater is contacted in a controlled manner with a low salinity solution such as secondary treated wastewater, to produce energy and/or decrease the seawater salinity. A new technology, assisted reverse electrodialysis (ARED), is introduced to increase the economic viability of RED, by decreasing the required membrane area compared to RED. ARED operation and its potential in an ARED-RO hybrid are investigated in **Chapter 5**, which investigates transport behaviour in ARED in more detail.

In the hybrid processes discussed above, IEM are used to allow controlled seawater pre-desalination with secondary treated wastewater, whereby the wastewater is only used as a sink for ions (in the case of (A)RED), and no mass transfer occurs. However, the wastewater may contain contaminants, such as (trace) organics, which could be transferred to the seawater during pre-desalination. Transport behaviour of organic components in IEM has not yet been studied thoroughly. However, a fundamental understanding of this behaviour could result in the development of membranes capable of the selective separation of salts and organics. This would not only benefit the hybrid technologies discussed here, but could also benefit organics separation in for example membrane electrolysis (ME), and could also aid in selective separation of organics and salts, thus enabling more efficient treatment of complex industrial waste streams, which is currently often hampered by the joint presence of both organic and inorganic solutes. That is why **Part 3** of this thesis focuses on the fundamental interaction between organics and ion-exchange membranes and the resulting transport of the organics through these IEM. In **Chapter 6**, the influence of operational parameters, such as the presence and magnitude of an applied electrical current, on the transport of organics is investigated. Trace organic contaminants (TOrCs) are used as model organic components in a pure NaCl matrix. The effect of changes in the matrix, such as the presence of $MgCl_2$ and Na_2SO_4 instead of NaCl, on the transport of organics is investigated in **Chapter 7.** Furthermore, in many applications, the organics and salts can be present in different

compartments, for example in the controlled mixing of seawater with impaired water as discussed before. The influence of the transport direction of the organics relative to the salt transport is therefore investigated as well. The study concludes with an investigation on the behaviour of organic acids, another group of organics that is frequently encountered in ion-exchange processes (e.g. ME). By investigating and determining the transport characteristics of organic compounds, the parameters that influence a selective separation between inorganics and organics can be identified.

Chapter 8 discusses the overall viability and applicability of hybrids with ion-exchange technologies based on the different research chapters. An outlook with respect to future applications and remaining research questions is provided.

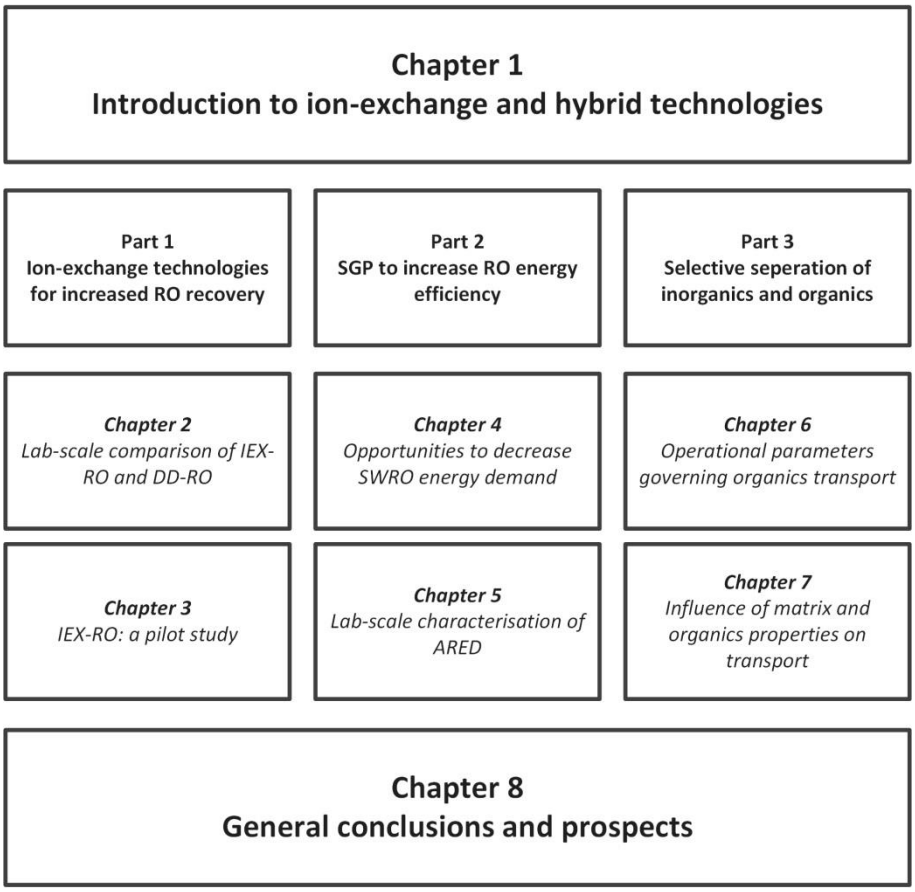

Figure 1.8 Overview and interconnection of the different thesis chapters.

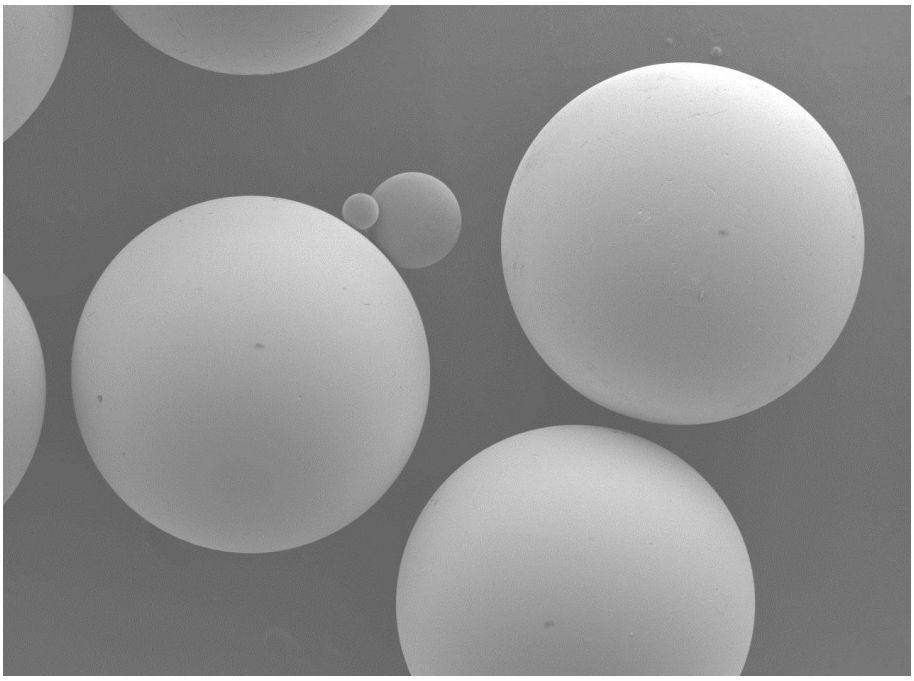

Part 1: Classic ion-exchange technologies for an increased RO water recovery

Picture: SEM of ion-exchange resin beads (100X magnificantion)

Chapter 2: Increasing RO efficiency by chemical-free ion-exchange and Donnan dialysis: Principles and practical implications

This chapter has been published as

Vanoppen, M., Stoffels, G., Demuytere, C., Bleyaert, W., Verliefde, A.R.D. Increasing RO efficiency by chemical-free ion-exchange and Donnan dialysis: Principles and practical implications. *Water Res.* **2015**, *80*, 59-70.

1. Introduction

Industrial water uptake constitutes around 20% of the total worldwide water withdrawal [3]. Due to increasing pollution and decline of fresh water resources, in combination with higher water quality demands in industry, alternative water sources are increasingly investigated. These alternative sources (e.g. secondary treated wastewater, industrial wastewater, …) often require extensive treatment to meet the stringent quality standards for drinking water or process water purposes. Reverse osmosis (RO) is one such treatment option that is used in a wide range of applications where a high water quality is desired. RO is for example of interest for the reclamation of water in industrial applications [44–46] and for the reuse of (secondary treated) municipal wastewater [38,47,48]. However, due to the presence of foulants and scale-forming components, the attainable water recovery in RO is often limited, resulting in high pre-treatment costs and high discharge volumes. New approaches to increase the attainable recovery, resulting in lower discharge volumes and higher water reuse efficiencies, are thus desired.

Ion exchange (IEX), a common and relatively cheap technology for the removal of unwanted ions from water (cations leading to water hardness, organics, boron, …), is sometimes coupled with reverse osmosis (RO) or nanofiltration (NF) for the production of drinking and/or process water [7,49,50]. Mostly, IEX is used to post-treat the water for removal of remaining trace elements, upon production of ultrapure water. IEX can also be used in the pre-treatment of the RO feed water. In this case, the reason is mainly to avoid either organic fouling (when using anion exchange resins), or scaling (when using cation exchange resins) of the RO membranes [33,51–54]. Recently, Indarawis and Boyer (2013) have shown indeed that combining anion- and cation exchange in RO pre-treatment results in a significantly improved flux in subsequent RO operations. Sarkar and SenGupta (2008) and Hilal et al. (2015) suggested a more advanced use of ion exchange as RO pre-treatment whereby an ion exchange method was implemented replacing chloride ions in the feed by sulphate ions to make the application of less energy consuming NF-membranes possible for the desalination of seawater and brackish water. Since the resulting NF concentrate was then high in sulphate, this concentrate could subsequently be used for the regeneration of the IEX after saturation with chloride [40,41]. A pilot-scale test confirmed the performance of the IEX-NF system [55]. However, such a system is mainly of interest for seawater applications, where the attainable water recovery is limited by the physical pressure limitations of the RO system. Due to the high osmotic pressure of seawater and a limitation of 60-80 bars in the RO equipment, the recovery is limited to about 50%. At this recovery, the risk of scaling

(due to for example $MgSO_4$ or $CaSO_4$) is small because of the limited increase in concentration in the RO concentrate. In industrial applications, the feed water osmotic pressure is lower, and thus the RO recovery is no longer limited by the pressure needed, but by the risk of scaling on the membrane.

In most IEX applications, the spent regenerant contains of a high concentration of the component used for regeneration (mostly NaCl in cation exchange for softening purposes, HCl in cation exchange for demineralisation (or decarbonation) and NaOH or NaCl in anion exchange). The spent regenerant also contains lower concentrations of the originally removed components (cations such as Ca^{2+} and Mg^{2+} or anions such as Cl^-, PO_4^{3-}, organics, …). Treatment and/or disposal of these high salinity streams (up to 10 wt.% of salts) is often a challenge, especially in inland regions. Reuse of these streams could therefore result in significant savings, both in disposal costs as well as in chemical costs. McAdam and Judd (2008) studied an anion exchange system for removal of organics, and tried to device methods to recycle the regenerant. By means of biological treatment, it was attempted to reduce the organic load in the regenerant, to make reuse feasible [56]. Jacob et al. (2005) on the other hand, studied reuse of the NaCl regenerant of a cation exchanger used for softening [57]. They suggested the precipitation of the multivalent cations with sodium carbonate to replenish the sodium in the regenerant and remove the multivalent ions before reuse. Although promising, these options require the implementation of (several) additional technologies for the treatment of the regenerant, reducing the economic attractiveness.

A very simple and elegant way to decrease chemical usage for regeneration of IEX resins, is an option which has been largely overlooked in recent literature. This option is particularly useful in cases where RO is used to produce good quality water, with a resulting RO concentrate that needs to be disposed of. In typical industrial RO applications for process water production on low- to medium-salinity water, the water recovery of the RO is limited by the risk of precipitation of sparingly soluble salts (i.e., scaling) in the RO. As stated above, cationic IEX pre-treatment can be an option here to increase RO recovery. Since multivalent cations such as Ca^{2+}, Ba^{2+}, Fe^{2+}/Fe^{3+} and Mg^{2+} are largely replaced by Na^+ in the cationic IEX, the RO recovery can be increased, since Na^+ salts are typically more soluble. As the RO recovery is increased, an RO concentrate is formed with a higher concentration of Na^+ (and other monovalent cations such as K^+). In this case, it is interesting to study whether the RO concentrate can be used to recharge the cationic IEX placed before the RO. This would provide a chemical-free possibility to increase RO recovery, with a useful application of the

RO concentrate before discharge, without the need for additional technologies. This envisioned hybrid process is shown in Figure 2.1.

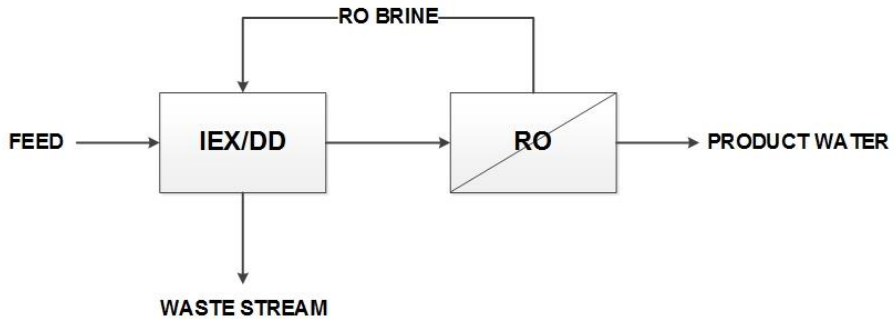

Figure 2.1 Schematic view of the envisioned hybrid IEX/DD-RO process.

An alternative, less developed ion exchange technique is Donnan dialysis. Here, the ion exchange is not reached by selective resins, but rather by CEM: a feed solution, containing the ions that should be removed (e.g. Ca^{2+}) is fed on one side of the ion exchange membrane, while a "concentrate" solution, containing another electrolyte (e.g. Na^{+}) at a relatively higher concentration compared to the feed solution, is fed on the other side. Because of the concentration difference between the two solutions, there is a net driving force for calcium transport from the feed to the concentrate and for sodium from the concentrate to the feed. Since the anions present can't move across the CEM, for every calcium molecule, two sodium molecules move from the concentrate to the feed to maintain electroneutrality. However, when the calcium concentration on both sides of the membrane is equal, transport will still carry on, due to the higher electrochemical potential of sodium compared to calcium, causing calcium to transport against its concentration gradient to allow sodium transport. Transport across the membrane continues until the electrochemical potential difference across the membrane is equal to the Donnan potential of the membrane. At this point, Donnan equilibrium across the membrane is reached and the solutions are in equilibrium. No more transport will thus occur. The potential difference (E) across the membrane for a species i can be described by the following equation (Davis 2000):

$$E = \frac{R_g \cdot T}{F} \cdot \ln\left(\frac{a_{i,C}}{a_{i,F}}\right)^{1/z_i} \tag{2.1}$$

With R the universal gas constant (J/(mol.K)), T the absolute temperature (K), F the Faraday constant (C/mol), $a_{i,C}$ and $a_{i,F}$ the activity coefficient of electrolyte i in the concentrate and feed solution respectively and z_i the ionic valence of electrolyte i.

The main advantage of DD over IEX is that the use of membranes provides a continuous ion-exchange process. In DD, the concentrated solution flows along one side of the membranes, while the feed solution flows on the other side, providing a driving force for ion exchange, as shown in Figure 2.2. In other words, the RO concentrate could be continuously recycled to the DD unit, without the need for a process interruption. This means that the investment cost for IEX could be higher, since an additional resin column is needed to take over operations when regeneration of the other column is being carried out. Research into DD has thus far mainly focussed on the removal of unwanted ions from water, such as fluoride [24–26], borate [22,23], calcium and magnesium [21] and many others [58]. In hybrid processes, Donnan dialysis has mainly been investigated in conjunction with electrodialysis (ED) [59–61]. Removing the multivalent ions from the ED feed water has two important advantages. First of all, the limiting current density can be increased, resulting in a higher salt flux and thus a lower required membrane area in ED. Secondly, because of the lower resistance of the solution after DD (as monovalent ions are generally more mobile than multivalent ions), the energy demand is decreased as well. A similar use of DD could of course be foreseen in RO applications.

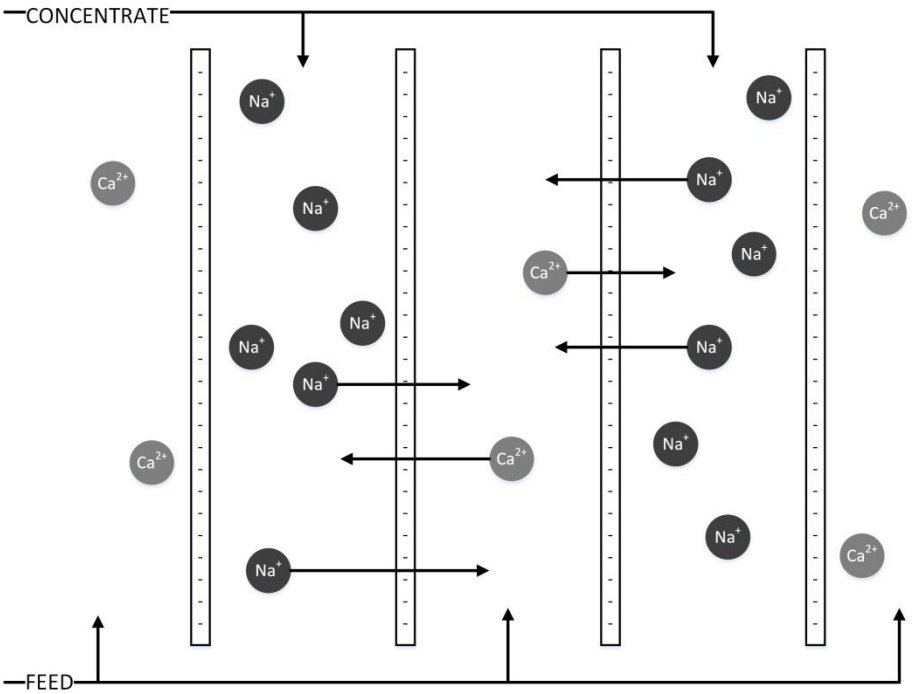

Figure 2.2 Schematic representation of the DD set-up, where multivalent cations (e.g. calcium) from the feed are exchanged for monovalent cations (e.g. sodium) for the concentrate over negatively charged cation exchange membranes.

This kind of hybrid process could be interesting for all kinds of applications where RO recovery is limited by scaling, such as seawater desalination and process water production. In this study, both IEX and DD were investigated as a pre-treatment step before RO in industrial applications. Two practical RO-processes, whereby recovery was limited by scaling, were investigated: 1) the desalination of tap water for steam production (a common application of RO in small-to-medium sized enterprises) and 2) the desalination of biologically treated industrial wastewater (a common application of RO in industrial water reuse schemes; in this typical case, the wastewater originated from a potato-processing company). In both case studies, the IEX and DD pre-treatment allowed to increase RO recovery compared to the reference case whereby no pre-treatment was implemented. In both cases the potential of using the RO concentrate to regenerate the IEX or provide a "concentrate" solution for the DD was studied. DD and IEX and the possibility to reuse the RO concentrate to regenerate, were investigated and compared for the two case study streams (tapwater and wastewater RO), based on technological and economical applicability.

2 Theoretical considerations

The goal of this study is not to provide a detailed theoretical background on the exact mechanisms of IEX and DD. However, since DD is a less known process compared to IEX, some theoretical considerations on DD applicable to this research will be presented here.

Donnan dialysis is a technique which is based on the establishment of Donnan equilibrium across an IEM. When two salt solutions of different composition are placed on different sides of an IEM, a flow of ions will occur until this Donnan equilibrium is reached. The basic principles have already been discussed in literature [20,62], but for clarity to the reader, we will briefly repeat them here. In this theoretical consideration, the stream from which we want to remove certain ions is called the 'feed', while the stream providing ions for exchange is called the 'concentrate', because of its higher concentration. More specifically in this research, we look into the ion exchange across a CEM for a binary mixture of salts. We consider ions i and j, at the left and right side of the membrane respectively. For Donnan equilibrium to be reached, the electrochemical potential for both species, as expressed by Equation 2.1, needs to be equal, as shown in Equation 2.2. Here, the activity is assumed to be equal to the concentration of the species.

$$\left(\frac{CE_{i,F}}{CE_{i,C}}\right)^{\frac{1}{z_i}} = \left(\frac{CE_{j,F}}{CE_{j,C}}\right)^{\frac{1}{z_j}} \quad (2.2)$$

Here, CE is the equilibrium concentration (mol/l) and z the valence (-) of the ions in the feed (F) and concentrate (C). This equation, however, does not take into account the potential volume difference between both streams. For example, consider two streams with different volumes, the feed containing mainly a bivalent cation i (e.g. Ca^{2+}) and the concentrate containing mainly a monovalent cation j (e.g. Na^{+}). Defining x as the amount of i (in moles) that needs to be transported across the membrane (from the feed to the concentrate) to obtain the electrochemical equilibrium, Equation 2.2 can be adapted to calculate the total amount of transport of both species (x moles for divalent species i, 2x moles for monovalent moles for species j) [20]:

$$\left(\frac{CI_{i,F} - \frac{x}{V_F}}{CI_{i,C} + \frac{x}{V_F}}\right)^{\frac{1}{2}} = \frac{CI_{j,F} + \frac{2x}{V_C}}{CI_{j,C} - \frac{2x}{V_C}} \tag{2.3}$$

With CI the initial concentrations of both species and V_F and V_C the initial volume of the feed and concentrate respectively. Solving for x results in the following third order polynomial:

$$\begin{aligned} -\frac{8}{V_F \cdot V_C^2} \cdot x^3 + \left(\frac{4 \cdot CI_{i,F} - 4 \cdot CI_{i,C}}{V_C^2} + \frac{4 \cdot CI_{j,C} - 4 \cdot CI_{j,F}}{V_C \cdot V_F}\right) \cdot x^2 \\ - \left(\frac{4 \cdot CI_{i,F} \cdot C_{j,C} + 4 \cdot CI_{i,C} \cdot CI_{j,F}}{V_C} + \frac{CI_{j,C}^2 + CI_{j,F}^2}{V_F}\right) \cdot x + CI_{i,F} \cdot C_{j,C}^2 \\ + CI_{i,C} \cdot C_{j,F}^2 = 0 \end{aligned} \tag{2.4}$$

Equation 2.4 can be applied to the DD-RO process, where the RO concentrate is recycled as the DD concentrate to pre-treat the RO feed. In Figure 2.3, the removal efficiency of calcium from the feed is presented for different ratios of sodium to calcium in the feed by solving Equation 2.4 numerically for x in Python 2.7 using the SymPy package [63]. In the ideal scenario, the theoretical removal of calcium from the feed is calculated neglecting the concentration of sodium in the feed and the concentration of calcium in the concentrate. In this case, the removal efficiency in DD is independent of the RO recovery. In practice, the calcium removal will be lower due to several reasons; (1) the feed contains sodium and (2) the concentrate contains calcium. The maximum amount of calcium that can be removed

from the feed can be estimated by taking into account the sodium concentration in the concentrate, which can be predicted based on the RO recovery (assuming total rejection of ions by RO). The resulting removal efficiencies are also shown in Figure 2.3. Because of the potential presence of calcium in the concentrate (neglected in this approach), the removal efficiency will be lower in practice. From this figure, it is clear that the ideal case is approximated more closely at higher RO recoveries, because of the higher sodium concentration in the concentrate in these cases. When the sodium/calcium ratio in the feed drops below 5, especially at lower RO recoveries, the calcium removal drops rapidly because of the decreasing sodium concentration in the concentrate.

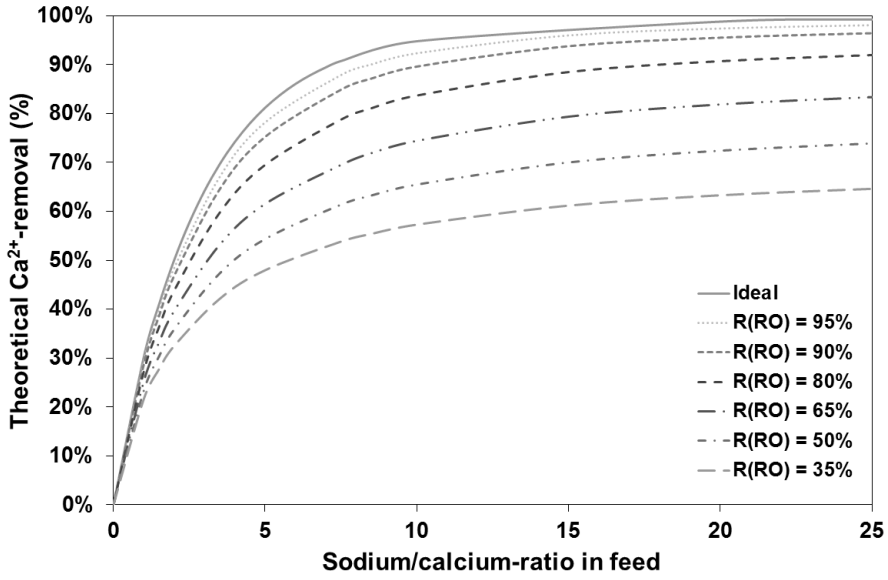

Figure 2.3 Theoretical removal of calcium by Donnan dialysis at different sodium/calcium ratios in the feed and different subsequent RO recoveries. In the ideal case, the concentration of sodium in the feed and calcium in the concentrate is neglected.

3 Materials and methods

3.1 Feed water samples

Two different water types were investigated in this study. On the one hand, tap water from the city of Ghent (Belgium) was used. This tap water is constant in composition, and is used by many companies to produce demineralised water using RO. On the other hand, biologically treated wastewater from a potato-processing factory was used. These waters will be referred to as 'tap water' and 'wastewater' in the remainder of the study. The average composition of both feed waters is given in Table 2.1.

Table 2.1 Average composition of used tap water and wastewater.

	Wastewater (mg/l)	Tap water (mg/l)
Ca^{2+}	17.6	78.9
Na^{+}	681.0	25.0
K^{+}	1 416.0	1.4
Mg^{2+}	53.2	7.9
CO_3^{2-}	12.9	0.9
HCO_3^{-}	1 383.0	197.1
NO_3^{-}	38.1	15.3
Cl^{-}	1 809.0	42.4
F^{-}	0.5	0.3
PO_4^{3-}	15	-
SO_4^{2-}	109.5	68.4
SiO_2	16.5	5.9
H_3BO_3	-	0.2

The pH of the tap water is 8.6, while that of the wastewater is slightly lower at 7.7. Both are used in industry as an RO feed. The flow of the wastewater stream to RO is about 60 m^3/h in the case considered, while that for tap water is 25 m^3/h.

3.2 Ion-exchange

For the ion-exchange experiments, the cation exchange resin Marathon C (Dow, USA) was used. The properties of this resin as provided by the manufacturer are given in Table 2.2. A glass column with a diameter of 2.6 cm was operated as IEX column for all experiments. For the tap water experiments, 100 ml of cation resin was used and the feed and regenerant were both fed in a downflow configuration. Upflow regeneration was tested but proved to be only marginally better than the downflow configuration, so the downflow configuration was further used due to practical considerations. Due to clogging problems as a result of the high suspended solids load in preliminary experiments, the wastewater experiments and regenerations were conducted in an upflow configuration. 50 ml of the cation resin was used in these experiments. The resin was used in the Na-form initially.

First of all, preliminary experiments were conducted to evaluate the regeneration capacity of the resin using NaCl versus KCl solutions, since the RO concentrate could contain high concentrations of both Na^+ and K^+ (see Table 2.1). Traditionally, IEX resins for softening are regenerated using at least 2 bed volumes of a 80-120 g/l NaCl solution [64]. For this experiment, 10 bed volumes (to ensure full saturation of the resin) of a 100 g/l NaCl solution

and equimolar KCl solution (i.e. 1.7M or 128 g/l KCl) were used for the regeneration of the 50 ml cation resin discussed above. The regeneration with both solutions was carried out twice and a 2 g/l $CaCl_2$ solution was used for the resin depletion.

Table 2.2 Properties of used ion-exchange resin.

Property		Dowex Marathon C
Exchange capacity	eq/l	2.0
Mean particle size	µm	585 ± 50
Matrix and porosity	-	Styrene-divinyl benzene copolymer, gel
Functional group	-	Sulfonate

In all IEX experiments, a flow rate of 6 SV (bed volumes per hours or space velocity) was applied during the regeneration phase, after which the resins were washed with deionised (DI) water. This washing consisted of a slow rinse with 2.5 times the bed volume in DI water (at 6 SV) and a fast rinse with 10 times the bed volume in DI water (21 SV). For the depletion of the resins, a flow rate of 21 SV was applied. The depletion was carried out until Ca^{2+} was detected in the effluent (breakthrough point, Ca^{2+}-detection limit of 0.2 mg/l). After depletion, before the next cycle, the resin was backwashed with DI water for 10 minutes at a flow rate of 21 SV. Based on the treated volume of feed solution, the capacity of the resin (eq/l) can be determined with the following equation:

$$\text{Resin capacity} = \frac{2 \cdot V_{treated} \cdot C_{Ca^{2+}}}{V_{resin}} \tag{2.5}$$

With $V_{treated}$ the feed volume treated before Ca^{2+}-breakthrough (l), C_{Ca2+} the calcium concentration in the feed (mol/l) and V_{resin} the volume of resin used. Calcium was chosen as an indicator here, since calcium is of major importance for scaling in RO (e.g., in the formation of $CaCO_3$ and $Ca_3(PO_4)_2$). It must be noted however that the IEX capacity for specific waters depends not only on the calcium concentration but also on the concentration of other cations such as magnesium, barium, iron, strontium,…

To assess the effect of using the RO concentrate as a regenerant on the resin capacity, several depletion-regeneration cycles were carried out for both the tap water and wastewater. The concentrate volume used for regeneration depends on the RO recovery that can be reached with the treated streams. For the study on IEX capacity, it was determined that the attainable RO recovery when removing all multivalent cations is 95%. This recovery is based

on the detailed prediction of the RO system behaviour by the ROSA and Genesys® software discussed in 3.4. The total volume of concentrate used was thus 20 times lower than the volume treated by IEX before Ca^{2+}-breakthrough occurred. The composition of the model concentrate used was simulated in our lab based on the composition of the respective feed streams and will be discussed with the results.

3.3 Donnan dialysis

For the Donnan dialysis experiments, four membranes with a total active area of 256 cm^2 were used to separate the feed and the concentrate solution (the concentrate solution being the high concentration salt solution which is produced as RO concentrate). This set-up is similar to the one shown in Figure 2.2.

The membranes used were Fujifilm II (Fujifilm, the Netherlands) CEM. The properties of the membranes, as given by the manufacturer, are given in Table 2.3. The experiments were carried out in batch, with the volume of the concentrate depending on the simulated RO recovery. This batch process allows for the estimation of the needed membrane area in a full-scale, continuous process, as implemented in the economic analysis (section 4.5). However, a full-scale DD system would be more efficient, as counter-flow would be implemented (assuring a maximal driving force), effectively decreasing the required membrane area. As discussed above, it is assumed for the experiments (based on initial recovery calculations) that the attainable RO recovery when removing all multivalent cations is 95%, resulting in 5% concentrate production. In other words, in Donnan dialysis, the volume of the concentrate was 5% of the volume of the feed. In practice, a volume of 2l was used for the feed and thus a volume of 0.1l for the concentrate solution. Both were circulated in co-current by a peristaltic pump (Masterflex 06402-17, Cole-Parmer, USA) at a flow rate of 100 ml/min. Experiments were run until no significant change in calcium concentration occurred anymore and thus equilibrium was reached. From this, the exchange rate of ions through the IEM could be calculated, thus allowing for a calculation of required CEM surface in practical applications.

Table 2.3 Properties of ion-exchange membranes used in Donnan dialysis experiments.

Properties		
Membrane type	-	Homogeneous
Thickness	μm	160
Permselectivity	%	96
Electrical resistance	Ω.cm²	6.1
Functional group	-	Sulfonate

3.4 Reverse osmosis

The effect of the suggested pre-treatments (IEX/DD) on RO-operation was modelled using the ROSA 9.1 software (Dow, USA) supplemented with the Genesys® software (Genesys International, UK). Both software packages are currently considered as the industrial reference standard for RO design. ROSA was developed by The Dow Chemical Company specifically for the modelling of reverse osmosis systems based on feed water composition, pre-treatment options and system configuration. The results obtained by the software were verified and supplemented by the Genesys® modelling software. This software allows a detailed prediction of the saturation degrees vs. the solubility limit of the salts present. This way, not only the attainable RO recovery could be predicted, but also the components limiting this recovery could be identified. In the modelling, the application of anti-scalants was avoided. Only pH changes were included and mentioned in the discussion where necessary. Any adaptations to the RO system, needed to accommodate higher pressures associated with higher recoveries, were modelled through the ROSA software.

3.4.1 RO concentrate preparation

As the small scale of the IEX and DD experiments did not allow for any RO experiments, the RO concentrate used was simulated. The composition of the simulated concentrate depends on the attainable RO recovery, as simulated by the software, discussed above. In both the tap water and wastewater case, a recovery of 95% can be reached theoretically. Consequently, the concentration of ions in the simulated concentrate is 20 times higher than in the feed. Complete exchange of Ca^{2+} and Mg^{2+} for Na^{+} were assumed and the resulting simulated concentrate was prepared using NaCl and KCl.

3.5 Analytical methods

All relevant cation concentrations (Na^{+}, K^{+}, Ca^{2+} and Mg^{2+}) were determined using inductively coupled plasma with optical emission spectroscopy (ICP-OES, Varian VISTA-

MPX, Palo Alto, VS). The standards for the calibration curve and the samples were acidified with 1% HNO_3.

4 Results and discussion

4.1 Preliminary experiments on resin capacity when regenerating with K^+

Since both feed water samples used for the testing contain not only Na^+, but also (some) K^+, the RO concentrate after IEX and DD is expected to contain both cations. However, regeneration of strong acidic ion-exchange resins for water softening is typically carried out with a pure NaCl solution. Therefore, some preliminary experiments were carried out to compare the effect of potassium and sodium on the regeneration capacity of a strong acid cation IEX resin. The results (Figure 2.4) show that there is no significant difference in capacity when using NaCl or KCl as the regenerating solution. It is thus expected that any effects on resin capacity observed during the IEX tests, where the RO concentrate is used for regeneration, are attributable solely to the concentration and/or volume of the regenerating solution and not to the exact monovalent composition.

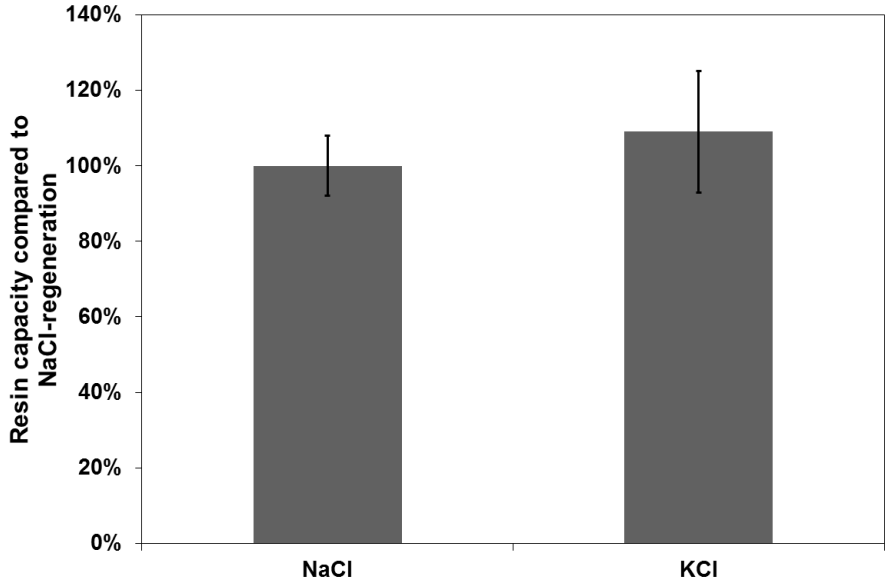

Figure 2.4 Measured capacity after regeneration with a classical 100 g/l NaCl solution and a 128 g/l KCl solution (both 1.7 M) calculated from two consecutive regenerations for both solutions. All capacities are relative to the capacity after classical NaCl regeneration, which was rescaled to 100%.

4.2 Wastewater

Besides cations, the wastewater stream also contains large amounts of phosphate as anion, increasing the risk of scaling in IEX or DD if this phosphate ends up in the regenerate/concentrate. In IEX, the calcium removed from the resin during regeneration

with the RO concentrate could potentially form $Ca_3(PO_4)_2$ with phosphate retained by the RO membrane. However, IEX regeneration is usually carried out in counter-flow and additional flushing is performed, effectively removing any precipitates formed in the resin [65]. This was also confirmed during experiments shown in Appendix A. In Donnan dialysis, phosphate retained in the concentrate during RO might form $Ca_3(PO_4)_2$ with the calcium transported from the wastewater. Thus, phosphate removal in an additional pre-treatment step, by anionic IEX or DD with anion-exchange membranes, was tested but proved to be ineffective due to the presence of negatively charged organics in the feed stream (Appendix A), which were exchanged more specifically than phosphate. Another option would be to treat the RO concentrate in an additional precipitation step before entering the DD unit, which could remove not only phosphate but other anions such as carbonate as well. This should however be looked into further on a more practical scale.

When treating this stream with cationic IEX, Ca^{2+} and Mg^{2+} are successfully removed. At calcium breakthrough (0.2 mg/l Ca^{2+}), the IEX effluent contained an average magnesium concentration of 11.8 mg/l. After calcium breakthrough was detected, the IEX resin was regenerated with the simulated RO concentrate as discussed above. Because of the high ratio of monovalent to multivalent cations of about 25 in the wastewater (monovalent:multivalent cation ratio or MMR, see Table 2.1), the simulated RO concentrate contains enough sodium and potassium for the regeneration to be successful, as shown in Figure 2.5. The resin capacity shows no significant deviation from the original capacity after two consecutive regenerations. Although the simulated concentrate only contained 1.5 eq/l (compared to 1.7 eq/l for a classic regeneration solution), the total volume was 9 BV (compared to about 2 BV used for a classic regeneration), ensuring an efficient regeneration of the resin.

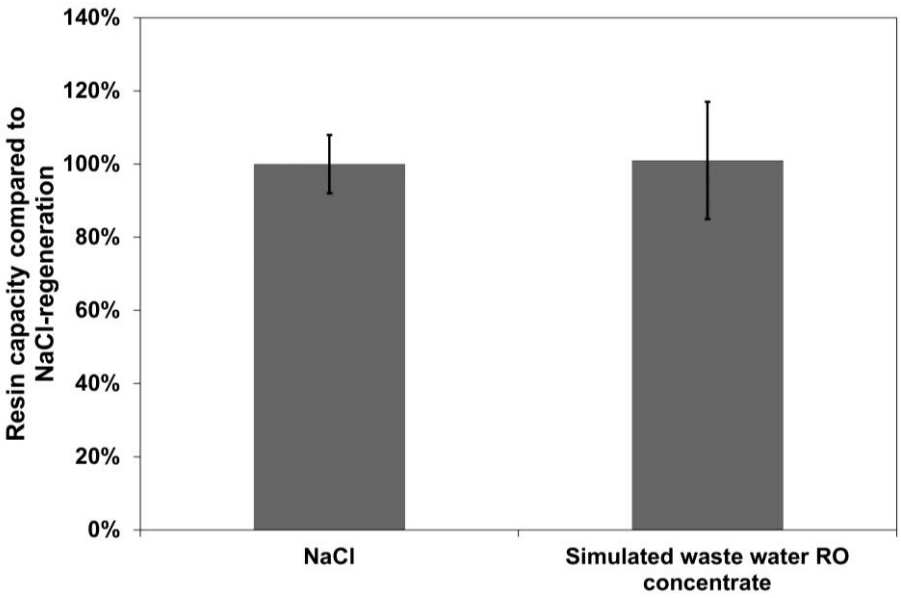

Figure 2.5 Measured resin capacity after regeneration with a simulated reverse osmosis concentrate after ion-exchange treatment of the wastewater, calculated from two consecutive regenerations for both solutions. All capacities are relative to the capacity after classic NaCl regeneration, which was rescaled to 100%.

The results for DD are shown in Figure 2.6. Here, the same simulated RO concentrate was used as the DD concentrate, at a volume 20 times lower than the feed stream (95% RO recovery). The removal efficiency of Ca^{2+} and Mg^{2+} after 6 hours is 77% and 70% respectively, much lower than what is obtained in IEX. This results in a calcium concentration of 4.0 mg/l and a magnesium concentration of 15.9 mg/l in the wastewater after DD treatment with a resulting flux of 19 mmol/(m².h) for the multivalent cations. It has to be mentioned that after about 6 hours, the removal levels off, but no real equilibrium is reached yet.

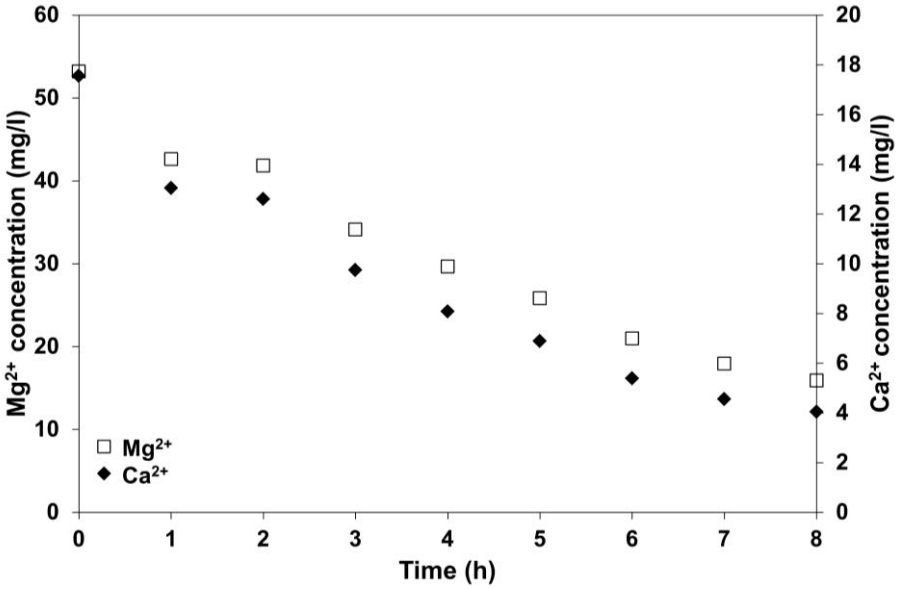

Figure 2.6 Calcium and magnesium concentration over time during Donnan dialysis treatment of the wastewater.

In theory, based on Equation 2.4, the removal efficiency for multivalent cations in this case should be around 98%, when no multivalent cations are present in the concentrate. The lower removal efficiency observed can be attributed to several effects, such as the non-ideality of the membranes (permselectivity <1, allowing some anions to pass), the non-optimised system design and operations, etc. Because the removal of multivalent cations in DD in this case is not optimal, some calcium and magnesium will end up in the RO concentrate in practice. This will have an effect on the removal of multivalent cations from the feed, decreasing the overall removal efficiency. This effect can again be theoretically determined using Equation 2.4, now taking into account the presence of multivalent cations in the concentrate and the expected RO recovery in practice (Section 4.4). Because of the high concentrations of sodium and potassium in the feed compared to the calcium and magnesium concentrations, the further decrease in removal efficiency is expected to be less than 5%, resulting in an only slightly higher calcium and magnesium concentration in the RO feed after DD in practice. This small decrease is not expected to have an effect on the achievable RO recovery, which was confirmed by the ROSA and Genesys® software. Furthermore, the treated wastewater contains some organics (11 mg/l of total organic carbon) which might result in membrane and resin fouling. However, during the short-term lab experiments, no organic fouling was observed and since organics are generally negatively charged, no significant influence on the cationic resins and cation-exchange membranes is expected.

These results show that when a sufficiently high MMR is achieved in the feed water, the IEX and DD processes operated with the RO concentrate are very efficient. Since this ratio is the

most important parameter determining the efficiency, the pre-treatment and concentrate recycling could also be considered in other applications, such as seawater or brackish water desalination with RO.

4.3 Tap water

The hardness of the tap water used is relatively high, with a calcium concentration of about 80 mg/l and a magnesium concentration of 8 mg/l. IEX was able to efficiently remove the calcium and magnesium present, resulting in an IEX effluent concentration of around 0.2 mg/l for both cations. The sodium and potassium concentrations of the sample were, however, low in comparison to the initial multivalent cation concentration (MMR of 0.5). Because of this low MMR, regeneration of the IEX resin with the simulated concentrate results in a significantly decreased IEX capacity, as shown in Figure 2.7.

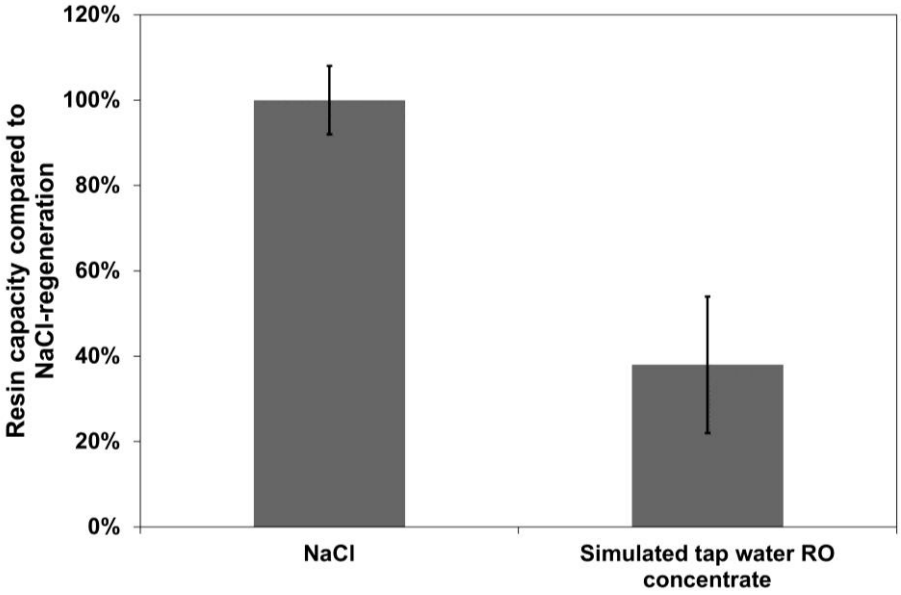

Figure 2.7 Measured resin capacity after regeneration with a simulated reverse osmosis concentrate after ion-exchange treatment of the tap water, calculated from two consecutive regenerations for both solutions. All capacities are relative to the capacity after classic NaCl regeneration, which was rescaled to 100%.

The tap water stream contains about double the amount of multivalent cations compared to the monovalent cations, resulting in a concentrate that contains too little sodium and potassium to create sufficient driving force to efficiently remove all calcium and magnesium from the resin during regeneration. To overcome this issue, an experiment was carried out whereby NaCl was added to the simulated concentrate in an attempt to increase the resulting resin capacity after regeneration. The measured capacity after regeneration as a function of the different amounts of NaCl added, in comparison with the initial capacity of the resin (obtained by regenerating with 100 g/l NaCl), is shown in Figure 2.8. To determine the total

NaCl concentration needed to achieve 100% resin regeneration, a second order polynomial (chosen because of the relatively narrow range of data-points) was fitted to the data. 100% was included as the maximum for the resulting curve, which has a correlation coefficient of 0.99. Extrapolating the resulting curve to 100% resin capacity results in a total NaCl concentration of 35.3 g/l needed to achieve full regeneration. This means that about 28.4 g/l NaCl would have to be added to the RO concentrate before regeneration. However, since the volume of the simulated concentrate in this case is about 20 bed volumes, this would mean adding up to 568 g NaCl per liter resin, while a classic regeneration requires only about 200 g NaCl per liter resin. From an ecological point of view, a classic regeneration would therefore be more interesting in this case. However, adding the traditional amount of NaCl (100 g/l) to a part of the produced RO concentrate could mitigate the use of fresh water and reduce consumption of NaCl compared to traditional regeneration. The efficiency of this regeneration would have to be investigated further.

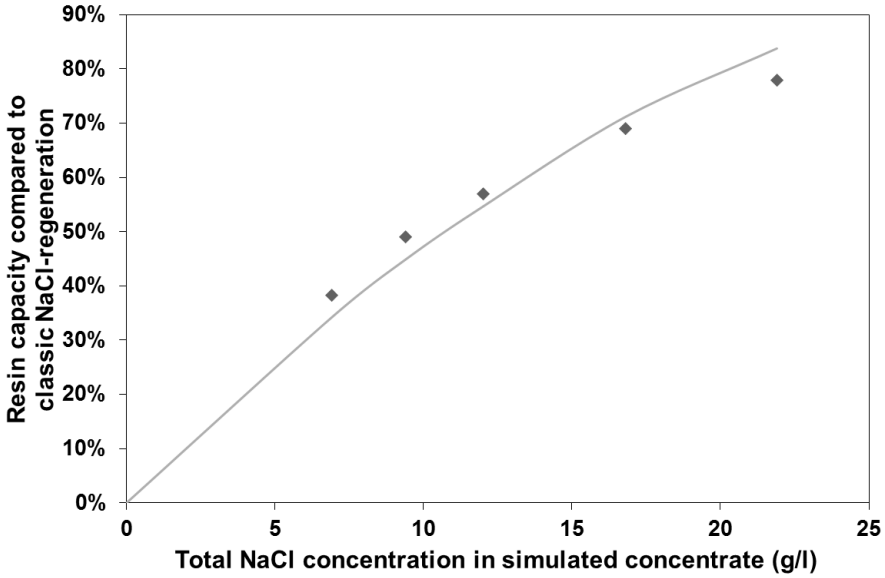

Figure 2.8 Measured resin capacity (compared to the capacity with a classic 100 g/l NaCl regeneration) and fitted second order regression ($R^2 = 0.99$). For this test, NaCl was added to the simulated RO concentrate to increase the resulting resin capacity, resulting in total NaCl concentrations as shown on the x-axis.

Donnan dialysis achieved 79% removal of calcium and 71% removal of magnesium when the same simulated RO concentrate as discussed for IEX was used as the DD-concentrate solution, without addition of NaCl. This results in an RO feed with relatively high calcium and magnesium concentrations of 17 and 2.6 mg/l respectively with a total multivalent cation flux of 18 mmol/m²/h. The evolution of the calcium and magnesium concentration over time in the batch Donnan dialysis experiment (Figure 2.9) shows a trend towards

levelling of both cation concentrations (i.e., reaching equilibrium) after about 5.5 hours. However, theoretically, the low MMR in the tap water stream should only allow for about 30% removal of the multivalent cations. Since the removal discussed above is based on the feed water concentration, it is possible that some of the calcium and magnesium precipitated on the membrane. Indeed, the concentration of both cations measured in the concentrate is much lower than would be expected from the decrease in the feed stream. Because of the higher concentration of magnesium and calcium in respect to the sodium and potassium concentrations in the feed, it is also possible that some of the multivalent cations are bound to the functional groups of the membrane, replacing the sodium initially present. Both phenomena can (partially) explain the impossibly high removal efficiency observed.

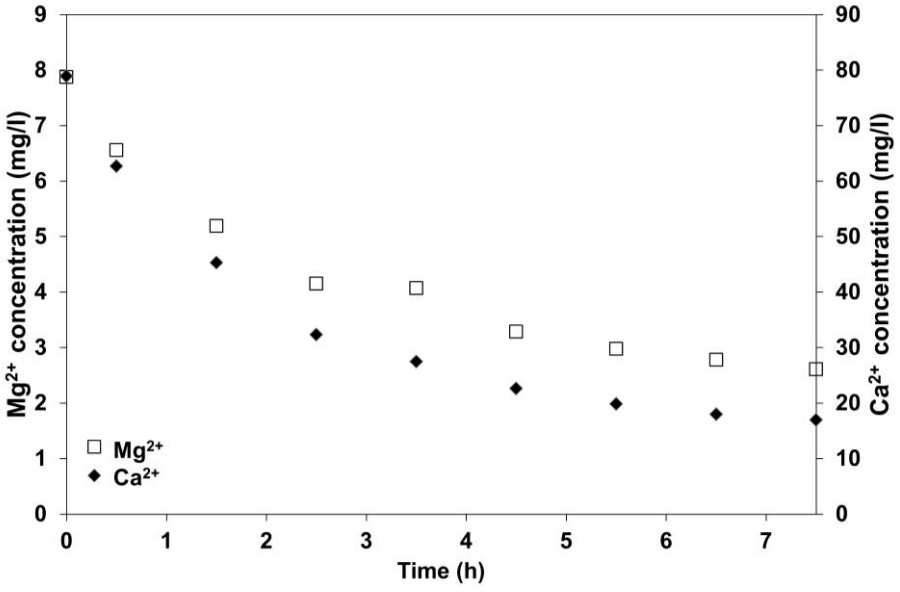

Figure 2.9 Calcium and magnesium concentration over time during the Donnan dialysis treatment of tap water.

Because of the low theoretical removal in DD, Equation 2.3 was used to determine what the required NaCl-concentration would need to be in the DD concentrate to achieve the same calcium and magnesium removal in DD as in IEX. For this calculation, the removal of scale-prone anions from the concentrate was assumed. A total NaCl concentration of 29.4 g/l would be needed, which means 29.0 g/l NaCl would have to be added to the produced concentrate. This NaCl would need to be added directly to the concentrate, and not to the feed, as this would increase the energy consumption in RO due to a higher osmotic pressure in the feed.

At the theoretical removal of 30% in DD as discussed above, the additional water recovery in RO would be negligible. Assuming DD would reach the same efficiency as IEX when

adding NaCl, the increase in water efficiency for both cases would be around 47% (from 46% to 93%, see 4.4), despite the need to add NaCl to the regenerate/concentrate. A trade-off between additional chemical use (NaCl) and an increased water recovery will thus have to be made. This will be looked at in more detail in the economic analysis of both cases.

4.4 Reverse osmosis

Based on the composition of the treated streams after treatment with IEX/DD as obtained during the lab experiments, an estimation of the attainable RO recovery can be made. This was done by simulating an RO system in the ROSA and Genesys® software (saturation of different scalants as calculated by Genesys® are included in Appendix A). In Table 2.4, the possible RO recovery for the original streams and the streams after IEX and DD treatment is shown.

Table 2.4 Attainable reverse osmosis recovery after the treatment of tap water and wastewater with ion-exchange and Donnan dialysis, as modelled by the ROSA and Genesys® software packages. The removal efficiency for multivalent cations in the tap water was assumed to be similar to that of the IEX in the wastewater case when sufficient NaCl is added to the RO concentrate. The removal efficiencies assumed in the wastewater simulations are those obtained during the lab experiments.

		Tap water	Wastewater
Untreated	%	46	76
Treated with IEX	%	93*	92
Treated with DD	%	93*	89

* With addition of a sufficient amount of NaCl to the concentrate

Due to the presence of HCO_3^- in the tap water, the effective RO recovery without pre-treatment is limited to 46% because of $CaCO_3$ scaling (incorporating a pH decrease from 8.6 to 6.3). The low MMR causes a low efficiency regeneration of the IEX resins and a limited removal efficiency (theoretically 30%) in DD. However, incorporating the addition of sufficient NaCl to the regenerate/concentrate in both cases, the RO recovery could be increased to 93%, ultimately limited by the formation of $CaCO_3$. Without the addition of NaCl, the application of both IEX and DD as an RO pre-treatment would be of little value due to their low efficiency. The low capacity of the IEX resin would result in short depletion cycles which would result in lower RO concentrate volumes. This would lead to even lower IEX capacities, eventually rendering the system obsolete. In Donnan dialysis, the situation is similar, since the low removal efficiency would result in lower RO recoveries, decreasing the concentration of NaCl in the concentrate and decreasing the removal efficiency in DD even further.

The RO recovery of the raw, untreated, wastewater is limited to 76% because of $CaCO_3$ scaling, with a similar pH decrease (from pH 7.7 to pH 6.3). However, here, the more favourable MMR assures an efficient removal of multivalent cations in IEX and DD. For the IEX-RO hybrid, this results in a possible RO recovery of 92%, only limited by the total TDS concentration in the concentrate (70 g/l to assure the stream can still be transported efficiently). This is very close to the 95% recovery adopted during the tests and no significant impact of this slightly lower recovery on the hybrid process is expected. In DD-RO, the RO recovery is limited to 89% due to $CaCO_3$ scaling. This would result in a higher volume and lower concentration of the produced RO concentrate. However, because of the very high MMR in this stream, this is not expected to have a significant effect on the removal efficiency in DD section 4.2.

4.5 Economical assessment

The overall outlook for the envisioned IEX/DD-RO process does not only depend on its technological performance, but also on its economic viability. Although the hybrid processes will lead to a higher water production, the additional implementation of technology will come at a certain cost. To assess the economic viability of both proposed hybrids, a more traditional IEX-RO with conventional regeneration (100 g/l NaCl, 2 bed volumes) was chosen as a reference scenario, resulting in the same high attainable RO recovery as the hybrid with concentrate recycling. These cases were compared to an RO scenario without pre-treatment, which achieves a much lower recovery. The costs for technologies and supplies are listed in Table 2.5, together with their origin. The RO cost estimate is based on ROSA simulations and is included in Appendix A. For DD, an emerging technology, it is very difficult to find data on CAPEX. Thus, CAPEX is estimated based on the current membrane costs. The DD module is envisioned to be spiral-wound, with a total membrane area of about 50 m². Based on the current membrane cost (€300/m²), this results in a total module cost of €15 000. For the tap water stream, addition of NaCl to the IEX regenerate and DD concentrate was incorporated, resulting in similar efficiencies in both scenarios. Most other costs were supplied by VITO, the Flemish institute for technological research, and technology suppliers. The feed to the RO unit was considered to be constant, at 60 m³/h for the wastewater and 25 m³/h for the tap water. Any adaptations to the RO unit to accommodate higher pressures (necessary because of higher recoveries) were modelled in ROSA and included in the cost analysis. The ROSA simulation can be found in Appendix A.

Table 2.5 Costs and constants used in the economical assessment and their references.

			Reference
Water	€/m³	1.5	Average in Flanders
Energy	€/kWh	0.1	Average in Flanders
Concentrate discharge	€/m³	2.6	Average in Flanders
NaCl	€/ton	100	VITO
Labor	€/h	50	VITO
Buffer tank 5m³	€	4 000	Technology supplier
Pump	€	3 000	Technology supplier
Interest on loan	%	4	VITO
Depreciation time	Years	10	VITO
Ion-exchange			
Columns	€/m³/h	757	Technology supplier
Resin	€/m³	3 800	Technology supplier
Lifetime resins	Years	7.5	Technology supplier
Donnan dialysis			
Membranes	€/m²	300	Technology supplier
Modules	€	15 000	Estimated based on membrane cost
Lifetime membranes	Years	5	[66]

The economic analysis (Table 2.6) clearly shows that the recycling of the RO concentrate for IEX regeneration is economically interesting for the wastewater case. Compared to the conventional IEX-RO case without concentrate recycling, this option results in a halving of the pre-treatment cost, from 0.14 €/m³ to 0.07 €/m³. These savings can be completely attributed to the total avoidance of fresh water and NaCl use. In DD, there is no need for additional buffer tanks because of the continuous nature of the process. Also, no back-up unit needs to be provided, as in IEX, since there is no need for regeneration. However, due to the high membrane cost, these savings and the savings due to water and NaCl avoidance are cancelled out, resulting in a pre-treatment cost that is about 10 times higher than the reference. Overall, including RO and concentrate discharge, the total cost is thus higher than the reference cases for DD-RO. Because of the higher RO recovery achieved after pre-treatment, the RO design needs to be expanded to allow for the higher permeate flow. This is why the total RO cost is higher when pre-treatment is included. This additional cost however, is compensated by the higher water production and consequently lower concentrate discharge when the RO feed is pre-treated by IEX. A potential drawback in this case could be the need to implement an additional precipitation unit, but the cost of this unit would most likely be very low.

Table 2.6 Detailed cost analysis for the ion-exchange and Donnan dialysis pre-treatment of the considered tap water and wastewater samples and two reference scenarios; simple RO of the stream and conventional IEX pre-treatment without RO concentrate recycling (CAPEX = capital expenses, OPEX = operational expenses, IEX = ion-exchange, DD = Donnan dialysis, RO = reverse osmosis).

		Wastewater				Tap water			
		RO	**IEX-RO conventional**	**IEX-RO study**	**DD-RO**	**RO**	**IEX-RO conventional**	**IEX-RO study**	**DD-RO**
Water consumed	**m³/h**	60	60	60	60	25	25	25	25
Water produced	**m³/h**	46	55	55	53	12	23	23	23
Concentrate produced	**m³/h**	14	5	5	7	14	2	2	2
				CAPEX					
Technology	**€**	-	56 820	56 820	1 845 000	-	23 675	23 675	540 000
Buffer tank	**€**	-	0	20 000	0	-	0	4 000	0
Pumps	**€**	-	6 000	6 000	6 000	-	6 000	6 000	6 000
				OPEX					
Replacements	**€/y**	-	1 520	1 520	369 000	-	633	633	108 000
Maintenance[1]	**€/y**	-	387	511	11 411	-	183	208	3 366
Labor[2]	**€/y**	-	9 125	9 125	9 125	-	9 125	9 125	9 125
Pumping energy[3]	**€/y**	-	14 016	14 016	14 016	-	7 008	7 008	7 008
Water	**€/y**	-	4 308	0	0	-	1 564	0	0
NaCl	**€/y**	-	28 721	0	0	-	10 428	54 115	44 457
Total technology[4]	**€/m³ produced**	**0**	**0.14**	**0.07**	**1.4**	**0**	**0.16**	**0.37**	**1.1**
RO cost	€/y	436 805	642 351	642 351	606 248	66 912	273 855	273 855	273 855
Concentrate discharge	€/y	327 974	109 325	109 325	150 322	307 476	39 858	39 858	39 858
Total*	**€/m³***	**1.9**	**1.7**	**1.6**	**3.0**	**3.7**	**1.7**	**1.9**	**2.6**

[1] Estimated as 5% of the investment cost, contains all physical maintenance costs except replacement of membranes and resin (= "Replacements")
[2] Estimated to be on average 0.5 hours per day both for IEX and DD
[3] This includes pumping energy for the IEX and DD system only. Energy costs for RO are included in "RO cost".
[4] Costs expressed per m³ of water produced by the system

For the tap water case, the recycling of the RO concentrate is not interesting from an economic point of view when compared to conventional IEX-RO. When considering the IEX-RO case, this is mainly due to the cost of the NaCl that needs to be added before regeneration. However, when considering using only part of the RO concentrate for the regeneration, supplemented with NaCl to a concentration of 100 g/l, the total cost would be similar as the IEX-RO reference (1.7 €/m³). The main difference between this option and conventional IEX-RO is the water savings achieved by re-using the RO concentrate. The major cost factor for DD is not the added NaCl (although significant) but more the membrane cost, which dominates the overall cost in this case as well.

Overall, pre-treatment of RO results in a significant decrease in the overall costs (except for DD-RO for the wastewater case). This decrease is mainly due to the lower amount of RO concentrate that needs to be discharged and to the higher amount of permeate produced. When comparing both pre-treatment options, DD-RO is more expensive due to the high membrane costs. However, membrane cost of IEM is expected to decrease in coming years due to more efficient production and higher market demands for ion-exchange membranes. The process efficiency can probably be increased in practice as well, by implementing a counter-flow system for example. These cost-factors were investigated by performing a sensitivity analysis, varying the membrane cost as well as the process efficiency. This is shown for both the tap water and the wastewater stream in Figure 2.10.

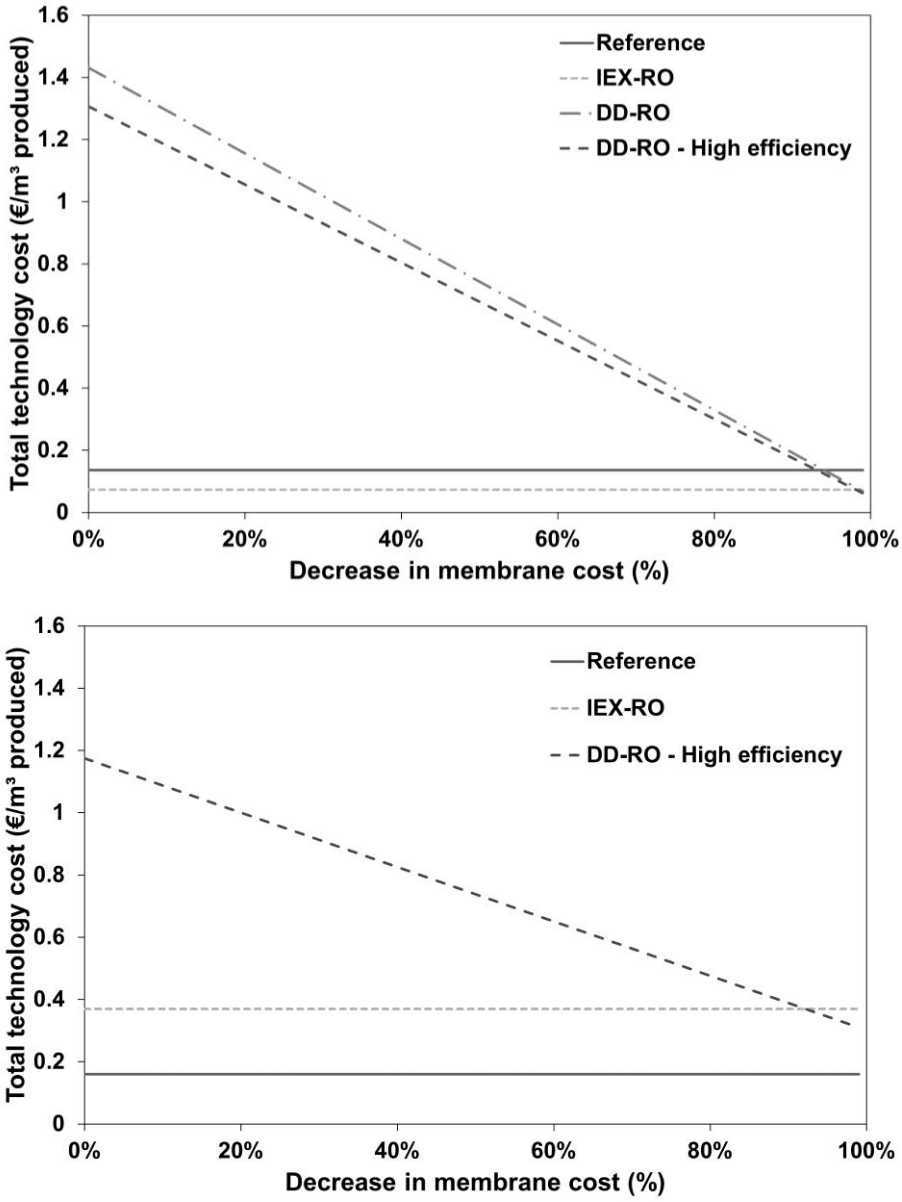

Figure 2.10 Sensitivity analysis of the total technology cost. While the membrane cost is expected to decrease, the process efficiency is expected to be higher in practice. The impact of the membrane cost is shown for the Donnan dialysis removal efficiency reached in the lab experiments (only wastewater) and for the case where Donnan dialysis reaches the same removal efficiency as the ion-exchange treatment (DD-RO – High efficiency). The wastewater case is shown on top, the tap water case below.

On the one hand, the decrease in IEM cost was investigated. On the other hand, costs were calculated for the current case and for the case where the DD removal efficiency increases up to the same level as IEX. Only the high efficiency case was considered for the tap water, since the removal efficiency without NaCl addition would be too low in practice. From the results, it is clear that for the wastewater case, the membrane cost would have to come down by 98-99% to be economically competitive with the IEX case. Since the achievable RO recovery is already quite high in this case, the higher efficiency DD-RO case does not have a

significant impact on the overall cost. For the tap water case, where the MMR is much less favourable, the membrane cost would have to decrease by about 97% to reach the same level as the IEX-RO scenario. In this case, both hybrids remain significantly more expensive than the reference scenario. Overall, it can be concluded that the cost of IEM membranes would have to come down to the same level as current state-of-the-art RO membranes, at 10-30 €/m².

5 Conclusions

This research looked into the recycling of RO concentrates for the regeneration of IEX or as a concentrate in DD. Both IEX and DD can be used to increase the RO recovery for the production of drinking and/or process water by removing multivalent cations from the feed water. The following conclusions can be made:

- DD is interesting when the MMR in the RO feed water is higher than 5 and an RO recovery >50% can be reached.
- The wastewater stream contained a favourable MMR, making an efficient hybrid process possible. The RO recovery could be increased from 72% to 89% and 92% for the DD-RO and IEX-RO hybrid respectively.
- For the low salinity tap water, the RO recovery could be increased from 46% to 93% for both DD and IEX. However, due to the very low MMR in the feed stream, the ion-exchange in DD and regeneration of IEX was much less efficient and NaCl should be added to the concentrate in practice.
- The economic analysis shows that pre-treating the RO feed results in lower overall water costs, mainly due to a higher permeate volume and consequently lower concentrate volume for discharge.
- Recycling the RO concentrate to the IEX pre-treatment results in a 50% cost reduction of the pre-treatment for the wastewater case. For the tap water, the costs were similar due to the need to add NaCl to the concentrate to achieve an efficient regeneration.
- Donnan dialysis showed to be much more expensive than IEX. Despite its advantages (no need for buffer tanks or back-up units), the membrane cost needs to decrease >90% before this technology becomes economically competitive, to a cost of 10-30 €/m² - which is comparable to current reverse osmosis membranes.

Chapter 3: A hybrid IEX-RO process with concentrate recycling for increased RO recovery without chemical addition: a pilot-scale study

This chapter has been published as

Vanoppen, M., Stoffels, G., Buffel, J., De Gusseme, B., Verliefde, A.R.D. A hybrid IEX-RO process with brine recycling for increased RO recovery without chemical addition: a pilot-scale study. *Desalination*. **2016**, 394, 185-194.

1 Introduction

In Chapter 2, the value of a hybrid IEX-RO system to increase the RO recovery without addition of anti-scalants was demonstrated on lab-scale. Especially at high MMR in the feed water, there was no need for the addition of chemicals of any kind to the system and the RO recovery could be increased significantly. Based on the economic analysis, classic IEX is preferred over the newer DD technique.

This chapter focuses on the implementation of the IEX-RO hybrid on a larger scale. A pilot-scale study was performed at a water production site producing demineralised water of different qualities. The treatment train of interest to this study consists of UF followed by single-pass RO, which currently operates at an average recovery of 75% with the aid of anti-scalants. The main goal of the pilot-scale tests is to show the performance of the hybrid at higher RO recoveries without the addition of anti-scalants to the feed. Three important hypotheses were formulated and tested in this study: (1) at higher RO recoveries, the higher concentration of monovalent cations in the RO concentrate will result in a higher IEX regeneration efficiency, (2) a higher MMR in the IEX-RO feed stream will result in a higher IEX regeneration efficiency and (3) at a low MMR, adding NaCl to the RO concentrate prior to IEX regeneration results in full restoration of the IEX to its original capacity. Based on the obtained results, the CNK-index (Concentrate Na^+ and K^+) is developed. This index, based on feed concentrations, gives an indication of the IEX-RO performance and allows to tune the hybrid operation in case of fluctuating feed compositions. By monitoring the CNK-index for example, the required addition of NaCl to the RO concentrate can be determined, assuring efficient operation of the hybrid without dosing excessive amounts of salts. The study is concluded with an economic analysis for a hypothetical 25 m^3/h RO skid.

2 Materials and methods

2.1 Feed water

For this study, surface water from the Rodenhuizedok in Ghent, Belgium was used. The water was taken after passing a 300 μm strainer and an ultrafiltration (UF) step before entering the pilot set-up. The UF consists of a dead-end hollow fibre system with PVDF membranes (Microza UNA-620A, Pall). Due to its enclosed nature but connection and proximity to the (brackish part of the) Scheldt river and the North Sea, the composition of the incoming feed water varies depending on the season. In general, low TDS (total dissolved solids) concentrations are observed in the colder months, while these concentrations start to

increase at the beginning of the Belgian summer (mainly in terms of NaCl concentrations), reaching a peak by the end of September. The alkalinity of the feed remains quite constant during the year. Table 3.1 gives the composition of the water between June 2014 – July 2015. The often large standard deviation shows the variability of the water during the year. Using RO modelling software allows to estimate the possible RO recovery and scaling potential based on the feed water composition as given here. The modelling software used here is ROSA 9.1 (Dow, USA) and Proton™ (American Water Chemicals Inc, USA). These predict that the main scaling potential for this particular feed water is $CaCO_3$ and that by removing the multivalent cations present in the feed, the RO recovery could be increased to 90%, limited mainly by SiO_2.

Table 3.1 Composition of the feed water, from the Rodenhuizedok in Ghent, Belgium, from June 2014 – July 2015.

Parameter	Unit	Value
Cond	µS/cm	3987 ± 2544
pH	-	7.6 ± 0.2
T	°C	14 ± 6
Al^{3+}	µg/l	685 ± 591
Ba^{2+}	µg/l	41 ± 8
Ca^{2+}	mg/l	135 ± 21
Cl^-	mg/l	1449 ± 608
Cu_{tot}	µg/l	25 ± 0
Fe_{tot}	µg/l	1600 ± 0
HCO_3^-	mg/l	292 ± 30
K^+	mg/l	47 ± 22
Mg^{2+}	mg/l	99 ± 57
Na^+	mg/l	826 ± 508
NH_4^+	mg/l NH_4	0.5 ± 0.5
NO_3^-	mg/l	21 ± 3
N_{tot}	mg/l N	7 ± 2
Si_{tot}	mg/l Si	6 ± 2
SO_4^{2-}	mg/l	260 ± 133
Sr^{2+}	µg/l	995 ± 689
COD	mg/l	19 ± 4

The experiments described in this paper ran from the end of February until the end of June 2015. During the pilot-testing, regular samples of the feed were taken and analysed. During the first half of the experiments, the concentration of the main ions of concern (Na^+, K^+, Ca^{2+} and Mg^{2+}) remained quite constant, as can be seen in Figure 3.1. During the second half however, the concentration of mainly sodium, potassium and magnesium increased

significantly, while the concentration of calcium remained relatively constant. This causes the MMR to vary from 0.95 in the first half of the experiments to 5.2 at the end.

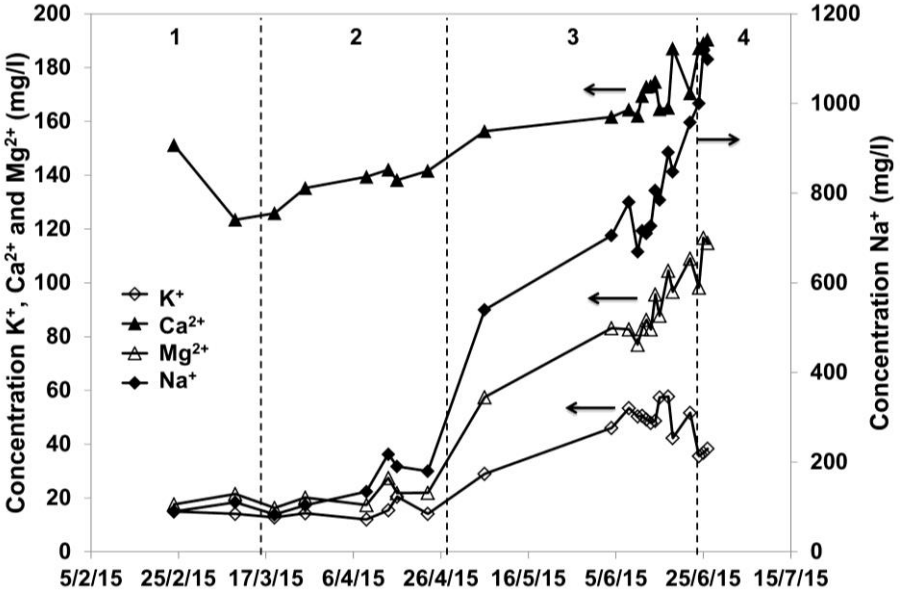

Figure 3.1 Feed concentration of Na^+, K^+, Ca^{2+} and Mg^{2+} during the course of the experiments. 4 series of experiments were carried out, the timing of which is indicated by the numbers 1-4 (see Table 3.3).

2.2 Pilot set-up and experimental protocol

The used pilot set-up consisted of a co-current IEX column and a 4-inch RO module. The IEX column contained 35 l of a strong cation-exchange resin (Lewatit® C 249, Lanxess, Germany), the properties of which are presented in Table 3.2. Flow through the column during exhaustion is sustained through the feed pressure delivered by the RO booster pumps of the water production site (± 5 bar). During regeneration, the regeneration liquid was provided using a Grundfos® presscontrol® pump. The RO set-up consisted of a 4 inch A/S pressure vessel (Eurowater, Denmark, 2014) containing a DOW-Filmtec brackish water membrane (LC HR-4040). A Grundfos® high pressure pump was used for RO operation. A schematic overview of the set-up is given in Figure 3.2.

Table 3.2 Ion-exchange resin properties.

Characteristic	Unit	
Uniformity coefficient	-	1.6
Bead size	mm	0.4-1.25
Effective size	mm	0.50 ± 0.06
Bulk density	g/l	832
Density	g/ml	1.26
Water retention	wt.%	45-48
Total ion exchange capacity	Min. eq/l	2.0
Stability	pH range (-)	0-14
	Temperature range (°C)	1-140
Storability	Max years	2

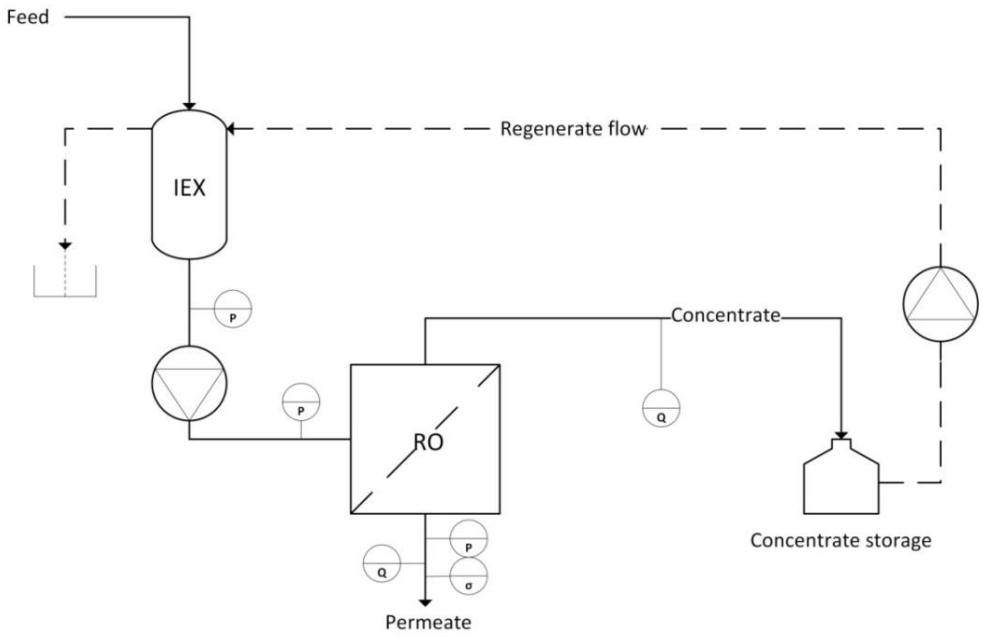

Figure 3.2 Schematic overview of the pilot IEX-RO set-up. Full lines represent the RO production phase, dotted lines represent the IEX regeneration phase. (P = pressure, Q = flow rate, σ = conductivity)

In the first three experiments, a minimum of four consecutive regeneration-exhaustion cycles were performed. If the resulting IEX capacity drops below 50%, indicating limited overall efficiency of the hybrid, no more cycles were executed. In the last experiment, just two cycles were performed to shortly test the hypotheses that adding NaCl to the RO concentrate can fully restore the IEX capacity upon regeneration. For each experiment, the resin was first regenerated with 4 bedvolumes (BV) of a 10 wt.% NaCl solution at a flow rate of 5 BV/h. This regeneration scheme falls within the manufacturers recommendations to ensure full recovery of the IEX capacity [67]. After the regeneration, a slow rinse (2 BV, 5 BV/h) and a

fast rinse (5 BV, 8-10 BV/h) of the resin with RO permeate were performed to remove any excess salt solution. After this regeneration step, an exhaustion cycle was started again and the IEX effluent was fed to the RO. For practical reasons, regeneration of the IEX was carried out in co-current, in other words, the regeneration solution followed the same top-to-bottom path as the feed solution during exhaustion. RO permeate flux was kept constant at 23 lmh, and the total RO recovery was controlled by adjusting the concentrate outlet valve. Four different experiments were carried out, of which the main parameters are given in Table 3.3. For each experiment, the RO concentrate was stored in 1 m³ storage vessels. RO operation and IEX exhaustion cycles were maintained until breakthrough of hardness from the IEX column was detected. After hardness detection, the RO operation was stopped, after which the collected RO concentrate from the storage tank was used as a regenerant for the IEX (with the rest of the regeneration cycle carried out as stated above). For each experimental setting, the first regeneration was always performed with a 10 wt.% NaCl solution regeneration (to restore the IEX capacity to the baseline capacity), and the consecutive regenerations were performed with the stored RO concentrate collected in the previous exhaustion cycle.

Table 3.3 Overview of the four executed experiment series.

Experiment series	Cycle	IEX regenerant	RO recovery
1 (Low feed Na^+)	1	10 wt.% NaCl	75%
	2	Concentrate cycle 1	
	3	Concentrate cycle 2	
	4	Concentrate cycle 3	
2 (Low feed Na^+)	1	10 wt.% NaCl	85%
	2	Concentrate cycle 1	
	3	Concentrate cycle 2	
	4	Concentrate cycle 3	
3 (High feed Na^+)	1	10 wt.% NaCl	75%
	2	Concentrate cycle 1	
	3	Concentrate cycle 2	
	4	Concentrate cycle 3	
4 (NaCl addition)	1	Concentrate after 2 cycles + NaCl	75%

2.3 Analysis

For the detection of exhaustion of the IEX column, hardness was analysed using a Duroval® Type A test kit (Gebrüder Heyl, Germany) on the IEX effluent. Also, at regular intervals during the pilot testing, IEX feed and IEX effluent samples were taken and

analysed for Na^+, K^+, Ca^{2+} and Mg^{2+}. This, in combination with the produced RO concentrate in each cycle, allowed the calculation of the exact capacity of the IEX resin. After each exhaustion cycle and before regeneration, a sample of the cumulatively collected RO concentrate was also taken and analysed for the same parameters. All relevant cations were analysed using inductively coupled plasma with optical emission spectroscopy (ICP-OES, Varian VISTA-MPX, Palo Alto, VS). All used standards and the analysed samples were acidified with 1% HNO_3 prior to analysis.

3 Results and discussion

3.1 Effect of regeneration with RO concentrate on IEX efficiency

3.1.1 Influence of the RO recovery: 75% versus 85% RO recovery

In the first two series of experiments, the performance of the hybrid at 75 and 85% RO recovery was compared. As can be seen in Figure 3.3, a higher recovery (and thus higher monovalent salt concentration in the RO concentrate, but a smaller volume of RO concentrate) seems to result in overall higher IEX regeneration efficiencies. In this figure (and all following similar figures), the IEX capacity resulting from a regeneration with a 10 wt.% NaCl solution was used as a baseline and rescaled to 100% to facilitate comparison. However, although the feed composition was relatively stable during this period, the MMR did increase from an average of 1.1 during the first experiment to 1.9 during the second experiment. To account for this change, the achieved IEX regeneration efficiency was divided by the MMR, as shown in Figure 3.4. This figure shows that the difference between the first two series of experiments is small and no clear trend can be observed. The third series of experiments, discussed further on, does differ from the other two.

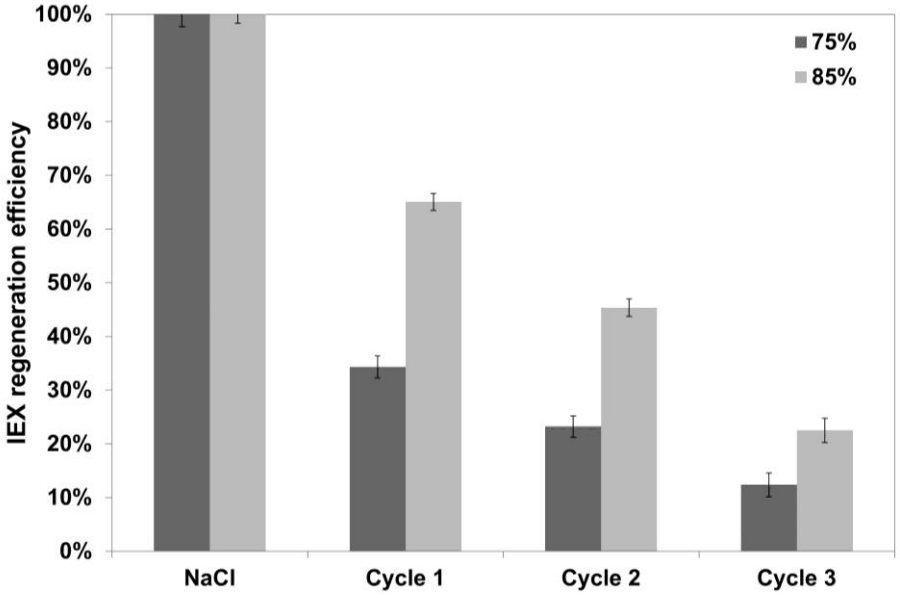

Figure 3.3 Regeneration efficiency of the ion-exchange column at 75% and 85% RO recovery over 3 cycles of regeneration with the RO concentrate. Regeneration with a 10 wt.% NaCl brine was used as a baseline and rescaled to 100% to facilitate comparison.

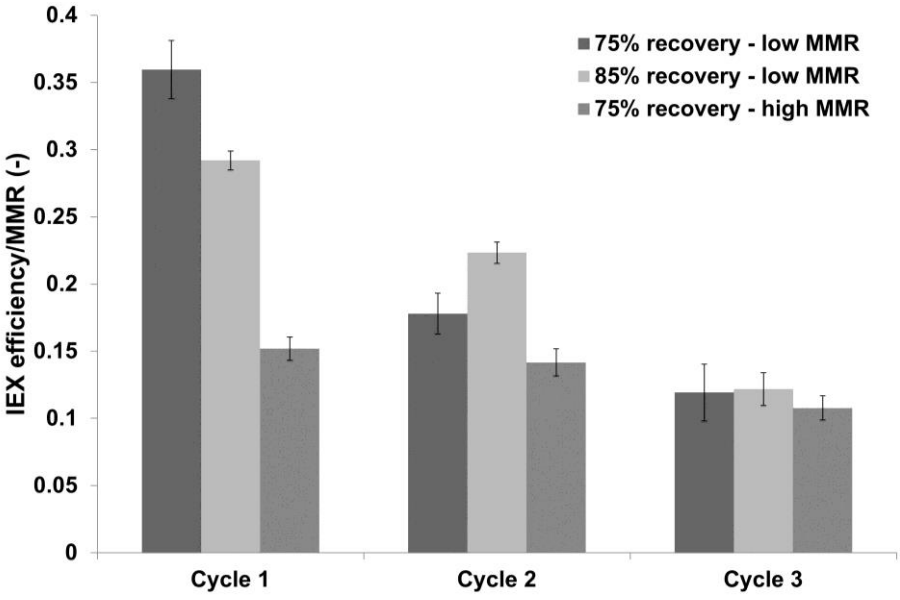

Figure 3.4 Achieved IEX regeneration capacity divided by the MMR in the feed.

Contrary to what was hypothesized, these experiments thus show that a higher RO recovery does not ensure a higher IEX regeneration capacity. This means that the determining factor for the regeneration of the resin is not the concentration, but the total amount of monovalent cations (sodium and potassium) present in the regenerant. Because the volume and concentration in the RO concentrate do not determine the regeneration efficiency, the only determining factor is the MMR in the feed water, which determines the final amount of monovalent cations in the concentrate. At high amounts of multivalent cations in the feed,

the total amount of feed treated by the IEX will be limited, resulting in a low amount of monovalent cations in the RO concentrate for the regeneration of the IEX. However, this can be counterbalanced by a higher monovalent cation concentration in the feed. In other words, the higher the MMR in the feed, the higher the regeneration efficiency will be.

3.1.2 Influence of the monovalent:multivalent cation ratio in the feed

In the last two pilot runs, all ion concentrations in the feed increased (see Figure) due to the seasonal effect. The main increase in concentration was observed for sodium, which increased from about 80 to 1100 mg/l. Consequently, the MMR in the feed increased from 1.1 at the beginning of the testing period to 5.2 at the end of the testing period. From the results in Chapter 2, we expect that the higher ratio will result in a more efficient IEX regeneration. This is confirmed in Figure 3.5, where the effect of the higher MMR is clearly shown. At 75% RO recovery (experiments 1 and 3), the higher ratio results in a higher efficiency and recovery of the ion-exchange capacity, even when compared to 85% RO recovery at a lower cation ratio (experiment 2, shown in Figure 3.3). In Figure 3.4 it was already demonstrated that there is a significant difference between both experiments, so this conclusion is valid.

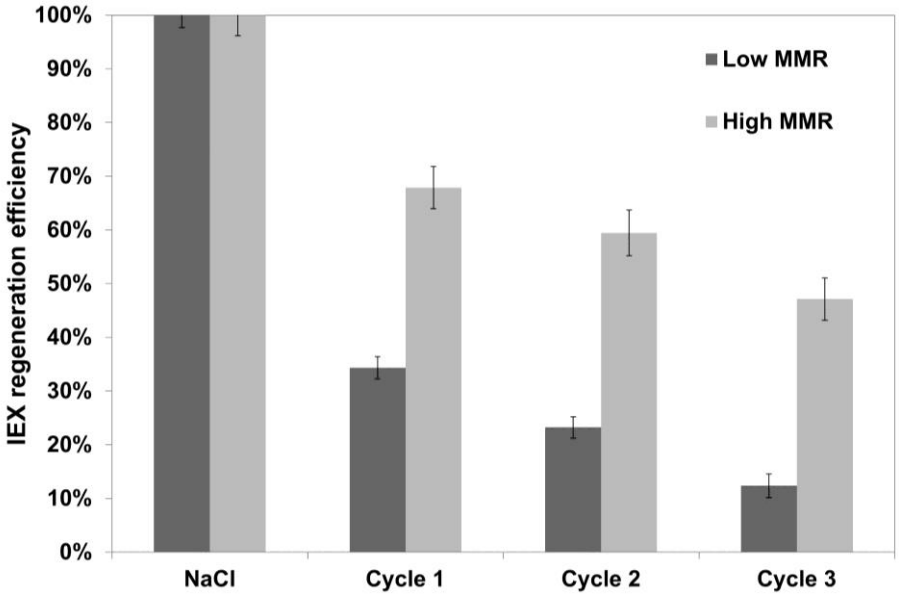

Figure 3.5 Regeneration efficiency of the ion-exchange column at 75% RO recovery at a low and high monovalent:multivalent cation ratio in the feed. 3 cycles of regeneration with the resulting RO concentrate. Regeneration with a 10 wt.% NaCl brine was used as a baseline and rescaled to 100% to facilitate comparison.

3.1.3 Influence of adding NaCl to the RO concentrate prior to IEX regeneration

To demonstrate that adding additional NaCl to the RO concentrate can recover the full IEX capacity, a final test was executed, in which the RO concentrate was supplemented with

NaCl. Enough NaCl was added in excess to raise the sodium content of the concentrate by 50% (arbitrarily chosen). Figure 3.6 shows the result of this test, compared to a classical 10 wt.% NaCl regeneration and the final regeneration of run 3 at 75% RO recovery as discussed before. The figure shows that adding NaCl to the RO concentrate indeed allows the IEX capacity to be restored to 100%.

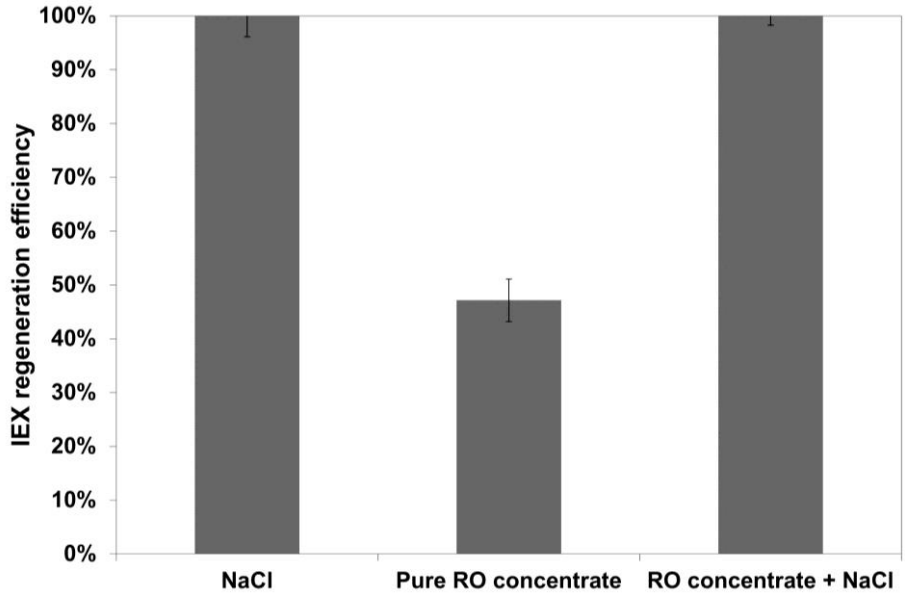

Figure 3.6 Regeneration efficiency of the ion-exchange column at 75% RO recovery without and with the addition of NaCl (50% of sodium present) to the RO concentrate. Regeneration with a 10 wt.% NaCl brine was used as a baseline and rescaled to 100% to facilitate comparison.

Based on the results obtained, some theoretical calculations can be made as to what the optimal conditions should be for an IEX-RO hybrid to be applicable in practice. For this purpose, the total amount of monovalent cations (sodium and potassium) in the RO concentrate can be used, termed the CNK-index (Concentrate Na^+ and K^+) for the remainder of the discussion. As discussed before, this total amount is an important parameter determining the IEX regeneration efficiency. CNK (in mol/m³ resin) is determined by the MMR in the feed and the IEX capacity, as shown by the following equation:

$$\begin{aligned} \mathrm{CNK} &= \frac{\mathrm{Cap_{IEX}}}{2 \cdot \left(\mathrm{C_{Ca^{2+}}} + \mathrm{C_{Mg^{2+}}}\right)} \cdot \left[\mathrm{C_{Na^+}} + \mathrm{C_{K^+}} + 2 \cdot \left(\mathrm{C_{Ca^{2+}}} + \mathrm{C_{Mg^{2+}}}\right)\right] \\ &= \mathrm{Cap_{IEX}} \cdot \left(1 + \frac{\mathrm{MMR}}{2}\right) \end{aligned} \tag{3.1}$$

With Cap_{IEX} the capacity of the IEX (eq/m³ resin), C the concentration of the ion (mol/m³) and MMR the monovalent:multivalent cation ratio in the feed. To allow comparison between different systems, the obtained amount of monovalent ions is divided by the volume of resin in the IEX column. The left hand side of the top equation represents the total volume treated by the IEX before breakthrough per m³ of resin, the right hand side includes the total amount of monovalent ions ending up in the concentrate. The factor 2 is included in the denominator on the left hand side to account for the double charge of the multivalent cations. In the numerator on the right hand side, this factor 2 is included to take into account that for every calcium and magnesium ion removed by the IEX, two monovalent ions end up in the RO concentrate, again because of the double charge. This elaborate equation can be simplified to the one shown on the bottom, including only the IEX capacity and the MMR. The relation between CNK and the IEX regeneration efficiency as obtained during the four experiment series is provided in Figure 3.7.

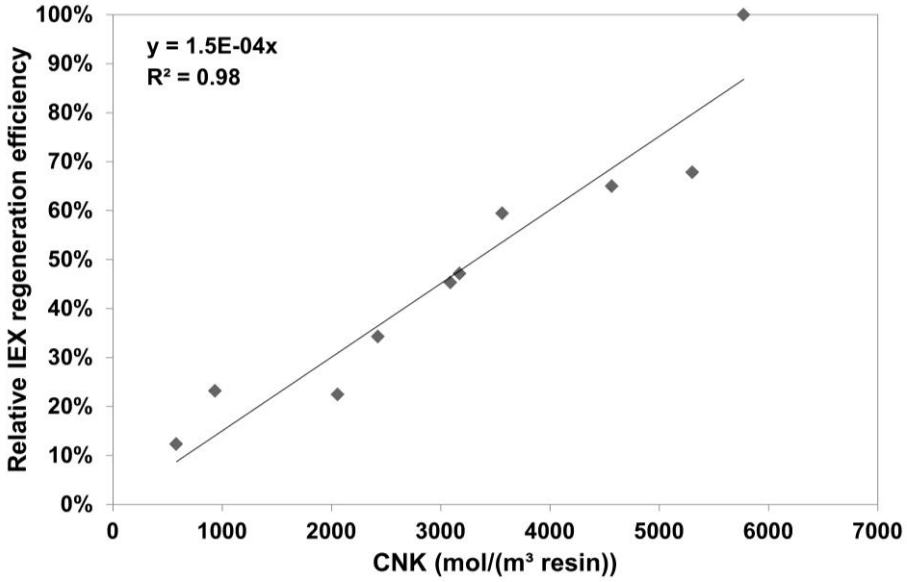

Figure 3.7 The relative IEX regeneration efficiency, compared to a classic 10 wt.% NaCl regeneration, in relation to CNK.

The linearity of the relation obtained between CNK and the regeneration efficiency, with a coefficient of determination (R^2) of 0.98 (t-test: 21.85, p-value: 4.15E-09), further emphasises that the obtained regeneration efficiency is independent of the RO recovery and is influenced mainly by the total amount of monovalent cations present in the concentrate. The fitting data (R^2, t and p) shows the validity of the linear fit, despite the limited number of data-points. From this relation, it can be estimated that theoretically, a CNK of 6 667 mol/(m³ resin) is needed to achieve 100% regeneration efficiency, although in the final experiment, the CNK was only 5 772 mol/(m³ resin) after addition of NaCl to the concentrate. Without NaCl

addition, the CNK in the last experiment would be 3 950 mol/(m³ resin), predicting a regeneration efficiency of 59%. In comparison, a classic regeneration with a 10 wt.% NaCl solution as performed in this study corresponds to a CNK of about 7 330 mol/(m³ resin). It has to be mentioned that this correlation is valid for this specific resin, and has to be re-evaluated for different resins used. However, for this resin, the index can give an indication for a wide range of feed water types. Furthermore, during these experiments, regeneration was carried out in co-current mode. In full-scale applications, regeneration would be carried out in counter-current, which is expected to result in a more efficient regeneration and thus lower CNK needed for full regeneration to be reached.

When the hybrid system is characterised as discussed above, the CNK-index can be used as a control-parameter in the steering of the system. By monitoring the CNK-index of the incoming water, based on the MMR, the system can perform optimally. During periods where the CNK-index is low for example (i.e. in winter in the example discussed here), the regeneration efficiency of the IEX will be low. However, based on the index, an estimation can be made on how much NaCl needs to be added to the RO concentrate to ensure an efficient regeneration. This not only ensures an efficient operation of the system, but also avoids the presence of excess salts in the waste stream (the RO concentrate/IEX regenerate). In the case discussed here, the feed composition fluctuates during the year and the CNK would have to be closely monitored to ensure efficient operation of the system. On-line measurement of the CNK and subsequent automated control of the NaCl dosing is necessary for cases where the feed is highly variable. However, if the feed composition is rather stable, manual periodic measurement of the CNK is sufficient to ensure efficient NaCl dosing.

3.2 Stability of IEX-RO hybrid performance

To assess the long-term operational stability of the hybrid process, both the IEX resin integrity and stable operation of the RO system are important. If the RO concentrate would have an irreversible effect on the IEX resin (e.g. due to fouling with organics present in the feed water), this would result in a steady decrease of the IEX capacity during the experiments. This can be assessed by the IEX capacity after full regeneration of the resin, which was performed three times during the experiments (at the beginning and after the first 2 experiment series with pure NaCl and at the very end with concentrate supplemented with NaCl). The absolute resin capacity (eq/l) at these three times shows no decline (Figure 3.8), indicating no irreversible effects of the concentrate on the resin.

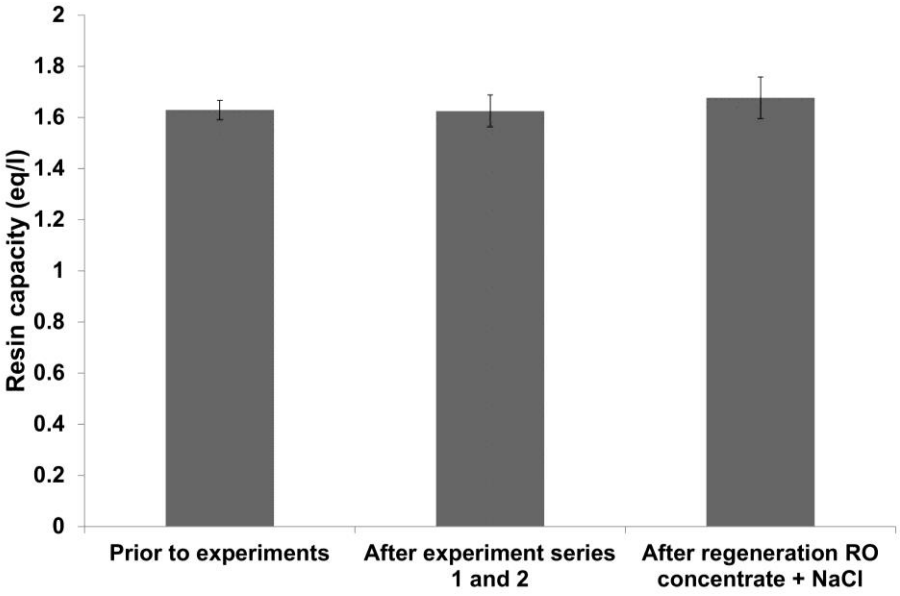

Figure 3.8 Absolute resin capacity during the course of the experiments.

While performing the experiments as described above, both at 75% and 85% recovery, the RO system showed stable performance, as shown by Figure 3.9. This figure shows that the permeability over the RO membrane is always around 1.5 l/(m².h.bar) at the high cross-flow of 0.1-0.2 m/s used, indicating that no significant deterioration or fouling of the membrane occurred, and thus that no scaling formed. Furthermore, the effectively achieved RO recovery showed a deviation of only ±3% maximum, further indicating stable operations.

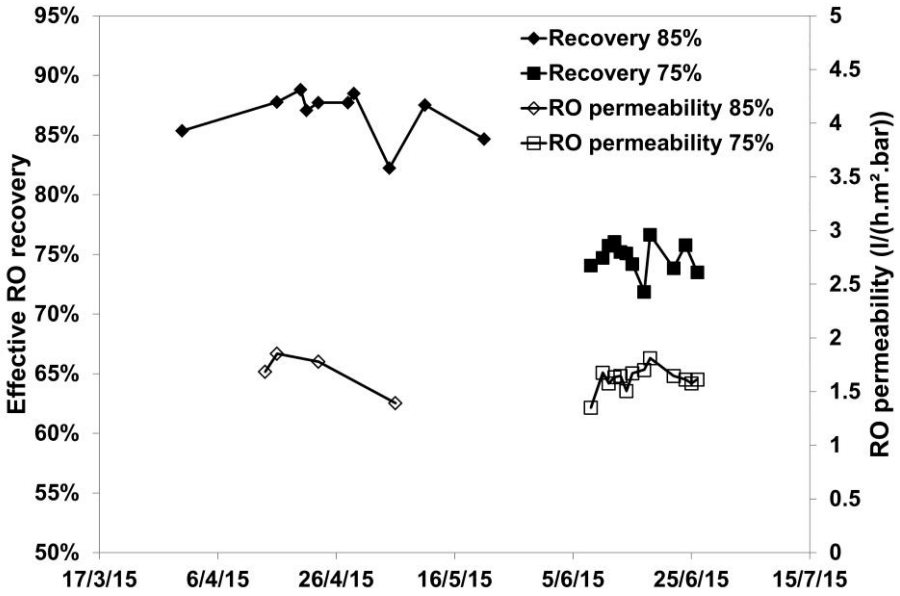

Figure 3.9 Effectively attained RO recovery and inlet RO pressure during the 85% and second 75% RO recovery experiment series.

3.3 Economic analysis

The research discussed here indicates that the pre-treatment of an RO system with IEX, including the recirculation of the RO concentrate for regeneration, is technologically feasible. However, to be implemented in practice, the economic feasibility needs to be taken into account as well. The economic analysis discussed in this part is based on the last part of the experiments, where the IEX capacity was fully restored after adding NaCl to the RO concentrate. Only in such cases, the system is fully sustainable, as the IEX capacity will not decrease continuously. As a feed water composition, the composition of the feed at the end of the experiments, during the last exhaustion cycle, was taken. This composition is assumed to represent an average composition of the water when looking at a whole year, as the concentrations before this point were at the winter-time low and they were still rising to the summer-time maximum values. This assumption is supported by the average water composition given in Table 3.1. The composition corresponds to a CNK of 6 103 mol/(m³ resin). At an RO recovery of 85%, this means that 2.5 g/l NaCl needs to be added to the concentrate to achieve 100% regeneration efficiency (CNK = 6 667 mol/(m³ resin)) as predicted by the linear regression model discussed before.

Three scenarios were considered for the economic analysis: (1) the baseline scenario, which is the RO operation as it is now at the site in question, where the single-pass RO system stands on its own and reaches an average RO recovery of 75% with the addition of anti-scalants, (2) an IEX-RO hybrid system whereby scaling cations are removed prior to RO, but without recirculation of the RO concentrate. Here, the IEX is regenerated using a classic regeneration step as described by the manufacturer and (3) the same IEX-RO hybrid, but now with recirculation of the RO concentrate and including the addition of 2.5 g/l NaCl to achieve full IEX capacity recovery. Based on these scenarios, the cost or benefit of retro-fitting an IEX system to and existing RO installation was estimated, based on the CAPEX and OPEX for a 25 m³/h RO installation. Conceptual flow schemes of all scenarios are given in Figure 3.9.

Scenario 1: Stand-alone RO, 75% recovery

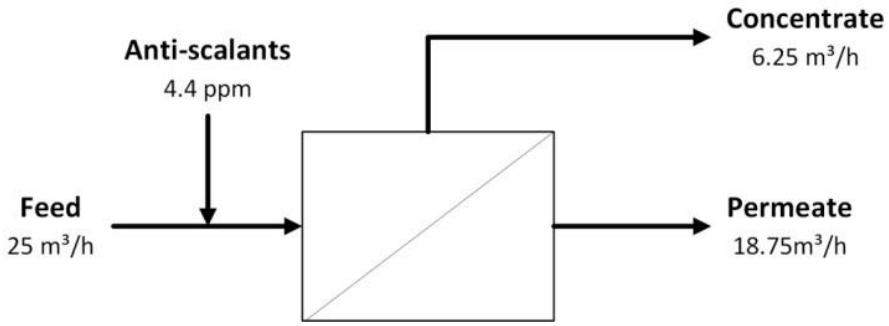

Scenario 2: IEX-RO, 85% recovery, classic IEX regeneration

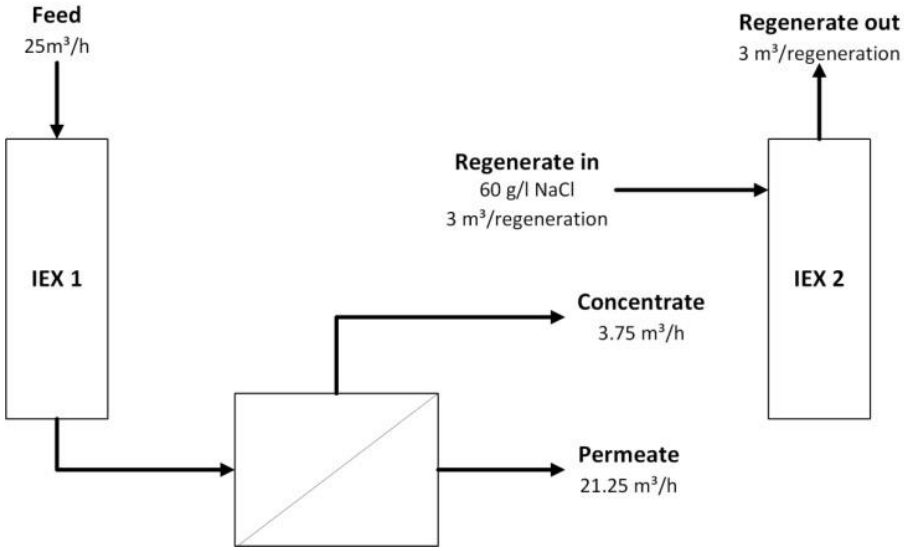

Scenario 3: IEX-RO, 85% recovery, regeneration with RO concentrate

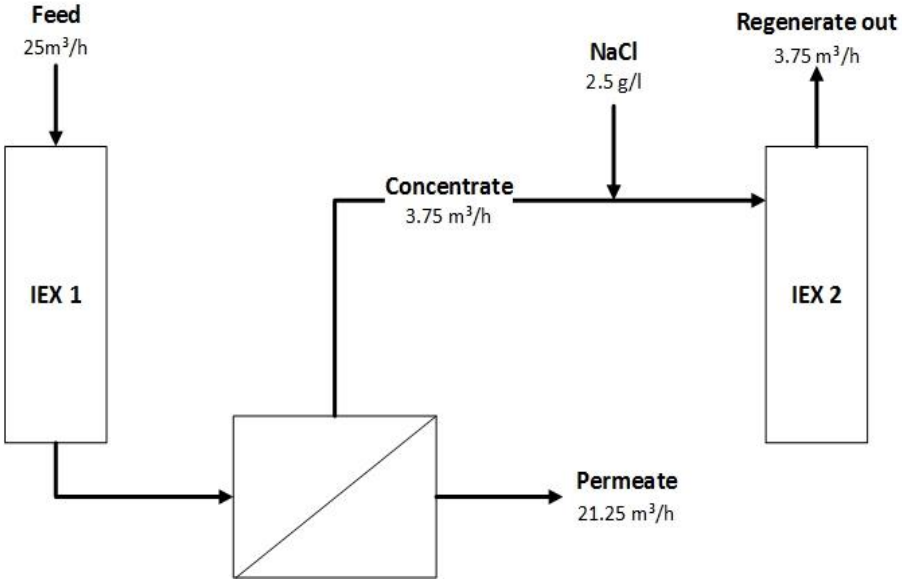

Figure 3.9 Different scenarios considered in the economic analysis.

Table 3.4 Costs and constants used in the economic assessment.

Cost	Unit	Amount	Reference
General			
Energy	€/kWh	0.1	Average in Flanders
Labor	€/h	50	VITO
Discharge	€/m³	2.6	Average in Flanders
Product water	€/m³	-1.5	Average in Flanders
Scenario 1: stand-alone RO at 75% recovery			
Anti-scalant	€/kg	4	Technology supplier
Scenario 2 and 3: IEX-RO at 85% recovery			
IEX-columns	€	52 500	Technology supplier
Resin	€/m³	3 625	Technology supplier
Installation	€	4 500	Technology supplier
NaCl	€/ton	100	VITO
Salt storage	€	35 000	Technology supplier
Auxiliary equipment	€	3 500	Technology supplier
Additional RO membrane cleaning[1]	€/year	3 000	Technology supplier
Additional RO membrane replacement[2]	€/year	5 000	Technology supplier

1 This includes the concentrate-vessel and pump and the software controls

2 Needed here because of the higher RO recovery reached

Table 3.4 gives an overview of the general costs included in the economic analysis. For the baseline scenario, anti-scalants need to be added in a dosage of 4.4 mg/l. This dosage was based on the Langelier and Stiff Davis indices for $CaCO_3$ saturation. Based on the manufacturer's data, an IEX column of 2000 liters of resin is needed to treat 25 m³/h of the considered feed in scenarios 2 and 3. To ensure continuous operations, 2 columns are needed, one to treat the feed water while the other one is being regenerated (1 + 1 redundancy). In scenario 3, no additional buffer tank for the concentrate is required, as the produced concentrate can continuously flow over the IEX column not in operation. Flow rates over the resin in this case meet the standards set by the IEX resin manufacturer [67]. To accommodate the higher RO recovery achieved in the last scenarios, the technology supplier estimates that only additional membrane cleanings and replacements will be necessary, and no expansion of the RO equipment itself is needed. The cost of additional cleanings and membrane replacements was estimated at 3000 and 5000 €/year, respectively. The cost for product water is negative, as this is an income in this analysis. In all cases, a depreciation time of 10 years and an interest on loan of 4% were assumed. A detailed overview of the cost analysis is included in Table 3.5. The total cost at the bottom is a

negative value, because the product water does not cost money but instead is a source of revenue, the value of which is represented by the negative cost.

Table 3.5 Detailed cost analysis for stand-alone RO and IEX-RO including classic regeneration and regeneration with RO concentrate.

		RO	IEX-RO No recirculation	IEX-RO Recirculation
Feed flow	m³/h	25	25	25
Water produced	m³/h	18.75	21.25	21.25
CAPEX				
Duplex IEX	€/year	-	6 473	6 473
Resin	€/year	-	1 788	1 788
Auxiliary equipment	€/year	-	4 747	4 747
Installation	€/year	-	555	555
OPEX				
Anti-scalants	€/year	3 854	-	-
Energy	€/year	15 108	28 538	28 538
NaCl	€/year	-	24 638	8 048
Resin replacement	€/year	-	1 933	1 933
Additional membrane replacement	€/year	-	3 000	3 000
Additional membrane cleaning	€/year	-	5 000	5 000
Personnel	€/year	-	4 800	4 800
Discharge	€/year	142 350	93 951	85 410
Product water revenue	€/year	-246 375	-279 225	-279 225
Total	€/year	-85 063	-103 804	-128 934
	€/m³ produced	**-0.52**	**-0.56**	**-0.69**

This analysis shows that retrofitting an IEX to an existing RO system brings a similar product water income compared to a stand-alone RO system when a classic regeneration scheme is implemented (-0.56 €/m³ versus -0.52 €/m³ respectively). When the RO concentrate is used for the regeneration of the IEX however, the income of the product water increases with 0.17 €/m³, to -0.69 €/m³. This results in a pay-back period (the amount of time needed to balance the investment costs with the added value of the hybrid system) of 2.5 years. The main difference between the latter and a stand-alone RO system is the lower cost for discharge, as the concentrate volume decreases due to the higher RO recovery achieved. When comparing scenario 3 to scenario 2, the biggest avoided cost is the added NaCl, which is about three times lower when the RO concentrate is used as a regenerant.

Depending on the feed water composition, the amount of NaCl to be added in scenario 3 can vary, as well as the energy required in the RO system. This influences the economic viability of the system. In the case studied here for example, the CNK in the winter is around 2 500, but because of the lower ion concentrations, the energy requirements in the RO system decrease as well. This results in a product water income of 0.70 €/m³, approximately the same as the scenario discussed above. Assuming the monovalent cation concentrations double in summertime, but the multivalent cation concentrations stay similar, the CNK would be 14 000 at this point and no NaCl would need to be added to the RO concentrate. However, the RO energy requirements would increase significantly due to the higher osmotic pressure of the feed. This would result in a product water income of about 0.63 €/m³. In other words, because of the trade-off between the monovalent ion content of the feed and the RO energy requirements, the economic viability of the system remains quite the same during the whole year. Besides the osmotic pressure, the seasonal temperature variations of the feed water influences the energy requirements as well. Another important cost factor is the discharge cost, as much of the added benefit of the IEX-RO hybrid is in the decrease of the discharged waste water volume. An average discharge cost of 2.6 €/m³ (the average Flemish cost for discharge onto the sewer system, including additional costs for treatment in a central WWTP) was assumed for the analysis here, as this cost is highly case-specific. Keeping all other parameters constant, the economic analysis shows that the water revenue for the hybrid case reaches the same value as that for stand-alone RO at a discharge cost of 1.5 €/m³. At lower discharge costs, the cost for the hybrid system would exceed that of the stand-alone RO.

In Figure 3.10, the total product water cost is given for different water types at varying equivalent sodium concentrations in the feed. All parameters as discussed in the economic analysis were assumed constant, except for the energy demand of the RO system and the required NaCl addition. Both were calculated based on the feed concentrations. As in the system studied here, it is assumed that the equivalent calcium concentrations in the feed remain constant. These equivalent concentrations are calculated by combining sodium and potassium concentrations (in mol/l) and calculating the equivalent amount of sodium (in mg/l). The same is done for the combination of calcium and magnesium in the equivalent calcium concentration. Five different equivalent calcium concentration levels are compared in Figure 3.10. This figure shows that at higher equivalent calcium concentrations, the product water revenue decreases (total costs become less negative or even positive at high equivalent sodium concentrations). This is to be expected, as the amount of sodium in the

concentrate required to assure efficient IEX regeneration increases at higher equivalent calcium concentrations in the feed (which corresponds to a lower MMR). At all equivalent calcium concentrations, except for the lowest, a sharp inflection point in the curve is seen. In the first part of the curves, the amount of NaCl that needs to be added to the RO concentrate decreases due to the increasing equivalent sodium concentration in the feed. The added benefit of this decrease in salt addition surpasses the additional cost caused by the increasing energy demand of the RO at higher sodium feed concentrations. At the inflection point, the NaCl that needs to be added to the RO concentrate decreases to 0. From then on, at higher sodium concentrations, no more NaCl needs to be added, and the increase in total cost is caused by the increase in the required energy in the RO system. The only difference between the curves after the inflection point is the feed calcium concentrations. Since multivalent ions are replaced by monovalent ions in the IEX system, a higher calcium feed concentration entails a higher RO energy demand after the IEX as well, which explains the slight difference between the curves. At an equivalent calcium concentration of 5 mg/l in the feed, the NaCl needed in the RO concentrate is negligible and the curve is linear.

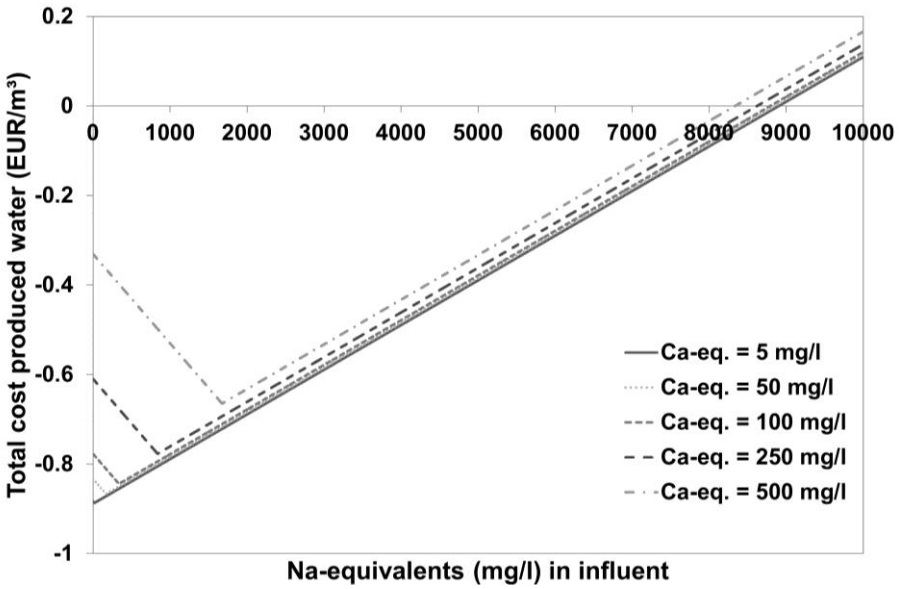

Figure 3.10 Comparison of the total cost of water produced by the hybrid IEX-RO process (EUR/m³) for different constant equivalent calcium concentrations in the feed, over a wide range of equivalent sodium concentrations.

Figure 3.11 shows the effect of varying MMR on the total cost for the produced water. Shown on the figure are four numbers, which correspond to four different water types typically encountered in RO systems; brackish surface water (as discussed in this study), secondary treated wastewater, fresh surface water and seawater. A typical composition of these streams is shown in Table 3.6. Moreover, as product water prices for the customer

differ depending on the region and will also probably change in the future, the figure compares product water prices (PW) of 0.75, 1.5 and 3 €/m³. Again, all parameters stay the same, only the added NaCl and RO energy demand are taken into account. The x-axis shows the varying equivalent sodium concentration in the feed, the corresponding equivalent calcium concentration was based on the different MMR compared (1, 5, 10 and 25).

Table 3.6 Composition of the feed waters considered in the comparison.

		1	2	3	4
		Brackish surface water	**Secondary treated wastewater**	**Fresh surface water**	**Seawater**
Reference		This study	Chapter 2	Coupure water, Ghent (own analysis)	Lenntech [83]
Na^+	**mg/l**	1 108	681	44.6	10 556
K^+	**mg/l**	37.6	1 416	13.4	380
Ca^{2+}	**mg/l**	189.7	17.6	94.9	400
Mg^{2+}	**mg/l**	115.8	53.2	12.1	1 262
MMR	**-**	5.18	25.1	0.8	7.58
CNK	**mol/m³ resin**	6 103	22 997	2 378	8 140

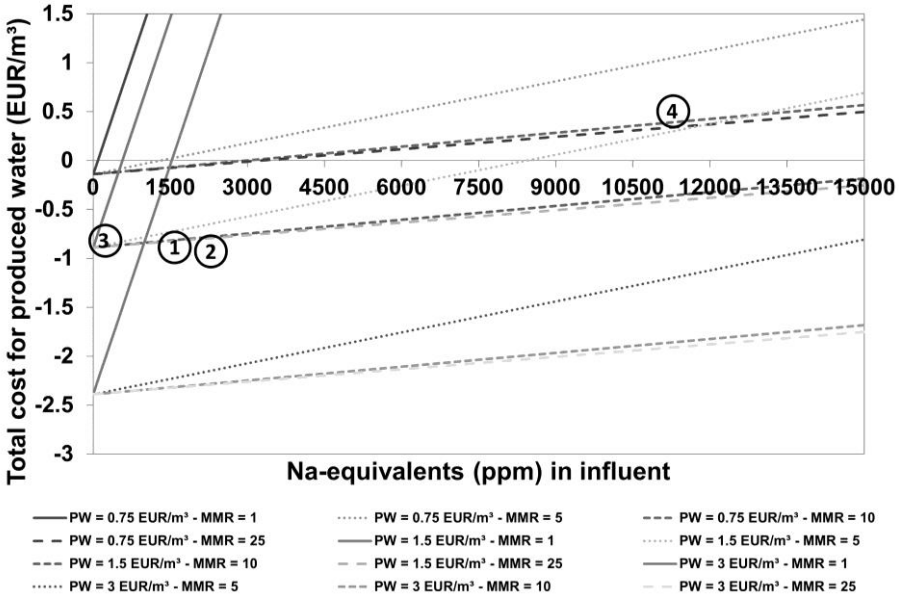

Figure 3.11 Comparison of the total cost for produced water for different monovalent:multivalent cation ratios (MMR) over a range of equivalent sodium concentrations in the feed. Three different product water prices (0.75, 1.5 and 3 EUR/m³, PW) are compared. The numbers indicate the position of the feed waters mentioned in Table 3.6 on the graph at a water price of 1.5 EUR/m³.

The figure shows that a feed with an MMR of around 1 (as is the case for the fresh surface water, 1) will only be interesting with regards to the hybrid process at very low equivalent sodium concentrations. However, in that case, because of the low feed concentrations, stand-alone RO will probably be more economically viable. At higher MMR, less NaCl needs to be added and the system becomes more interesting. For example in the case of brackish surface water as discussed here, only 2.4 g/l NaCl needs to be added to the RO concentrate. In the case of secondary treated wastewater, no addition of NaCl is needed because of the favourable MMR (as shown in Chapter 2). The balance between the equivalent sodium concentration in the feed and the MMR in the first three examples results in a net profit when considering these for the hybrid system discussed. For the seawater example however, although no addition of NaCl would be needed, the energy demand in the RO to reach 85% recovery is so high, that no net profit can be achieved here. This case is only added as an example, as seawater RO at 85% is not achieved in practice due to excessive material costs to cope with the very high osmotic pressure reached.

The figure also shows that at a product water price of 0.75 €/m³, there is only a very small region of feed composition that allows for a net profit in the hybrid system. In this region however, due to the low sodium concentrations in the feed, stand-alone RO would most likely be more interesting. As expected, a product water price of 3 €/m³ results in a much more interesting economic case, as only at very low MMR the net profit drops to 0 for the concentration range discussed here. Even at a product water price of 1.5 €/m³, considered as the average in Flanders today, the hybrid system proves interesting for a wide range of feed compositions. For MMR above 5 and certainly above 10, the total cost of produced water is negative, resulting in a net profit.

4 Conclusions

Ever more stringent regulations on discharge, the need for more and purer water and the decrease in available water sources push existing water treatment technologies to the limit. In this research, a hybrid IEX-RO system was introduced to increase the achievable RO recovery by pre-treating the feed stream and thus removing multivalent cations, without addition of anti-scalants. The hybrid technology had already proven to be feasible on lab-scale, and this research presents the pilot-scale results. The major conclusions are:

- By implementing an IEX pre-treatment before RO, the singe-pass RO recovery can easily be increased to at least 85%.

- Increasing the RO recovery does not increase the IEX regeneration efficiency. In other words, the concentrate volume is not important, the regeneration efficiency will be similar as long as the total amount of monovalent cations in the concentrate stays the same.
- The MMR in the feed water is the only factor determining the IEX regeneration efficiency and thus the viability of the system. When the MMR in the feed increases, the IEX regeneration efficiency increases as well.
- By adding a limited amount of NaCl to the RO concentrate, the full capacity of the IEX resin can be restored. This amount can be estimated theoretically based on simple measurements of the incoming water hardness and the monovalent ion concentration of the feed.
- Compared to stand-alone RO, operating at 75% recovery, a hybrid system including IEX regeneration with the concentrate operating at 85% recovery is more economically interesting. The revenue increases from 0.52 €/m³ to 0.69 €/m³.
- The hybrid system is interesting for a wide variety of feed waters. Both the RO energy demand and the MMR play an important role in the economic assessment.

Overall, the hybrid IEX-RO system does seem applicable to a range of brackish and fresh water qualities and for the reuse of secondary treated wastewater effluent. Not only does it increase the possible RO recovery, it also avoids the use of expensive and environmentally unfriendly anti-scalants. Continued research will need to focus on implementing this technology with other feed waters and at a larger scale. Furthermore, the influence of the resin type needs to be investigated.

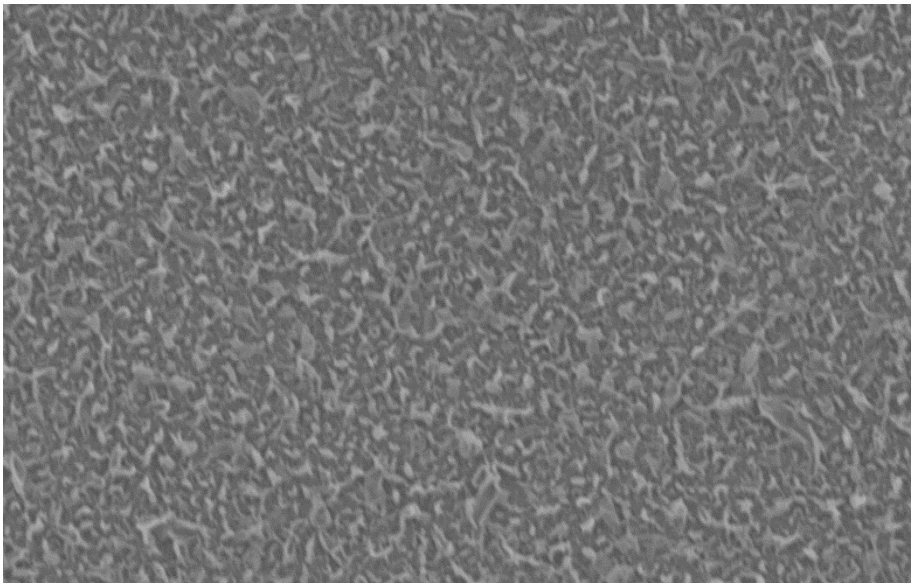

Part 2: Salinity gradient power as a pre-treatment step to increase RO energy efficiency

Picture: SEM of an RO membrane (10 000X magnification)

Chapter 4: Opportunities to decrease seawater reverse osmosis energy demand

This chapter has been published as

Vanoppen, M., Blandin, G., Derese, S., Le Clech, P., Post, J., Verliefde, A.R.D. Chapter 9: Salinity gradient power and desalination, in: Cipollina, A. & Micale, G. (2016) Salinity gradient power and desalination. Sustainable energy from salinity gradients. London: Woodhead publishing, Elsevier.

1 Introduction

With the world population ever increasing, water scarcity and resource depletion have become pressing problems. In 2015, 660 million people worldwide lacked access to improved drinking water sources, being forced to use unprotected wells, springs and surface water [68]. With freshwater resources being increasingly limited, depleted or contaminated, the use of alternative water resources such as desalinated seawater and recovered wastewater for drinking water purposes are highly studied. So far, the focus has shifted more to seawater, a seemingly endless source of clean water. Today, more than 60% of the installed desalination capacity worldwide operates on seawater and in 2018, desalinated water production is forecasted to exceed 36 million m^3 [36,69,70]. However, seawater desalination remains energy intensive, limiting its broader application. As energy consumption is expected to grow by 50% between 2007 and 2035, the water-energy nexus forces researchers to look for more energy efficient ways to desalinate seawater. This chapter introduces and discusses the hybridisation of seawater reverse osmosis (SWRO) with electrochemical and pressure driven membrane processes for a more energy efficient seawater desalination process.

2 State-of-the-art seawater desalination

Originally, seawater desalination was developed to provide drinkable water and steam aboard ships. The first large-scale desalination plants emerged around the 1950s to desalinate seawater in the Middle East, an arid region suffering from water shortages [33]. These early plants were based on thermal desalination processes; that is, multistage flash (MSF) and multieffect distillation (MED). However, due to their high energy demand (20-37 kWh/m^3 for MSF and 14-30 kWh/m^3 for MED [71,72]), membrane-based processes have gained popularity as alternative technologies for seawater desalination. The fastest growing technology in this respect is RO, which has taken a world-wide leading position due to its lower water production costs and energy demand [73]. Seawater RO specific energy consumption (SEC) has decreased from around 16 kWh/m^3 in 1970 to as low as 2.2 kWh/m^3 in state-of-the-art desalination plants operating at 50% water recovery [33,36,74]. The RO recovery (R) is defined as the ratio of the produced water flow rate (Q_p, m^3/h) to the feed flow rage (Q_f, m^3/h) (Eq. 4.1).

$$R = \frac{Q_p}{Q_f} \tag{4.1}$$

Some pilot plants have even demonstrated RO desalination energy consumption as low as 1.8 kWh/m³ [69,72]. Further improvements are theoretically possible but limited, as the thermodynamic limit of SEC is 1.06 kWh/m³ when considering seawater at 35 g/l TDS as RO feed and operation at 50% RO recovery [36,72].

The observed decrease in energy consumption over the last decades is mainly due to optimisation of the RO process itself. In RO, the main source of energy consumption is connected to the hydraulic pressure needed to overcome the osmotic pressure, to allow water to permeate through the membranes and to overcome the frictional losses inside the membrane modules. Important optimisations have been implemented in the RO design, both on a module level – using mathematical models and computational fluid dynamics to limit pressure drop and promote mass transfer phenomena – as well as on the overall RO setup by adapting the design to a multistage system [75]. Furthermore, the development of highly permeable membranes has allowed the limitation of hybraulic resistance to water transport, allowing the water to pass the membranes more easily, further reducing the energy required [76]. Finally, one of the most important breakthroughs in limiting RO energy use is the implementation of intelligently engineered energy recovery devices that are currently able to recovery up to 95% of the pressure energy still contained in the produced concentrate, and use it to pressurize the feed water [77,78]. Besides the improvements to the RO process itself, additional efforts were put into the pre-treatment systems, to further limit RO fouling (organic fouling, scaling), to protect the membranes, and to avoid the decrease of performance of time. All of these improvements led to a significant decrease in RO energy consumption and to the optimisation of RO operation; however, at the cost of additional capital expenses (CAPEX). Moreover, the amount of energy needed is still substantial and undesirable if a sustainable desalination process is envisioned. Elimelech and Phillip (2011) concluded that future energy savings in seawater RO will have to focus on pre- and post-treatment, because actual RO energy demand is already very close to the thermodynamic limit. Decreasing the need for pre- and post-treatment requires the development of novel membranes with higher selectivity (e.g. for boron) and fouling resistance, a daunting task that entails the development of new surface chemistries.

For the majority of the currently operational RO desalination plants, energy represents on average about one-third of the total desalination cost, another third being due to capital costs, and the last third attributed to all other operational costs (maintenance, labour, …) [79]. It has to be mentioned that not all these costs are directly related to the RO itself, as important

costs can be associated with pre- and post-treatment (i.e. energy consumption of pre-treatment can exceed 1 kWh/m³). On average, the cost of seawater desalination with RO is estimated to be 0.7 €/m³, but values fall within a wide range of 0.5-2 €/m³, depending in particular on the local energy cost, quality of feed stream and installation site [70].

3 RO hybridisation for an increased energy efficiency

3.1 Improved water management by the combination of different water sources

Diversification of water sources for all types of water usage (potable, irrigation, industrial, …) has been established as a key evolution in water management, especially in regions facing water scarcity or droughts [80]. Current water managements strategies clearly mention the importance of increasing both water reuse and seawater desalination capacities to battle water shortage. As 40% of the world's population lives in coastal areas, these highly populated regions bring together many different water sources of different salinity levels (river water, wastewater, treated wastewater, seawater, …). This means that the effluent of wastewater treatment plants and seawater intake points will often be very close. Due to the proximity of different water sources and the occurrence of water scarcity, both desalination and water reuse will have a role to support water demand in these regions. Examples of coexistence of water reclamation and seawater desalination facilities already exist (Singapore, California, Australia), but so far have not been combined.

The combination of water reclamation and desalination appears naturally attractive in these dry urban coastal areas. To integrate a useful application of impaired water with RO seawater desalination, SGP and osmotic dilution (OD) technologies can be used. SGP harvests the energy from a salinity gradient through the use of membranes either by allowing the transport of salts (reverse electrodialysis, RED) or water (pressure retarded osmosis, PRO) along their natural concentration gradient. In osmotic dilution technologies, these same membranes are used in a different configuration in forward osmosis (FO), short-circuited RED (scRED) (i.e. there is osmotic dilution, but no energy generation), assisted RED (ARED) and pressure-assisted osmosis (PAO) (i.e. there is osmotic dilution, aided by a small additional externally provided driving force). These technologies will be discussed further in Section 3.3.

When using SGP or OD technologies as a pre-treatment to RO, a suitable low-salinity water source has to be identified. Considering the water management scheme shown in Figure 4.1, reusing impaired water (e.g. secondary treated effluent) would make sense, as this is often

discharged directly into the sea in coastal areas. However, contaminants present in the impaired water represent a risk to the RO system (i.e. contamination of the produced water and fouling or scaling of the RO membranes). Fouling and rejection of contaminants in SGP and OD technologies are two main topics to be considered when looking into the SGO/OD-RO hybrid. Considering that direct reuse of impaired water is often not desired or allowed, creating a double barrier integrating SGP/OD and RO offers the opportunity of integrating impaired water into the water production scheme.

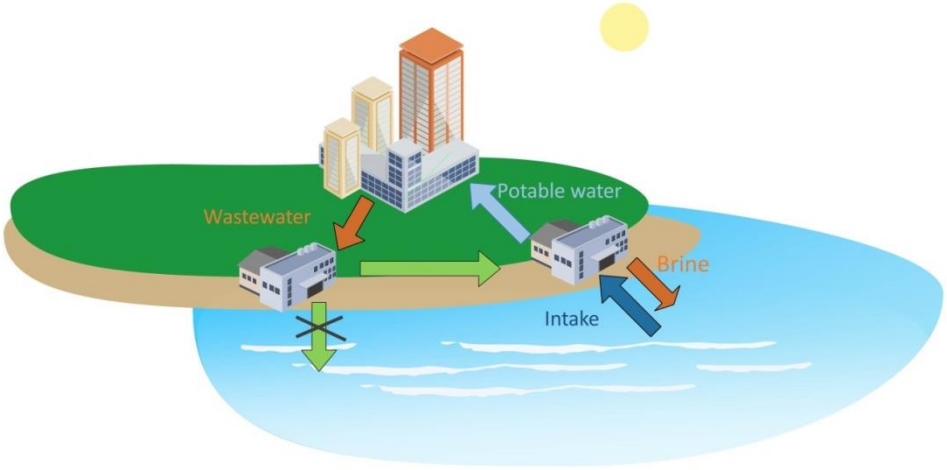

Figure 4.1 Conceptual drawing of the opportunities of combining water reuse and desalination.

3.2 Theoretical considerations for the hybridisation of RO with SGP/OD

Typically, two approaches to SGP/OD-RO hybrids may be considered (although many variations to these two basic approaches are possible): (1) SGP or OD can be used to decrease the salinity of the seawater, using a low-salinity impaired water stream for a pre-dilution within the SGP/OD unit before entering the RO unit to decrease RO energy demand, whilst some energy is also recovered if SGP is used; and (2) the unused osmotic energy in the RO concentrate is harvested by SGP to recover energy. The advantages of coupling SGP/OD with RO are twofold: (1) a lower concentration of the seawater/concentrate entails a lower osmotic pressure, resulting in a lower energy demand for desalination or facilitating the brine discharge and decreasing its environmental impact [81–83]; and (2) the produced energy in case of SGP can be used on-site to further decrease the overall net energy requirements of the desalination process [84]. Both options are shown in Figure 4.2 and Figure 4.3. Although mixing RO concentrate with an impaired water source, as shown in Figure 4.3, allows for a higher energy density than mixing the concentrate with seawater, the availability of impaired water might be limited. As an alternative, integrating the two concepts into a single hybrid process allows the use of the brackish impaired water from

the first SGP/OD step into the second SGP/OD unit for the dilution of the RO concentrate, as shown in Figure 4.4.

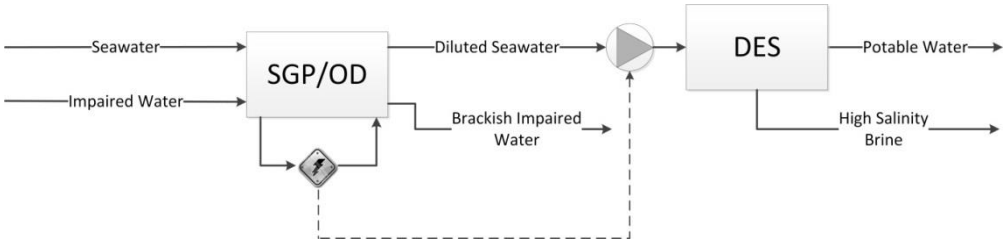

Figure 4.2 Hybridisation of SGP/OD technologies as pre-treatment for RO ro reduce RO energy demand (SGP = salinity gradient power, OD = osmotic dilution, DES = desalination).

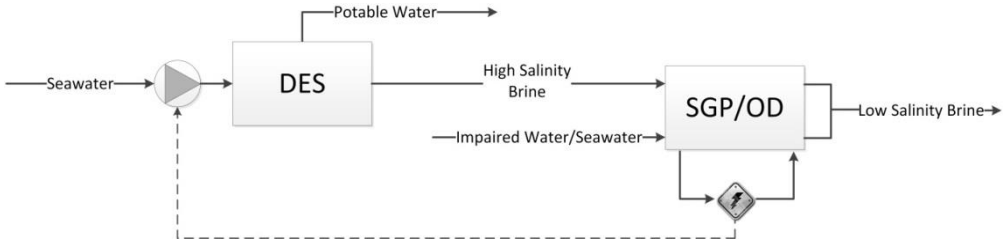

Figure 4.3 Hybridisation of SGP/OD technologies as a post-treatment for RO to reduced RO energy demand (DES = desalination, SGP = salinity gradient power, OD = osmotic dilution).

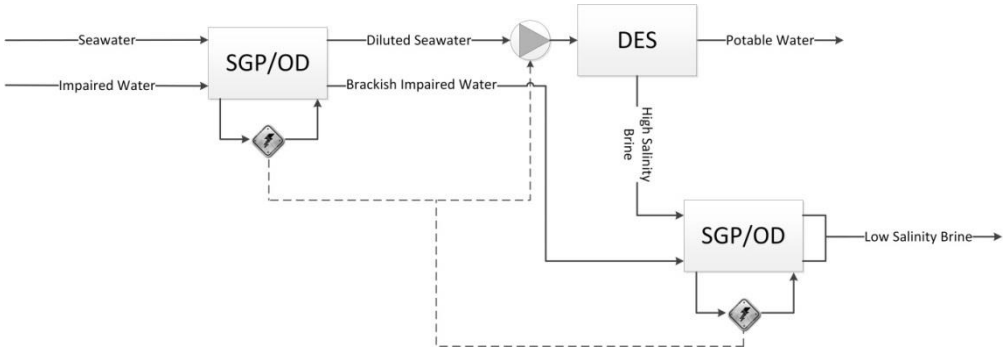

Figure 4.4 Envisioned hybrid technology incorporating salinity gradient power (SGP) or osmotic dilution (OD) devices to decrease the RO energy demand (DES = desalination).

In the pre-treatment step, focus is not only on energy production (if SGP is used), but also on decreasing the seawater salt concentration. In the post-treatment step, the goal is to recover as much of the remaining salinity gradient power as possible. OD technologies are only of interest here if the resulting diluted RO concentrate can be reused in the process itself.

Optimisation of the proposed hybrid requires the study of several operational parameters that control both the amount of energy harvested and the extent of pre-dilution obtained [42,85,86]:

- The mixing ratio (MR): it represents the ratio of fresh (impaired) water versus seawater (Q_{iw} and Q_{sw}, in m^3/h, respectively) used:

$$MR = \frac{Q_{iw}}{Q_{sw}} \tag{4.2}$$

  When SGP is used as a pre-treatment step, higher MRs of impaired water versus seawater will result in a higher extent of pre-dilution (lower concentration of the diluted seawater) and a higher possible energy recovery in the first SGP step. However, this will also entail an additional energy cost for the possible pre-treatment and pumping of the impaired water before entering the SGP step. Furthermore, the availability and recovery of impaired water will be a determining factor in the system, as overall water balances in water scarce regions will limit the achievable MR in practice.

  In the post-treatment SGP step, the MR will mainly depend on the low-salinity stream selected for mixing. Both seawater and impaired water are an option here. The lower concentration of the impaired water would entail a higher energy production when compared to seawater. However, the MR would again be limited by the impaired water availability. Although the concentration of seawater is higher, its virtually unlimited availability enables higher MRs. The use of fresh streams, either seawater or impaired water, will entail an increased pre-treatment cost.

  When considering the full hybridisation, the brackish impaired water from the first SGP/OD step could be used, and the attainable MR would depend on this first step.

- The extent of mixing: the effective extent of mixing (termed SGP or OD recovery) achieved by the SGP/OD step can be expressed as the fraction of salt removed (Δn_{NaCl}, mol/h) compared to the maximal removable amount ($\Delta n_{NaCl,max}$, mol/h) for electrochemical SGP/OD processes, and as the amount of water transported (Δn_{H2O}, mol/h) with respect to the maximum transportable amount ($\Delta n_{H2O,max}$, mol/h) for osmotic SGP/OD processes (equations 4.3 to 4.7).

$$R_{EC} = \frac{\Delta n_{NaCl}}{\Delta n_{NaCl,max}} \tag{4.3}$$

$$\Delta n_{NaCl,max} = Q_{sw} \cdot (C_{sw,in} - C_{eq}) = Q_{iw} \cdot (C_{eq} - C_{iw,in}) \tag{4.4}$$

$$R_O = \frac{\Delta n_{H_2O}}{\Delta n_{H_2O,max}} \tag{4.5}$$

$$\Delta n_{H_2O,max} = \frac{(C_{sw,in} - C_{iw,in}) \cdot Q_{iw,in}}{MR \cdot C_{iw,in} + C_{sw,in}} \cdot \frac{1000 \cdot \rho_{H_2O}}{MW_{H_2O}} \tag{4.6}$$

Similarly as Equation 4.4, Equation 4.6 is based on the amount of dilution of the seawater needed to achieve the equilibrium salt concentration, taking into account the mixing ratio MR. The factor $(1000 \times \varrho_{(H2O)})/(MW_{(H2O)})$ in mol/m³, with $\varrho_{(H2O)}$ the density of water (kg/m³) and MW_{H2O} the molecular weight of water (g/mol), is needed to convert the volumetric flow rate to a molar flow rate of water.

$$C_{eq} = \frac{MR \cdot C_{iw,in} + C_{sw,in}}{MR + 1} \tag{4.7}$$

Where R_{EC} and R_O are the recovery of electrochemically and osmotically driven processes, respectively. $C_{sw,in}$ and $C_{iw,in}$ (mol/m³) are the incoming seawater and impaired water concentrations, respectively, while C_{eq} is the equilibrium concentration, reached at complete mixing of both streams. In theory, complete mixing until equilibrium (whereby the osmotic pressure on both sides is the same) is possible, but in practice this will require infinite time and/or membrane area. Indeed, when considering SGP/OD technologies as a pre-treatment for RO, the extent of mixing will determine the salt concentration going to RO. A lower salt concentration means a lower energy demand in RO, but also a larger required membrane area in the pre-treatment. A good trade-off between energy savings and membrane costs will have to be found. If SGP is implemented as a post-treatment, again the consideration is between the produced energy and the required membrane area.

In general, when considering equal membrane areas, the mixing extent for the considered processes (considering a single pass configuration) normally decreases in this order: PAO/ARED > FO/scRED > PRO/RED. Combining SGP with or replacing SGP by other OD technologies could thus limit the required investment costs (because of the lower required membrane area), but an optimisation between reduced energy recovery in the system and overall system costs is necessary. This optimisation will depend mainly on the local conditions and on the specific requirements of the hybrid system.

- RO recovery (R): as the salt concentration in the feed will be decreased by pre-dilution, operation of the RO at higher recoveries is theoretically possible. The overall RO recovery can be calculated by Eq. 4.1. As an example, recovery in traditional seawater RO is usually limited to 50% due to limitations in hydraulic pressure and possible scaling. Decreasing the RO feed salt concentration by a factor 2 for example, theoretically allows the RO recovery to be increased to 75% without suffering of the above limitations.

Several studies [42,43,85,87,88] have already indicated the theoretical potential of the above-mentioned hybrid configurations. While Li et al. (2013) showed the potential of different combinations of RED and RO, Feinberg et al. (2013) also included PRO in their study. Both show that it is even theoretically possible, based on thermodynamics, to obtain an energy-neutral and even energy-producing seawater desalination system in this way. In a previous study [42], we also included OD technologies, and added practical loss factors (due to imperfect thermodynamic reversibility of the processes). It was shown that, even when accounting for irreversible system losses, and with current state-of-the-art SGP technology, a significant decrease in energy demand of RO desalination is possible, even when including only an SGP pre-treatment step. Energy considerations for the hybrid processes will be discussed in Section 4.

3.3 Comparison of the different SGP/OD technologies

The main difference between PRO and RED is their physical mode of operation, as shown schematically in Figure 4.5. In PRO, water is transferred from the low-salinity source to the seawater, allowing for a higher overall water recovery in a hybrid PRO-RO system. However, although the PRO membranes provide a physical barrier to possible pollutants from reclaimed water, this means that the low-salinity source water is indirectly used for the

production of drinking water in the RO stage, which might cause some social acceptance issues. At the contrary, in RED, the low-salinity source is only used as a sink for the ions coming from the seawater. Ideally, no water from the low-salinity source passes to the seawater side. This results in a lower overall recovery of the hybrid system, but avoids water from (treated) wastewater ending up into the RO system.

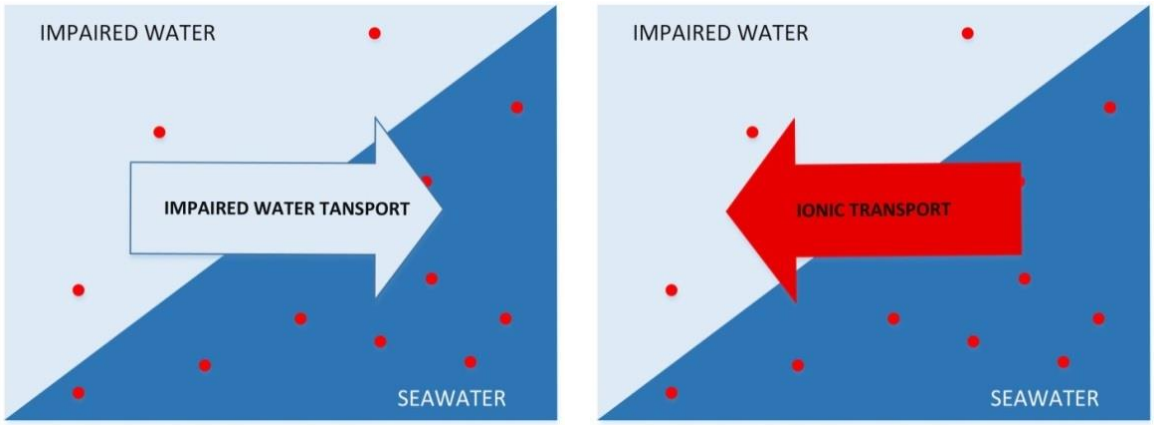

- Higher water recovery
- Added barrier for impaired water
- Reuse of impaired water

- Lower water recovery
- Impaired water acts as ions sink
- No reuse of impaired water

Figure 4.5 Comparison between PRO and RED as a pre-treatment option for RO.

As already mentioned, OD technologies serve as a valuable option to complement SGP technologies in RO hybrid schemes. In general, OD differs from SGP technologies as no energy is generated in the former. Instead, a small amount of energy can be added to achieve an increased dilution rate. A schematic overview of these OD-RO hybridisations in comparison to the SGP-RO technologies is shown in Figure 4.6. The main desired result in OD is a faster transport rate of salts or water, resulting in a decreased membrane area and consequently, in lower overall CAPEX. Depending on the type of SGP/OD technology used, and the local context in terms of energy cost, these OD-RO systems might even be more economical than SGP-RO systems.

FO (Figure 4.6A) differs from PRO (Figure 4.6B) as the priority is given to the permeation flux rather than to the production of energy. In PRO, fluxes are typically lower than in FO as the applied pressure on the draw solution decreases the driving force for water transport. Typically, when considered as a pre-treatment for RO, FO will lead to a higher degree of dilution than PRO and thus more energy reduction in the RO step. In addition, considering that the hydraulic turbine to recover energy is not required, FO might represent a more cost-effective alternative to PRO. This of course depends largely on current and future energy

prices. To further enhance dilution fluxes and decrease the required membrane surface area, it is possible to pass to a third scheme (Figure 4.6C). In this PAO configuration, a moderate hydraulic pressure is applied on the impaired water side, to add an extra hydraulic pressure driving force to the natural osmotic driving force.

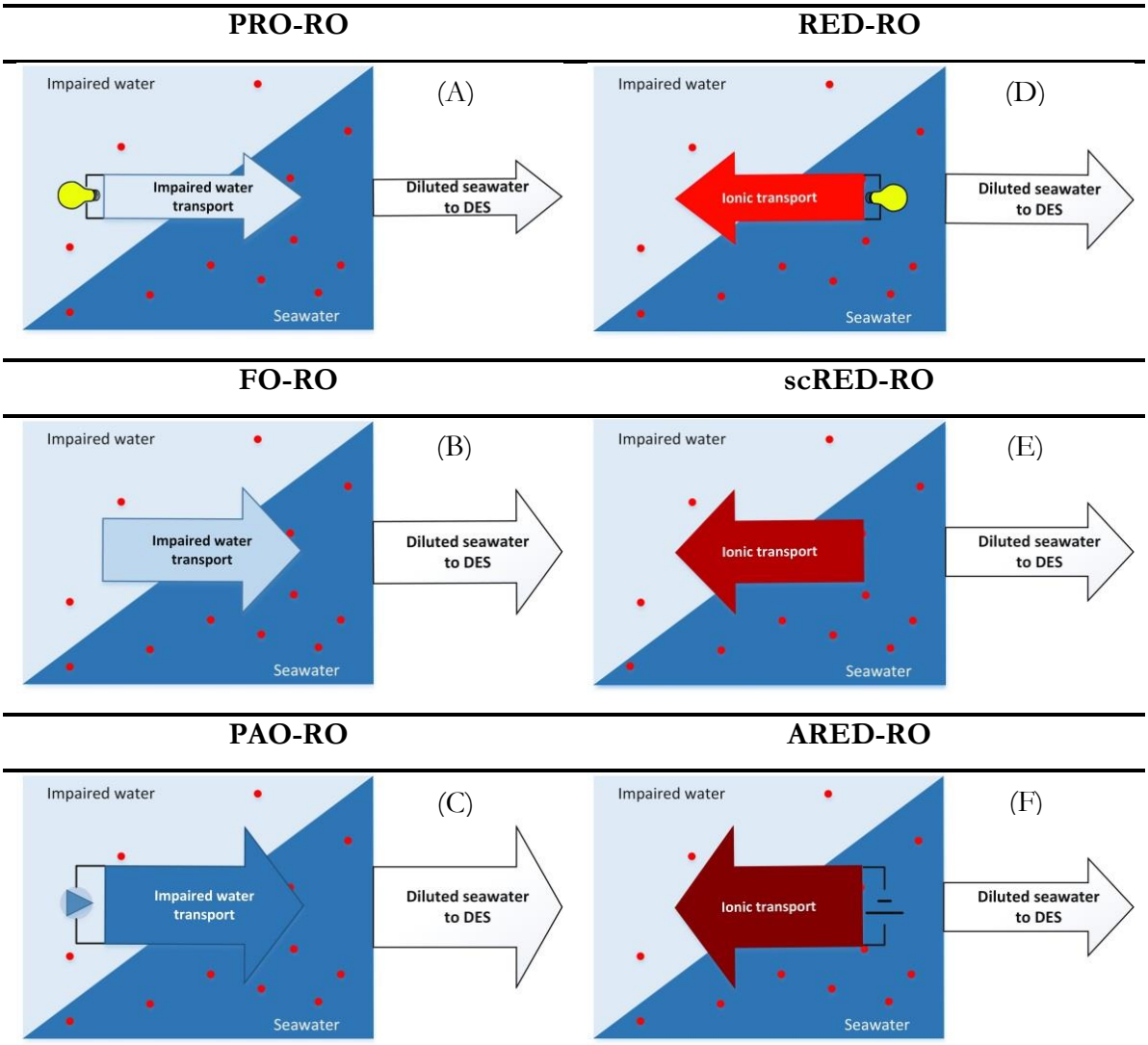

Figure 4.6 Schematic overview of the six possible SGP/OD-RO hybridisations. (A) pressure retarded osmosis – RO, (B) forward osmosis –RO, (C) pressure assisted osmosis – RO, (D) reverse electrodialysis – RO, (E) short-circuited reverse electrodialysis – RO, (F) assisted reverse electrodialysis – RO.

Similar concepts can be developed for RED (Figure 4.6D). In scRED (Figure 4.6E), dilution of seawater is achieved solely through the passage of salts through the IEMs. No external driving force is applied, the electrodes are short-circuited, and salt transport becomes solely driven by the electrochemical potential difference between the seawater and the low-salinity stream. Although no energy is produced here, the dilution process takes place faster than in RED, due to the higher current density related to the absence of an external resistance. Another RED-related option is ARED (Figure 4.6F). In ARED, a small electrical potential is

used to enhance the ion transport through the membrane from high to low salinity streams. This results in an even faster pre-dilution process, further reducing the required membrane area.

A theoretical comparison of the different SGP and OD processes is shown in Figure 4.7. The figure on the left (Figure 4.7A) shows the osmotically driven processes, including RO, PRO, FO and PAO. On the right (Figure 4.7B), electrochemically driven processes are shown, including ED, RED, scRED and ARED. The most important parameter here is the direction of water/ions flux. A positive flux is defined as a flux against the concentration gradient (i.e. from low to high salinity for ions and vice versa for water) and is thus not desirable for dilution purposes, while it is typical of RO and ED desalination processes. In all other schemes, the flux is negative, providing an effective decrease in the seawater concentration.

Similarly, in Figure 4.8, a comparison is made between the different energy production/requirements in all SGP/OD processes. As discussed before, PRO and RED generate power, though allowing low dilution fluxes; FO/scRED do not required any external energy input, allowing a larger flow of water/ions according to the natural salinity gradient; while for PAO and ARED, an additional energy input is needed, enhancing the water/ions flux according to the natural salinity gradient and resulting in a faster dilution.

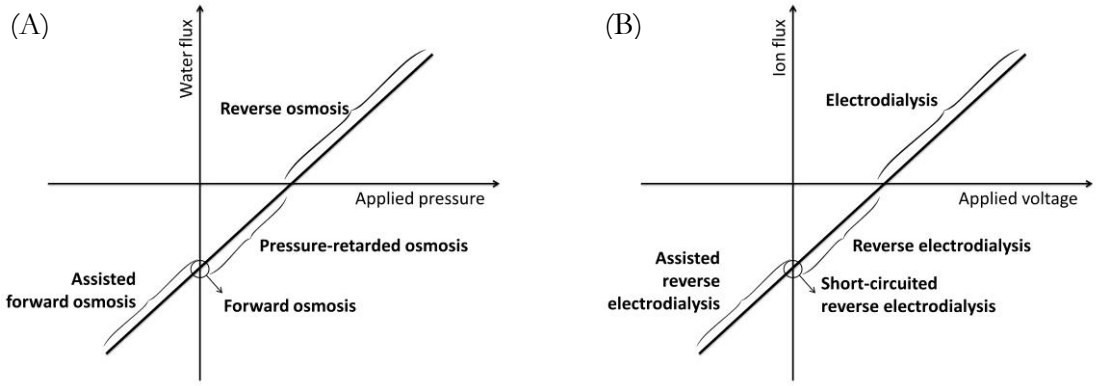

Figure 4.7 Comparison between (A) osmotic and (B) electrochemical desalination/dilution processes.

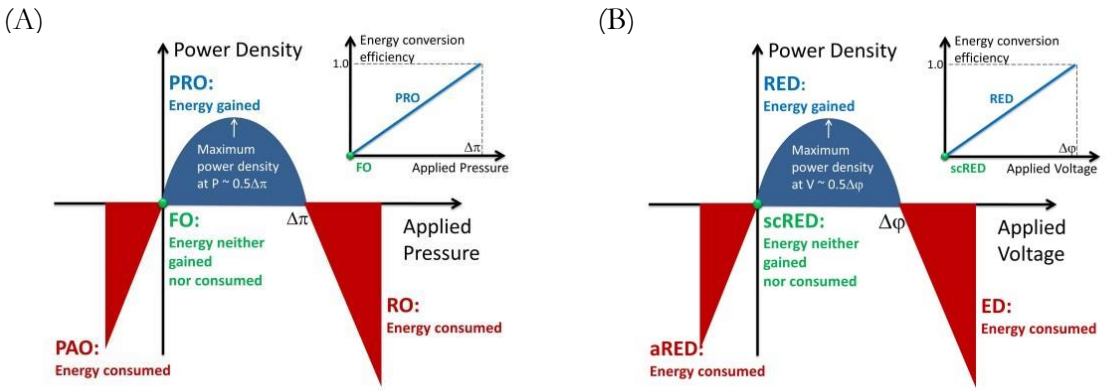

Figure 4.8 Energetic comparison between osmotically driven (A) and electrochemically driven (B) desalination processes.

Several studies have demonstrated the potentials of the FO-RO concept for energy reduction in seawater desalination, whereby typically (treated) wastewater is used as a low-salinity solution [79,89,90]. A 30% energy reduction for FO-RO is currently considered feasible, when the FO recovery is 50% (this means that the FO permeate is equal in volume to the feed seawater stream). Lab-scale demonstrations of the concept have shown a specific energy decrease for RO seawater desalination from 2.5-4 kWh/m³ down to 1.5 kWh/m³ with the FO-RO hybrid at high MR [91].

FO-RO schemes thus demonstrate promising potential because they can uniquely combine water reuse and desalination, and have the advantage of a double-barrier protection against pollutants from the impaired water and of decreasing membrane fouling risks [89,92]. Due to the current limitations of low permeation flux for presently available FO membranes, the concept of PAO (also called assisted forward osmosis of pressure enhanced osmosis) has been recently developed [93–95]. The PAO concept, despite its additional energy needs for pressurisation of the low-salinity stream, demonstrated to be economically relevant when compared to FO-RO, thanks to significant savings in FO plant capital costs, mainly related to required membrane surface area [79].

Similar to PRO, RED is limited by a relatively low ion flux and high required membrane area. Therefore, also in this case, two variations of the RED technology have been recently proposed an analysed, namely scRED and ARED. However, though some promising outcomes of theoretical modelling work were obtained [42], they have not received much attention in the scientific literature yet.

4 Efficiency analysis of proposed hybrids

The coupling of SGP and OD technologies with RO was modelled. A semi-empirical numerical model based on first principle equations with empirically determined parameters was implemented.

The minimal energy needed to achieve desalination can be calculated based on thermodynamic considerations. Figure 4.9 shows the specific energy consumption (SEC, kWh/m³) for different RO recoveries (R), assuming a seawater concentration of 35 g/l TDS. These calculations are based on the energy of mixing, which originates from the entropy of mixing, given by the following equation (for a reference volume of 1 m³):

$$\Delta S_{mix} = -n \cdot R_g \sum_{0}^{i} x_i \cdot \ln(x_i) \tag{4.8}$$

Where n is the amount of moles in the solution (mol), R_g is the universal gas constant (J/mol.K), and x_i is the mole fraction of component i. From this entropy of mixing, the energy needed to separate a salt solution into its components can be calculated:

$$\Delta G_{sep} = T \cdot \Delta S_{mix} \tag{4.9}$$

With T the absolute temperature (K). The thermodynamically determined SEC (in kWh/m³) ranges from about 0.6 kWh/m³ (at low recoveries) to almost 2 kWh/m³ (R = 90%). At a recovery of 50%, the thermodynamic SEC is 1.06 kWh/m³. Modern RO systems are already very close to this limit (1.8 – 2.2 kWh/m³). In other words, from a thermodynamic point of view, RO is not very energy intensive. However, considering the energy-water nexus, the energy demand for seawater desalination is still substantial and a decrease in this energy demand, beyond the thermodynamic limit for stand-alone desalination, would be desirable.

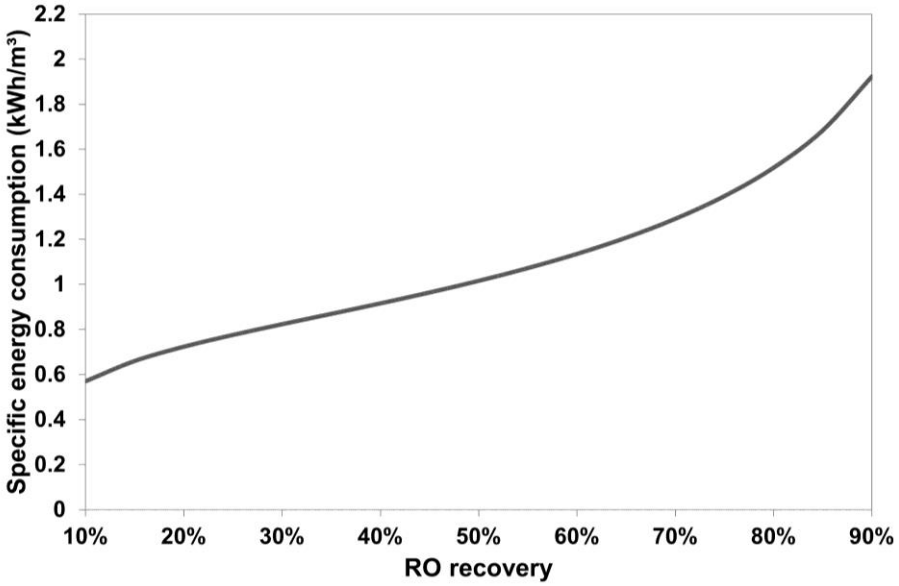

Figure 4.9 Theoretical specific energy consumption of RO at different process recoveries.

Concerning the energy consumption predicted by the model for the SGP-RO schemes, Figure 4.10 shows the ideal (i.e. neglecting any non-ideal phenomena affecting the performance of the real systems) SEC for both RED-RO and PRO-RO as a function of SGP recovery (R_{EC} and R_O) and at different mixing ratios (MR), fixing an RO recovery of 50%. This figure shows that the hybrid systems can significantly reduce the system SEC and could theoretically be even energy-producing when operated at MRs of 1 and 2 for a high SGP recovery. It also shows that, although the SEC for RED and PRO hybrid schemes is the same when approaching the equilibrium dilution, it differs for intermediate SGP recoveries. This difference is caused by the physical difference between the dilution mechanisms in the two processes. This causes the seawater salt concentration to decrease faster as a function of transported salt (and thus recovery) in RED than of transported water in PRO, which is why RED-RO shows a lower SEC at intermediate SGP recovery.

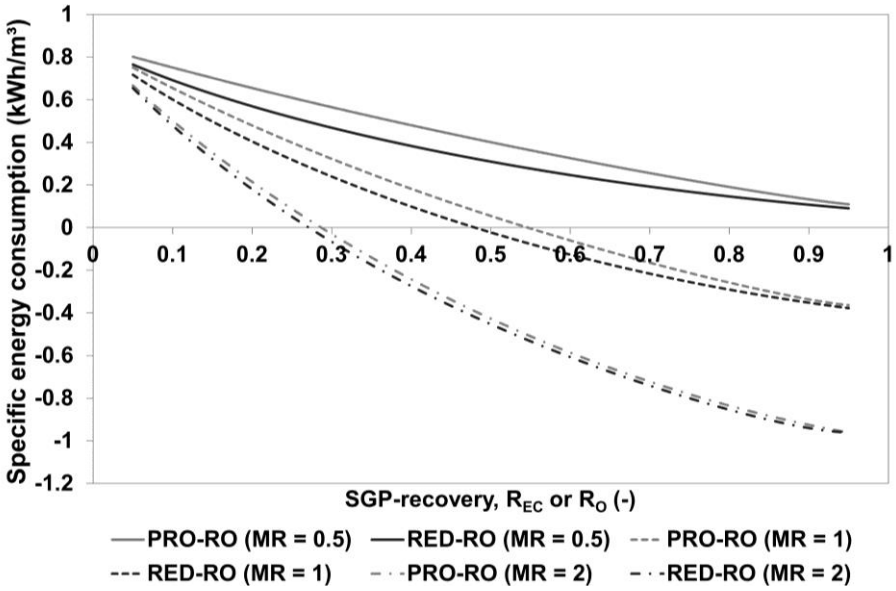

Figure 4.10 Theoretical SEC for PRO-RO and RED-RO at three different mixing ratios (0.5, 1 and 2) at a RO recovery of 50% (MR = mixing ratio).

In reality, SGP/OD systems are faced with non-ideality losses that will decrease the actual energy efficiency of the hybrid desalination systems. For example, in osmotic processes, water transport through the membrane is limited by internal and external concentration polarisation [84,96]. The reverse salt diffusion (RSD, i.e. diffusion of solute from the seawater to the impaired water) is also responsible for a reduction of the osmotic pressure driving force [97]. Despite intense research and significant improvements in membrane materials (e.g. manufacturing of more selective membranes, thinner support layers, …), flux limitation remains an issue in commercially available osmotic membranes, as shown by several researchers [98–104]. This results in low power densities for PRO and low permeation fluxes in FO, affecting the economic viability of these processes.

On the other side, the efficiency of electrochemically driven processes can be limited also by water transport through the membranes, reducing the driving force for ion transport. Furthermore, the presence of multivalent ions (e.g. Ca^{2+}, Mg^{2+}, SO_4^{2-}, PO_4^{3-}, metals, …) in the impaired water can reduce the overall energy efficiency by uphill transport and membrane plugging phenomena [105,106]. An overview of the most important non-ideality losses for both processes is given in Table 4.1.

Table 4.1 Major non-ideality factors influencing the overall energy efficiency of both PRO/FO/PAO and RED/scRED/ARED.

PRO/FO/PAO	RED/scRED/ARED
Concentration polarisation	Concentration polarisation
Reverse salt diffusion	Water transport
Transmembrane pressure losses	Co-ion transport
Parasitic friction losses	Parasitic friction losses
Module and pumping inefficiencies	Membrane and solution resistance

Thus, in order to allow a more realistic modelling approach, the main non-ideality factors above mentioned were also considered, and the operation of real membrane modules has analysed. In particular, it was assumed that 90% of the applied hydraulic pressure is retained in the RO concentrate and pressure exchangers with an efficiency of 98% were used. Pumps were assumed to have an efficiency of 95%.

For RED/scRED/ARED, a module consisting of 50 cell pairs of 0.5x0.5 m^2 membrane area was assumed, with compartment thicknesses of 0.2 mm (including spacers with a shadow factor of 0.6) for both seawater and impaired water compartments. For the properties of the IEMs, the characteristics reported for Neosepta AMX-SB and CMX-SB membranes were used.

For PRO/FO/PAO, modules with 4 m^2 of membrane area were implemented, assuming the membrane properties of the HTI CTA-W membrane. The flow channels were assumed to be spacer-filled, with a specific surface of 11 600 m^2/m^2 and a porosity of 90%.

For all processes, modules were added in series until the desired recovery was reached. NaCl solutions with a concentration of 0.5M and 0.01M were considered as seawater and impaired water feed streams, respectively. A complete overview of the equations and assumptions used can be found in Appendix B.

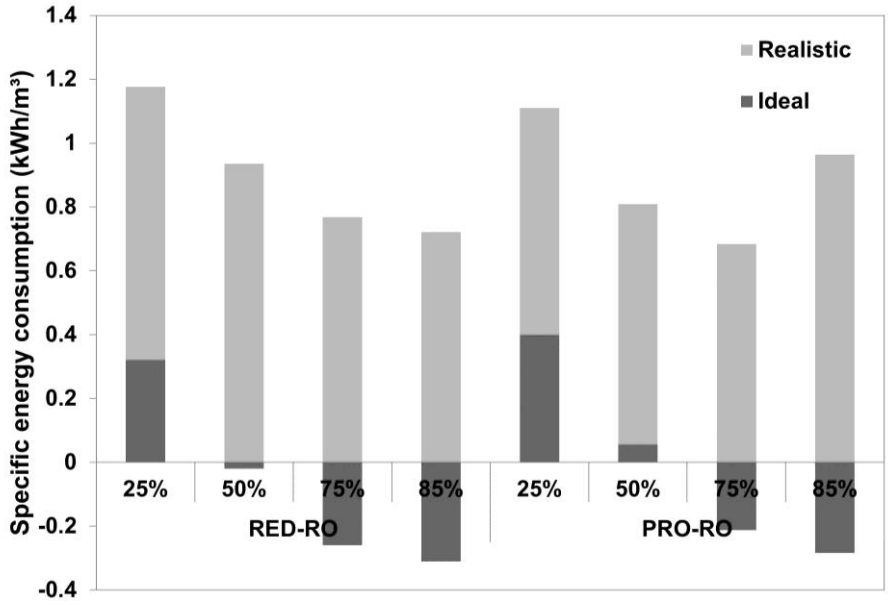

Figure 4.11 RED-RO and PRO-RO specific energy consumption at different SGP recoveries. 50% RO recovery and unitary MR are fixed. An 85% SGP recovery was identified as the practical upper limit.

SEC values predicted under such "more realistic" conditions are compared to the previously reported ideal values in Figure 4.11, which shows the SEC at different SGP recoveries, with the RO recovery fixed at 50% and the MR at 1. These figures show that the hybrid processes are no longer energy neutral when accounting for non-idealities. At low and intermediate SGP recoveries, PRO-RO seems to be slightly more energy efficient. At high SGP recovery, the energy efficiency is higher for RED-RO, which suffers less from pressure losses in each module. Although the losses associated with state-of-the-art SGP operation prevent the hybrid from being energy neutral, the coupling of SGP and RO still results in a significant decrease in energy requirements when compared to current state-of-the-art RO. At high SGP recoveries, a SEC below the thermodynamic limit of 1.06 kWh/m³ can even be reached.

Figure 4.12 compares the SGP-RO hybrid schemes to the associated OD-RO schemes previously discussed. All processes are compared at 50% RO recovery, unitary MR and maximal SGP/OD recovery (i.e. R_{EC} or R_O = 85%). Clearly, from an energetic point of view, the PRO-RO and RED-RO hybrids are preferred. Even, taking into account major non-ideality factors, the SGP-RO hybrids can achieve a SEC around 1 kWh/m³ (PRO-RO) and 0.75 kWh/m³ (RED-RO). For the OD-RO hybrids, the SEC falls just below 1 and 1.1 kWh/m³ for scRED-RO and FO-RO, respectively. The energy demand for ARED-RO and PAO-RO is, as expected, slightly higher and predicted around 1.2 kWh/m³ for both processes. These technologies were modelled assuming an additional external driving force

with a magnitude equal to 20% of the natural driving force (salinity gradient) between the seawater and the impaired water.

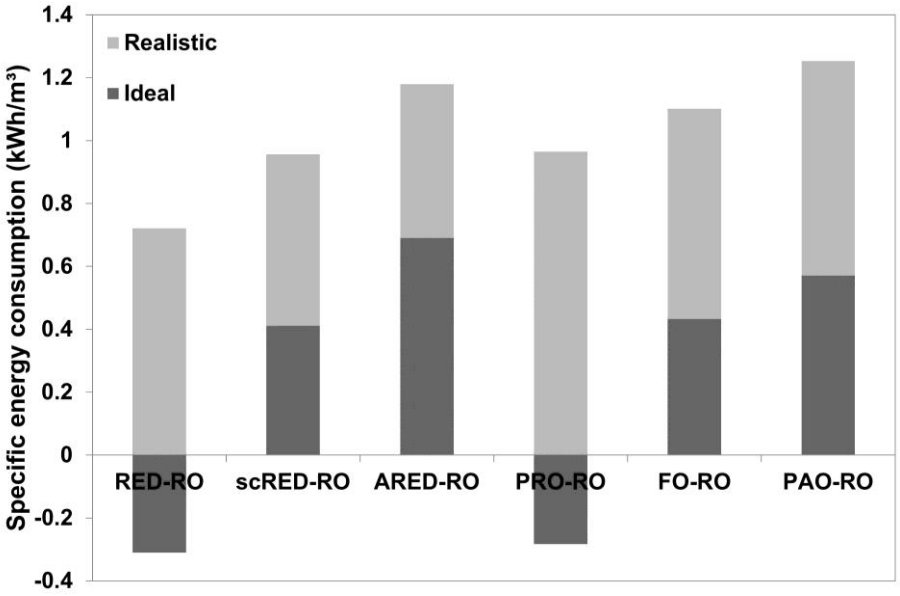

Figure 4.12 Specific energy consumption for all different SGP/OF-RO hybrids at 50% RO recovery, unitary MR and maximal SGP/OF recovery (85%).

Although OD technologies present slightly higher energy consumptions, they still achieve a significant reduction in SEC compared to the current state-of-the-art RO energy demand of around 2 kWh/m³ at 50% recovery. Moreover, OD technologies require a lower membrane surface area to achieve the same mixing extent as SGP-RO, thus requiring lower CAPEX.

This is shown in Figure 4.13, indicating the required membrane area per m³/h of water production capacity for the SGP/OD technologies in the above-discussed scenarios. Notably, the membrane area required in electrochemically driven processes is up to 10 times higher than for osmotically driven processes. Furthermore, the power density, which is generally higher in PRO, will have a significant effect on the overall process performance. This means that, although the difference in SEC between RED-RO and PRO-RO is small and the SEC is even higher for PRO-RO at high recoveries, a higher membrane area would be needed in RED-RO. Economic considerations will then be necessary for the design and optimisation of the process.

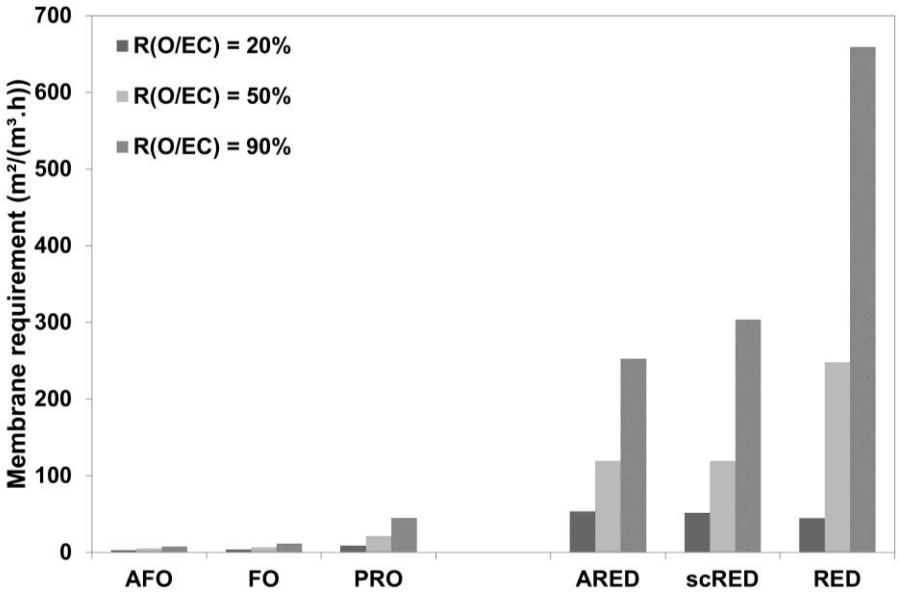

Figure 4.13 Comparison of the required membrane area per m³/h of water produced (50% RO recovery) for osmotically and electrochemically driven processes at different SGP recoveries (R_O/R_{EC}).

5 Challenges for the application of SGP/OD-RO hybrids

Two important factors further influencing the overall efficiency of the hybrid processes are hard to be taken into account in models. First of all, both seawater and impaired water contain their own mixture of foulants, which will affect the process efficiency by fouling the membranes. Besides fouling phenomena in the SGP/OD technologies themselves, the pre-treatment will also have an effect on fouling phenomena in the RO unit. Transfer of foulants from the impaired water to the seawater is possible, but will be limited. In PRO/FO/PAO, the water transport to the seawater will result in an effective decrease in concentration of salts but also of foulants, resulting in decreased fouling risks in the RO process. In RED/scRED/ARED, no dilution of the foulants in the seawater will occur, but the ionic strength of the seawater will be significantly lower compared to untreated seawater. This is expected to have a clear effect on fouling propensity in the RO stage, due to changes in charge properties and aggregation behaviour of organic matter and colloids, and on their interaction with the membrane and the present ions.

Furthermore, contaminants present in these streams could impact the final product quality, which is a key element in such systems, where the overall goal is to produce drinking water. SGP/OD-RO hybrids as discussed here have the added benefit of providing a double barrier for potential contaminants, such as endocrine-disrupting chemicals, pharmaceutically active compounds, pesticides and disinfection by-products which could be present in the impaired

water [107]. These compounds are generally called trace organic contaminants (TOrCs), due to the low concentrations in which they are present (ng/l to µg/l), and can represent a human and environmental threat, even at these trace concentrations. Although TOrC rejection in RO is generally quite high and well understood [108–110], an additional membrane barrier can further decrease the amount of TOrCs in the produced potable water and indeed increase consumer confidence.

5.1 Osmotically driven SGP/OD processes

Research on fouling in osmotically driven processes, mainly FO and PRO, is extensive and includes the behaviour of several model foulants (humic acids, alginate, proteins, silicates) and real impaired water types under different operating conditions [92,111–123]. Most of the studies so far have been performed using the cellulose triacetate benchmark membrane from Hydration Technology (HTI, Albany, Oregon, USA), which is characterised by a relatively low permeation flux. The development of new generations of membranes, allowing for higher fluxes, already demonstrated more severe fouling. An overview of the expected dominant fouling mechanisms when combining seawater and impaired water is graphically represented in Figure 4.14.

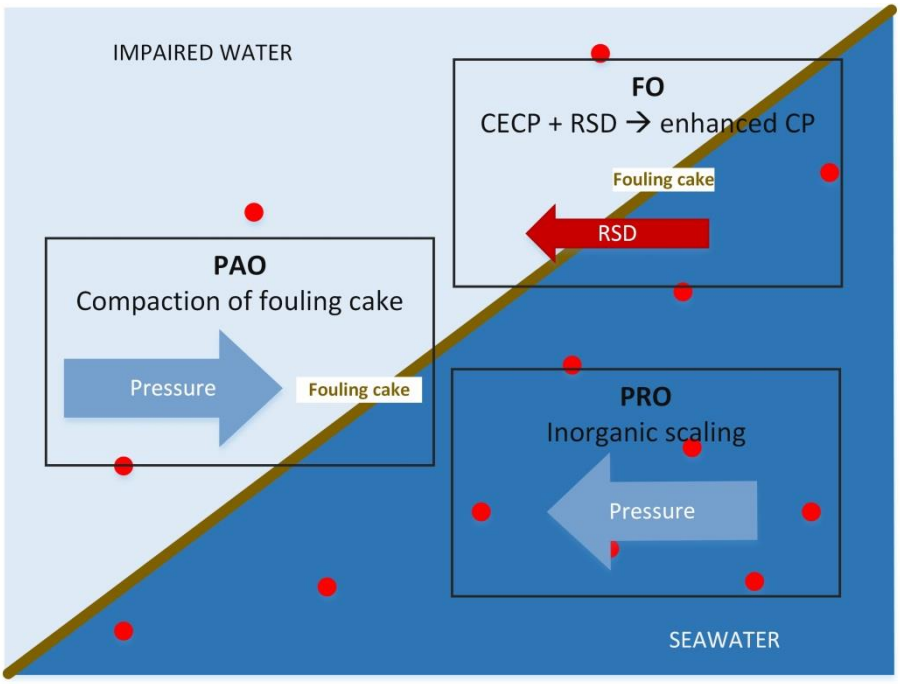

Figure 4.14 Summary of the dominant fouling mechanisms in the different osmotically driven SGP/OD processes (CECP = cake-enhanced concentration polarisation, RSD = reverse salt diffusion, CP = concentration polarisation).

Rejection of TOrCs in FO has been recently intensively investigated and FO was shown to be a robust barrier for TOrCs [124]. Owing to a low solute permeability (due to size

exclusion, especially in newer membranes) and electrostatic repulsion, the rejection of TOrCs in FO is high [125]. However, in PAO the rejection is lower. This is hypothesized to be an effect of membrane deformation due to the applied hydraulic pressure. The same deformation has been observed in PRO, indicating that in this process as well the rejection of TOrCs is lower than in FO [93,126].

5.2 Electrochemically driven SGP/OD processes

In contrast to the R&D efforts focused on fouling in osmotically driven processes, the effects of fouling on process efficiency in RED have barely been investigated. Vermaas et al. (2013) observed a significant increase in pressure drop over an RED system operated on untreated sea- and river water. A fouling mixture of diatoms, clay minerals and organic foulants at the anion-exchange membranes and of calcium and phosphate scaling at the cation-exchange membranes was observed [127]. In depth studies on biofouling in RED have shown that the economy of the process will depend largely on the strategies developed to control biofilm formation [128,129]. However, no research on the fouling phenomenon that come with using impaired water as a low-salinity water stream has been conducted so far. In addition, ARED operation will most likely result in significantly different fouling behaviour, comparable to the difference between PRO and PAO.

As for the transport of TOrCs in RED/scRED/ARED, it is expected that the charge density of the membrane will play a more important role compared to osmotically driven processes. It has been shown that larger, more hybrophobic molecules tend to adsorb onto IEMs [130] and that the transport of TOrCs is mainly diffusion-driven and independent on the electric driving force (see Chapter 6 and Chapter 7). This indicates that in slower desalination processes, where there is more time for diffusion, TOrC rejection will be lowest. In other words, the transport of TOrCs from impaired water to seawater is expected to be highest in RED and lowest in ARED.

6 Outlook for full-scale applications

Both RED/scRED/ARED and PRO/FO/PAO in a hybrid process with RO have been found potentially effective in decreasing the overall desalination energy cost significantly, due to the combination of OD and energy production. However, when economic aspects are considered, nog only energy, but all operational costs as well as CAPEX need to be taken into account. It is expected that by implementing SGP/OD technologies as RO pre-treatment, the cleaning costs will decrease if RO is operated at a lower hydraulic pressure.

However, additional operational costs related to cleaning and membrane replacement have to be considered for the SGP/OD. Of course additional investment cost should also be considered with regard to the implementation of the additional SGP/OD unit. As such, in all hybrid systems, an important trade-off between CAPEX and energy savings will have to be found.

Economic studies executed so far have indicated that PRO/FO/PAO-RO is economically more attractive than RED/scRED/ARED-RO, with PAO being the most interesting option for RO pre-treatment [42,77,79,90]. However, current economic estimations are largely based on performance characteristics achieved on lab-scale. Research from Feinberg et al. (2015) indicates that the translation of these lab-scale performance characteristics to full-scale applications is not so straightforward and that in reality, power densities would, for example, be a lot lower than expected. Notably, they even predict the actual system size requirements of PRO to exceed those of RED in full-scale applications [131]. Furthermore, economic analysis of RED and related processes depend on IEM prices which are still very high at around € 100/m² [132], while the potential for IEMs development is still very big, resulting in an expected cost reduction and performance increase in the near future.

7 Conclusions

The integration of SGP/OD into hybrid SGP/OD-RO desalination schemes has been demonstrated to have multiple advantages, ranging from decreasing energy needs for desalination, whilst contributing to increase water production, to a decrease in the environmental impacts of concentrate discharge. The SGP/OD-RO hybrid schemes have been shown to be thermodynamically very promising, and have also demonstrated significant energy savings even after integrating practical limitations and irreversible losses within the numerical analysis of performance. However, to allow SGP/OD-RO to reach full implementation on a large scale, several barriers still have to be overcome. Most importantly, improvements in membranes and modules are required for economic sustainability. As for now, no clear preference for either osmotically driven or electrochemically driven processes can be made based on the data available. Although some studies indicate PRO/FO/PAO to be more economically sustainable in a hybrid scheme, others indicate that future developments could favour RED/scRED/ARED hybrids.

It is expected that SGP/OD-RO hybrid schemes will have the highest potential in dry urban coastal areas, where wastewater effluents and seawater are often closely located, and the

hybrid scheme complements efforts to improve local water management strategies. As most of the world's largest cities are located close to the sea, these represent a huge potential catchment area, where the hybrid schemes could be very useful.

Chapter 5: Assisted RED as a novel pre-desalination technology to decrease seawater RO energy demand – a lab-scale system characterisation

This chapter is in preparation for submission to Energy & Environmental Science as

Vanoppen, M., Criel, E., Walpot, G., Andersen, S., Prévoteau, A., Verliefde, A.R.D. Assisted reverse electrodialysis: a novel technique to decrease reverse osmosis energy demand – a lab scale system characterisation.

1 Introduction

In Chapter 4, several options for the reduction of the specific energy demand of seawater RO were discussed. One of the new technologies in this respects is ARED, in which a small potential difference is applied in an RED system to increase the rate of desalination. Although modelling results show that an ARED-RO hybrid system can be beneficial in terms of energy consumption and especially membrane requirements, the system has only been attracting interest recently. GE has presented some interesting work on using ARED and RED to treat the RO concentrate and extract energy by mixing the concentrate with impaired water [133,134], but no further literature exists to the best knowledge of the authors. Especially as a pre-desalination step for RO, no research has been done so far.

In this chapter, the basic working principles of ARED on lab-scale are investigated. Attention is given to the relation between the applied potential difference and the resulting current density, as this determines the energy requirements for the pre-desalination, and to the influence of flow rate and concentrations, as these influence concentration polarisation effects and overall resistance in the system respectively.

2 Theoretical considerations

In the electrochemical membrane systems as discussed here, the potential difference across the stack, E_{stack}, (V), depends on the potential difference caused by the concentration difference across the membranes E_{OCV} (or open circuit voltage, in V) and the total stack resistance R_{stack}, ($\Omega.m^2$) according to the following equation:

$$E_{stack} = E_{OCV} + i \cdot R_{stack} \tag{5.1}$$

With i (A/m^2) the current density through the stack. E_{OCV} and R_{stack} are given by the following equations:

$$R_{stack} = \frac{N}{A_m} \cdot \left(\frac{R_{AEM}}{1-\beta} + \frac{R_{CEM}}{1-\beta} + \left(\frac{h_C}{\kappa_c \cdot \varepsilon^2} \right) + \left(\frac{h_D}{\kappa_d \cdot \varepsilon^2} \right) \right) \tag{5.2}$$

$$E_{OCV} = N \cdot \alpha \cdot \frac{R_g \cdot T}{z \cdot F} \cdot \ln\left(\frac{C_C}{C_D} \right) \tag{5.3}$$

With N (-) the number of cell pairs, A_m (m^2) the active membrane surface for one membrane, R_{AEM} and R_{CEM} ($\Omega.m^2$) the membrane resistances for the AEM and CEM, β (-) the spacer shadow factor, h (m) the compartment thickness, $\varkappa$ (S/m) the conductivity of the solutions and ε (-) the spacer porosity. α (-) is the permselectivity, R_g (8.314 J/(mol.K)) is the universal gas constant, T (K) is the temperature, z (-) is the ion valence, F (96 485 C/mol) is the Faraday constant and C (mol/m^3) is the concentration. Subscripts C and D denote the concentrate and diluate compartments, respectively.

Based on the above equations, a theoretical current-voltage relationship can be determined for ED, RED and ARED (full line in Figure 5.1). However, concentration polarisation phenomena (CP) cause a deviation from this ideal line, as shown by the dashed line.

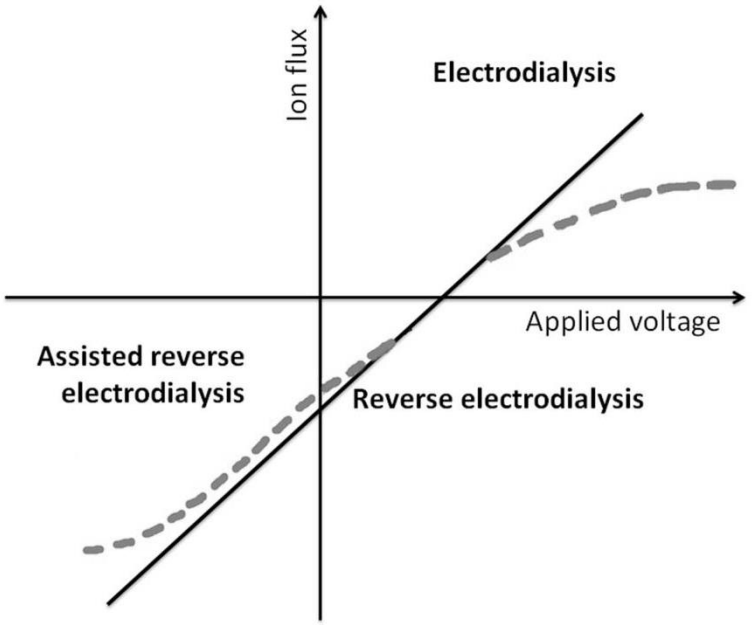

Figure 5.1 Schematic representation of the ideal (full line) and expected (dashed line) current-voltage curve in electrochemical membrane processes.

In ED (positive current and potential difference), CP causes the concentration at the membrane interface to decrease at the low salinity side and to increase at the high salinity side. This causes the overall resistance to increase, as the concentration difference over the membrane increases (as shown in Figure 5.2). Therefore, when concentration polarisation occurs, the current at a certain potential difference will be lower than ideally expected, resulting in a lower efficiency and higher energy demand of the process. Because the salt is forced to move against its concentration gradient, the effect of CP in ED is very clear even at low current densities – as the concentration in the diluate compartment may become limiting. In the RED region (negative current, positive potential difference), due to the low currents

generated, CP is expected to have only a limited influence on the process, mainly causing the natural driving force to decrease. In ARED (negative current, negative potential difference), a (small) additional potential difference is applied to the system, along with the concentration gradient, to increase the speed of desalination. This will also increase the current density in the system, increasing the effect of CP. However, since transport occurs from the high salinity to the low salinity side in ARED, the overall effect of CP is expected to be limited – it mainly results in a decrease in driving force along with the concentration gradient. At a high additional potential difference, the concentration of the high salinity water at the membrane interface could theoretically decrease below the concentration of the low salinity compartment, thereby significantly increasing the effect of CP. However, this would require very high potential differences, which are not envisioned in ARED, as this would result in high energy costs. In the region of potential differences where ARED would be interesting, the current-voltage curve is expected to follow the ideal line more or less, with only a slight deviation due to non-idealities in the system.

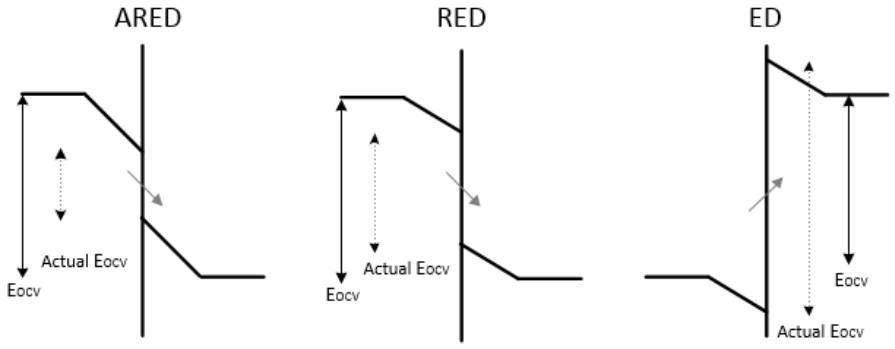

Figure 5.2 Schematic representation of the effect of concentration polarisation on the concentration profile in the diluate (left) and concentrate (right) compartments. The direction of salt transport is indicated by the light grey arrow, the theoretical open-circuit voltage is indicated by the black arrow and the actual open-circuit voltage is indicated by the dotted arrow.

3 Materials and methods

3.1 Electrochemical membrane cell

The electrochemical membrane cell consisted of a plexiglass encasement, containing a stretched titanium anode with an iridium mixed metal oxide coating and a stretched titanium cathode with a ruthenium mixed metal oxide coating (Magneto Special Anodes B.V., the Netherlands). In all experiments, 5 cell pairs were used, containing either Fujifilm type I (F I) or type II (F II) membranes (Fujifilm, the Netherlands) with an active surface area of 7.8x11.2 cm^2. A compartment thickness of 485 μm was achieved by the use of polyamide

spacers (Nitex 06-700/53, Sefar, Switzerland). The properties of the membranes and spacers are depicted in respectively Table 5.1 and Table 5.2.

Table 5.1 Properties of the membranes used in the experiments [Fujifilm, personal communication].

Membrane properties	**Unit**	**AEM Type I**	**CEM Type I**	**AEM Type II**	**CEM Type II**
Membrane type	-	Homogeneous	Homogeneous	Homogeneous	Homogeneous
Thickness	μm	125	135	160	160
Permselectivity	%	92	95	95	96
Electrical resistance 2M NaCl	Ω.cm²	0.8	1.3	3.5	6.1
Water permeability	ml/(bar.m².h)	6	10	3	3.5
Burst strength (wet)	kPa	2.4	2.7	5	4.7
pH stability	-	2-10	4-12	2-10	4-12

Table 5.2 Properties of the spacers used in the experiments

Spacer properties	**Unit**	
Fiber material	-	Polyamide
Weight fabric	kg/m²	0.14
Porosity (ε)	-	0.8
Shadow factor (β)	-	0.47
Thickness	μm	485
Mesh opening width	mm	0.7
Open area	-	0.53
Wire diameter	mm	0.265

To exclude any losses associated with redox reactions occurring at the electrodes, in both end plates, close to the electrodes, a reference electrode (Ag/AgCl) was inserted (RE-5B, BASi, USA) to measure the actual potential difference across the membrane stack. This stack potential difference was recorded using an Agilent 34970A Data Acquisition/Data Logger Switch Unit (Agilent Technologies, USA). The highest measurable current for this unit is ± 1.2A, corresponding to ± 136 A/m² for the set-up used. This current was used as the end-point for all continuous experiments. A DC current was applied to the stack using an adjustable DC power supply (PS 5005, HQ Power, Belgium).

3.2 Continuous experiments

To compare the practical behaviour of the (A)RED system to the theoretical expectations as shown in Figure 5.1, continuous experiments were performed to construct actual current-voltage curves. Continuous here means that the stack was fed in once-through mode with solutions with a constant concentration and no recycling of the solutions occurred. Instead, after flowing through the system, the solutions were discarded. Only the electrolyte (0.25M NaCl) was recycled in batch mode. To exclude any losses associated with the feed water matrix (e.g. scaling or poisoning by multivalent ions (Ca^{2+}, PO_4^{3-}, …) or fouling by organics), only pure NaCl solutions were used.

Several experiments were conducted. Firstly, the influence of a varying concentration of the diluate compartment on stack performance was investigated, as the diluate concentration has an important effect on the system resistance. Secondly, the flow velocity was varied, to investigate the influence of concentration polarisation - which is more severe at lower flow velocities – on stack performance. Flow velocities of 30, 50 and 100 ml/min ($2.6 \cdot 10^{-3}$, $4.4 \cdot 10^{-3}$ and $8.8 \cdot 10^{-3}$ m/s respectively) were compared. In each experiment, the current was adjusted step-wise and the corresponding stack potential was recorded after stabilisation of the signal (indicated by a standard deviation <5% between 5 consecutive measurements, taken every 30 seconds). The current was applied in the direction of the ion transport, from the high to the low concentration compartment, represented in this study as a negative current. NaCl solution conductivities and the corresponding NaCl concentrations at the inlet and outlet (as derived from calibration curves) were determined using a conductivity probe (SK23T, Consort, Belgium).

4 Results and discussion

4.1 Comparing theory and practice

In the first exploratory experiments, ARED experiments were carried out with both membrane types in two separate experiments, with artificial sea- and wastewater (0.5M and 0.01M NaCl respectively) at a flow rate of 100 ml/min. The corresponding current-voltage curves are shown in Figure 5.3. Also included in this figure is the theoretical line, based on equations 1-3, which shows the ideal current-voltage curve neglecting concentration polarisation. A permselectivity of 95%, as given by the manufacturer, was assumed in the theoretical curve. The Ohmic resistance in the theoretical curve was calculated based on a

constant feed solution concentration and assuming a constant membrane resistance as given by the manufacturer.

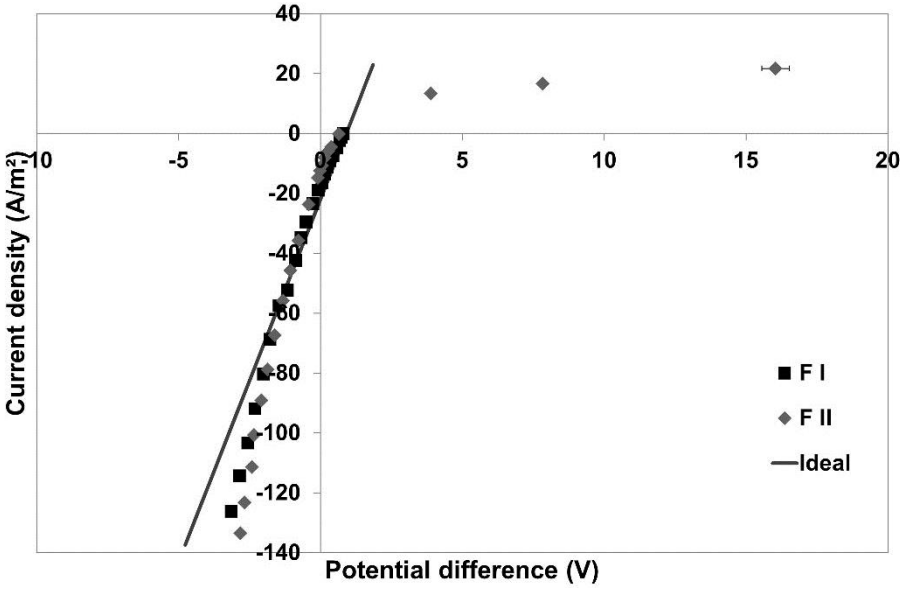

Figure 5.3 Exploratory experiments comparing the theoretically expected ideal current-voltage relation and the measured data points for both membranes.

As expected, the experimental data points show that the current densities level of while the potential difference increases drastically at higher current densities in the ED region (positive current density and potential difference, quadrant 1). This is consistent with previous literature, and is due to CP phenomena, causing depletion of the salt concentration in the diluate compartment and thus a resistance increase in the diluate compartment (as resistance is inversely related to the conductivity). In the RED region (positive potential difference, negative current density, quadrant 2), the experimental data points almost coincide with the theoretical curve, but are positioned slightly above it. This indicates that in practice a lower current density is reached than expected in the ideal case. This is caused by non-idealities in the system, such as for example a lower effective permselectivity (since permselectivity depends on the concentrations), a small decrease in E_{OCV} due to CP phenomena as discussed before or water transport. In the ARED region (negative potential difference and current density, quadrant 3) however, the points shift from above the ideal case at low current densities, to below this curve at higher current densities. In other words, the obtained current density is higher than expected in the ideal case, and thus the required energy in practice is lower than expected. This is very surprising, and reasons for this behaviour will be investigated in more detail in the next paragraph. The ARED region is shown in more detail in Figure 5.4.

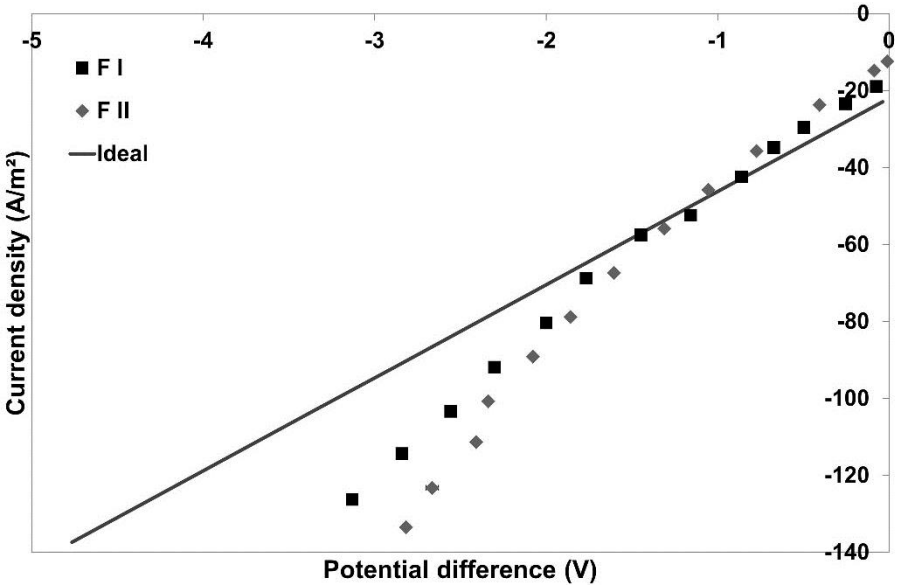

Figure 5.4 Detailed view of the ARED region in the exploratory experiments.

Overall, the observed potential difference corresponding to a certain current density depends on several parameters, of which the boundary layer effect (CP effect) and the resistance of the bulk solutions and membranes are the most pronounced. In the ARED region and at the relatively low current densities used in these experiments, CP is not expected to play a significant role, as discussed before, since current is moving from high to low concentration. Therefore, the most logical explanation for the unexpected behaviour in ARED, is an important drop in solution and/or membrane resistance which decreases the resistance of the system and thus decreases the potential difference corresponding to a certain applied current. The drop in solute/membrane resistance can be more clearly explained as follows: in ARED, compared to RED, the faster rate of desalination (caused by the added external potential) causes a rapid increase in the bulk concentration of the low salinity compartment during passage through the stack. This causes the resistance of this compartment to drop significantly during passage. Geise et al. (2013) and Galama et al. (2014) already showed that the low salinity compartment concentration not only determines the resistance of the low salinity compartment, but in addition mainly determines the membranes resistance, while the effect of the high salinity compartment on membrane resistance is negligible [135,136]. The lower the salinity of the low salinity compartment, the larger the membrane resistance. Because of the increased salt transport rate in ARED, the rapidly increasing concentration in the low salinity compartment (resulting in an on average higher concentration in the low salinity compartment) causes the membrane resistance and the low salinity compartment resistance to decrease. The decrease in solution resistance with increasing salt concentrations shows a rather exponential curve, as shown in Figure 5.5. The decrease in resistance starts to

level of above a concentration of 0.2M. This shows that any changes in the seawater concentration (initially 0.5M) will not influence the overall resistance as much as the increase in concentration in the low salinity compartment. The latter, starting at 0.01M, is positioned in the rapidly decreasing zone of Figure 5.5, indicating a significant effect of an increasing concentration on the resistance of the compartment (and the membranes). Galama et al. derived an equation that correlates the membrane resistance to the low salinity solution concentration through the relative diluate concentration K_d:

$$R_{IEM} = a + \frac{b}{K_d} \tag{5.4}$$

$$K_d = \frac{C_D}{C^0} \tag{5.5}$$

With K_d (-) the diluate concentration (C_D) with reference to a standard concentration C^0 of 1M and a and b ($\Omega.m^2$) parameters that represent the resistance resulting from the ion distribution inside the membrane. Both a and b are constants that depend on the membrane properties and should be experimentally determined. The equations show an inverse linear relationship of the diluate concentration with the membrane resistance. In other words, the membrane resistance is expected to follow a similar exponential trend of decreasing resistance with increasing diluate concentration.

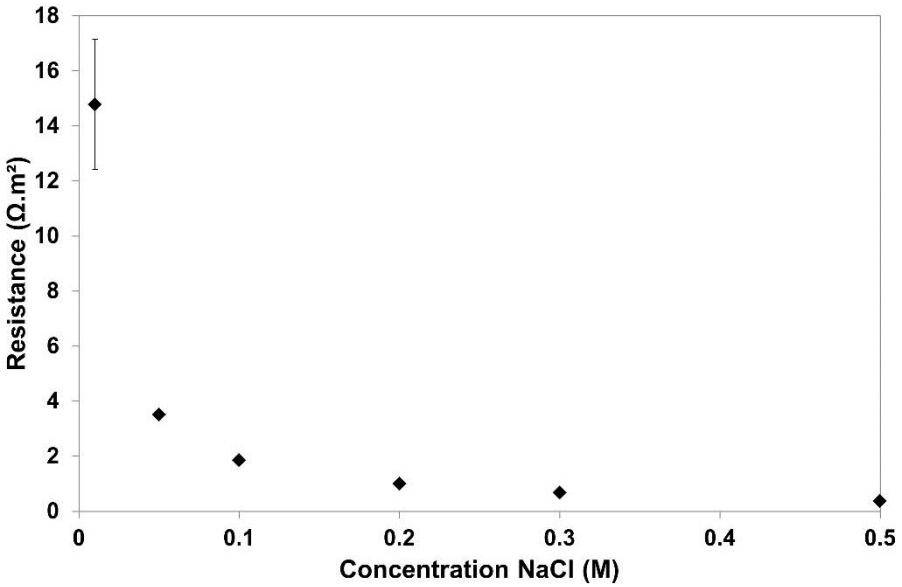

Figure 5.5 Solution resistance as a function of the concentration of NaCl.

A combination of both a decrease in membrane resistance as well as a decrease in solution resistance are thus most likely the cause of the observed unexpected behaviour in ARED, namely a below linear increase in potential difference with increasing current density. This hypothesis will be further investigated by varying the flow rate in the next paragraph. Flow rate will largely influence the degree of desalination in the stack, as a lower flow rate results in a higher residence time. As the relation between solution resistance and concentration is not linear, the effect of different concentrations for the low salinity compartment on stack performance were investigated as well.

4.2 Effect of changing flow rates on the current-voltage relation

The difference in stack behaviour between flow rates of 30, 50 and 100 ml/min is shown in Figure 5.6 for both membrane types. The flow rate has two important and distinct influences on stack behaviour: at a higher flow rate (and thus a higher cross-flow velocity), mixing at the membrane surface will be higher. This results in a decreased thickness of the diffusion boundary layer. E_{OCV} in this case will be less affected by CP and thus a higher actual E_{OCV} will be present across the membranes, resulting in a decrease in total potential difference across the stack at constant current density and stack resistance. However, an increase in flow rate also results in a decrease in residence time and hence a lower concentration in the diluate compartment due to a shorter residence time in the stack compared to a lower flow rate. This lower concentration results in a higher membrane resistance, by the effects discussed before. A slightly higher potential difference is obtained at higher flow rates, confirming that a decrease in solution and membrane resistance due to the higher extent of salt transfer at lower velocities causes the decrease in potential difference.

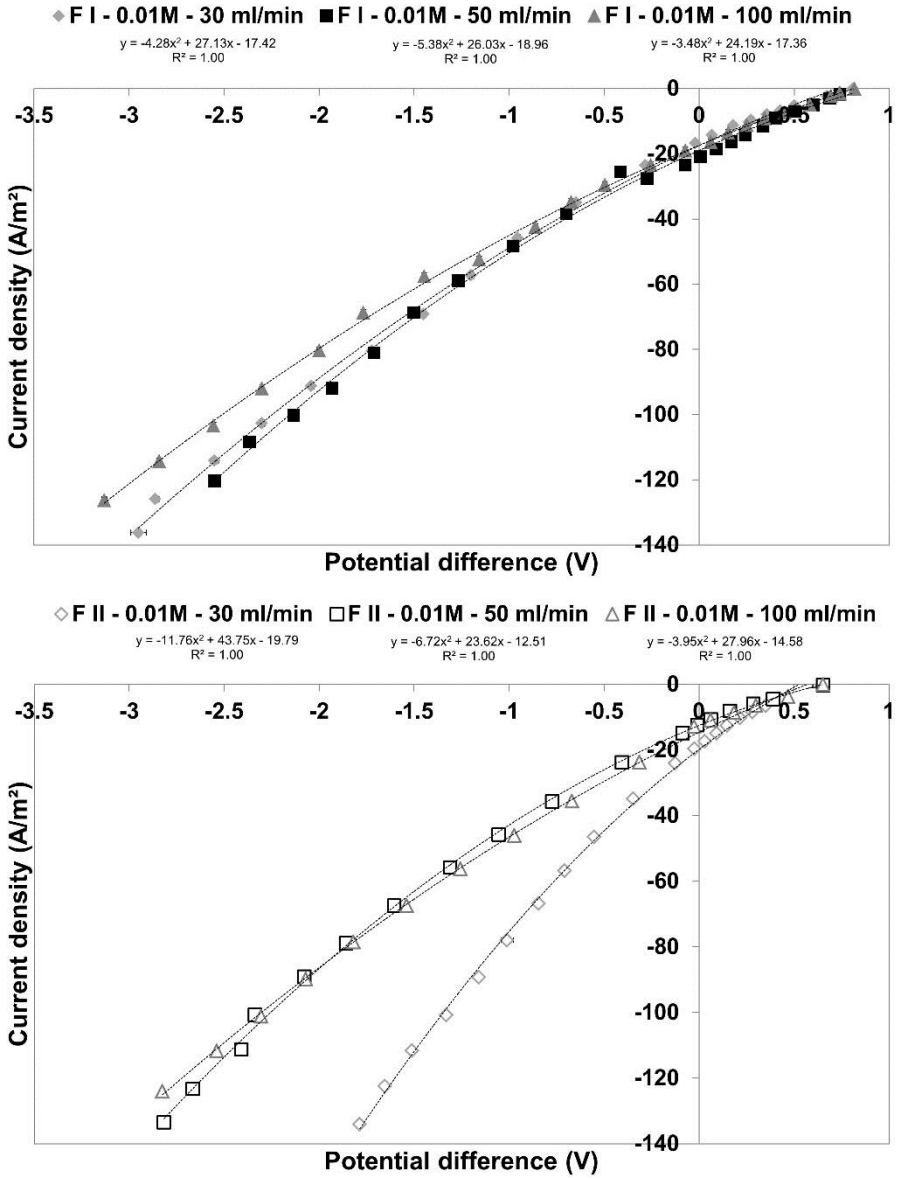

Figure 5.6 Effect of a changing flow rate on the current-voltage relation in the RED and ARED region (C_D = 0.01M, C_C = 0.5M) for F I (top) and F II (bottom) type membranes. Curve fitting polynomial degree is based on highest R^2 reached. Error bars are included but overall too small to be visible.

However, the differences between different flow rates are small for the F I type membranes, and all curves show a clear downward deflection, as shown by the negative second order coefficient for the polynomial fit. A similar trend is observed for the F II type membranes but for these membranes the difference between the lowest flow rate and the higher flow rates is much larger. This can be explained by the higher inherent resistance of these membranes (see Table 5.1), which causes the effect of the higher desalination degree at the lowest flow rate to be much larger.

4.3 Effect of changing diluate concentrations on the current-voltage relation

The initial diluate concentration is important, as it determines the membrane resistance and solution resistance of the low-salinity compartment, which is the largest contributor to the overall resistance of the system. In these experiments, the diluate concentration was varied (at a constant C_C of 0.5M), as shown in Figure 5.7. The concentrate concentration was kept constant to ensure the effects seen can be attributed to the diluate compartment only. Because of the change in C_D, E_{OCV} varies (i.e. it decreases with an increasing C_D because the salinity gradient between the concentrate and diluate decreases). At the lowest diluate concentrations (0.01 and 0.05M), the downward declination of the current-voltage curve is clear, both visually and from the second order coefficient in the polynomial fit. At higher concentrations, however, the curves (and fit) become linear. It is clear that when the initial diluate concentration is already high, the effect of further increasing diluate concentration through ARED does not have a large effect on the compartment and membrane resistance, since at these concentrations, the overall resistance remains quite constant (see Figure 5.5). Furthermore, it is now also clearly proven that the currents applied in ARED are too low to cause significant CP effects, since otherwise no linear current-voltage relations would be obtained. Similar results were obtained with the type II membranes (Figure 5.7 bottom), which shows a declination at C_D concentrations of 0.01 and 0.05M and a linearization from a concentration of 0.1M on.

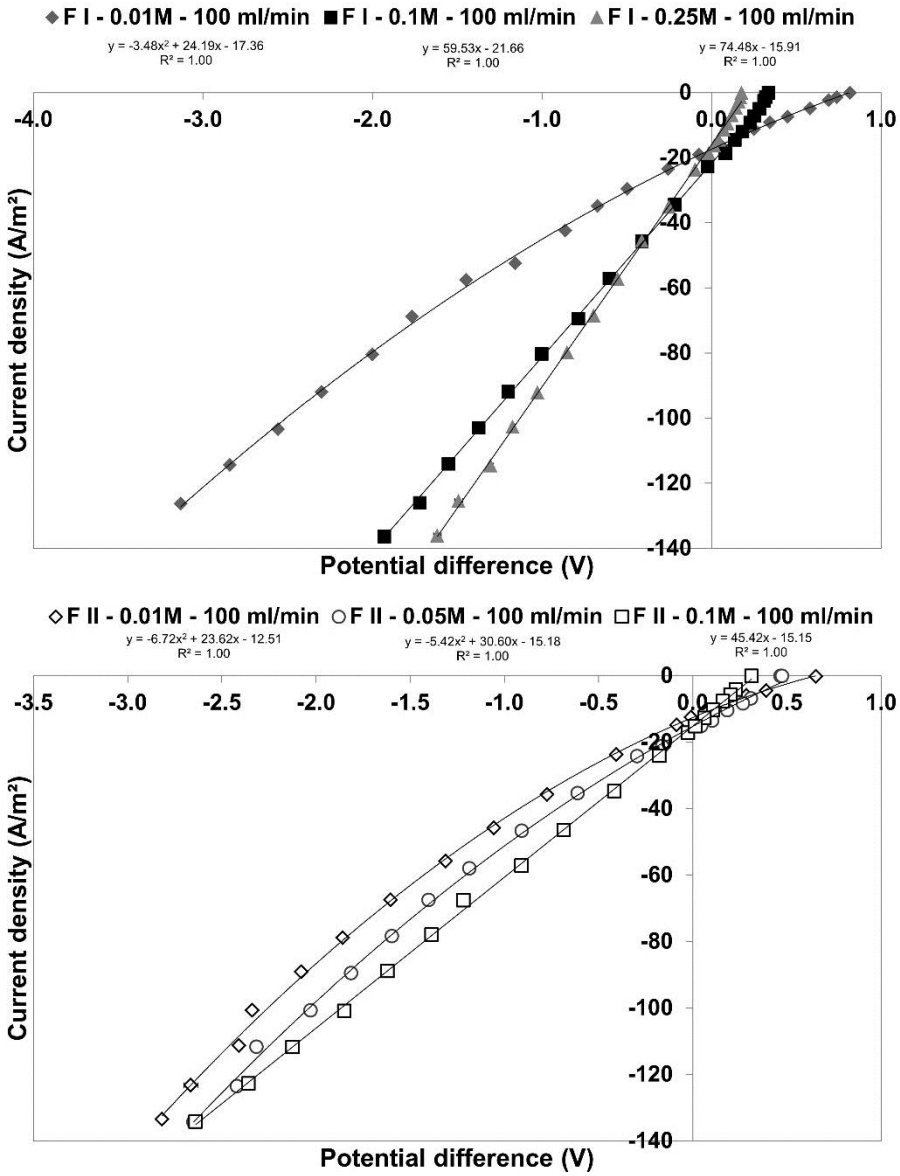

Figure 5.7 Influence of different C_D concentrations on the current-voltage relation in the RED and ARED region (C_C = 0.5M, flow rate = 100 ml/min) for F I (top) and F II (bottom) type membranes. Curve fitting polynomial degree is based on highest R^2 reached. Error bars are included but overall too small to be visible.

The results at 30 and 50 ml/min are similar, as shown in Appendix C.

4.4 Membrane and solution resistance in (A)RED

Using equation 5.2, in combination with the measured C_D and C_C concentrations, the average CEM and AEM membrane resistance can be calculated from the current-voltage data discussed before. The resistance of the low salinity compartments in these equations is calculated based on the average of the incoming and outgoing solutions. Figure 5.8 shows the combined membrane and low salinity solution resistance, the two major contributors to the overall resistance, at a flow rate of 100 ml/min. The initial solution resistance is 2.6, 0.3 and 0.1 Ω.cm² for the 0.01, 0.1 and 0.25M solutions respectively. The average membrane

resistance given by the manufacturer is 1 Ω.cm² in a 2M NaCl solution for the F I type membranes. From the measurements at low current densities (where the effect of desalination on the resistance is limited) it is clear that a similar resistance is obtained in the 0.25M and 0.1M solutions but that the membrane resistance is significantly higher in the 0.01M solution, as predicted before. In the ARED region, roughly from -20 A/m² downwards to -140 A/m², the overall resistance remains quite constant, while in the RED region it decreases significantly with increasing current density.

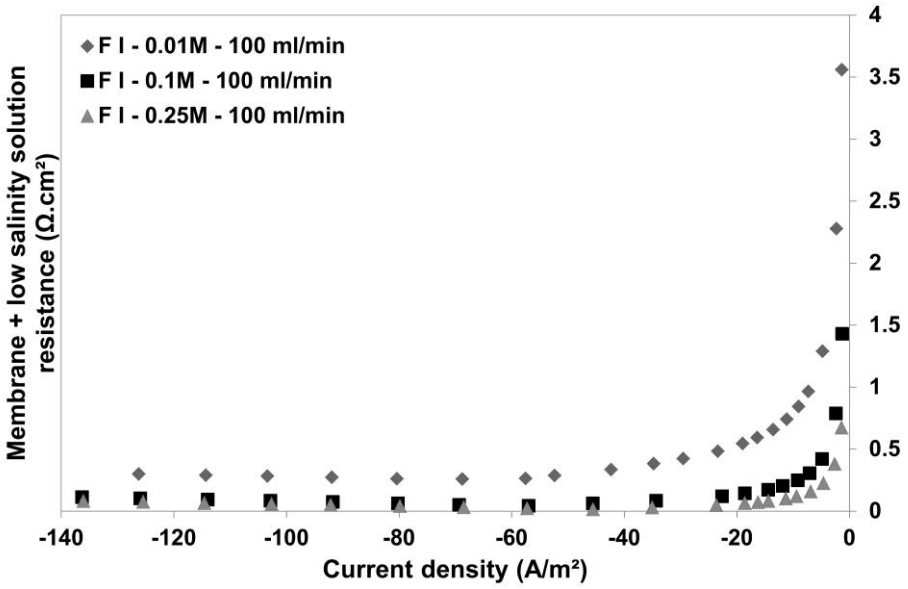

Figure 5.8 Combined membrane and low salinity solution resistance for F I type membranes at a C_D of 0.01, 0.1 and 0.25M (C_C = 0.5M, flow rate = 100 ml/min).

These results further confirm the influence of the decrease in resistance of both the membrane and the solution on stack performance at low C_D. The results also indicate that the highest resistance to overcome, causing the largest losses in RED systems, is in the RED region at low C_D. In the RED region, the resistance is 60-74% and 81-88% lower for the 0.1 and 0.25M solutions respectively compared to the 0.01M solution. In RED, desalination is hampered by the low salinity of for example impaired water, which causes a slow desalination and hence a high required membrane area. ARED however, does not seem to suffer from the same limitations. To decrease the membrane requirement of pre-desalination with RED, ARED could be implemented as a first step, to overcome the initial high resistance of the low salinity compartment and the membranes. When the low salinity compartment reaches a sufficiently high concentration (and thus low resistance), energy production with RED can be started.

5 The future of the ARED in a hybrid seawater desalination system

The results presented in this study clearly show the added value of an ARED system, as this system is able to provide a boost in the pre-desalination system at low energy cost. If only RED would be used as pre-desalination step, membrane cost would be very high since the desalination rate in RED is initially low due to the high diluate resistance. ARED is able to overcome this important drawback of RED. In Chapter 4 it was shown that when ARED is used as a single pre-desalination step in an ARED-RO hybrid, the overall energy consumption of the hybrid is still significantly lower than that of a stand-alone RO system. However, this research has shown that the value in the ARED system is mainly at lower concentrations, where the decrease in resistance significantly reduced the added energy requirement. At higher concentrations, this added benefit is lost. Based on these results, a new hybrid system can be thought of, in which ARED and RED are combined in the hybrid system, as shown in Figure 5.9.

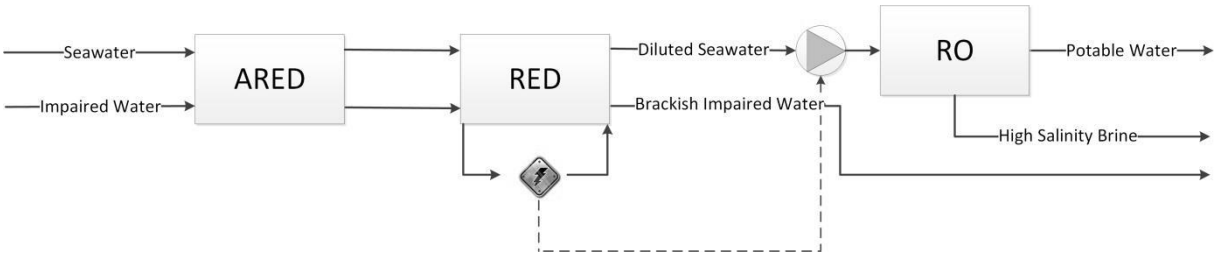

Figure 5.9 Envision hybrid process including ARED and RED as pre-desalination steps before RO.

In this extended hybrid system, a small amount of energy can be added in the ARED system to overcome the initial high resistance of the low salinity stream (shown here as impaired water for example), after which an RED system can be placed to harvest the rest of the remaining salinity gradient power. Due to the reduced resistance of the solutions (and thus of the membranes) in the RED system, the membrane requirement will be much smaller. This combination of ARED and RED thus reduces membrane area requirements at low energy cost, and can thus further optimise the overall cost efficiency of (A)RED-RO hybrids for seawater desalination for drinking water purposes.

6 Conclusions

In this study, the ARED system was investigated as a pre-desalination step for seawater RO at lab-scale for the first time. The main conclusions can be summarised as follows:

- Fast desalination kinetics in ARED cause the system to perform better than theoretically expected, due to a decrease in both solution and membrane resistance.

- At low diluate concentrations (0.01 and 0.05M), the positive effect of the decreasing resistance is the largest, as the relationship between salinity and resistance is not linear.
- At higher diluate concentrations (0.1 and 0.25M), the current-voltage relationship becomes linear, as both the solution and membrane resistance are relatively constant.
- By combining ARED and RED in the pre-desalination step, the initial high resistance region can be overcome by ARED and the remaining salinity gradient power can be harvested by RED, optimising the overall energy demand and membrane requirement for the seawater RO hybrid.

This system will have to be further optimised and some more detailed studies are required to thoroughly confirm the hypotheses postulated in this research. Tests with real impaired water and seawater are needed to confirm ARED performance in practice and to quantify the effects of the presence of foulants and of ions other than Na^+ and Cl^-. Further hybrid system optimisation can be done by modelling ARED and RED to determine the optimal amount of pre-desalination by both systems to minimise both energy and membrane requirements of the overall hybrid system.

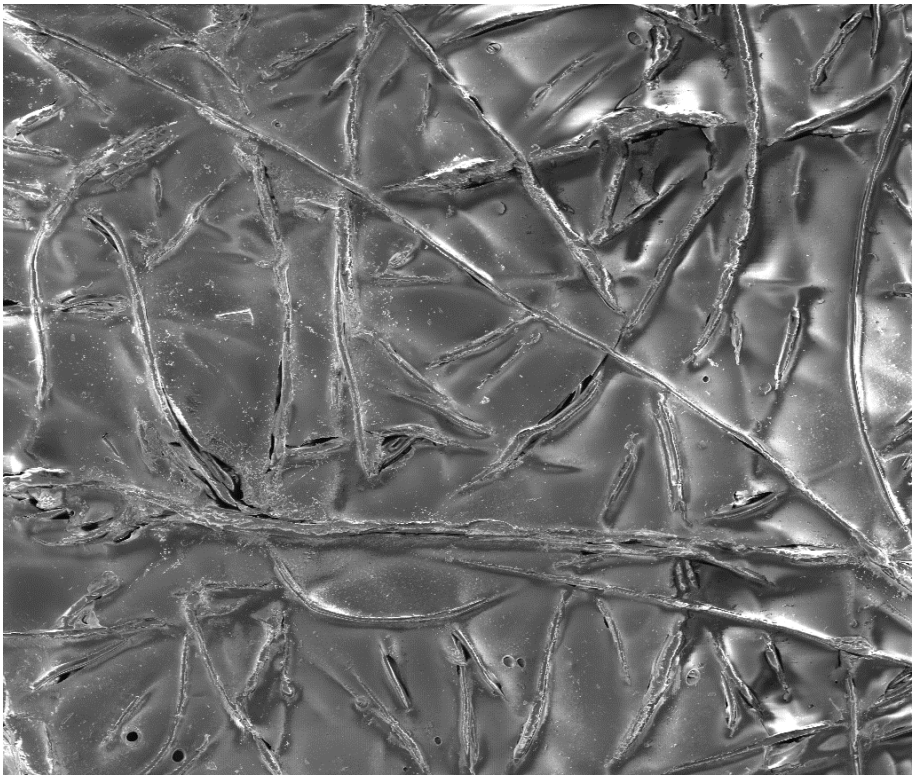

Part 3: Selective separation of inorganics and organics through ion-exchange membranes

Picture: SEM of an ion-exchange membrane (300X magnification)

Chapter 6: Properties governing the transport of trace organic contaminants through ion-exchange membranes

This chapter has been published as

Vanoppen, M., Bakelants, A.F.A.M., Gaublomme, D., Schoutteten, K.V.K.M., Vanden Bussche, J., Vanhaecke, L., Verliefde, A.R.D. Properties governing the transport of trace organic contaminants through ion-exchange membranes. *Environ. Sci. Technol.* **2014**, *49*, 489-497.

1 Introduction

The production of large volumes of aqueous waste streams is inherent to many industrial activities. These streams are often complex, containing high salt concentrations as well as high concentrations of organics. For example in the food industry, salt is used to treat potatoes, olives, cheeses, etc, resulting in a salt and organic rich wastestream, but also the concentrate from reverse osmosis (RO) operations contains both [137,138]. Because of the high salt concentration, conventional biological treatment of these streams to remove the organics before discharge is hampered, while the organic matter restricts the applicability of conventional physico-chemical techniques [139,140]. Pressure driven membrane processes such as nanofiltration (NF) and RO suffer from fouling when used to treat these complex streams, due to high rejection of the salts as well as the organics, leading to a complex interplay of scaling and/or (compacted) organic fouling layers on the membrane surface by the high applied pressure, leading to an uneconomic process [33,141–143].

Simple separation of the organics and inorganics could lead to the reuse and/or valorisation of both organic and inorganic fractions. Besides being more economical for this type of separation, ion-exchange membrane (IEM) technologies are expected to be less prone to fouling when treating these complex streams, since they are not subjected to high pressures. Still, fouling of IEM can occur, which is corroborated by literature on inorganic scaling [144–147] and organic fouling [130,148–151] of IEM.

IEM are implemented in a wide range of applications [152] and both electrodialysis (ED) and membrane capacitive deionisation (MCDI) could be viable candidates to perform the selective separation of organics and inorganics in complex streams [153–156]. ED, for example, has already been finding its way into industrial applications in the food industry, biotechnology-applications and many more [15]. Despite the thorough research on organic fouling, a more fundamental insight in what phenomena govern organic solute transport through IEM is still lacking [157]. Literature on the subject is limited and focuses mainly on the sorption of organics [130,158] and/or a limited set of mainly negatively charged organic components [153], despite evidence that their transport can be a real problem [159]. This contrasts with the vast amount of knowledge on transport of organic solutes through NF/RO membranes [110,160,161]. In these membranes, the rejection/transport is governed by three important mechanisms: (1) steric hindrance, determined by the size of the organic relative to the size of the membrane pores, (2) membrane affinity, leading to a better exclusion of solutes with a low membrane affinity compared to ones with a high membrane

affinity of the same size and (3) electrostatic interactions, in the case of charged organics [162]. Although the importance of these factors is expected to be different, the mechanisms of solute rejection and transport are expected to be the same in IEM. As IEM are highly charged, electrostatic effects are expected to be more important, but the cross-linking degree of the membranes and properties of the polymeric backbone will still have a significant effect on steric hindrance and membrane affinity as well.

This lack of knowledge on organics transport in IEM is even more surprising given the fact that IEM are often used in combination with microbial communities, requiring and producing organic components. In microbial electrolysis cells (ME) and microbial fuel cells (MFC), the IEM are often in contact with very organic-rich streams [163–165]. The applications of ME and MFC technologies are very versatile [166–169] and transport of organics across the IEM is often unwanted [168], or selective transport of certain organics is desired [170].

It is thus clear that a more thorough understanding of transport phenomena of organics through IEM is urgently required and could benefit a wide variety of applications. This study therefore focuses on the phenomena governing the transport of organics across IEM. As a general model for a wide variety of organic components, a set of 16 trace organic contaminants (TOrCs) with a wide range of physico-chemical properties such as charge, hydrophobicity and size is used in this study. Although these organics are relatively small, it is believed that they can serve as a model for a lot of small, charged organic molecules such as for example organic acids and short chain carboxylates, which are often of interest for recovery and valorisation [170,171]. The well-known ED-process is chosen to investigate the influence of an external potential difference. Altogether this allows the study to focus on the identification of the dominant solute and membrane properties governing the transport of organics through IEM and makes it possible to apply the results to other IEM-technologies facing organics, such as MCDI, ME, MFC and many more.

2 Materials and methods

2.1 Electrodialysis set-up

The electrodialysis cell used in this study was a PCCell ED64004 (PCA GmbH, Germany), containing two titanium electrodes coated with a platinum/iridium mixed metal oxide coating for the cathode/anode respectively. Four cell pairs were formed with a CEM at each electrode (thus using five CEM and four AEM) using 0.5 mm silicone/polyethylene spacers.

2.2 Membranes and analysis

The Type II AEM and CEM used were provided by Fujifilm and described as standard homogenous membranes with a cross-linked structure. The AEM contain quaternary amines as functional groups, while the CEM contain sulfonic groups. The membranes were specifically developed for their high permselectivity even at high salt concentrations. They were cut to size with a resulting effective membrane area of 64 cm^2. The properties of the membranes are given in Table 6.1, comparing the manufacturer's data with properties measured in this study. The apparent hydrophilicity of the membranes, shown by the relatively low contact angle, was explained by the manufacturer as a result of the homogeneity of the membranes.

Table 6.1 Properties of ion-exchange membranes used as given by the manufacturer and measured in this study (Man. = manufacturer, Meas. = measured).

		AEM		CEM	
		Man.	**Meas.**	**Man.**	**Meas.**
Thickness	μm	160	148 ± 1	160	170 ± 4
Permselectivity	%	95	94 ± 2	96	-
Electrical resistance	Ω.cm^2	3.5	2.7 ± 0.1	6.1	3.7 ± 0.2
Water permeability	ml/(bar.m^2/h)	3	-	3.5	-
Burst strength	kPa	5	-	4.7	-
Swelling degree	%	-	14 ± 0	-	18 ± 0
Contact angle	°	-	33 ± 7	-	32 ± 5

2.2.1 Membrane thickness

The thickness of the dry AEM and CEM, as received by the manufacturer, was measured with an electronic micrometer (9664-0107, Limit, Sweden). The measurement was repeated three times on each membrane sheet.

2.2.2 Permselectivity

To determine the permselectivity, the membranes were equilibrated in 0.05M KCl for at least 16 hours. Then, one membrane was placed in the ED cell and 0.5M and 0.05M KCl was circulated on either side of the membrane for at least 5 minutes before the potential difference was noted. The Nernst-equation was used to determine the theoretical potential difference. Comparing the measured and theoretical values gives the permselectivity:

$$\Delta E_t = \frac{R_g \cdot T}{z \cdot F} \cdot \ln\left(\frac{a_c}{a_d}\right) \tag{6.1}$$

$$\alpha = \frac{\Delta E_m}{\Delta E_t} \tag{6.2}$$

With R_g the universal gas constant (J/(mol.K), T the absolute temperature (K), a_c and a_d the chemical activity of the concentrated and diluate solution (-), α the permselectivity (-), ΔE_m the measured potential difference (V) and ΔE_t the theoretical potential difference (V). This measurement was repeated three times for three different membrane sheets.

2.2.3 Electrical resistance

The electrical resistance of the membranes was determined with a self-made resistance clamp, based on previous studies by Bazinet and Arraya-Farias [147] and Lindstrand et al [172]. More details on the design and working can be found in Appendix D. The resistances of the solution and membranes were measured three times at three different places on the membrane.

2.2.4 Swelling degree (SD)

To determine the swelling degree, samples of the membrane (three AEM and three CEM) were equilibrated in DI water for at least 24 hours. To determine the wet weight of the membranes, the surface water was removed by blotting paper and the membranes were weighed. Then the membranes were dried at 50°C for at least 24 hours and weighed again. The swelling degree can be calculated by comparing the wet and dry weight of the membrane:

$$SD = \frac{W_{wet} - W_{dry}}{W_{dry}} \cdot 100\% \tag{6.3}$$

Where W_{wet} (g) and W_{dry} (g) are the weight of the wet and dry membranes respectively.

2.2.5 Contact angle

The contact angle measurements were conducted with a 'drop shape analysis system' (DSA10-Mk2, Krüss GmbH, Germany) through the sessile drop method. Contact angles were measured five times at five different places on each membrane with Milli-Q water.

2.2.6 Weight and conductivity

To monitor water transport, the weight of the diluate was logged with a balance with an accuracy of 1g (Xtreme W T51XW, OHAUS, USA). The extent of desalination was monitored using a conductivity electrode (SK23T, Consort, Belgium).

2.3 TOrCs

The advantage of using TOrCs as model components is that they are relatively small - thus avoiding issues related to fouling/poisoning of membranes by the organics during experiments - easy to analyse and distinguish quantitatively in a mixture, and their structure and properties are very well characterised. As such, they can serve as a model for a wide range of small organic molecules. The TOrC reference standards used were of analytical grade (Sigma Aldrich, USA) with a minimal purity of 98%. An overview of the 16 TOrCs and their physico-chemical properties is given in Table 6.2, the chemical structure of the TOrCs is included in Appendix D. A stock solution of 2 mg/l TOrCs was prepared and stored at 4°C. This solution was diluted into the diluate salt solution to give a final concentration of 100 µg/l prior to each experiment (see further).

Table 6.2 Main properties and limit of detection (LOD) of 16 used TOrCs. The charge, pKa, molecular weight (MW), and log D (pH-corrected octanol-water partition coefficient) were calculated using Marvin 5.11.5 software (ChemAxon, Hungary).

Component	Charge (pH 7)	pKa (-)	MW (g/mol)	Log D (pH 7)	LOD (µg/l)
Atrazine	0	3.2	215.68	2.20	0.25
Carbamazepine	0	-	236.27	2.77	0.015625
Chloridazon	0	-	215.68	1.11	0.125
Clofibric acid	-	3.4	214.65	-0.63	1
Diclofenac	-	4.0	296.15	0.73	2
Dimethoate	0	-	229.26	0.34	1
Diuron	0	-	233.10	2.53	0.125
Ketoprofen	-	3.9	254.28	0.08	0.03125
Metoprolol	+	9.7	267.36	-0.79	0.25
Paracetamol	0	9.5	151.16	0.91	2
Phenazone	0	-	188.23	1.22	0.125
Pirimicarb	0	5.0	238.29	1.79	0.5
Simazine	0	3.2	201.66	1.78	0.5
Sulfamethoxazole	-	2.0	253.28	0.15	0.25
Theophylline	-	7.8	180.16	-0.81	4
Triclopyr	-	2.3	256.47	-0.83	1

2.4 Experimental protocol

All experiments were carried out in DI water, to which NaCl and TOrCs were added. The actual experiments consisted of two phases; so-called "diffusion" and "electrodialysis" experiments. The diluate, concentrate and electrode rinse were recirculated in batch mode at a flow rate of 500 ml/min using a peristaltic pump (Masterflex L/S Economy Drive, Cole-

Parmer, USA). The electrode rinse consisted of 81 g/l $NaNO_3$, to assure a minimal osmotic potential difference between the rinse and diluate/concentrate compartments. This way, Na^+-transport from and to the rinse compartment is minimalized while NO_3^--transport is hindered by the outer CEM. An initial diluate NaCl-concentration of 100 g/l was chosen to mimic a high salinity wastewater and to assure a sufficient duration of the "electrodialysis" experiments, while the initial concentrate NaCl-concentration was 10 g/l to assure sufficient conductivity of this compartment. By choosing an initial diluate concentration higher than that of the concentrate, the influence of NaCl transport with and against its concentration gradient could be studied. The TOrCs were dosed in the diluate at a concentration of 100 µg/l to allow the determination of up to 99% of transport and to mimic an industrial wastestream. To determine the exact starting concentration of the TOrCs, a sample from the diluate was taken at the beginning of each experiment. The TOrC analyses were performed using UHPLC-HR-Orbitrap™-MS (Benchtop Exactive Orbitrap™ mass-spectrometer, Thermo Fisher Scientific, USA). To remove all NaCl from the samples, a solid phase extraction (SPE) with Oasis HLB cartridges (6cc, 200 mg of sorbent, Waters Corporation, Ireland) was performed on all samples. The UHPLC-HR-Orbitrap™-MS detection method was specifically developed for the optimal quantitative determination of the used TOrCs. Detailed information can be found in Appendix D.

2.4.1 "Diffusion" experiments

Here, the adsorption and transport of the TOrCs in the absence of an electrical potential difference were investigated. Adsorption of TOrCs onto the membranes is unavoidable but also undesirable, since adsorption can lead to a temporary underestimation of the transport of TOrCs [161,173]. Therefore, the equilibrium adsorption time, necessary to saturate the membranes, was determined from these experiments by looking at the adsorbed mass of TorCs at different times. To ensure saturation of the membranes used for the ED experiments, the membranes from the diffusion experiments were reused and flushed (based on the determined equilibrium time) before each ED experiment. Preliminary experiments (included in Appendix D) showed that adsorption onto the spacer material, stack and tubing was negligible. The adsorbed mass (µg) was determined by the following equation:

$$\text{Adsorbed mass}_t = C_{D,0} \cdot V_{D,0} - (C_{D,t} \cdot V_{D,t} + C_{C,t} \cdot V_{C,t}) \quad (6.4)$$

With C the TOrC concentration (µg/l) and V the volume of the compartment (l). C,t is the concentrate compartment at time t, D,0 is the diluate compartment at time 0 and D,t is the diluate compartment at time t.

Three separate diffusion experiments were conducted in which the NaCl-concentrations of the diluate and concentrate solutions were varied in order to gain more insight on its potential effect on the adsorption and diffusion behaviour of TOrCs. Fresh membrane sheets were cut for each experiment. It is expected that properties such as charge and hydrophobicity will have an important impact, with a higher adsorption for charged TOrCs. The diluate/concentrate NaCl-concentrations were as follows: 0/0 g/l, 100/100 g/l and 100/10 g/l NaCl (technical grade, VWR, USA), all in batches of 8l. These concentrations were chosen to mimic the concentrations used in the "electrodialysis" experiments (see further). In the first two experiments, no salt diffusion occurred, allowing to identify the influence of salt on the adsorption. In the last experiment, the concentration difference was the driver for NaCl-diffusion from diluate to concentrate so the effect of salt-transport on the adsorption can be assessed. 100 µg/l of TOrCs was dosed to the diluate in all experiments. All experiments were run for 48 hours and samples were taken at regular time intervals to be analysed for TOrC-concentration. The pH of diluate and concentrate was corrected to pH 7 ± 0.1 before the experiments. Conductivity and weight of the concentrate were measured to check the salt and water passage.

From the performed experiments, the relative transport and adsorption of TOrCs can be determined. The TOrC concentration of both the diluate and concentrate compartment were monitored as well as the water transport. Combining this data allows the calculation of the transport and adsorption at time t (%) through the following equations:

$$\text{Relative transport}_t = \frac{C_{C,t} \cdot V_{C,t}}{C_{D,0} \cdot V_{D,0}} \cdot 100\% \quad (6.5)$$

$$\text{Adsorption}_t = \frac{C_{D,0} \cdot V_{D,0} - (C_{D,t} \cdot V_{D,t} + C_{C,t} \cdot V_{C,t})}{C_{D,0} \cdot V_{D,0}} \cdot 100\% \quad (6.6)$$

2.4.2 "Electrodialysis" experiments

To investigate whether TOrC-transport is mainly driven by diffusion or by electrical effects, the transport from diluate to concentrate under the influence of different constant current densities during ED was investigated. If transport is mainly diffusion driven, it will be hard

to achieve a selective separation between the organic and inorganic fraction during ED-operation, while electrically driven transport can be tuned to allow for a more selective separation of charged compounds. Again, 8l batches of diluate (100 g/l NaCl + 100 μg/l TOrCs) and concentrate (10 g/l NaCl) were used. To minimalize effects due to non-steady-state adsorption of TOrCs onto the IEM, the membranes from the previous tests were used and equilibrated for an additional 24h with a 55 g/l NaCl (equilibrium concentration) solution containing 100 μg/l TOrCs. This timeframe was shown to be sufficient to guarantee saturation of the membranes with the TOrCs, by the tests discussed above. Before starting the actual experiments, the compartments were rinsed with an extra 1l of the appropriate solutions to remove any traces of the flushing solution from the compartments. This volume proved to be sufficient to avoid any influence of the flushing solution on the tests and to avoid desorption of TOrCs from the pre-loaded membranes. Tests were conducted with three different current densities: 100, 150 and 200 A/m², applied by using a DC current-source (AFX-2930SB, Velleman, Belgium). The weight and conductivity of the diluate were continuously monitored and logged to monitor water and salt transport. Samples of the diluate and concentrate were taken at 0, 25, 50, 75 and 95% of desalination for TOrC analyses. By varying the current density, the desalination speed is varied, resulting in an experimental time of approximately 128, 85 and 64 hours for the 100, 150 and 200 A/m² experiments respectively until a desalination extent of 95% was reached. This allows to distinguish between the TOrC-transport by diffusion, and the transport caused by the electrical potential gradient. In case the transport is mainly diffusion driven, the transported amount is expected to be higher at lower current densities. By linking the properties of the TOrCs and membranes (such as charge and hydrophobicity) to the transport phenomena, the dominant properties governing the transport can be revealed. It is expected that electrostatic interactions will dominate and transport of charged solutes will thus be greater than that of neutral compounds.

3 Results and discussion

3.1 Diffusion experiments - TOrC adsorption

As can be seen from Figure 6.1, the total amount of TOrC adsorbed onto the membranes appeared to reach a constant value after 24-36 hours, indicating equilibrium adsorption of the TOrCs. In this experiment, the salt concentration in the diluate and concentrate were 100 g/l NaCl and 10 g/l NaCl respectively, similar to the ED experiments. The adsorption experiments were also done at a high salt concentration (100 g/l NaCl) and in the absence of

salts. These results are shown in Appendix D. As for the adsorption experiment with different salt concentrations, the experiment with high salt concentration also showed an equilibrium around 24h, while the experiment in the absence of salt showed no equilibrium after 48h. Based on these results, it was decided to flush the stack and membranes with the TOrC solution prior to the electrodialysis experiments for at least 24 hours to ensure saturation of the membranes by the TOrCs. Since the membranes used in the ED experiments were first used in the adsorption experiments for 48 hours, they were already (partially) loaded with TOrCs, making 24h a sufficient timespan to ensure full saturation.

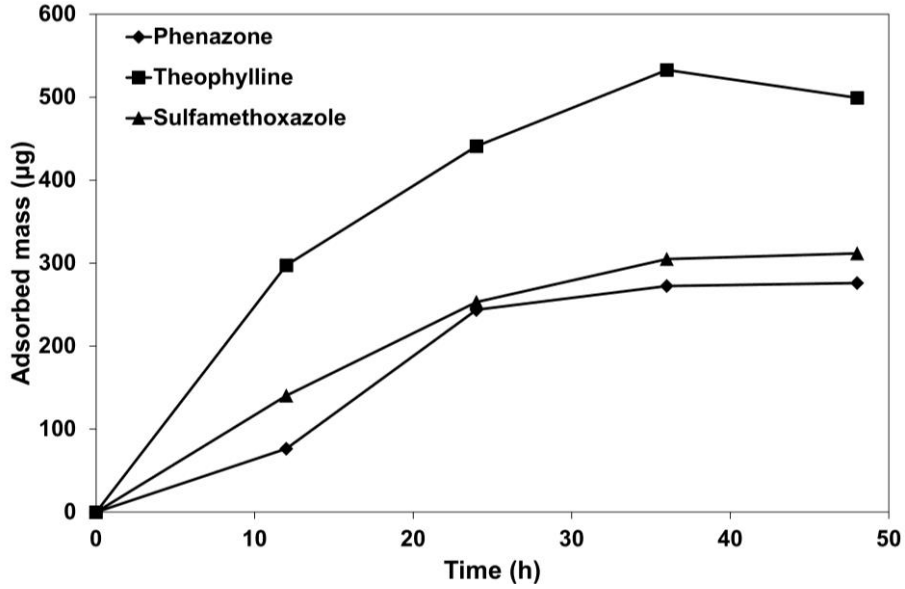

Figure 6.1 Adsorbed amount of TOrC (µg) during 48-hour diffusion experiment (100 g/l NaCl + TOrCs | 10 g/l NaCl diluate | concentrate). Lines were included to guide the eye. Information for all TOrCs is included Appendix D.

The adsorption of TOrCs at the end of the experiments with different NaCl concentrations is shown in Figure 6.2. When the salt concentration in both compartments was 100 g/l NaCl, the adsorption of charged TOrCs (denoted (-) and (+)) was significantly lower compared to the adsorption in the absence of salt. The lower adsorption of TOrCs in the presence of NaCl could be explained by the preferred interaction of the membrane functional groups with smaller, more mobile sodium and chloride ions when these are present.

A weak correlation between the amount of adsorbed TOrC and their charge ($R^2 = 0.5$) and LogD ($R^2 = 0.3$) was found, but only in the absence of NaCl. It would thus appear as if adsorption is more pronounced for more hydrophilic solutes, which is in contrast with research on similar TOrCs for NF/RO membranes [110,161]. This suggests that hydrophobic-hydrophobic interactions only have a minor role in the adsorption process of TOrCs onto IEM and – logically – that charge and polar interactions play a more dominant

role. It is hypothesized that adsorption is mainly governed by electrostatic interactions between the TOrCs and the membrane and, due to the increasing adsorption for more hydrophilic TOrCs, also that electron-donor/-acceptor interactions between the TOrCs and the membrane functional groups (including the formation of hydrogen bonds) are important for neutral TOrCs. Both hypotheses seem rather logical, given the charged and rather hydrophilic character (see Table 6.1) of the membranes and corroborate with earlier work [157]. When the NaCl concentration in both compartments is different, these effects are less clear, although the adsorption of neutral compounds seems to be higher. A possible explanation for this elevated adsorption could be a "salting out" effect, a phenomenon which causes the solubility of non-electrolytes to decrease in the presence of high salt concentrations. The high affinity for water of the salt molecules causes a dehydration of the TOrCs, decreasing their solubility, a process which is often used in the extraction of various organic components [174,175]. In this experiment, the high salinity of the diluate compartment forces the TOrCs into the low salinity compartment, where their solubility is higher. This causes more TOrC-membrane contact, increasing the adsorption of neutral compounds onto the membrane. However, this is merely a hypothesis that needs further research.

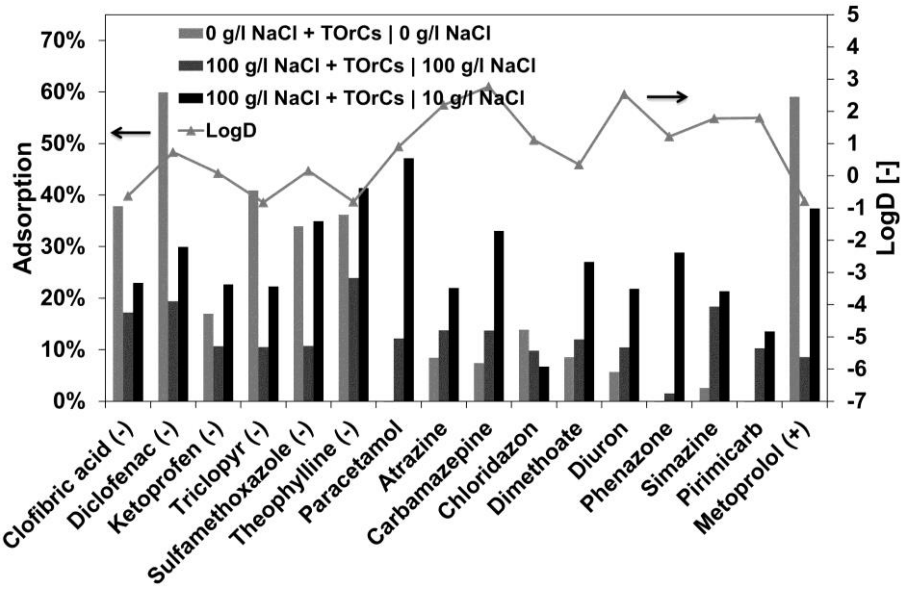

Figure 6.2 Total adsorption (%) after 48 hours with different diluate | concentrate concentrations as a function of logD (-). Based on quantitative analysis with a calibration curve with an $R^2 > 0.99$.

3.2 Diffusion experiments – TOrC transport

The net transport (%) of TOrCs from diluate to concentrate during these experiments is shown in Figure 6.3. Since adsorption reaches an equilibrium after approximately 24 hours,

the effect of the different salt concentrations on transport after 48 hours can be compared. Clearly, charged TOrCs are transferred across the membrane more easily when no NaCl is present. Although no correlation was found between the size of the TOrCs and the transport in absence of NaCl, the higher transport of paracetamol (despite its neutral charge) could be explained by its smaller size compared to the other compounds.

When NaCl is present, whether the concentration is the same or different in concentrate and diluate, the transport of TOrCs is much lower. This again shows a preferential interaction of the IEM with the salt ions, similar to the adsorption experiments, which suppresses the transport of TOrCs. This preferential interaction can be explained by the smaller size and higher mobility of the Na^+ and Cl^- ions, but also by their high concentration in respect to the TOrC concentration. Indeed, the chemical equilibrium across the membrane is restored in this case mainly by transport of NaCl. Another explanation for the lower transport in the presence of NaCl could be found in the diffusion coefficient of organic compounds, which tends to decrease in the presence of high salt concentrations. This phenomenon has been found to decrease the self-diffusion coefficient by up to 27% at high NaCl concentrations during tests in our laboratory (results are shown in Appendix D). A decrease of up to 12% in the diffusion coefficient can be expected at the salt concentrations used in this study, which could partially explain the lower transport of TOrCs in the presence of NaCl.

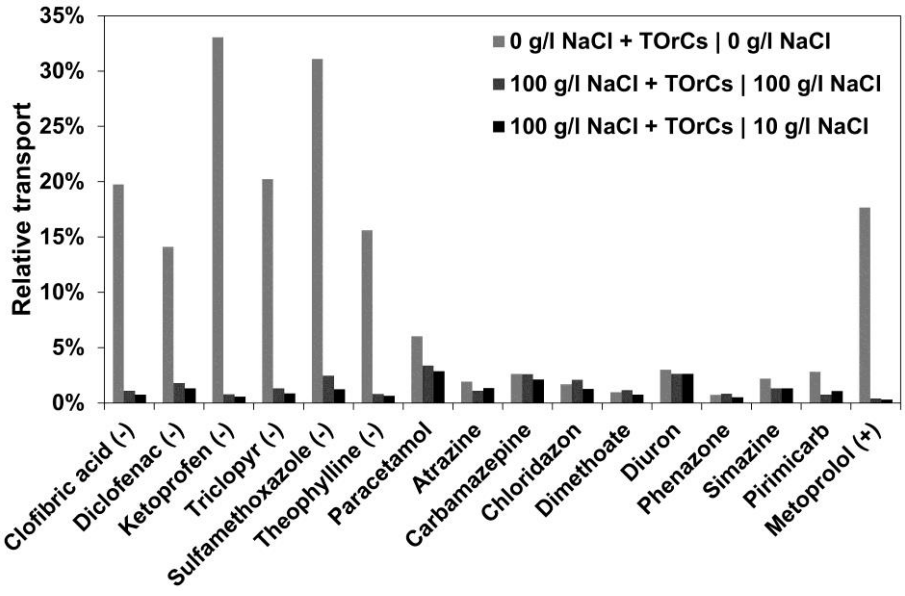

Figure 6.3 Transport of TOrCs (%) in the presence of different salt concentrations in diluate | concentrate. Based on quantitative analysis with a calibration curve with an $R^2 > 0.99$.

3.3 Diffusion experiments – TOrC and salt diffusion

Figure 6.4 shows a more detailed overview of the net transport of TOrCs over time during the experiment with different NaCl concentrations in diluate and concentrate. When closely analysing this transport versus time, an almost linear trend is seen for the neutral TOrCs (with an average R^2 for the neutral TOrCs of 0.9 ± 0.1 for the regression). Given the rather limited amount of transport (<10%), which causes the concentration gradient of the TOrCs across the membrane to stay more or less the same, one would speculate that the transport of especially neutral compounds is purely diffusion driven, and thus irrespective of water and/or salt transport. For the charged compounds, this linear relation with time is less clear: R^2 values of 0.7 ± 0.2 and 0.1 ± 0.1 for negatively and positively charged compounds respectively indicate that (especially for positive compounds) other mechanisms play a role here. This was already indicated above, by the differences in transport of charged TOrCs with different salt concentrations in the different compartments.

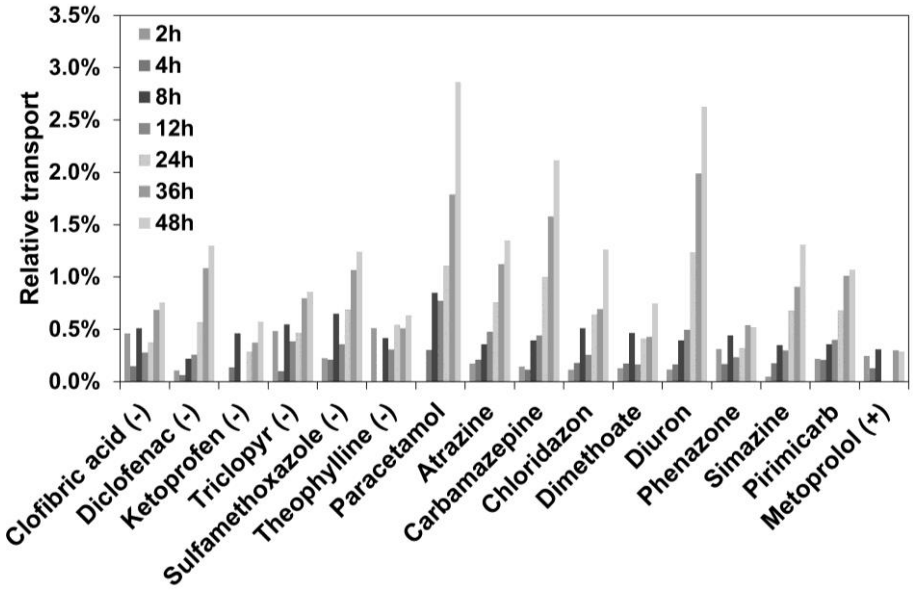

Figure 6.4 Transport (%) versus time (h) with a 100 g/l NaCl + TOrCs | 10 g/l NaCl diluate | concentrate concentration difference. Based on quantitative analysis with a calibration curve with an $R^2 > 0.99$.

Transport of the positively charged TOrC metoprolol appears to be the lowest of all compounds, despite the charged character of the CEM, which should allow for electrostatic interactions with the charged membrane surface. The smaller amount of transport of the positively charged TOrC could potentially be explained by the higher crosslinking of the CEM membranes through which these TOrCs would preferentially move (given their positive charge), hindering their transport. This higher crosslinking was confirmed by the membrane characterisation as shown by a higher resistance compared to the AEM and

relatively low swelling degree. In addition, the positively charged TOrC used is metoprolol, which is also one of the largest compounds in the mixture. These considerations make it difficult to make any general conclusions on the behaviour of positively charged compounds. Since the neutral compounds can diffuse through both the AEM and CEM, their total transport in the presence of NaCl is higher than that of the negatively charged TOrCs, which are repelled by the negatively charged CEM. The transport of neutral compounds through the CEM might however also be limited by the crosslinking of the CEM. Whether or not transport of the neutral TOrCs occurs mainly through the AEM can not be assessed from this study. The transport of phenazone is significantly lower when compared to other neutral compounds, and seems to be limited to about 0.5%. However, no clear explanation for this anomalous behaviour was found.

3.4 Electrodialysis experiments

During ED operation, there are two main drivers for (ionic) transport; the concentration difference between diluate and concentrate and the applied electrical potential. The influence of the latter on TOrC-transport was investigated by applying three different current densities (100, 150 and 200 A/m²) during the desalination of a model waste stream (100 g/l NaCl + 100 μg/l TOrCs). The resulting amount of TOrC-transport at the end of these experiments is shown in Figure 6.5.

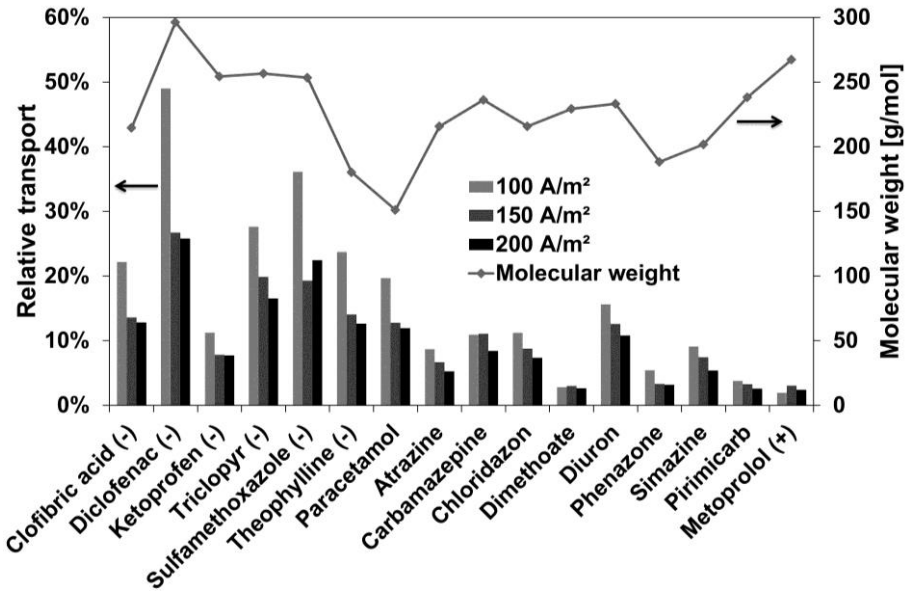

Figure 6.5 Net transport (%) at 95% desalination for electrodialysis at three different current densities (100, 150 and 200 A/m²) as a function of the molecular weight (g/mol). Based on quantitative analysis with a calibration curve with an $R^2 > 0.99$.

More transport of TOrCs occurs at lower current densities, in contrast to what would be expected given the lower driving force for ionic transport. This again provides an indication that the TOrC-transport of negative and neutral TOrCs is mainly diffusion driven, as experiments run at lower current densities lasted longer (since all experiments were run until 95% desalination was reached), and thus had more time for diffusion of TOrCs. This is supported by the course of the transported amount over time (results shown in Appendix D), which shows a good linear correlation ($R^2 = 0.94 \pm 0.06$) for all compounds. If the external potential difference would have a significant effect, one would expect the transport to be more exponential, increasing with a decreasing NaCl concentration during desalination. Further proof for this diffusion driven transport is given in Figure 6.6, where the transported amount of TOrCs is given after approximately the same amount of time has passed (50% desalination at 100 A/m², 75% desalination at 150 A/m² and 95% desalination at 200 A/m²). This graph clearly shows that the transported amount is not very different between the 100 A/m² and 150 A/m² experiments, resulting in an average standard deviation of 0.9% when comparing the transport between these two experiments, despite the different experimental conditions. However, the transport seems to increase for the 200 A/m² experiment for the negatively charged components. This increase is probably due to the very low NaCl concentration at that point, causing the increased transport of TOrCs as charge carriers. The transport of negatively charged components is thus diffusion driven up to the point that the diluate is almost completely depleted of NaCl.

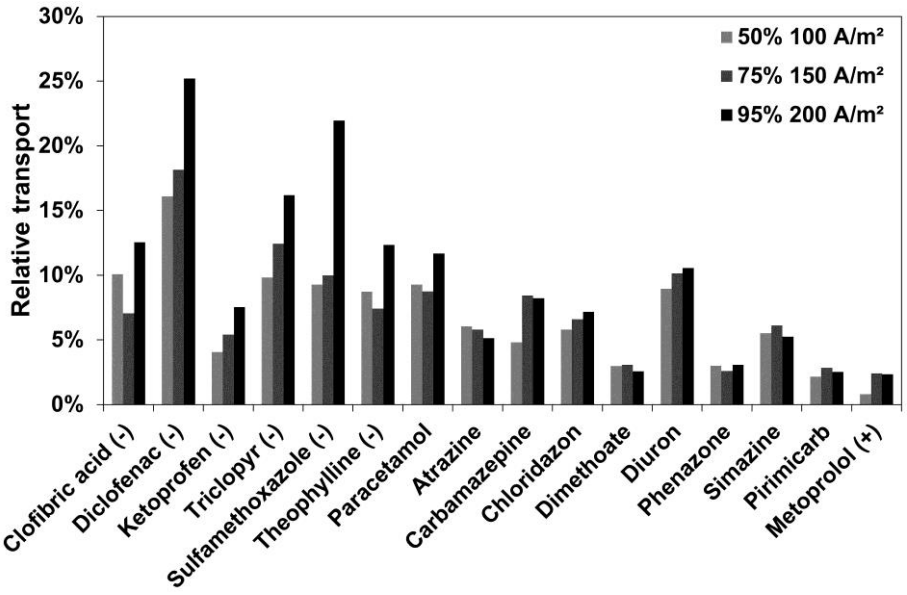

Figure 6.6 Transported amount of TOrCs after a similar amount of time (36 hours) has passed for the three different ED experiments (100 A/m², 150 A/m² and 200 A/m²). Based on quantitative analysis with a calibration curve with an $R^2 > 0.99$.

4 Conclusions

The transport mechanisms of organics, based on TOrCs as a model, were examined in this study. The influence of NaCl as well as of the external potential difference was looked into. The major findings can be summarised as follows:

- Electrostatic and hydrophobic interactions as well as a possible 'salting out' effect affect the adsorption of the TOrCs onto the membranes.
- The transport of charged TOrCs is higher in the absence of NaCl, showing the preferential interaction of the membranes with the small, mobile NaCl ions.
- The transport of especially negatively charged TOrCs is higher at lower current densities at the same desalination degree. Furthermore, the transport is similar at equal time intervals. This indicates that the transport of TOrCs is mainly diffusion driven.
- Although the behaviour of positively charged organics is expected to be similar to that of the negatively charged ones, this should be confirmed in experiments with a wider range of positively charged compounds.

Diffusion as the driver for organics transport is of major importance for transport of organics in high salinity environments, as it shows that it is very difficult to get preferential transport of (charged) organics. In Chapter 7, the diffusive nature of the organics transport is looked into further. The influence of the matrix is investigated as well as the behaviour of other organics.

Chapter 7: Organics transport in ion-exchange membranes: influence of solution matrix and organics properties

This chapter was submitted to Environmental Science and Technology as

Vanoppen, M., Stoffels, G., Ma, L., De Meyer, E., Schoutteten, K.V.K.M., Vanden Bussche, J., Vanhaecke, L., Verliefde, A.R.D. Organics transport in ion-exchange membranes: influence of solution matrix and organic properties.

1 Introduction

Chapter 6 described the behaviour of TOrCs in ED under different operational circumstances. However, not only the operational conditions, but also the solution matrix and the properties of the organics have an important impact on their transport behaviour.

Depending on the specific application, transport of organics may be desired [170,176] or unwanted [168]. Gildemyn et al. (2015) for example, discusses the selective production, extraction and concentration of acetate in a microbial electrosynthesis (MES) configuration, using IEM. Here, selective transport of the acetate over the IEM is preferred over the transport of e.g. chlorides present in the catholyte [176]. On the other hand, in the hybrid combination of IEM technologies with RO to decrease seawater RO energy demands as discussed in Chapters 4 and 5, organics from the wastewater should be retained from the IEM as they risk ending up in the RO feed, potentially causing fouling in the RO membrane or contamination of the produced water.

A different study by Andersen et al. (2014) showed an increased flux of acetate at increased current densities in a membrane electrolysis system [170]. In these systems, the broth containing the organics is usually low in salts and the transport of organics is against the dominating salt flux, as in this study where Na_2SO_4 was present in the anolyte. Furthermore, an increase in concentration of this salt in the anolyte proved to enhance the organics transport to the anolyte by Donnan dialysis effects.

The aim in this study is to further investigate the transport of organics in the presence of salts other than NaCl as well as the effect of their transport direction relative to the dominating salt flux direction. Both $MgCl_2$ and Na_2SO_4 were investigated in this respect, where one of the ions (either Na^+ or Cl^-) is kept constant in comparison to NaCl, and the other ion is replaced by a bivalent ion (Mg^{2+} or SO_4^{2-} respectively) to isolate the effect of multivalent anions and cations on the transport of the organics. Also, the concentration of the organics relative to the salt concentration seems to play an important role in the transport characteristics, which is why both of these concentrations were varied as well. As in the previous study, TOrCs were used as a model for organics, but this study also looks into the transport of organic acids, which are important in typical microbial electrosynthesis processes. Both types of organics are small (i.e. they don't cause fouling or poisoning of the membranes), easy to analyse and easy to distinguish quantitatively in a mixture, which makes them the ideal candidates for this study on the general transport of organics through IEM.

Based on the results obtained in this study, the understanding of transport of organics through IEM will be further expanded and documented. This will ultimately lead to an understanding of the parameters that govern the transport, and this knowledge can be used for the development of specific IEM focussed on the selective transport or retention of organics in a wide range of applications.

2 Materials and methods

2.1 Electrodialysis set-up and membranes

The ED set-up used in this study is the same as the one described in Chapter 6. The same Fujifilm type II membranes were used, the properties of which are reported in Table 6.1.

2.2 Organics

TOrCs and organic acids are chosen here as a model for organic compounds in general. The exact compounds used and their general properties are listed in Table 7.1.

A stock solution of the TOrCs (analytical grade, Sigma-Aldrich; >98%) of 2 mg/l was prepared and stored in the freezer. Before use, the solution was thawed and subsequently stored at 4°C for a maximum of 4 weeks. For the experiments, the stock solution was diluted to yield a final concentration of 100 µg/l in the diluate or concentrate (depending on the specific experiment). As the behaviour of compounds with identical charge was shown to be similar in our previous study, the mixture was limited to four compounds with a negative, neutral and positive charge, respectively. The chemical structure of the TOrCs is included in Appendix E.

Table 7.1 Main properties and limit of detection (LOD) of 12 used TOrCs and 4 used organic acids. The charge, pKa, molecular weight (MW), and log D (pH-corrected octanol-water partition coefficient) were calculated using Marvin 5.11.5 software (ChemAxon, Hungary).

Component	Charge (pH 7)	pKa (-)	MW (g/mol)	Log D (pH 7)	LOD (µg/l)
Carbamazepine	0	-	236.27	2.77	0.015625
Clofibric acid	-	3.4	214.65	-0.63	1
Dimethoate	0	-	229.26	0.34	1
Diuron	0	-	233.10	2.53	0.125
Ketoprofen	-	3.9	254.28	0.08	0.03125
Metoprolol	+	9.7	267.36	-0.79	0.25
Pirimicarb	0	5.0	238.29	1.79	0.5
Sulfamethoxazole	-	2.0	253.28	0.15	0.25
Lincomycin	+	7.97	406.54	-1.33	0.125
Lidocaine	+	7.75	234.34	2.02	1
Propanolol	+	9.67	259.34	0.04	1
Triclopyr	-	2.3	256.47	-0.83	1
Propionic acid	-	4.8	74.08	0.48	$12 \cdot 10^3$
Butyric acid	-	5.0	88.11	0.92	$14 \cdot 10^3$
Valeric acid	-	5.0	102.13	1.37	$17 \cdot 10^3$

Propionic, butyric and valeric acid, obtained from Sigma-Aldrich at a purity >99%, were used as an alternative model for organics, as these are commonly encountered in MES and ME systems for example. Furthermore, their higher solubility compared to the TOrCs enables the study of the concentration of the organics relative to the salt concentration. The acid concentrations in diluate and concentrate during the experiments were measured by gas chromatography (GC-2014, Shimadzu®, The Netherlands) with DB-FFAP 123-3232 column (30m x 0.32 mm x 0.25 µm; Agilent, Belgium) and a flame ionization detector (FID) [170].

2.3 Experimental protocol

All experiments were carried out in DI water, to which salts, TOrCs and/or organic acids were added. A constant concentration of 100 µg/l was used when TOrCs were examined, while experiments with an organic acid dosing of 1 and 10 g/l were carried out. All experiments were carried out in two different operational modes: one without an external potential difference (so-called 'diffusion' experiments) and one with a constant current density (so-called 'ED' experiments). This current density was 100 A/m² unless specified otherwise. Experiments were carried out with NaCl, $MgCl_2$ and Na_2SO_4 in different concentrations in diluate and concentrate, and with TOrCs added to the diluate and the

concentrate in separate experiments. The initial salt concentration was adjusted to correspond to either 0.86 eq/l (50 g/l) or 1.71 eq/l (100 g/l) NaCl in the diluate and 0.17 eq/l (10 g/l) NaCl in the concentrate. In all experiments, the electrolyte consisted of 81 g/l $NaNO_3$. An overview of all experiments with the respective compositions of diluate and concentrate is given in Table 7.2.

Table 7.2 Overview of experiments carried out in this study (TOrC = Trace Organic Contaminants, OA = Organic Acids). To avoid an overload of data and assure overall clarity, results of experiments marked with a * will be presented in Appendix E, as they confirm the conclusions discussed in this study but do not offer any new insights. ** ED experiments for experimental series 5 were carried out at 0, 23, 44 and 100 A/m².

Experiment	Salt	Diluate (eq/l)	Concentrate (eq/l)
1	NaCl	0.86 + TOrC	0.17
2	NaCl	0.86	0.17 + TOrC
3	NaCl	1.71 + OA (1g/l)	0.17
4	NaCl	1.71 + OA (10 g/l)	0.17
5**	NaCl	OA (10 g/l)	0.17
6	$MgCl_2$	0.86 + TOrC	0.17
7*	$MgCl_2$	0.86	0.17 + TOrC
8	Na_2SO_4	0.86 + TOrC	0.17
9*	Na_2SO_4	0.86	0.17 + TOrC

Volumes of the solutions were chosen so that during the ED experiments, 90% desalination would be theoretically reached after 48 hours. For a diluate concentration of 1.71 eq/l, this corresponds to 3 l of solution, for a concentration of 0.86 eq/l it is 6 l. 1 l of electrolyte was used in all experiments. All solutions were recycled through the stack and back to their vessel in batch mode at a flow rate of 500 ml/min. Samples were taken at 0, 24 and 48h for the experiments with TOrCs and at 0, 8, 24, 32 and 48 hours for experiments 3 and 4 with organic acids. In experiment series 5, where no salt was dosed to the diluate, experiments were run for 8 hours (at the same volumes as experiments 3 and 4) to avoid complete desalination because of the low concentration of charges available, and samples were taken at 0, 2, 4, 6 and 8h. Weight and conductivity were monitored to check the progress of the desalination process. Exact solution volumes were measured after each experiment.

This study specifically looks into the transport of the organics. However, due to non-steady-state adsorption of the organics onto the IEM, transport might be underestimated because of adsorption of the organics onto the membranes, spacers and other materials. To avoid these phenomena, the complete stack was equilibrated with the organics for 24h before each

experiment. The equilibrating solution consisted of 4 l with an average diluate/concentrate salt solution of the appropriate salt and 100 µg/l TOrC or the appropriate concentration of organic acids (1 or 10 g/l, depending on the experiment). Before the start of the actual experiments, each compartment (diluate, concentrate and electrolyte) was flushed with 1 l of the appropriate starting solution to remove any traces of the equilibrating solution. These experimental conditions were validated in Chapter 6. The results are shown as relative transport (%), which is the transported mass (taking into account volume changes) relative to the total mass initially present in the diluate (see Equation 6.5).

3 Results and discussion

This study focuses on the matrix composition and the properties of different model organics and their effect on the transport of organics through IEM. The influence of the salt type and direction of organics transport with respect to the salt flux are examined for TOrCs. The study concludes with a study of the behaviour of organic acids. In all cases, both diffusion experiments (in the absence of an external potential difference) and electrodialysis experiments (with a constant current density) are discussed.

3.1 Influence of Na_2SO_4 and $MgCl_2$ on TOrC transport

3.1.1 Diffusion experiments – no external potential difference

The effect of the presence of NaCl, $MgCl_2$ and Na_2SO_4 on the transport of TOrCs (dosed to the diluate) during the diffusion experiments was investigated in experiments 1, 6 and 8. The results after 48 hours are shown in Figure 7.1. The presence of multivalent ions in the matrix is expected to have an effect mainly on the charge interactions between the ions and the IEM. That is why for neutral compounds no significant effect of the change in matrix composition is expected. This is confirmed by the results, which show that there is no detectable difference in transport for the neutral compounds between the three experiments. For the negatively charged compounds, no difference in transport of the organics is detected between the experiments where NaCl is in the diluate matrix versus when $MgCl_2$ is used. The transport of positively charged compounds however is higher in the presence of $MgCl_2$ compared to NaCl. This can be (partially) explained by the lower diffusion rate of Mg^{2+} compared to Na^+ (the diffusion coefficient in water at 25°C for Na^+ is 13.3 x 10^{-10} m^2/s and for Mg^{2+} is 7.05 x 10^{-10} m^2/s [177]). In both experiments, the electrochemical potential difference over the membrane drives the transport of ions across the membrane. Since Mg^{2+} diffuses slower than Na^+, relatively more positively charged organics will be transported to

balance the equilibrium difference across the membrane when Mg^{2+} is present in the diluate than when Na^+ is present. For the negatively charged TOrCs, there is no difference between these two experiments, as the anion (Cl^-) remains the same. When Na_2SO_4 is present in the diluate compared to when NaCl is present, the same phenomenon can explain the higher transport of negatively charged compounds (the diffusion coefficient in water at 25°C for Cl^- is $20.3x10^{-10}$ m²/s and for SO_4^{2-} is $10.7x10^{-10}$ m²/s [177]). However, the transport of positively charged compounds is also higher in the presence of Na_2SO_4 in the diluate. Based on the data available here, no clear explanation for this behaviour can be found. The same behaviour for all three experiments can also be seen in the data after 24 hours, which is included in Appendix E.

It is expected that the higher charge (of Mg^{2+} and SO_4^{2-}) makes up, at least in part, for the lower diffusion coefficient. The increased transport of organics however shows that the increased charge might not make up for the decreased diffusion coefficient entirely, but the increased transport of positively charged TOrCs in the presence of SO_4^{2-} points at other phenomenon playing a role. It is possible that the diffusion coefficient of the organics is influenced by dehydration in the presence of high salt concentrations, and that this dehydration (increasing the diffusivity) is more severe in the presence of multivalent ions. The hydration of ions and solutes was already shown to play an important role in their rejection by NF membranes [178,179]. Furthermore, complexation of the organics with the multivalent ions should looked into, as research has already shown that multivalent cations for example are prone to complexation with carboxylic functional groups [178,180,181]. However, this is expected to result in a decline of the transport rather than an increase. More thorough research is needed to elucidate the exact mechanisms causing the increased TOrC transport in the presence of multivalent ions.

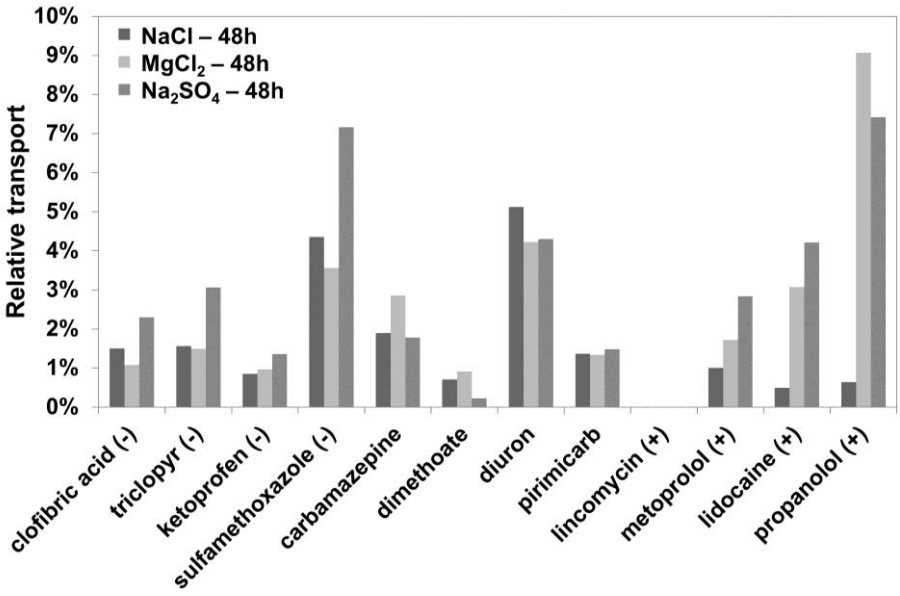

Figure 7.1 Relative transport of TOrCs in the absence of an external potential difference in the presence of different salt (NaCl, $MgCl_2$ and Na_2SO_4) at 48h (the results after 24h are included in Appendix E). Based on quantitative analysis with a calibration curve with an $R^2 > 0.99$.

3.1.2 Influence of a constant current density in electrodialysis experiments

From the transport results under influence of an external potential difference, a similar conclusion can be drawn, as shown in Figure 7.2 (experiments 1, 6 and 8). Again, the transport of negatively charged compounds is higher in the presence of Na_2SO_4 and the transport of positively charged compounds is higher in the presence of $MgCl_2$, as discussed above. There is also no distinguishable difference for the neutral compounds. Surprisingly however, the transport of positively charged TOrCs is again highest in the presence of Na_2SO_4. Again, the data available is insufficient to explain why the transport of positive TOrCs is higher in the presence of Na_2SO_4 and more research is needed to explain this phenomenon.

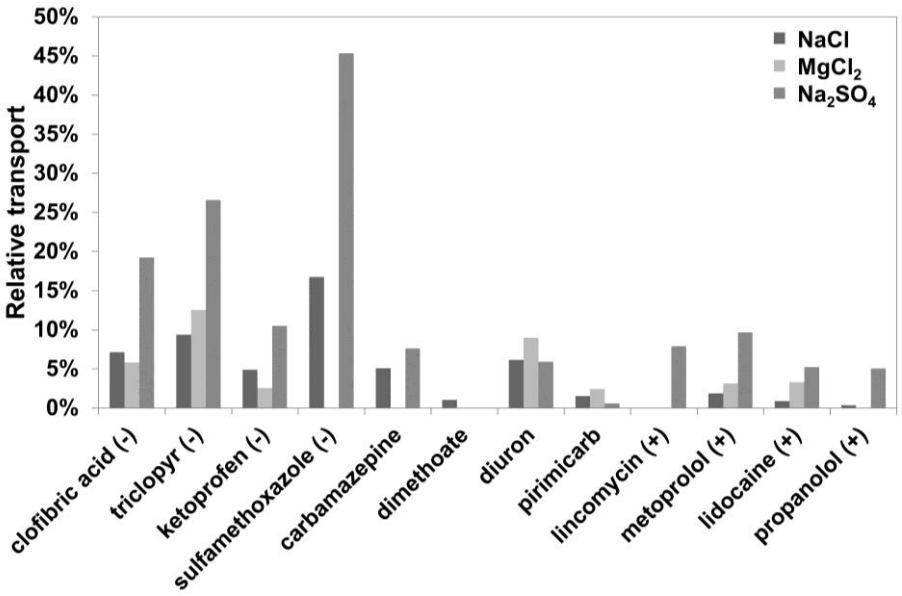

Figure 7.2 Relative transport of TOrCs during electrodialysis in the presence of different salt (NaCl, $MgCl_2$ and Na_2SO_4) at 48h (the results after 24h are included in Appendix E). Based on quantitative analysis with a calibration curve with an $R^2 > 0.99$.

As in the diffusion experiments, the results after 24 hours show the same results, and are included in Appendix E.

3.2 Influence of the TOrC transport direction relative to the dominant salt flux

3.2.1 Diffusion experiments – no external potential difference

In Figure 7.3, transport of the organics is shown for experiments where the TOrCs are dosed in different compartments (experiments 1 and 2). Experiments where the TOrCs are dosed to the diluate (D + TOrCs) are compared to experiments where they are dosed to the concentrate (C + TOrCs) initially. This induced transport of the organics with or against the dominant salt flux respectively. Since the transport of neutral components is not influenced by charge effects, their diffusion over the membrane according to their concentration difference across the membrane should not be influenced by their direction of transport relative to the dominant salt flux. This is confirmed in the experiments, where no difference between both kinds of experiments is detected for the neutral compounds.

For the charged compounds however, it is clear that transport is higher when the TOrCs move from the concentrate to the diluate, i.e. against the direction of the salt transport from diluate to concentrate (with the salt concentration gradient). This can be explained by the phenomenon of Donnan dialysis, by which species of the same charge are exchanged across IEM according to their difference in electrochemical potential across this membrane. In ED, transport across the membrane can occur in different ways. Commonly, to maintain

electroneutrality, an ion and its counter-ion(s) are exchanged across the CEM and AEM simultaneously. E.g. when a sodium ion crosses the CEM, a chloride ion for example will cross the AEM at the same time. However, when the electrochemical potential difference across the membrane is high such as in this case, Donnan dialysis may occur as well. In this case, sodium for example can be exchanged across the CEM for another ion (such as a positively charged TOrC) with the same charge, decreasing the electrochemical potential difference and maintaining electroneutrality by transport across only one kind of IEM. The effect is more pronounced for the negatively charged compounds as the positively charged compounds are much bigger and the CEM has a highly crosslinked structure, limiting easy exchange of organic cations across the CEM and favouring the transport of the small Na^+ ions instead. The same conclusions can be obtained from similar tests with $MgCl_2$ and Na_2SO_4, included in Appendix E.

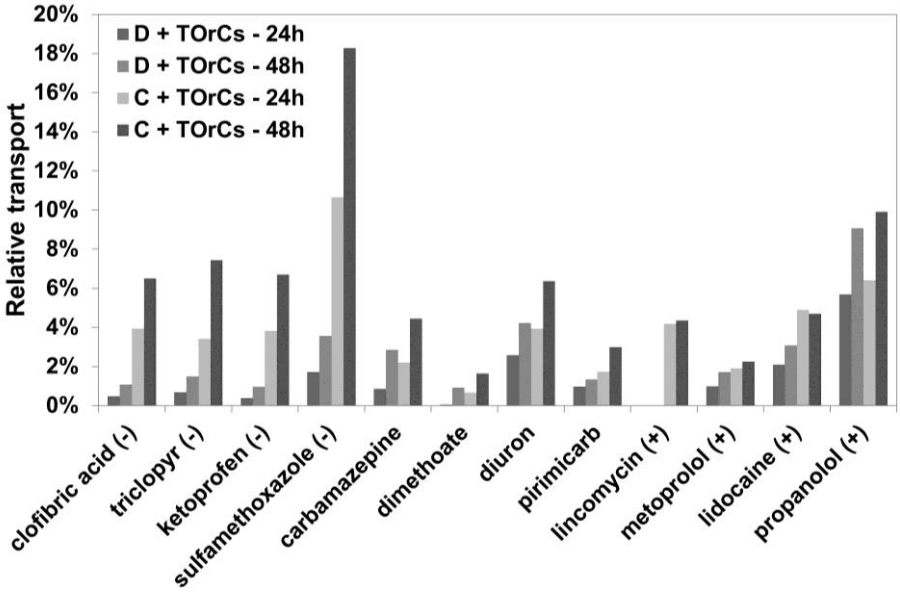

Figure 7.3 Relative transport of TOrCs in the absence of an external potential difference with the initial dosing of the TOrCs in the concentrate (C) or diluate (D) after 24 and 48h. The initial diluate contained 50 g/l NaCl. Based on quantitative analysis with a calibration curve with an $R^2 > 0.99$.

3.2.2 Influence of a constant current density in electrodialysis experiments

In ED experiments 1 and 2, results show a different trend compared to the diffusion experiments, as shown in Figure 7.4. The transport after 24 hours is unaffected by the direction of salt transport both for neutral compounds and for negatively charged compounds. This indicates that transport is mainly diffusion driven, as it is the same independent of the direction relative to the applied potential difference, further confirming the observations in our previous research. After 48 hours, the transport of negatively charged species peaks when the direction of the organics transport is the same as the salt flux, as

discussed before. However, when the organics move against the dominant salt flux (i.e. when they are initially dosed in the concentrate), the transported amount of TOrCs decreases slightly between 24 and 48 hours, indicating transport back into the concentrate. This could have been caused by the phenomenon of salt depletion in the diluate, resulting in an increased transport of the TOrCs that were earlier transported to the diluate, back to the concentrate to carry the charge. For the positively charged species however, the transport from concentrate to diluate is higher than the transport from diluate to concentrate under the same experimental conditions. However, this trend, contrary to the other trends observed, is not reproduced in the experiments with different salts (Appendix E), where, as expected based on the behaviour of the negatively charged compounds, the transport of positively charged TOrCs is lower when they are dosed to the concentrate.

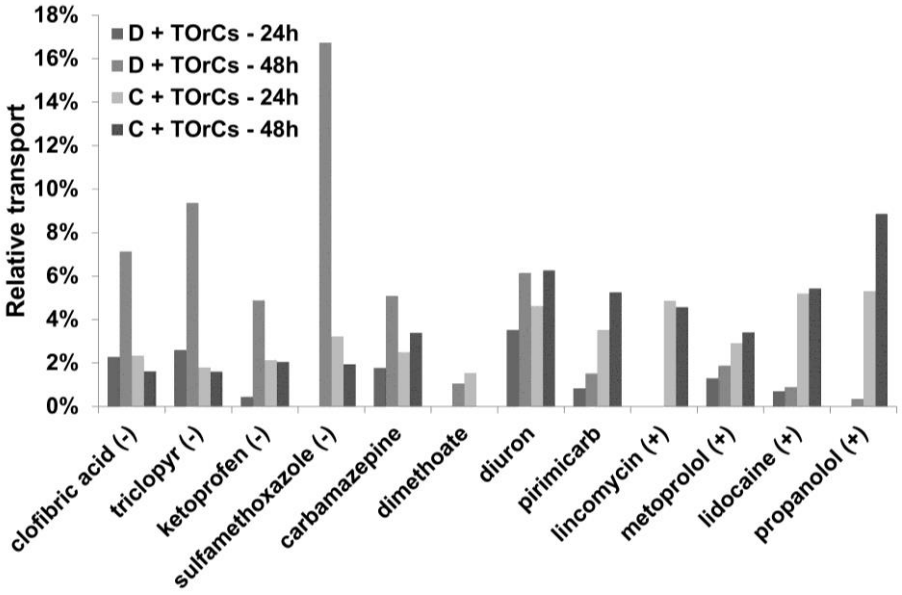

Figure 7.4 Relative transport of TOrCs during electrodialysis with the initial dosing of the TOrCs in the concentrate (C) or diluate (D) after 24 and 48h. The initial diluate contained 50 g/l NaCl. Based on quantitative analysis with a calibration curve with an $R^2 > 0.99$.

3.3 Behaviour of organic acids

In MES or MFC processes, the ratio of salts to organics in the broth to be treated is typically lower, and the concentration of the organics is higher. Organic acids are common in these systems and are usually the target compounds to be transported. In a last part of this study, experiments with three different organic acids were performed; propionic, butyric and valeric acid. Because of their higher solubility compared to TOrCs, different concentration ratios of salt versus organics could be tested and ED experiments without salts could be carried out for a significant amount of time without risking a fast complete desalination. This allowed to

study the transport mechanisms more closely and made it possible to distinguish between diffusion and electromigration more clearly. Experiments were performed with different acid concentrations (1 and 10 g/l), at different current densities (0, 23, 44 and 100 A/m²) and in the presence and absence of NaCl in the diluate.

3.3.1 Transport of organic acids at different concentrations, in the presence of salt

By varying the concentration of the organic acids (experiments 3 and 4), the ratio of the salt:organics concentration was varied. At a lower salt:organics ratio, it could be expected that more current will be carried by the organics since they are then present in higher relative amounts. Also, as the organics concentration is increased, their diffusional transport rates are expected to increase. As can be seen in Figure 7.5, increasing the organics concentrations does not result in an increase in relative transport of the organics (i.e. the rate of transport increases linearly with concentration). Both in the ED (left) and diffusion (right) experiments, the relative transport of the organics is comparable at different acid concentrations. However, since both diffusion and electromigration are expected to increase at a higher concentration, no clear distinction between the two can be made based on these figures, and it is yet unclear why transport increases linearly with organics concentration.

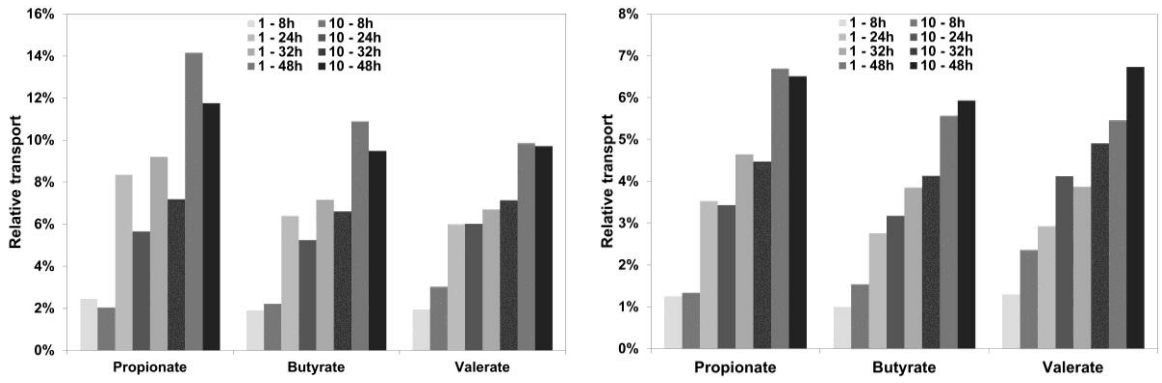

Figure 7.5 Relative transport over time of organic acids during the electrodialysis (left, at a constant current density of 100 A/m²) and diffusion (right) experiments, for a dosing of 1 and 10 g/l of the organic acids.

To make a more clear distinction between the transport phenomena taking place during the diffusion and ED experiments, the transport rate of the different organics was calculated. As the total transport is low in all experiments (<15%), it is expected that the driving force for transport remains constant during the experiments and thus the transport rate should be constant. Based on this assumption, Figure 7.6 was constructed, using the average fluxes during the experiments. As diffusion should theoretically be 10 times higher when the concentration increases 10 times as in these experiments (assuming no concentration

polarisation occurs and membrane selectivity is constant), the transport rate is expected to be around 10 times higher in the diffusion experiments with a higher acid concentration. If the external potential difference would also have a significant effect on the transport of the acids, the average transport rates would be higher during the electrodialysis experiments compared to the diffusion experiments.

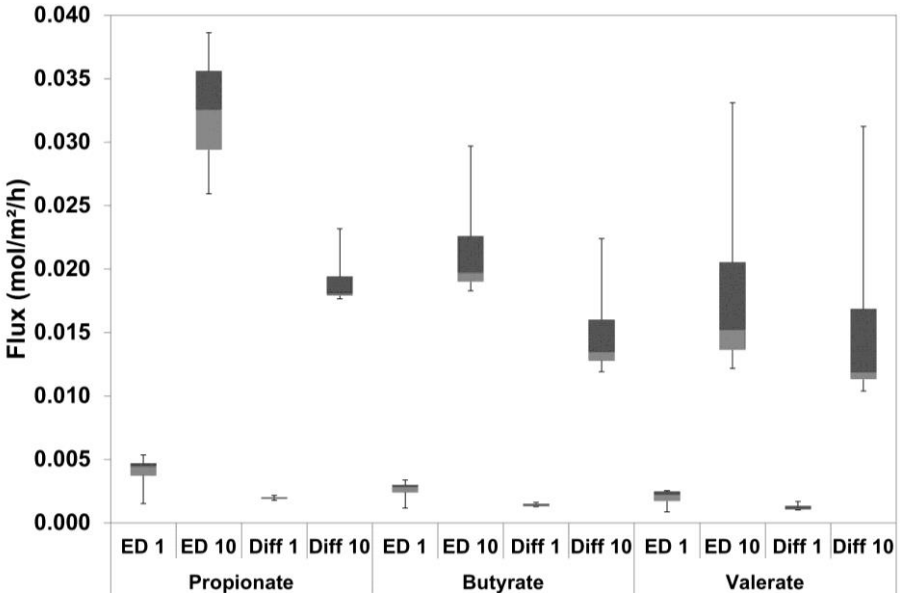

Figure 7.6 Flux of the organic acids through the ion-exchange membranes during the electrodialysis (ED) and diffusion (diff) experiments at an initial organic acid concentration of 1 and 10 g/l in the diluate.

The figure shows that the transport rates are indeed an order of magnitude higher when the concentration of acids is higher. However, the figure also shows that the difference in flux between the diffusion and ED experiments is limited, although the rate does seem to be somewhat higher in ED when comparing the averages. The latter is especially true for propionic acid, the smallest of the three. For butyrate and valerate, both bigger, the difference between the average transport rates in diffusion and ED experiments is smaller. This appears to confirm the hypothesis postulated in Chapter 6 that transport of organics in the presence of salts is mainly diffusion driven.

Another way of comparing the transport of organics at different concentrations, is the coulombic efficiency. As the organics concentration increases and the ratio of salt versus organics decreases, the coulombic efficiency for the organic acids would be expected to increase, as more charge would be carried across the membranes by organic acid transport. The coulombic efficiencies are shown in Table 7.3. These are based on the difference in transport between the diffusion and the ED experiments.

Table 7.3 Coulombic efficiencies for experiments at different organic acid concentrations.

		Coulombic efficiency	
		1 g/l	**10 g/l**
Propionate	%	0.06	0.4
Butyrate	%	0.04	0.2
Valerate	%	0.02	0.1

As expected, the coulombic efficiencies indeed increase at higher acid concentrations. It is however clear that, when salts are present, the coulombic efficiency for the organic acids is very low and the influence of the external potential difference on the acid transport is practically negligible – Coulombic efficiencies are below 1%, despite the fact that the salt concentration is only 13-17 times higher than the organics concentration in the 10 g/l organic acids case. This again points at the likeliness of diffusion being the main driving force for organics transport in the presence of salts. However, to more clearly assess the effect of the salt, experiments with organic acids in the absence of salt are discussed in the next section.

3.3.2 Transport of organic acids at different current densities without salts

In the absence of NaCl (experiment 5), the organic acids are the only ions that can carry charge across the membranes when the potential difference is applied (assuming no water splitting is occurring). Experiments were carried out with a diluate containing 10 g/l of the different organics in the absence of a potential difference and at three different constant current densities (23, 44 and 100 A/m²). It is expected that, as the current density increases, the transport of the acids will also increase. Figure 7.7 shows the transport of all three acids after 8 hours. The transport over the whole experiment appears to be linear for each acid in each experiment (linear slope with an average R^2 of 0.99 ± 0.01). It is clear that the transport is significantly higher when only organic acids are present, compared to when the transport occurs in the presence of NaCl.

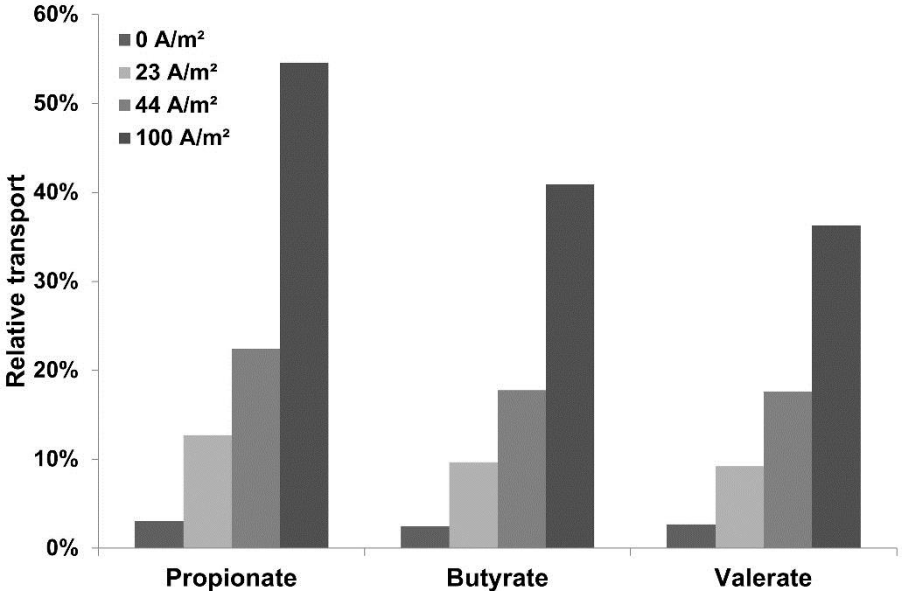

Figure 7.7 Total transport after 8h of organic acids at different current densities.

The relationship between the applied current density and the transport is linear for all acids, at an average R^2 of 1.00 ± 0.00. With the acids being the only charge carriers present, the coulombic efficiency for these compounds also increases dramatically. The overall coulombic efficiency, based on the average of the four sample points, is now 94% for the 23 and 44 A/m² experiments and 83% for the 100 A/m² experiment. The latter shows that in this case the limiting current density was probably exceeded. This is however not expected to influence the conclusions drawn from this experiment. These experiments show that indeed the presence of salt decreases the transport of organic acids and that charge is preferentially carried by the small, mobile salt ions in salt-organic mixtures. This is an important conclusion for all MES/MFC experiments, as it shows that it is imperative to keep salt concentrations low if transport of charged organics is aimed for.

3.3.3 Diffusion as the main transport mechanism for organics in ED

The Nernst-Planck equation (Equation 7.2), typically used to model transport of charged species, shows that in the presence of an external potential difference, transport is determined by both diffusion (first part) and electromigration (second part). Convection can be neglected in ED, since the feed flow is parallel to the membrane surface and only a negligible flow of water through the membranes occurs.

$$J_s = D \cdot \frac{\Delta C}{\Delta x} + \frac{F \cdot C}{R_g \cdot T} \cdot z \cdot D \cdot \frac{\Delta E}{\Delta x} \qquad (7.2)$$

In Equation 7.2, J_s is the solute flux (mol/(m².h)), D the diffusion coefficient in the membrane (m²/h), ΔC the concentration difference across the membrane (mol/m³), Δx the thickness of the membrane (m), F the Faraday constant (96 485 J/(mol.K)), C the concentration in the diluate (mol/m³), R_g the universal gas constant (8.31 J/(mol.K)), T the temperature (K), z the ion valence (-) and ΔE the potential difference across the membrane. Diffusion only depends on the diffusion coefficient in the membrane and on the concentration difference across the membrane. As such, if the concentration difference remains unchanged, diffusion should be the same whether an external potential difference is applied or not. This is why it can be assumed that in the diffusion experiments and the ED experiments with salts present, the diffusion is the same, since the concentration difference across the membrane barely changes, as discussed before. In the ED transport experiments for organic acids where no NaCl is present, this assumption of constant concentration difference across the membrane, can only be stated to hold for the experiment at 23 A/m², as in the other cases the transport is much higher and the concentration difference changes significantly. Based on these assumptions, the total observed flux of organics in the ED experiments can theoretically be split in a diffusion and an electromigration part. The average of both parts, based on the four measurements carried out during the experiments, is shown in Figure 7.8.

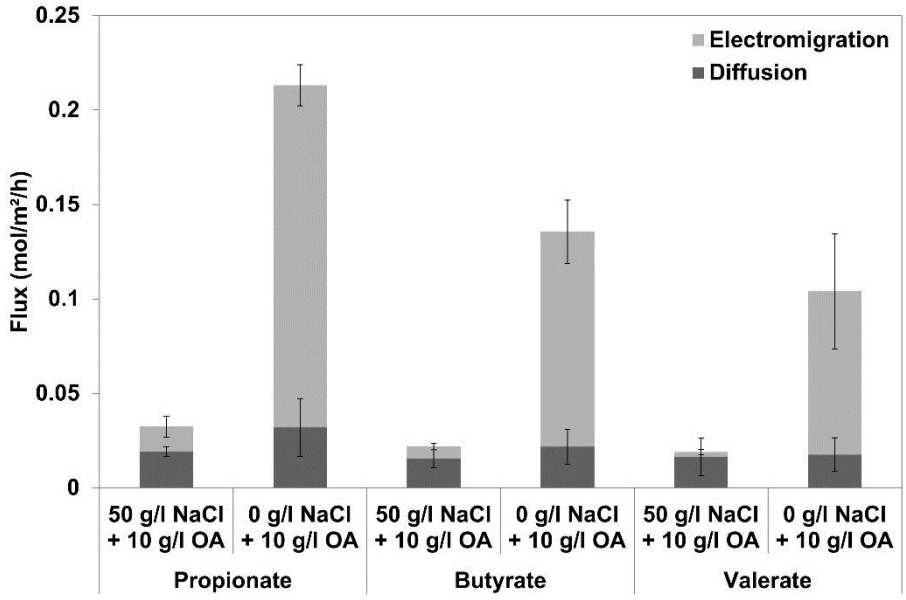

Figure 7.8 Diffusion and electromigration driven transport of organic acids in the presence and absence of NaCl.

As clearly seen from the figure, there is no significant difference in diffusive organic acids transport, whether NaCl is present or not. In other words, NaCl does not influence diffusion of the organic acids. There is however a clear difference in electromigration between the

experiments with and without NaCl for all organic acids. The contribution of electromigration is 14 (propionate), to 17 (butyrate), to 33 (valerate) times larger when no NaCl is present. This shows that electromigration indeed only plays a small role in the transport of organics in the presence of salts. When comparing the different organic acids, it is clear that the effect of electromigration becomes smaller as the component's size increases.

4 Conclusions

Selective separation of organic and inorganic compounds in mixtures would be beneficial in many applications. IEM, due to their lower fouling propensity, are considered a suitable candidate to achieve this and are already used in a variety of applications faced with both salt and organics. In a previous study, it was shown that transport of organics through IEM is mainly diffusion driven. The main conclusions from this new study are:

- As expected, the transport of negatively charged compounds is higher in the presence of Na_2SO_4 and the transport of positively charged compounds is higher in the presence of $MgCl_2$. This is due to the lower diffusion constants of SO_4^{2-} and Mg^{2+} compared to Cl^- and Na^+ respectively, increasing the relative transport of TOrCs.
- In diffusion experiments, Donnan dialysis causes the transport of charged species to increase when they are dosed to the concentrate. In ED experiments, transport is higher when TOrCs are dosed to the diluate, but only after 48 hours (i.e. when salt depleting conditions are reached).
- Organic acids behave similar to TOrCs. The diffusive character of the organics transport is again supported by the fact that there is no significant difference in organic acid flux between the diffusion and ED experiments and by the low coulombic efficiencies and low contribution of electromigration observed in the presence of NaCl.

More research is needed to explain why the transport of positively charged TOrCs is higher in the presence of Na_2SO_4 and to explain the deviant behaviour of the positively charged TOrCs during the ED experiments with different transport directions. However, it was again clearly confirmed that diffusion is the main transport mechanism for the studied organics in the presence of salt.

All of the experiments discussed here and in Chapter 6 were conducted using the same membranes. Future research will focus on the effect of membrane characteristics (thickness, polymeric backbone, cross-linking degree, …) and their influence on the diffusion behaviour

of organics. This can ultimately lead to the development of new membranes, tailored to the specific selective separation between organics and inorganics needed in different applications.

Chapter 8: General conclusions and prospects

This thesis discusses the possibilities of the hybridisation of ion-exchange technologies with reverse osmosis and some of the challenges that go with it. The ultimate goal is to develop processes that can provide sustainable water treatment solutions with improved energy and water efficiency. The work was divided in three different parts; (1) the hybridisation of classical IEX with RO for process water production, where lab-scale and pilot-scale studies were discussed from a technological and economic point of view (Chapter 2 and Chapter 3), (2) The hybridisation of SGP and the newly developed ARED technologies with RO for energy-efficient seawater desalination, where modelling predicts significant energy savings for the hybrid and first lab-scale performance of ARED are presented (Chapter 4 and Chapter 5) and (3) the transport of organics through IEM, which could have an important impact on the produced water quality in ion-exchange/RO hybrids (Chapter 6 and Chapter 7). In this final chapter, the main results and conclusions are discussed, together with some additional contemplations and suggestions for future research.

1 Conclusion 1: IEX is a viable pre-treatment method to increase process water RO recovery, especially if the RO concentrate is used to regenerate the IEX

As the demand for high quality (process) water increases while environmental legislations become ever more stringent, innovative process schemes are needed to provide water at an acceptable ecological and economical cost. RO is a popular technique to treat all kinds of feed waters for process water production and reuse - besides surface, ground and tap water, focus is shifting more and more towards the treatment of wastewater for reuse in the process as a cheap water source. However, most of these water sources often contain sparingly soluble salts (e.g. $CaCO_3$, $CaSO_4$, …) that can cause scaling on the RO membrane. To deal with this, utilities mostly add anti-scalants and/or limit the water recovery in the RO. Anti-scalants are however expensive and may cause discharge problems with the RO concentrate (especially in the case of P-containing anti-scalants).

In Chapter 2, two techniques are compared for RO pre-treatment to exchange cations responsible for the formation of sparingly soluble salts by cations forming more soluble salt. These techniques (IEX and DD) are compared with tap water and secondary treated wastewater as a feed. Both IEX and DD succeed in the exchange of Ca^{2+} and Mg^{2+} from the feed streams for Na^+ coming from the RO concentrate, although IEX is more efficient at the removal. Both processes result in the potential to increase the RO recovery to ± 90% without the addition of anti-scalants. The innovative part of this study lies in the reuse of the RO concentrate to regenerate the IEX/DD, as the RO concentrate is low in multivalent

cations but rich in monovalent cations. In DD, the concentrate serves as a source of monovalent ions to be exchanged for multivalent ions from the feed across IEM. In IEX, the concentrate is used as a regenerating solution when the IEX is saturated. The main parameter influencing the efficiency of the ion-exchange in DD and the regeneration of the IEX is the initial monovalent:multivalent cation ratio in the feed. For the tap water used, in this case tap water with a high hardness, the monovalent:multivalent ratio is low (around 0.5), resulting in a low IEX regeneration efficiency and a low ion-exchange in DD. To resolve this issue, NaCl could be added to the RO concentrate prior to recycling this concentrate to the IEX or DD. The ratio in the wastewater, however, was ±25, resulting in full regeneration of the IEX and higher ion-exchange rates in DD. An economic assessment points at IEX-RO as the most interesting hybrid option here, with savings of up to 10% compared to stand-alone RO and 6% compared to IEX-RO without concentrate recycling.

Based on the higher efficiency of IEX and the economic assessment, it was decided to test the IEX-RO hybrid system at pilot-scale. The industrial location in the Ghent harbour provides a brackish surface water feed with variable composition: the sodium content increases significantly during the warmer months of the year while the hardness remains quite constant. This results in higher monovalent:multivalent cation ratios in summer. The pilot was operated at different RO recoveries (75 and 85%) and ran from January to June, thus providing a variable feed. Again it was shown that the monovalent:multivalent cation ratio was the determining factor in the IEX regeneration efficiency. The RO recovery, and thus the monovalent cation concentration in the concentrate, did not influence the obtained regeneration efficiency. However, the monovalent:multivalent cation ratio in the feed was never sufficient to reach full IEX regeneration efficiency, and thus tests with added NaCl were carried out as well. Based on the obtained results, a prediction of the NaCl needed in the RO concentrate to obtain full IEX regeneration can be made with basic information on the feed water composition. This enables process operators to estimate the NaCl need day by day and ensures an efficient process where excessive addition of salt is avoided. Despite the (low) need for NaCl addition in this process, avoiding anti-scalant use and increasing the RO recovery to 85% results in an economically interesting process, with an increased revenue of the water of up to 30%.

This research clearly shows the technological feasibility of an IEX-RO hybrid system with concentrate recycle. However, some important considerations and research questions remain.

An important operational factor with RO is avoiding biological growth on the membranes and in the complete hybrid system. Often, biocides are added to the system, which end up in the RO concentrate. Some of the most popular biocides used in RO are non-oxidizing biocides such as aldehydes, dithiocarbamates, organobromines, isothiazolones and quaternary ammonium compounds [182]. During the pilot-scale experiments, no biocides were added but no issues with biofouling were encountered. Biofouling is however a slow process and it can take several months for a biofilm to develop. Therefore, the duration of the pilot-tests might not have been sufficient to observe any potential problems with biological growth. Biocides in RO concentrate might have a negative effect on the regeneration efficiency obtained in the IEX in IEX-RO hybrids, because of (irreversible) binding to or damaging of the resins itself. The potential effects of such biocides should thus be considered when a full-scale installation is designed and developed.

Another factor to take into account is possible scaling on the IEX resins. The concentration of anions in the feed will be increased in the RO concentrate, as these are not removed in the cationic IEX. During regeneration with the RO concentrate, these anions will come into contact with the cations on the resins, such as Ca^{2+} and Mg^{2+}. This might cause precipitation of for example $CaCO_3$ of $CaSO_4$ on the resin. However, contrary to the experiments executed in this research, regeneration and flushing of the resin is often carried out in counter flow. Especially the high velocity rinse at the end of the regeneration cycle is usually able to remove the precipitations formed.

The efficiency of the hybrid scheme is limited by the amount of monovalent cations present in the RO concentrate. To remove the multivalent ions from the resin in favour of the monovalent ions during regeneration, a certain concentration of the monovalent ions is required to switch the affinity of the resin from the multivalent to the monovalent cations. Although in the study conducted here the concentrations encountered turned out not to influence the regeneration efficiency, at lower monovalent:multivalent cation ratios the RO concentrate will contain less monovalent cations in a lower concentration, which will negatively affect the regeneration efficiency. Purolite® has developed an IEX resin with a higher regeneration efficiency at low regenerant concentrations, the so-called Shallow Shell Technology™ resins [183]. These resins contain an inert core, while only the outer, easily accessible shell contains the reactive sites, as shown in Figure 8.1. This shorter diffusion path results in a more efficient elution of the multivalent cations, even at regenerant

concentrations as low as 0.5% [184]. This can improve the efficiency of the IEX-RO and expand it applicability to lower MMR.

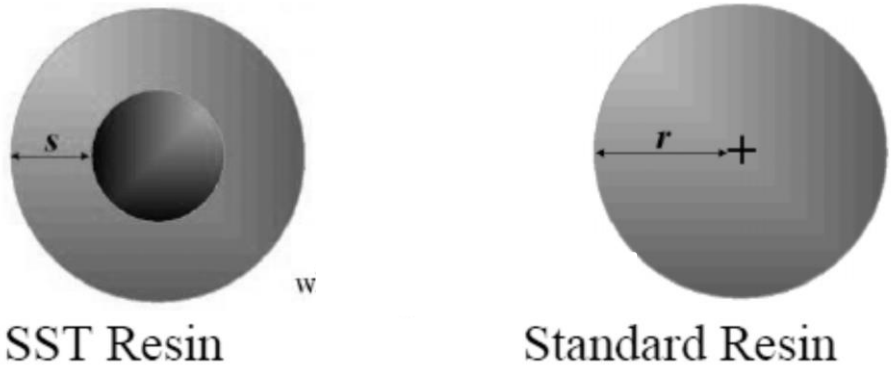

Figure 8.1 Comparison of Shallow Shell Technology ™ (SST) resin to standard resin beads [183].

In the scheme considered in this study, the IEX-RO hybrid operates directly on one feed stream. However, situations where the RO and IEX are available at different locations in a company are also possible. As the main issue with IEX is the production of a highly concentrated waste stream after regeneration (typically NaCl for softeners), the question remains if RO concentrate produced in the same plant, but on another location, potentially also with another feed stream, might be a viable alternative to fresh NaCl brine as a regenerant for the IEX. An example of this is an industrial case that was investigated in this respect, as an addition to the work in this thesis. On this industrial site, an IEX system is used for softening of tap water for use as cooling tower make-up water, while a brackish water RO is used in another part of the plant to produce process water. As the RO concentrate is high in Na^+ (9 243 mg/l) and low in Mg^{2+} (869 mg/l) and Ca^{2+} (652 mg/l), it would appear to be possible to regenerate the IEX with the RO concentrate, which is produced in much larger quantities than would be needed for the IEX regeneration. However, the RO concentrate also contains anti-scalants and other products (i.e., biocides) added to ensure an efficient RO process. Interestingly and surprisingly, lab-scale tests show that the maximum regeneration efficiency that can be achieved for the IEX is ±35% after regeneration with this RO concentrate, independent on the amount of concentrate used for the regeneration. Adding NaCl to the RO concentrate only increased the efficiency to about 50%, as shown in Figure 8.2.

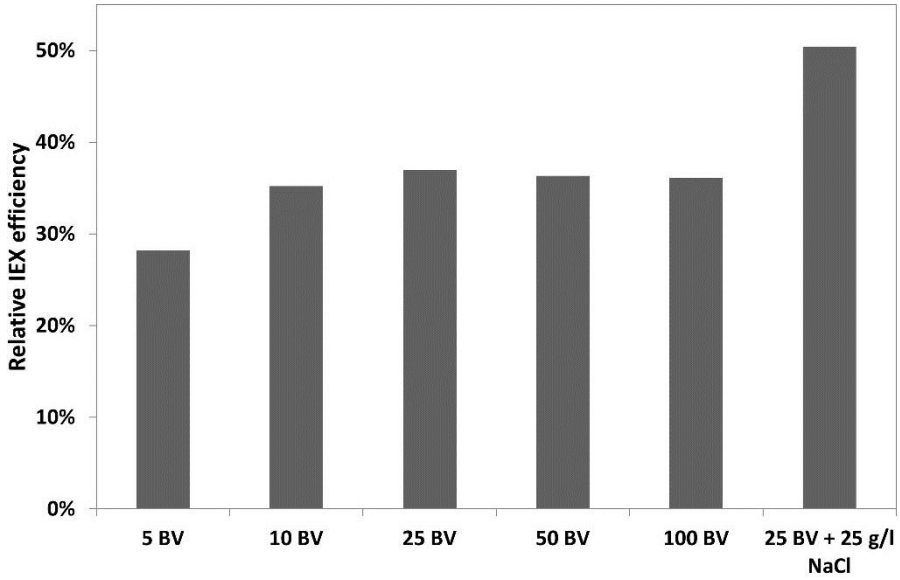

Figure 8.2 IEX regeneration efficiency relative to classic 100 g/l NaCl efficiency after regeneration with RO concentrate at different bed volumes (BV) used and with addition of 25 g/l NaCl to the RO concentrate.

Furthermore, the intrinsic capacity of the IEX resin seems to decline, as the efficiency of a classic NaCl brine regeneration after several cycles of regeneration with the RO concentrate also decreases to about 80%. The hypothesis for this is that some components in the RO concentrate bind irreversibly to the IEX resin, thereby blocking part of the active sites on the resin and decreasing the resin capacity. SEM and EDX analysis of the resin beads (shown in Table 8.1) however could not help to identify a clear cause for the decline in regeneration efficiency. Further research is therefore needed, as well as research to investigate if the same would be true for other RO concentrates, and how this can be prevented. One option would be to use different, more resistant ion-exchange resins. In this research, standard gel-based resins with a polystyrene backbone were used. Macroporous or polyacrylic resins for example generally have a better resistance against organic fouling, which might make them a better candidate to handle the biocides that might be present in the RO concentrate.

Table 8.1 Comparison of virgin resin (left) and resin after regeneration with the RO concentrate (right) and the composition of the surface

Virgin resin				**Resin after regeneration with RO concentrate**			
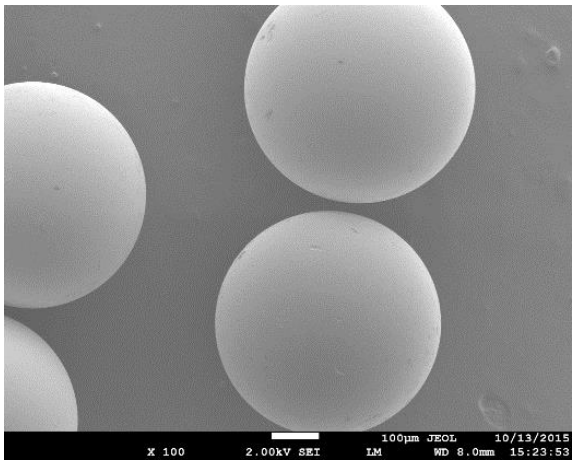				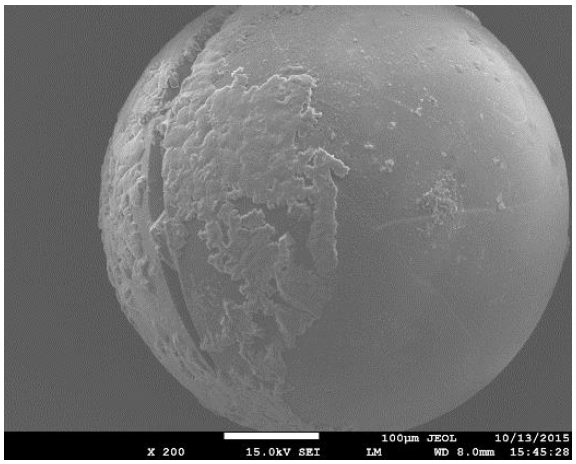			
C	56.2	±	0.3	**C**	22.7	±	1.2
O	21.6	±	0.3	**O**	4.0	±	0.2
S	13.8	±	0.1	**S**	-	±	-
Na	8.5	±	0.1	**Na**	32.5	±	0.5
				Cl	40.2	±	0.7

As with many cases where water reuse (or an increase in water use efficiency) is aimed at, the hybrid IEX-RO system does result in less volume discharge of wastewater, however, the wastewater is discharged with a higher salt concentration. In cases where no or little salt needs to be added to the RO concentrate, the total amount of salts discharged (in terms of salt load) remains the same. However, environmental permits in Flanders, which dictate discharge limits for a certain industry or company, are mostly based on concentrations and not on the total load discharged. This can lead to discharge issues and high fines, which can hamper the development of innovative water recovery systems and can discourage companies to implement water reuse and increased water efficiency schemes. The reasoning behind this is that higher salt concentrations, regardless of the total load, can increase the risk of local environmental damage at the discharge point. VITO (Vlaamse Instelling voor Technologisch Onderzoek/Flemisch Institute for Technological Development) suggests a differentiated discharge limit, based on the amount of water saved, including an absolute maximal concentration [185]. This approach has not been implemented in practice yet and a clear and open discussion with policy makers is urgently needed to look for good solutions

and send a positive signal to industries and companies willing to make an effort towards a higher water efficiency.

2 Conclusion 2: Salinity gradient power can theoretically lead to energy-neutral seawater desalination

Seawater is one of the main sources of potable water for the future. However, current state-of-the-art desalination of seawater RO is energy demanding, at 2-3 kWh/m³. In Chapter 4, a new way of reducing seawater RO energy demand is introduced. By mixing the seawater with impaired water in a controlled manner, the seawater salt concentration prior to RO can be decreased, decreasing the subsequent RO energy demand. Furthermore, depending on the mode of operation, this pre-dilution step can be used to generate energy as well. The latter is the case for RED, a technology that allows the production of energy directly from a salinity gradient across IEM. So far, RED has been considered mainly for the production of energy in places where fresh river water flows into the sea. However, other sources of impaired water could be used as ion sink as well. Theoretical research in this thesis has shown that as a pre-treatment for RO, RED can lead to an energy-neutral system for potable water production from seawater, depending on the amount of impaired water available. However, when considering losses and imperfections in the system, it becomes clear that this energy-neutrality is far from reality. Some of the main efficiency losses are associated with the membrane and solution resistances. This causes the overall energy demand of a realistic RED-RO system to be around 0.8-1.2 kWh/m³ (at 50% RO recovery), which is still a significant improvement when compared to stand-alone RO for seawater desalination. All of the predictions in this thesis are based on theoretical models, and lab-scale testing on RED on a combination of actual sea- and wastewater is yet to start. Such studies will shed light on some major question marks that remain in the envisioned hybrid system. Some issues might indeed require attention.

A first issue is the contamination of the seawater prior to RO, which could eventually lead to quality issues in the produced water. The composition of impaired water is very diverse and using this water to pre-dilute seawater (even in a controlled manner) can lead to several issues. An important category of contaminants in impaired water that might be of concern, are the trace organic contaminants (e.g. pharmaceuticals, pesticides, personal care products, …). Potentially, these could be transported across the membranes to the seawater. Other contaminants that are a risk are heavy metals, nutrients and micro-organisms. Although the rejection of these compounds is high in RO [108–110,186–188], their presence

in the seawater could alter the fouling behaviour of the seawater in RO. Furthermore, the use of impaired water could lead to significant fouling issues in RED, which are expected to be different than the ones encountered in a seawater-river water combination RED. Although some research has been performed on fouling in the latter configuration, fouling in RED remains largely unknown at this moment [127,189].

Besides issues with the feed streams, the design of the RED system needs to be improved as well. To bring the RED-RO potential closer to its theoretical performance, especially issues with resistances within the system need to be addressed. More specifically, membrane resistance has been identified as a key parameter and the need for low-resistance membranes in RED has been highlighted in literature [135,136,190]. Further efforts to decrease the resistance of the overall RED system have focussed on the low-salinity compartment, with the development of ion conductive spacers [191] and profiled membranes [192–194] (the latter allowing to completely avoid the use of spacers and to decrease the low-salinity compartment thickness as much as possible, shown in Figure 8.3 on the left). A recent study has looked into replacing the spacer with ion-exchange resin beads to further improve the compartment conductivity, as shown in Figure 8.3 on the right [195]. Furthermore, research by Veerman et al. (2011) has shown that by segmenting the electrodes, the power density can be increased by 15% [196].

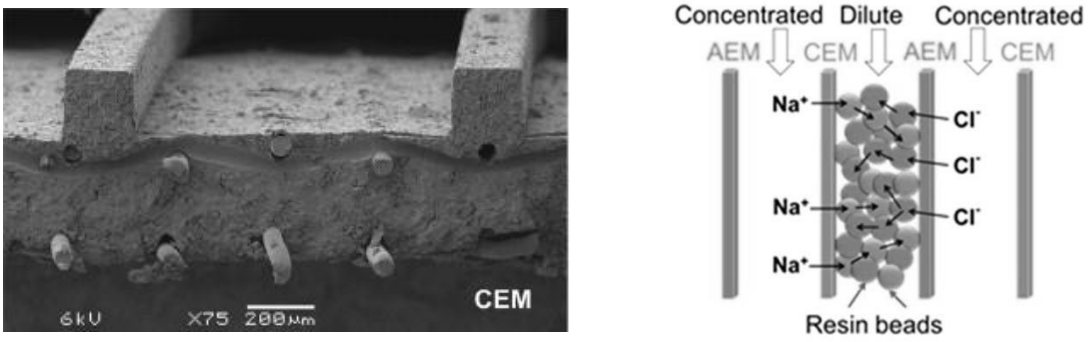

Figure 8.3 Profiled IEM (left) [192] and resin beads in the low-salinity compartment (right) [195], two possible developments to decrease the overall stack resistance in RED.

Despite the high interest in RED as a source of sustainable energy and as a pre-treatment method for seawater RO, its economic viability is currently still questionable. There is the question if direct potable reuse of the impaired water would not be more interesting (assuming the public acceptance is there). A recent study by Teusner, Blandin and Le-Clech has proven the economic potential of FO-RO systems for augmenting RO production, even compared to direct potable reuse of secondary treated wastewater [197]. This shows that direct potable reuse is not necessarily economically more interesting than pre-dilution.

However, to reach similar costs in (A)RED systems, some development is still needed. Due to a low ion flux in IEM, the power density and desalination rate in RED are still low, which leads to high required membrane areas. IEM are currently still expensive, at about € 100/m² for most commercial membranes, leading to excessive capital expenses [132]. In terms of energy production, the power density would have to come up to about 2.7 W/m² and the membrane prices would have to decrease to ± € 4/m² for RED to compete with established renewable energy technologies (e.g. wind power). In the context of an RED-RO hybrid, at current performances, the membrane price would have to drop to about the same amount [198]. Although power densities are coming up to this limit [199], current membrane prices are still too high. However, Fujifilm, an important player in the development and production of ion-exchange membranes, has set these competitive prices as the target to be reached within the next 5-10 years.

3 Conclusion 3: Assisted reverse electrodialysis increases the viability of the hybrid RO seawater desalination process

To avoid excessive costs due to a high required membrane area in an RED-RO seawater desalination hybrid, a new mode of RED operation was developed: assisted RED or ARED. In ARED, the rate of desalination/pre-dilution is increased by providing an additional driving force, on top of the natural salinity gradient. This driving force is provided by an external potential difference. Although this does mean that some additional energy is consumed in the ARED pre-dilution system, a theoretical estimation still predicts a significant decrease in energy demand for the ARED-RO hybrid system (at ± 1.2 kWh/m³) compared to stand-alone RO.

At the start of this PhD thesis, no research on ARED or similar processes was conducted yet. However, some preliminary experiments at our lab (Chapter 5) showed great promise for the technique, which shows efficiencies higher than theoretically expected. These high efficiencies are caused by a rapid decrease in resistance of the low salinity compartment and the membranes due to an increased desalination rate (and increased concentrations in the compartment) in ARED. Earlier research already pointed out that the low salinity compartment determines the resistance of the membranes. In ARED, due to a decrease in resistance of the low salinity compartment, the resistance of the membrane decreases as well. These benefits of ARED are especially observed at (and mostly limited to) a low salinity compartment concentration below approximately 0.1M NaCl. Below this concentration, a rapid decrease in resistance due to increased concentrations is observed, which is mostly due

to the non-linear relationship between concentration and resistance. Above 0.1M NaCl, the behaviour of the system is again as theoretically expected. It is thus especially at these very low concentrations, where RED suffers from the high resistance of the membranes and solution, that ARED would be an ideal first step in the (A)RED-RO hybrid, overcoming the initial high resistance before switching to energy production in RED.

The results presented here are preliminary, exploratory results of a new and innovative approach to RED and more research is needed. The effect of other components (e.g. multivalent ions, foulants, …) needs to be investigated and the effect of different membrane parameters (thickness, resistance, permselectivity, …) on the ARED process need to be studied. In the envisioned hybrid, impaired water is considered a viable option for the low salinity source. However, this water may contain important pollutants, such as pharmaceuticals, pesticides and personal care products, which are not removed in traditional wastewater treatment plants. Transport of these pollutants from the impaired water to the seawater should be avoided, as this might compromise the RO step and ultimately contaminate the produced water. However, little is known about the transport of organics through IEM, which is why this transport was focused on in this thesis (Chapters 6 and 7).

All of this practical research will allow more insight into the transport processes involved in ARED, and will lead to a more accurate modelling of the hybrid system. This type of modelling is needed to optimise the hybrid process in terms of energy and investment costs. Another option, that will be studied in the upcoming Horizon 2020 project REvivED (NMP-24-2015), is implementing ED to replace or complement RO for the final seawater desalination. Both RED-ED and ED-RO processes will be looked at, with the potential of combining all technologies in an optimal hybrid system as shown in Figure 8.4.

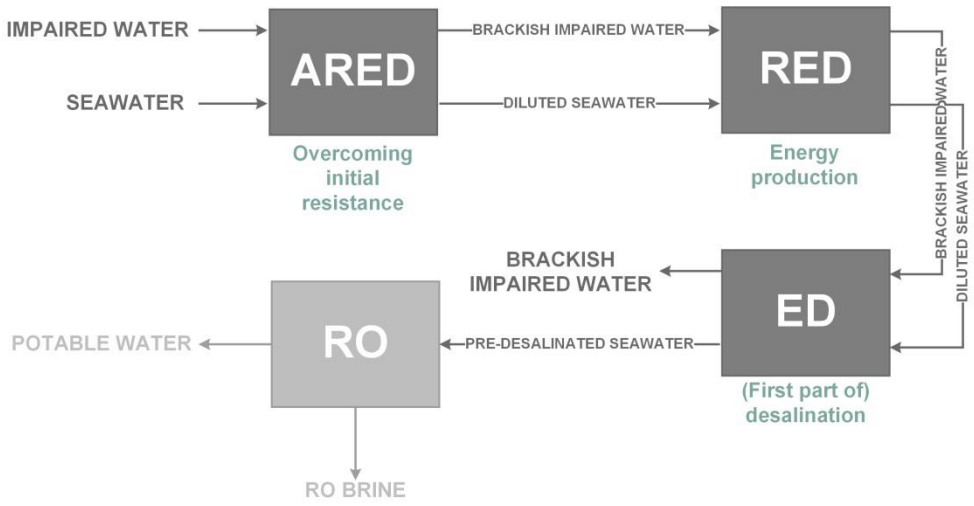

Figure 8.4 Envisioned hybrid system where RED, ARED and ED are incorporated to achieve an optimal configuration, with or without RO as a final desalination step.

Recently, GE Power and Water (Singapore) presented an idea similar to ARED, at the International Desalination Association World Congress on Desalination and Water Reuse, where a combination of RED and driven RED (dRED, similar to ARED) for the treatment of RO concentrate after seawater desalination was proposed [133,134]. GE envisions a process that combines seawater and wastewater to minimise the environmental impact of wastewater discharge into the sea while reducing the cost for seawater desalination and the impact of concentrate discharge. Their studies show a decrease in water cost of 16-18% and a decrease in energy demand of 6-24%. The advantage of implementing the ARED/RED stage on the RO concentrate is that the concentration of this stream is higher and thus a higher power density will be reached in the RED stage. However, the concentrate volume will be lower than the feed volume, so the comparison of the net produced energy is not that straightforward. Furthermore, although the overall water recovery can be increased by recycling the concentrate with reduced concentration back to the RO feed after the (A)RED step, the energy demand per m^3 of produced water will remain the same. When incorporating (A)RED before the RO step, energy can be produced and the energy demand in the RO system can be reduced by the reduction in seawater concentration. More detailed modelling of the systems needs to be carried out to make a definite assessment of which system would be most energetically and economically interesting. Energetically, it would no doubt be most interesting to incorporate (A)RED both on the feed and the concentrate. However, this would mean the incorporation of two separate ARED/RED systems and thus additional investment costs.

To avoid the need for two separate (A)RED systems and still benefit from both feed and concentrate (A)RED treatment, (A)RED can be coupled to closed-circuit RO (CCD™), developed recently by Desalitech. In this system, desalination is approached as a semi-batch process, in which the feed stream is recirculated in the system until the desired recovery is reached, as shown in Figure 8.5. At this point, the concentrate compartment is drained and new feed is added, resulting in a continuous process. During the process, the feed pressure is increased with the increasing osmotic pressure of the concentrate, resulting in a varying operating pressure that minimizes the net driving pressure (i.e. the difference between the feed pressure and the osmotic pressure). Energy demand for seawater desalination with this system is predicted to be between 1.6-2.3 kWh/m³ [200–202].

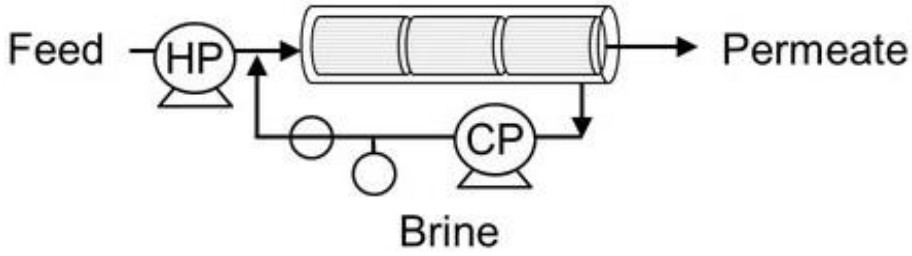

Figure 8.5 Schematic representation of the closed-circuit RO system [203].

An (A)RED process can be envisioned that takes advantages of the fact that this is a batch process. During operation, the (A)RED system can treat the discharged concentrate from the previous cycle and switch to treating the new batch of seawater RO feed before the next cycle. Only one (A)RED system would be needed in this case to treat both the feed and concentrate, opposed to two separate systems as discussed before. Although the system would be larger in this case, capital costs are expected to be less. Again, more detailed modelling is needed to predict the viability of such a system in practice.

4 Conclusion 4: The type and concentration of salt present, the direction of the salt transport and the properties of the organic determine the final transport of the organics in IEM

One of the major shortcomings in knowledge when looking into ion-exchange hybrid systems, is on the transport behaviour of organics in IEM. As discussed before, the transport of pollutants from wastewater to seawater across IEM can be important in (A)RED-RO hybrid systems, where the quality of the produced drinking water is at stake. Furthermore, in a more general sense, the separation of organics and inorganics is often paramount to allow the recovery and reuse of the organics, inorganics or both from different wastewaters. One

of the driving forces behind the study of organics transport in IEM were experiments carried out for the Blue Circle project, a project that focuses on the valorisation of inorganics from aqueous waste streams and the increase in water efficiency in industrial water loops. A very clear example that warrants the study of how organics are transport through IEM, is that of two very similar concentrated Na_2SO_4 streams, that both contained a significant amount of organics. The main difference was in the nature of the organics; in the first stream, the organics came from a starch modification process, while in the second case, their origin was in the dying of textiles. In the first case, shown at the top of Figure 8.6, the separation was successful using ED, and SO_4^{2-} could be recovered while the organics were mostly retained. In the case of the textile dyes, the organics were rapidly adsorbed onto and in the membrane, and no separation whatsoever was obtained. This irreversible adsorption is shown at the bottom of Figure 8.6.

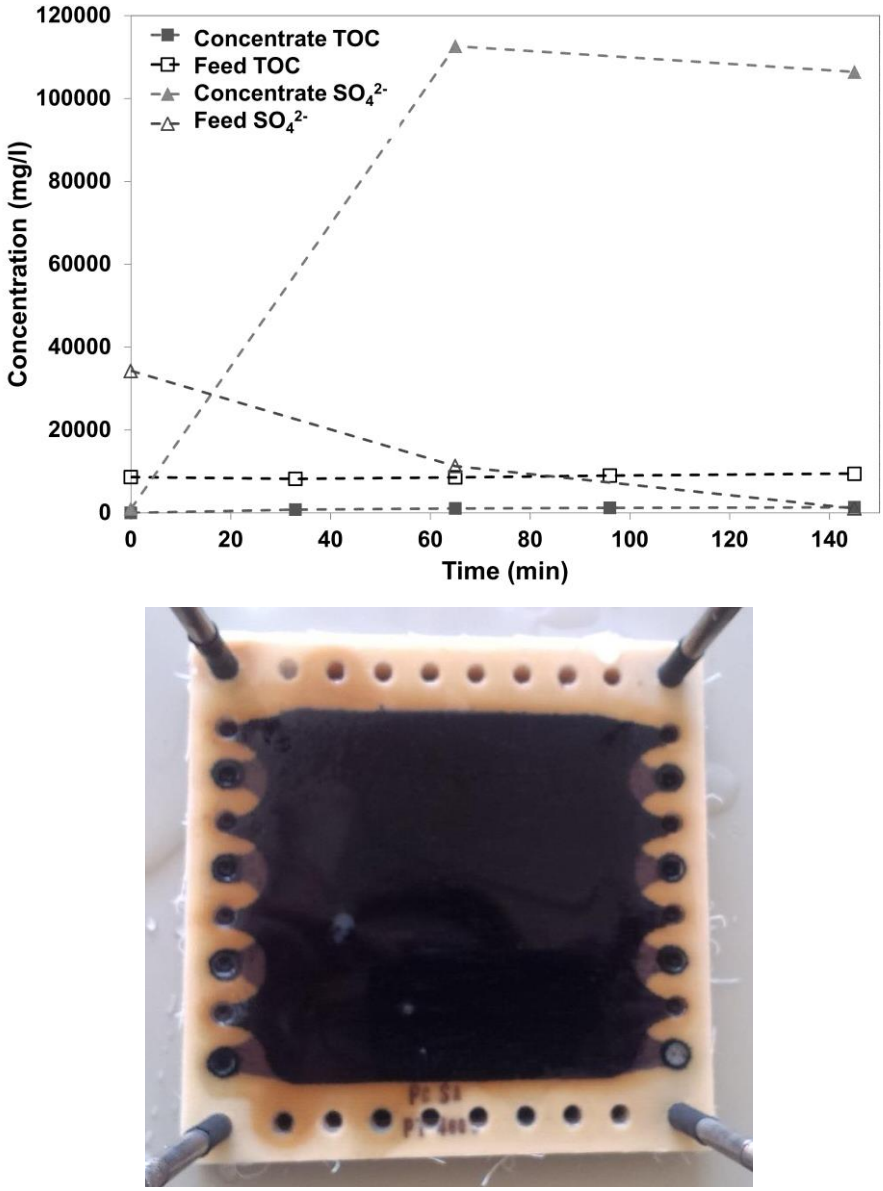

Figure 8.6 The research into organics transport in IEM was triggered by research into the separation of organics and inorganics in industrial waste streams using ED. The top graph shows the results for a stream containing Na_2SO_4 and starch-related organics, the bottom picture shows the effect of a stream containing Na_2SO_4 and textile dyes on an AEM (TOC = total organic carbon).

The first experiments on the more scientific study of organics transport in IEM, as discussed in Chapter 6, were conducted with a simple mixture of NaCl and TOrCs. These experiments showed first and foremost that if salt is present in the aqueous stream, the electrochemical equilibrium across the membranes is preferentially restored through transport of the salts rather than the organics. The organics are transported in higher amounts when no salt is present, though. Secondly, it was shown that the applied external potential difference did not have a significant influence on the transport of the organics when salts were present. Although the transport rate is higher when a potential difference is applied compared to when no potential difference is applied, the transport rates are similar for different applied potential differences.

In a large number of applications of IEM, such as the ones described before, NaCl is not the only salt present. Furthermore, as is the case in (A)RED for example, the organics do not always move in the same direction as the salt. In many applications, such as ME, MFC, RED, …, the organics move against the dominant salt flux. That is why in Chapter 7, the influence of different types of salt (Na_2SO_4 and $MgCl_2$) and of the direction of the organics transport relative to the salt transport was investigated. Furthermore, the behaviour of organic acids was studied as a different model for organic material. The advantage of using propionic, butyric and valeric acid is their higher solubility, allowing to study different salt:organic ratios and the effect of this ratio on the acid transport. It was clearly shown that the presence of multivalent salt ions promotes the transport of organics compared to NaCl. This is because the diffusion coefficient of the multivalent ions is lower compared to that of Na^+ and Cl^-, causing a slight increase in the TOrC transport to compensate for the reduced salt transport. Moreover, it was shown that Donnan dialysis plays an important role in the transport of organics against the dominant salt flux.

Some important questions remained unanswered by the presented results. Firstly, it was observed that in the presence of Na_2SO_4, the transport of not only the negatively charged but also the positively charged TOrCs increases, both in the diffusion and the ED experiments. The first is expected, as the diffusion coefficient of SO_4^{2-} is lower than that of Cl^-, causing a slight increase in the transport of the negatively charged organics. This should however not affect the transport of the positively charged TOrCs, as the cation is the same for Na_2SO_4 and NaCl, and until now, no clear explanation for this behaviour was found. To further look into this behaviour, experiments with different salts at different concentrations will be carried out. One such test was already conducted under the same circumstances but with Na_3PO_4 as a salt, in the absence of an external potential difference. The results of this test (Figure 8.7) show a similar trend as for Na_2SO_4, with an increased transport of the negatively and positively charged organics in the presence of Na_3PO_4 compared to NaCl. Due to the limited solubility of Na_3PO_4 and consequent risk of scaling due to concentration polarisation phenomena, no ED experiment could be carried out here.

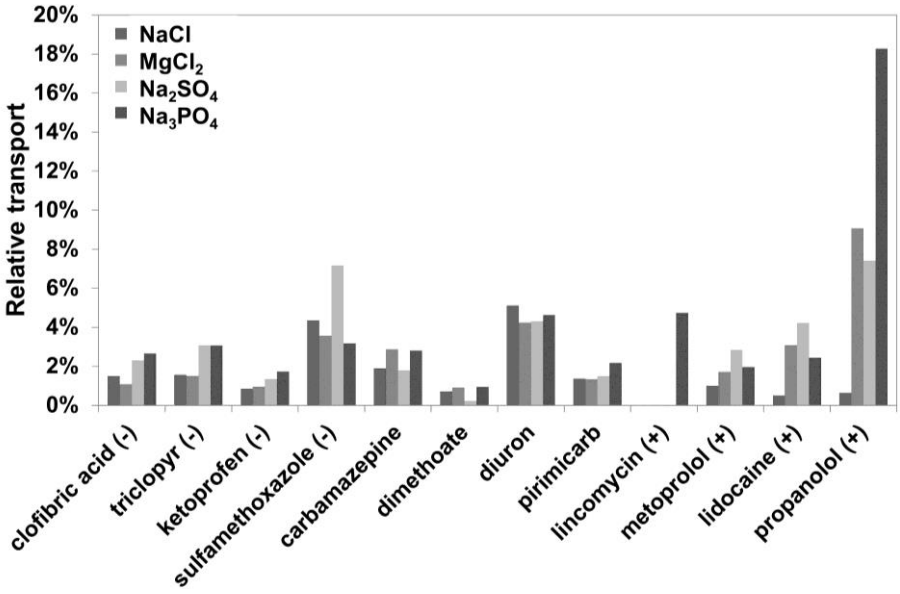

Figure 8.7 Relative transport of TOrCs in the absence of an external potential difference in the presence of different salts (NaCl, $MgCl_2$, Na_2SO_4 and Na_3PO_4) at 48h. Based on quantitative analysis with a calibration curve with an $R^2 > 0.99$.

The experiments with organic acids showed that, as the salt:organics ratio decreases and a higher concentration of organics relative to the salt concentration is present, the fraction of charge carried by the organics increases. When no salt is present, almost all of the charge is carried by the organic acids. This is of course accompanied by a steady increase in Coulombic efficiency. The overall behaviour of the organic acids is similar to that of the TOrCs, further confirming that both types of organics are a good model for organic material in general.

Another open question is whether transport of the organics is limited to transport as a counter-ion through membranes of the opposite charge, or if some of the transport takes place as a co-ion through membranes of the same charge. In the experiments presented in this thesis, no distinction between the two can be made. However, if co-ion transport is important, this can have important implications for the further development of the selective separation technology and the design of new membranes for selective separation (see conclusion 5). Currently, experiments are being carried out to study the transport of organics through individual membranes. In small glass cells, two different solutions (one with, one without organics) are separated by either an AEM or a CEM. Diffusion of the organics over time is monitored as the cells are stirred continuously. These experiments are expected to show the extent to which the organics diffuse through membranes with the same charge.

5 Conclusion 5: The transport of organics is mainly diffusion driven in the presence of salts

The most important conclusion about organics transport in ED presented in this thesis, indicated already in Chapter 6 and clearly confirmed in Chapter 7, is that in the presence of salts, the transport of organics is mainly diffusion driven. This is an important finding for many applications, as it indicates the time-dependence of the organics transport. In other words, faster desalination processes will result in less organics transfer across the membrane. When comparing RED and ARED as a pre-treatment for RO for example, ARED will likely result in less contaminants passing to the seawater than RED, because of the increased desalination rate. This is an added advantage of the ARED process in the hybrid system and should be taken into account when designing the full system.

The fact that transport of organics is mainly diffusion-driven in the presence of salts, also indicates that transport of organics might be controlled by controlling the diffusion through the membrane, by tuning certain membrane parameters. As discussed in Chapter 7, the total solute flux depends on diffusion and electromigration. The diffusion part can be expanded further as follows, based on the convection-diffusion model [204]:

$$J_s = \frac{\varphi \cdot \varepsilon \cdot D}{\Delta x} \cdot \Delta C \tag{8.1}$$

$$\varphi = (1 - \lambda)^2 \cdot e^{\left(\frac{-\Delta G_i}{k \cdot T}\right)} \tag{8.2}$$

$$\lambda = \frac{r_s}{r_p} \tag{8.3}$$

In Equation 8.1, J_s is the solute flux through the membrane pores, ϕ is the partition coefficient (the ratio of solute concentration in the membrane phase versus the bulk fluid phase), ε is the membrane porosity, D the diffusion coefficient of the solute in the membrane, Δx the membrane thickness and ΔC the concentration difference across the membrane. The partition coefficient depends on λ, which is the ratio of the solute radius (r_s) to the hypothetical pore radius (r_p), assuming the presence of uniform cylindrical pores in the membrane. Furthermore, ϕ depends on the Gibbs free energy of interaction ($-\Delta G_i$), the Boltzmann constant (k) and the temperature (T). In this context, $-\Delta G_i$ expresses the interaction energy between the solute and the membrane in the water phase.

Based on this set of equations (Equation 8.1 – 8.3), possible membrane adaptations for a better selective separation between salts and organics can be suggested. The diffusion coefficient and concentration difference across the membrane (Equation 8.1) are given and can not be adjusted. However, the solute flux is inversely correlated with the membrane thickness, indicating that membranes with a higher thickness will result in a lower flux. Although the higher thickness generally results in a lower conductivity of the membrane, it also results in a longer diffusion path for the organics, which is why these membranes are expected to retain the organics more efficiently. Furthermore, the membrane porosity (ε) and the radius of the pores (r_p) can be adjusted to decrease the solute flux. This can for example be achieved by a higher crosslinking of the membrane, resulting in physical hindrance of the diffusing organics. This was already shown in Chapter 6 and Chapter 7, where the diffusion of the positively charged TOrCs is lower due to a higher crosslinking of the CEM compared to the AEM.

The free energy of interaction includes both electrostatic and non-electrostatic interactions of the solute with the membrane. Tuning of the electrostatic interactions of the solutes with the membrane is an important tool, that nowadays is mostly used to create monovalent selective membranes, that not only have a higher selectivity for monovalent ions but often also exhibit increased anti-fouling properties. This was shown for example by Mulyati et al. (2013) and Güler et al. (2014). The first applied a layer-by-layer approach with alternating polyelectrolyte layers of poly(sodium 4-styrene sulfonate) and poly(allylamine) to increase the monovalent selectivity and hydrophilicity of AEM [205]. White et al. (2015) adopted a similar approach to modify a CEM used in ED [206]. Both Güler et al. (2014) and Li et al. (2015) focussed on the modification of CEM in seawater applications, the first by coating a commercial CEM with 2-acryloylamido-2-methylpropanesulfonic acid and N,N-methylenebis(acrylamide) as a cross-linker, the latter by applying a thin layer of N,N-dimethyl-N-2-propenyl-2-propene-1-ammonium chloride-2-propenamide (PQ7) on the CEM [207,208]. These are just some of the many examples where the surface of commercial membranes is modified, resulting in an increase in monovalent selectivity. The same mechanisms that ensure the monovalent selectivity and anti-fouling properties of these membranes are believed to also result in an increased retention of organics. This has been demonstrated during experiments in our lab with a mixed Na_2SO_4 and organics industrial waste stream (cfr. Figure 8.6), where standard SA and monovalent selective MVA AEM (PCA, Germany) were compared. In both experiments, >97% removal of SO_4^{2-} was reached. Although the experiments with the MVA took about 1.5 times longer than those with the standard membranes, the concentration of

organic carbon in the concentrate at the end was less than half the concentration in the case of the SA membranes for the same feed stream (140 mg/l TOC versus 360 mg/l TOC respectively), clearly showing a better selective separation between SO_4^{2-} and organics with the monovalent selective membranes.

The non-electrostatic interactions (e.g. hydrogen bonding or hydrophobic interactions [157]) between the organics and the membrane depend on the membrane material and functional groups used. Although most commercial membranes are based on polystyrene-divinylbenzene as a backbone, there exist many other possible materials that can be used. A comprehensive overview is outside the scope of this discussion, but some good reviews exist that summarise different possibilities for IEM formation [13,28,209]. However, a thorough literature review and study on the affinity of organics for different membrane materials is needed, which can form the basis for the further development of membranes capable of the selective separation between organics and inorganics.

6 Final conclusions

This thesis has clearly shown the strength of ion-exchange technologies in hybrid treatment schemes for water production with RO. In cases where the RO recovery is limited by the potential scaling of the membrane by multivalent ions in the feed water, as is often the case in industrial process water production, inclusion of an IEX step can increase the attainable water recovery. The recycling of the RO concentrate for the IEX regeneration ensures an efficient, sustainable process. When the RO recovery is limited by the osmotic pressure of the feed water and energy consumption is high, such as with seawater desalination, controlled mixing of the seawater with impaired water in an (A)RED system can ensure an energy efficient system. An overview of the advantages, challenges and range of applicability of the different hybrid technologies is given in Table 8.2. Broad ranges for application are given, as this is highly dependent on local considerations, such as energy and water prices, discharge limitations and water availability.

Table 8.2 Overview of the advantages, challenges and range of applicability associated with the IEX-RO and (A)RED-RO hybrids.

IEX-RO	**ARED-RED-RO**
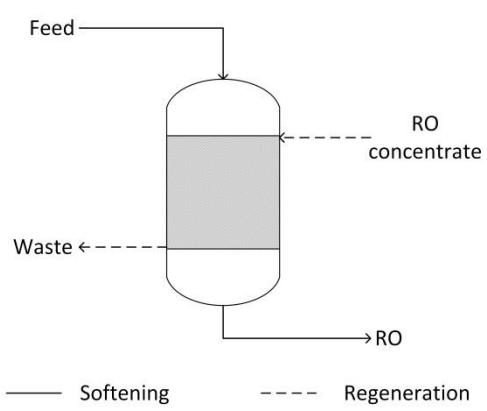	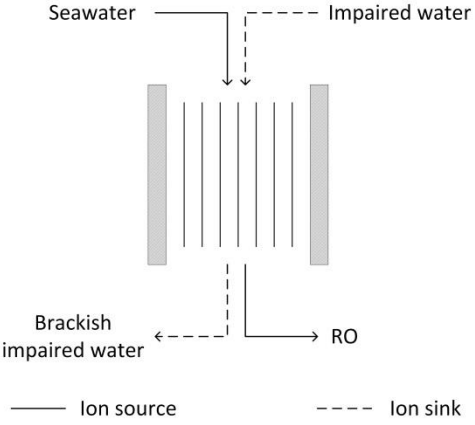
ADVANTAGES	
Increased RO recovery No anti-scalants	Increased energy efficiency Increased RO recovery Double barrier against contaminants
CHALLENGES	
NaCl addition not always avoidable Increased concentration brine discharge Potential resin fouling?	Trade-off energy savings vs CAPEX IEM price Optimal ARED-RED-RO configuration
USEFUL WHEN	
Scaling is limiting RO recovery MMR > 3.4 → no NaCl addition Discharge cost > 1.5 €/m³	Osmotic pressure is limiting RO recovery < 0.1M NaCl → ARED-RED-RO > 0.1M NaCl → RED-RO
POTENTIAL FEED STREAMS	
Brackish surface water Brackish groundwater Secondary treated wastewater Seawater (if osmotic pressure is not limiting)	For the low salinity feed stream: (Secondary treated) wastewater River water

An important challenge when using IEM is the lack of knowledge when it comes to the transport of organic contaminants. This is critical in applications where secondary treated wastewater is used, which can contain emerging contaminants such as pharmaceuticals and pesticides, but also in applications where IEM are used for the recovery of high value organics produced, for example in ME and MES. This thesis showed that the transport of organics depends on the composition of the matrix but is mainly diffusion driven. This means that membrane properties, such as thickness and hydrophobicity, are the parameters to tune in the development of IEM for selective organics separation.

References

[1] WRI. (2015) Water Risk Atlas [Internet]. Aqueduct. p. www.wri.org.

[2] Rodriguez, D. (2014) Thirsty Energy: Integrated Energy-Water Planning for a Sustainable Future [Internet]. Cornerstone. p. www.cornerstonemag.net.

[3] FAO. (2014) AQUASTAT database [Internet]. p. http://www.fao.org/nr/aquastat.

[4] EIA. (2015) U.S. Energy Information Administration [Internet]. p. https://www.eia.gov/tools/faqs/faq.cfm?id=447&t=1.

[5] Lucy, C. a. (2003) Evolution of ion-exchange: From Moses to the Manhattan Project to Modern Times. *Journal of Chromatography A*, **1000**, 711–24.

[6] Mulder, M. (1996) Basic principles of membrane technology. 2nd ed. Kluwer Academic Publishers, Dordrecht/Boston/London.

[7] Baker, R.W. (2004) Membrane technology and applications. Wiley.

[8] Hoek, E.M. V. and Tarabara, V. V., editors. (2013) Encyclopedia of membrane science and technology. Wiley, Hoboken, New Jersey.

[9] Kumar, S. and Jain, S. (2013) History, Introduction, and Kinetics of Ion Exchange Materials. *Journal of Chemistry*, **2013**, 1–13.

[10] Abrams, I.M. and Millar, J.R. (1997) A history of the origin and development of macroporous ion-exchange resins. *Reactive and Functional Polymers*, **35**, 7–22.

[11] GE. Chapter 08 Ion Exchange [Internet]. Handb. Ind. Water Treat. p. http://www.gewater.com/handbook/ext_treatment/ch_8.

[12] Lenntech. (2008) Ion exchange for dummies [Internet]. p. http://www.lenntech.com/Data – sheets/Ion – Exchange – f.

[13] Xu, T. (2005) Ion exchange membranes: State of their development and perspective. *Journal of Membrane Science*, **263**, 1–29.

[14] Reahl, E.R. (2006) Half A Century of Desalination With Electrodialysis. GE Water Process Technol.

[15] Strathmann, H. (2010) Electrodialysis, a mature technology with a multitude of new applications. *Desalination*, **264**, 268–88.

[16] Pattle, R.E. (1954) Production of electric power by mixing fresh and salt water in the hydroelectric pile. *Nature*, **174**, 660–660.

[17] Wick, G.L. and Schmitt, W.R. (1977) Prospects for renewable energy from the sea. *Marine Technology Society Journal*, **11**, 16–21.

[18] Tedesco, M., Scalici, C., Vaccari, D., Cipollina, A., Tamburini, A. and Micale, G. (2015)

Performance of the first Reverse Electrodialysis pilot plant for power production from saline waters and concentrated brines. *Journal of Membrane Science*, **500**, 33–45.

[19] Veerman, J. and Vermaas, D. a. (2016) Reverse electrodialysis: fundamentals. In: Cipollina A, and Micale G, editors. *Sustainable Energy from Salinity Gradients*, 1st ed. Woodhead Publishing-Elsevier, London. p. 77–134.

[20] Davis, T.A. (2000) Donnan dialysis. *Membrane Processes*, DESWARE.

[21] Wiśniewski, J. and Różańska, A. (2007) Donnan dialysis for hardness removal from water before electrodialytic desalination. *Desalination*, **212**, 251–60.

[22] Dydo, P. and Turek, M. (2013) Boron transport and removal using ion-exchange membranes: A critical review. *Desalination*, **310**, 2–8.

[23] Bryjak, M., Poźniak, G. and Kabay, N. (2007) Donnan dialysis of borate anions through anion exchange membranes: A new method for regeneration of boron selective resins. *Reactive and Functional Polymers*, **67**, 1635–42.

[24] Hichour, M., Persin, F., Sandeaux, J. and Gavach, C. (2000) Fluoride removal from waters by Donnan dialysis. *Separation and Purification Technology*, **18**, 1–11.

[25] Durmaz, F., Kara, H., Cengeloglu, Y. and Ersoz, M. (2005) Fluoride removal by donnan dialysis with anion exchange membranes. *Desalination*, **177**, 51–7.

[26] Tor, A. (2007) Removal of fluoride from water using anion-exchange membrane under Donnan dialysis condition. *Journal of Hazardous Materials*, **141**, 814–8.

[27] Velizarov, S. (2013) Transport of arsenate through anion-exchange membranes in Donnan dialysis. *Journal of Membrane Science*, **425-426**, 243–50.

[28] Nagarale, R.K., Gohil, G.S. and Shahi, V.K. (2006) Recent developments on ion-exchange membranes and electro-membrane processes. *Advances in Colloid and Interface Science*, **119**, 97–130.

[29] Ang, W.L., Mohammad, A.W., Hilal, N. and Leo, C.P. (2015) A review on the applicability of integrated/hybrid membrane processes in water treatment and desalination plants. *Desalination*, **363**, 2–18.

[30] Lee, J.W., Yeon, K.H., Song, J.H. and Moon, S.H. (2007) Characterization of electroregeneration and determination of optimal current density in continuous electrodeionization. *Desalination*, **207**, 276–85.

[31] DiMascio, F., Wood, J. and Fenton, J.M. (1998) Continuous Electrodeionization. Production of High-Purity Water without Regeneration Chemicals. *The Electrochemical Society - Interface*, 26–9.

[32] Wood, J., Gifford, J., Arba, J. and Shaw, M. (2010) Production of ultrapure water by

continuous electrodeionization. *Desalination*, Elsevier B.V. **250**, 973–6.

[33] Greenlee, L.F., Lawler, D.F., Freeman, B.D., Marrot, B. and Moulin, P. (2009) Reverse osmosis desalination: water sources, technology, and today's challenges. *Water Research*, **43**, 2317–48.

[34] Henthorne, L., Pankratz, T. and Murphy, S. (2011) The state of desalination. *Desalination: Sustainable Solutions for a Thirsty Planet*, IDA world congres, Perth.

[35] Vrouwenvelder, J.S., Manolarakis, S. a., Veenendaal, H.R. and van der Kooij, D. (2000) Biofouling potential of chemicals used for scale control in RO and NF membranes. *Desalination*, **132**, 1–10.

[36] Elimelech, M. and Phillip, W. a. (2011) The future of seawater desalination: energy, technology, and the environment. *Science*, **333**, 712–7.

[37] de Koning, J., Bixio, D., Karabelas, A., Salgot, M. and Schäfer, A. (2008) Characterisation and assessment of water treatment technologies for reuse. *Desalination*, **218**, 92–104.

[38] Van Houtte, E. and Verbauwhede, J. (2008) Operational experience with indirect potable reuse at the Flemish Coast. *Desalination*, **218**, 198–207.

[39] Indarawis, K. a. and Boyer, T.H. (2013) Evaluation of ion exchange pretreatment options to decrease fouling of a reverse osmosis membrane. *Desalination and Water Treatment*, **52**, 4603–11.

[40] Sarkar, S. and SenGupta, A.K. (2008) A new hybrid ion exchange-nanofiltration (HIX-NF) separation process for energy-efficient desalination: Process concept and laboratory evaluation. *Journal of Membrane Science*, **324**, 76–84.

[41] Hilal, N., Kochkodan, V., Al Abdulgader, H. and Johnson, D. (2015) A combined ion exchange–nanofiltration process for water desalination: II. Membrane selection. *Desalination*, **363**, 51–7.

[42] Vanoppen, M., Derese, S., Bakelants, A. and Verliefde, A. (2014) Reduction of specific energy demand of seawater RO by osmotic dilution/osmotic energy recovery - realistic modelling approach. *Desalination for the Environment: Clean Water and Energy*,.

[43] Li, W., Krantz, W.B., Cornelissen, E.R., Post, J.W., Verliefde, A.R.D. and Tang, C.Y. (2013) A novel hybrid process of reverse electrodialysis and reverse osmosis for low energy seawater desalination and brine management. *Applied Energy*, **104**, 592–602.

[44] Petrinic, I., Korenak, J., Povodnik, D. and Hélix-Nielsen, C. (2015) A feasibility study of ultrafiltration/reverse osmosis (UF/RO)-based wastewater treatment and reuse in the metal finishing industry. *Journal of Cleaner Production*, **101**, 292–300.

[45] Ochando-Pulido, J.M., Verardo, V., Segura-Carretero, A. and Martinez-Ferez, A. (2015) Analysis of the concentration polarization and fouling dynamic resistances under reverse osmosis membrane treatment of olive mill wastewater. *Journal of Industrial and Engineering Chemistry*, **31**, 132–41.

[46] Suárez, A., Fernández, P., Ramón Iglesias, J., Iglesias, E. and Riera, F.A. (2015) Cost assessment of membrane processes: A practical example in the dairy wastewater reclamation by reverse osmosis. *Journal of Membrane Science*, **493**, 389–402.

[47] Bunani, S., Yörükoğlu, E., Yüksel, Ü., Kabay, N., Yüksel, M. and Sert, G. (2015) Application of reverse osmosis for reuse of secondary treated urban wastewater in agricultural irrigation. *Desalination*, **364**, 68–74.

[48] Chon, K., Cho, J. and Shon, H.K. (2013) A pilot-scale hybrid municipal wastewater reclamation system using combined coagulation and disk filtration, ultrafiltration, and reverse osmosis: removal of nutrients and micropollutants, and characterization of membrane foulants. *Bioresource Technology*, **141**, 109–16.

[49] Jacob, C. (2007) Seawater desalination: Boron removal by ion exchange technology. *Desalination*, **205**, 47–52.

[50] Kabay, N., Sarp, S., Yuksel, M., Kitis, M., Koseoğlu, H., Arar, Ö. et al. (2008) Removal of boron from SWRO permeate by boron selective ion exchange resins containing N-methyl glucamine groups. *Desalination*, **223**, 49–56.

[51] Shanmuganathan, S., Nguyen, T.V., Shim, W.G., Kandasamy, J. and Vigneswaran, S. (2014) Performance of submerged membrane – Ion exchange hybrid system with Purolite A502PS in treating reverse osmosis feed. *Separation and Purification Technology*, **122**, 24–31.

[52] Víctor-Ortega, M.D., Ochando-Pulido, J.M., Hodaifa, G. and Martínez-Ferez, A. (2014) Ion exchange as an efficient pretreatment system for reduction of membrane fouling in the purification of model OMW. *Desalination*, **343**, 198–207.

[53] Dietz, K. (2009) The design of a desalination pretreatment system for brackish groundwater. Worcester polytechnic institute.

[54] Abdulgader, H. Al, Kochkodan, V. and Hilal, N. (2013) Hybrid ion exchange – Pressure driven membrane processes in water treatment: A review. *Separation and Purification Technology*, **116**, 253–64.

[55] Hilal, N., Kochkodan, V., Al Abdulgader, H., Mandale, S. and Al-Jlil, S. a. (2015) A combined ion exchange–nanofiltration process for water desalination: III. Pilot scale studies. *Desalination*, **363**, 58–63.

[56] McAdam, E.J. and Judd, S.J. (2008) Biological treatment of ion-exchange brine regenerant for re-use: A review. *Separation and Purification Technology*, **62**, 264–72.

[57] Jacob IV, W.A. and Valesquez, L. (US 2005/0051491 A1, 2005.) Regenerant reuse. United States.

[58] Wiśniewski, J., Różańska, A. and Winnicki, T. (2005) Removal of troublesome anions from water by means of Donnan dialysis. *Desalination*, **182**, 339–46.

[59] Rozanska, A. and Wisniewski, J. (2006) Brackish water desalination with the combination of Donnan dialysis and electrodialysis. *Desalination*, **200**, 615–7.

[60] Rozanska, A. and Wisniewski, J. (2009) Modification of brackish water composition by means of Donnan dialysis as pretreatment before desalination. *Desalination*, **240**, 326–32.

[61] Rozanska, A., Wisniewski, J. and Winnicki, T. (2006) Donnan dialysis with anion-exchange membranes in a water desalination system. *Desalination*, **198**, 236–46.

[62] Cwirko, E.H. and Carbonell, R.G. (1990) A theoretical analysis of donnan dialysis across charged porous membranes. *Journal of Membrane Science*, **48**, 155–79.

[63] SymPy Development Team. (2014) SymPy: Python library for symbolic mathematics [Internet]. http://www.sympy.org.

[64] Flodman, H.R. and Dvorak, B.I. (2012) Brine Reuse in Ion-Exchange Softening: Salt Discharge, Hardness Leakage, and Capacity Tradeoffs. *Water Environment Research*, **84**, 535–43.

[65] Venkatesan, A. and Wankat, P.C. (2012) Desalination of the Colorado River water: A hybrid approach. *Desalination*, **286**, 176–86.

[66] Bernardes, A.M., Rodgrigues, M.A.S. and Ferreira, J.Z. (2014) Electrodialysis and water reuse - novel approaches. Springer.

[67] Lenntech. (2012) Product information Lewatit(R) C 249.

[68] WHO/UNICEF. (2015) Progress on sanitation and drinking water - 2015 update and MDG assessment.

[69] Schiermeier, Q. (2008) Water: purification with a pinch of salt. *Nature*, **452**, 260–1.

[70] Desaldata [Internet]. p. http://desaldata.com.

[71] Al-karaghouli, A. and Kazmerski, L.L. (2013) Comparisons of Technical and Economic Performance of the Main Desalination Processes With and Without Renewable Energy Coupling. Sol. World Congr. ISES, Cancun, Mexico. p. 1–8.

[72] Semiat, R. (2008) Energy issues in desalination processes. *Environmental Science and Technology*, **42**, 8193–201.

[73] Semiat, R. and Hasson, D. (2012) Water desalination. *Reviews in Chemical Engineering*, **28**, 43–60.

[74] Malaeb, L. and Ayoub, G.M. (2011) Reverse osmosis technology for water treatment: State of the art review. *Desalination*, **267**, 1–8.

[75] Peñate, B. and García-Rodríguez, L. (2012) Current trends and future prospects in the design of seawater reverse osmosis desalination technology. *Desalination*, **284**, 1–8.

[76] Li, D. and Wang, H. (2010) Recent developments in reverse osmosis desalination membranes. *Journal of Materials Chemistry*, **20**, 4551–66.

[77] Kim, Y., Kang, M.G., Lee, S., Jeon, S.G. and Choi, J.S. (2013) Reduction of energy consumption in seawater reverse osmosis desalination pilot plant by using energy recovery devices. *Desalination and Water Treatment*, **51**, 766–71.

[78] Voutchkov, N. and Semiat, R. (2008) Seawater desalination. In: Li NN, Fane AG, Ho WSV, and Matsuura T, editors. *Advanced Membrane Technology and Applications*, Wiley, Hoboken, New Jersey. p. 87–100.

[79] Blandin, G., Verliefde, A.R.D., Tang, C.Y. and Le-Clech, P. (2015) Opportunities to reach economic sustainability in forward osmosis–reverse osmosis hybrids for seawater desalination. *Desalination*, **363**, 26–36.

[80] Hochstrat, R., Wintgens, T., Kazner, C., Melin, T. and Gebel, J. (2012) Options for water scarcity and drought management - the role of desalination. *Desalination and Water Treatment*, **18**, 96–102.

[81] Bamaga, O.A., Yokochi, A., Zabara, B. and Babaqi, A.S. (2011) Hybrid FO/RO desalination system: Preliminary assessment of osmotic energy recovery and designs of new FO membrane module configurations. *Desalination*, **268**, 163–9.

[82] Lattemann, S. and Höpner, T. (2008) Environmental impact and impact assessment of seawater desalination. *Desalination*, **220**, 1–15.

[83] Latorre, M. (2005) Environmental impact of brine disposal on Posidonia seagrasses. *Desalination*, **182**, 517–24.

[84] Achilli, A., Cath, T.Y. and Childress, A.E. (2009) Power generation with pressure retarded osmosis: An experimental and theoretical investigation. *Journal of Membrane Science*, **343**, 42–52.

[85] Feinberg, B.J., Ramon, G.Z. and Hoek, E.M. V. (2013) Thermodynamic analysis of osmotic energy recovery at a reverse osmosis desalination plant. *Environmental Science & Technology*, **47**, 2982–9.

[86] Yip, N.Y. and Elimelech, M. (2014) Comparison of Energy Efficiency and Power

Density in Pressure Retarded Osmosis and Reverse Electrodialysis. *Environmental Science and Technology*, **48**, 11002–12.

[87] Sarp, S., Yeo, I., Kim, S., Oh, J., Cheon, K. and Park, Y. (2014) Evaluation and implementation of SWRO-PRO hybrid process for less energy intensive desalination. *Conference and Exhibition on Desalination for the Environment, Clean Water and Energy*, p. 216–7.

[88] Kim, Y.C. and Park, S.-J. (2014) Osmotic power generation by pressure retarded osmosis: water resource, technology, and the renewable energy. *Conference and Exhibition on Desalination for the Environment, Clean Water and Energy*, p. 216.

[89] Cath, T.Y., Hancock, N.T., Lundin, C.D., Hoppe-Jones, C. and Drewes, J.E. (2010) A multi-barrier osmotic dilution process for simultaneous desalination and purification of impaired water. *Journal of Membrane Science*, **362**, 417–26.

[90] Yangali-Quintanilla, V., Olesen, L., Lorenzen, J., Rasmussen, C., Laursen, H., Vestergaard, E. et al. (2014) Lowering desalination costs by alternative desalination and water reuse scenarios. *Desalination and Water Treatment*, 1–9.

[91] Yangali-Quintanilla, V., Li, Z., Valladares, R., Li, Q. and Amy, G. (2011) Indirect desalination of Red Sea water with forward osmosis and low pressure reverse osmosis for water reuse. *Desalination*, **280**, 160–6.

[92] Cath, T.Y., Drewes, J.E. and Lundin, C.D. (2009) A Novel Hybrid Forward Osmosis Process for Drinking Water Augmentation using Impaired Water and Saline Water Sources. *Water Research Foundation, Denver, CO*, 1–84.

[93] Blandin, G., Verliefde, A.R.D., Tang, C.Y., Childress, A.E. and Le-Clech, P. (2013) Validation of assisted forward osmosis (AFO) process: Impact of hydraulic pressure. *Journal of Membrane Science*, **447**, 1–11.

[94] Lutchmiah, K., Harmsen, D.J.H., Wols, B. a., Rietveld, L.C., Jianjun Qin and Cornelissen, E.R. (2015) Continuous and discontinuous pressure assisted osmosis (PAO). *Journal of Membrane Science*, **476**, 182–93.

[95] Yun, T., Kim, Y.J., Lee, S., Hong, S. and Kim, G.I. (2014) Flux behavior and membrane fouling in pressure-assisted forward osmosis. *Desalination and Water Treatment*, **52**, 564–9.

[96] Tang, C.Y., She, Q., Lay, W.C.L., Wang, R. and Fane, A.G. (2010) Coupled effects of internal concentration polarization and fouling on flux behavior of forward osmosis membranes during humic acid filtration. *Journal of Membrane Science*, **354**, 123–33.

[97] She, Q., Jin, X. and Tang, C.Y. (2012) Osmotic power production from salinity

gradient resource by pressure retarded osmosis: Effects of operating conditions and reverse solute diffusion. *Journal of Membrane Science*, **401-402**, 262–73.

[98] Chung, T.-S., Li, X., Ong, R.C., Ge, Q., Wang, H. and Han, G. (2012) Emerging forward osmosis (FO) technologies and challenges ahead for clean water and clean energy applications. *Current Opinion in Chemical Engineering*, **1**, 246–57.

[99] Chung, T.-S., Zhang, S., Wang, K.Y., Su, J. and Ling, M.M. (2012) Forward osmosis processes: Yesterday, today and tomorrow. *Desalination*, **287**, 78–81.

[100] Song, X., Liu, Z. and Sun, D.D. (2011) Nano gives the answer: Breaking the bottleneck of internal concentration polarization with a nanofiber composite forward osmosis membrane for a high water production rate. *Advanced Materials*, **23**, 3256–60.

[101] Wang, R., Shi, L., Tang, C.Y., Chou, S., Qiu, C. and Fane, A.G. (2010) Characterization of novel forward osmosis hollow fiber membranes. *Journal of Membrane Science*, **355**, 158–67.

[102] Wang, H., Chung, T.-S., Tong, Y.W., Jeyaseelan, K., Armugam, A., Chen, Z. et al. (2012) Highly Permeable and Selective Pore-Spanning Biomimetic Membrane Embedded with Aquaporin Z. *Small*, **8**, 1185–90.

[103] Zhao, S., Zou, L., Tang, C.Y. and Mulcahy, D. (2012) Recent developments in forward osmosis: Opportunities and challenges. *Journal of Membrane Science*, **396**, 1–21.

[104] Saren, Q., Qiu, C.Q. and Tang, C.Y. (2011) Synthesis and characterization of novel forward osmosis membranes based on layer-by-layer assembly. *Environmental Science & Technology*, **45**, 5201–8.

[105] Post, J.W., Hamelers, H.V.M. and Buisman, C.J.N. (2009) Influence of multivalent ions on power production from mixing salt and fresh water with a reverse electrodialysis system. *Journal of Membrane Science*, **330**, 65–72.

[106] Vermaas, D. a., Veerman, J., Saakes, M. and Nijmeijer, K. (2014) Influence of multivalent ions on renewable energy generation in reverse electrodialysis. *Energy & Environmental Science*, **7**, 1434–45.

[107] Siegrist, H. and Joss, A. (2012) Review on the fate of organic micropollutants in wastewater treatment and water reuse with membranes. *Water Science and Technology*, **66**, 1369–76.

[108] Bellona, C., Drewes, J.E., Xu, P. and Amy, G. (2004) Factors affecting the rejection of organic solutes during NF/RO treatment--a literature review. *Water Research*, **38**, 2795–809.

[109] Verliefde, a. R.D., Cornelissen, E.R., Heijman, S.G.J., Verberk, J.Q.J.C., Amy, G.L.,

Van der Bruggen, B. et al. (2008) The role of electrostatic interactions on the rejection of organic solutes in aqueous solutions with nanofiltration. *Journal of Membrane Science*, **322**, 52–66.

[110] Verliefde, A.R.D., Cornelissen, E.R., Heijman, S.G.J., Hoek, E.M. V, Amy, G.L., Van der Bruggen, B. et al. (2009) Influence of solute-membrane affinity on rejection of uncharged organic solutes by nanofiltration membranes. *Environmental Science & Technology*, **43**, 2400–6.

[111] Boo, C., Lee, S., Elimelech, M., Meng, Z. and Hong, S. (2012) Colloidal fouling in forward osmosis: Role of reverse salt diffusion. *Journal of Membrane Science*, **390-391**, 277–84.

[112] Boo, C., Elimelech, M. and Hong, S. (2013) Fouling control in a forward osmosis process integrating seawater desalination and wastewater reclamation. *Journal of Membrane Science*, **444**, 148–56.

[113] Lee, S., Boo, C., Elimelech, M. and Hong, S. (2010) Comparison of fouling behavior in forward osmosis (FO) and reverse osmosis (RO). *Journal of Membrane Science*, **365**, 34–9.

[114] Xie, M., Nghiem, L.D., Price, W.E. and Elimelech, M. (2012) Comparison of the removal of hydrophobic trace organic contaminants by forward osmosis and reverse osmosis. *Water Research*, **46**, 2683–92.

[115] Mi, B. and Elimelech, M. (2008) Chemical and physical aspects of organic fouling of forward osmosis membranes. *Journal of Membrane Science*, **320**, 292–302.

[116] Mi, B. and Elimelech, M. (2010) Organic fouling of forward osmosis membranes: Fouling reversibility and cleaning without chemical reagents. *Journal of Membrane Science*, **348**, 337–45.

[117] Parida, V. and Ng, H.Y. (2013) Forward osmosis organic fouling: Effects of organic loading, calcium and membrane orientation. *Desalination*, **312**, 88–98.

[118] She, Q., Jin, X., Li, Q. and Tang, C.Y. (2012) Relating reverse and forward solute diffusion to membrane fouling in osmotically driven membrane processes. *Water Research*, **46**, 2478–86.

[119] Valladares Linares, R., Yangali-Quintanilla, V., Li, Z. and Amy, G. (2012) NOM and TEP fouling of a forward osmosis (FO) membrane: Foulant identification and cleaning. *Journal of Membrane Science*, **421-422**, 217–24.

[120] Zhao, S., Zou, L. and Mulcahy, D. (2011) Effects of membrane orientation on process performance in forward osmosis applications. *Journal of Membrane Science*, **382**,

308–15.

[121] Liu, Y. and Mi, B. (2012) Combined fouling of forward osmosis membranes: Synergistic foulant interaction and direct observation of fouling layer formation. *Journal of Membrane Science*, **407-408**, 136–44.

[122] Kim, D.I., Kim, J., Shon, H.K. and Hong, S. (2015) Pressure retarded osmosis (PRO) for integrating seawater desalination and wastewater reclamation: Energy consumption and fouling. *Journal of Membrane Science*, **483**, 34–41.

[123] Hoek, E.M. V and Elimelech, M. (2003) Cake-Enhanced Concentration Polarization: A New Fouling Mechanism for Salt-Rejecting Membranes. *Environmental Science and Technology*, **37**, 5581–8.

[124] Coday, B.D., Yaffe, B.G.M., Xu, P. and Cath, T.Y. (2014) Rejection of trace organic compounds by forward osmosis membranes: a literature review. *Environmental Science & Technology*, **48**, 3612–24.

[125] Alturki, A.A., McDonald, J. a., Khan, S.J., Price, W.E., Nghiem, L.D. and Elimelech, M. (2013) Removal of trace organic contaminants by the forward osmosis process. *Separation and Purification Technology*, **103**, 258–66.

[126] She, Q., Hou, D., Liu, J., Tan, K.H. and Tang, C.Y. (2013) Effect of feed spacer induced membrane deformation on the performance of pressure retarded osmosis (PRO): Implications for PRO process operation. *Journal of Membrane Science*, **445**, 170–82.

[127] Vermaas, D.A., Kunteng, D., Saakes, M. and Nijmeijer, K. (2013) Fouling in reverse electrodialysis under natural conditions. *Water Research*, **47**, 1289–98.

[128] Post, J.W. (2009) Blue Energy : electricity production from salinity gradients by reverse electrodialysis. Wageningen University.

[129] Ratkje, S.K., Holt, T. and Fiksdal, L. (1985) Effect of biofilm formation on salinity power plant output on laboratory scale. *Industrial Membrane Processes*,.

[130] Banasiak, L.J., Van der Bruggen, B. and Schäfer, A.I. (2011) Sorption of pesticide endosulfan by electrodialysis membranes. *Chemical Engineering Journal*, **166**, 233–9.

[131] Feinberg, B.J., Ramon, G.Z. and Hoek, E.M. V. (2015) Scale-up characteristics of membrane-based salinity-gradient power production. *Journal of Membrane Science*, **476**, 311–20.

[132] Daniilidis, A., Herber, R. and Vermaas, D. a. (2014) Upscale potential and financial feasibility of a reverse electrodialysis power plant. *Applied Energy*, **119**, 257–65.

[133] Edwin Moe, N., Han, Z., Guo, Y., Vipin Wagholikar, V., May Goh, L., Ramanan, H.

et al. (2015) Feasibility studies of a novel way to combine seawater desalination and wastewater treatment. *The Internation Desalination Association World Congress on Desalination and Water Reuse*, San Diego.

[134] Zhuang, H., Guo, Y., Vipin Wagholikar, V., Zhao, Y., Edwin Moe, N., Ramanan, H. et al. (2015) RED/DRED process development for desalination brine recovery. *The Internation Desalination Association World Congress on Desalination and Water Reuse*, San Diego.

[135] Geise, M., Curtis, A.J., Hatzell, M.C., Hickner, M.A. and Logan, B.E. (2014) Salt Concentration Differences Alter Membrane Resistance in Reverse Electrodialysis Stacks. *Environmental Science & Technology Letters*, **1**, 36–9.

[136] Galama, a. H., Vermaas, D. a., Veerman, J., Saakes, M., Rijnaarts, H.H.M., Post, J.W. et al. (2014) Membrane resistance: The effect of salinity gradients over a cation exchange membrane. *Journal of Membrane Science*, **467**, 279–91.

[137] Kabsch-Korbutowicz, M., Wisniewski, J., Łakomska, S. and Urbanowska, A. (2011) Application of UF, NF and ED in natural organic matter removal from ion-exchange spent regenerant brine. *Desalination*, **280**, 428–31.

[138] Kim, D.H. (2011) A review of desalting process techniques and economic analysis of the recovery of salts from retentates. *Desalination*, **270**, 1–8.

[139] Lefebvre, O. and Moletta, R. (2006) Treatment of organic pollution in industrial saline wastewater: a literature review. *Water Research*, **40**, 3671–82.

[140] Deorsola, A.B., Camarinha, G.C., Carvalho, D.D. and Sant'Anna Jr., G.L. (2013) Biological treatment of saline wastewaters in an aerobic sequencing batch reactor. *Environmental Progress & Sustainable Energy*, **32**, 198–205.

[141] Khan, M.T., Busch, M., Molina, V.G., Emwas, A.-H., Aubry, C. and Croue, J.-P. (2014) How different is the composition of the fouling layer of wastewater reuse and seawater desalination RO membranes? *Water Research*, **59**, 271–82.

[142] Goosen, M.F.A. and Sablani, S.S. (2004) Fouling of reverse osmosis and ultrafiltration membranes: a critical review. *Separation Science and Technology*, **39**, 2261–98.

[143] Wang, Y.-N. and Tang, C.Y. (2011) Protein fouling of nanofiltration, reverse osmosis, and ultrafiltration membranes—The role of hydrodynamic conditions, solution chemistry, and membrane properties. *Journal of Membrane Science*, **376**, 275–82.

[144] Casademont, C., Pourcelly, G. and Bazinet, L. (2007) Effect of magnesium/calcium ratio in solutions subjected to electrodialysis: characterization of cation-exchange membrane fouling. *Journal of Colloid and Interface Science*, **315**, 544–54.

[145] Casademont, C., Pourcelly, G. and Bazinet, L. (2008) Effect of magnesium/calcium ratios in solutions treated by electrodialysis: morphological characterization and identification of anion-exchange membrane fouling. *Journal of Colloid and Interface Science*, **322**, 215–23.

[146] Araya-Farias, M. and Bazinet, L. (2006) Effect of calcium and carbonate concentrations on anionic membrane fouling during electrodialysis. *Journal of Colloid and Interface Science*, **296**, 242–7.

[147] Bazinet, L. and Araya-Farias, M. (2005) Effect of calcium and carbonate concentrations on cationic membrane fouling during electrodialysis. *Journal of Colloid and Interface Science*, **281**, 188–96.

[148] Tanaka, N., Nagase, M. and Higa, M. (2012) Organic fouling behavior of commercially available hydrocarbon-based anion-exchange membranes by various organic-fouling substances. *Desalination*, **296**, 81–6.

[149] Lee, H.-J., Choi, J.-H., Cho, J. and Moon, S.-H. (2002) Characterization of anion exchange membranes fouled with humate during electrodialysis. *Journal of Membrane Science*, **203**, 115–26.

[150] Ping, Q., Cohen, B., Dosoretz, C. and He, Z. (2013) Long-term investigation of fouling of cation and anion exchange membranes in microbial desalination cells. *Desalination*, **325**, 48–55.

[151] Xu, J., Sheng, G.-P., Luo, H.-W., Li, W.-W., Wang, L.-F. and Yu, H.-Q. (2012) Fouling of proton exchange membrane (PEM) deteriorates the performance of microbial fuel cell. *Water Research*, **46**, 1817–24.

[152] Strathmann, H., Grabowski, A. and Eigenberger, G. (2013) Ion-exchange membranes in the chemical process industry. *Industrial & Engineering Chemistry Research*, **52**, 10364–79.

[153] Zhang, Y., Pinoy, L., Meesschaert, B. and Van der Bruggen, B. (2011) Separation of small organic ions from salts by ion-exchange membrane in electrodialysis. *AIChE Journal*, **57**, 2070–8.

[154] Lopez, A.M. and Hestekin, J.A. (2013) Separation of organic acids from water using ionic liquid assisted electrodialysis. *Separation and Purification Technology*, **116**, 162–9.

[155] Woźniak, M.J. and Prochaska, K. (2014) Fumaric acid separation from fermentation broth using nanofiltration (NF) and bipolar electrodialysis (EDBM). *Separation and Purification Technology*, **125**, 179–86.

[156] Huyskens, C., Helsen, J., Groot, W.J. and de Haan, A.B. (2013) Membrane capacitive

deionization for biomass hydrolysate desalination. *Separation and Purification Technology*, **118**, 33–9.

[157] Banasiak, L.J. (2009) Removal of inorganic and trace organic contaminants by electrodialysis. The University of Edinburgh.

[158] Banasiak, L.J. and Schäfer, A.I. (2010) Sorption of steroidal hormones by electrodialysis membranes. *Journal of Membrane Science*, **365**, 198–205.

[159] Ghyselbrecht, K., Silva, A., Van der Bruggen, B., Boussu, K., Meesschaert, B. and Pinoy, L. (2014) Desalination feasibility study of an industrial NaCl stream by bipolar membrane electrodialysis. *Journal of Environmental Management*, Elsevier Ltd. **140**, 69–75.

[160] Verliefde, A.R.D., Heijman, S.G.J., Cornelissen, E.R., Amy, G., Van der Bruggen, B. and van Dijk, J.C. (2007) Influence of electrostatic interactions on the rejection with NF and assessment of the removal efficiency during NF/GAC treatment of pharmaceutically active compounds in surface water. *Water Research*, **41**, 3227–40.

[161] Van der Bruggen, B., Verliefde, A., Braeken, L., Cornelissen, E.R., Moons, K., Verberk, J.Q.J.C. et al. (2006) Assessment of a semi-quantitative method for estimation of the rejection of organic compounds in aqueous solution in nanofiltration. *Journal of Chemical Technology and Biotechnology*, **1176**, 1166–76.

[162] Verliefde, A. (2008) Rejection of organic micropollutants by high pressure membranes (NF/RO). Technische Universiteit Delft.

[163] Zhang, Y. and Angelidaki, I. (2014) Microbial electrolysis cells turning to be versatile technology: recent advances and future challenges. *Water Research*, **56**, 11–25.

[164] Logan, B.E., Call, D., Cheng, S., Hamelers, H.V.M., Sleutels, T.H.J.A., Jeremiasse, A.W. et al. (2008) Microbial electrolysis cells for high yield hydrogen gas production from organic matter. *Environmental Science & Technology*, **42**, 8630–40.

[165] Kim, J.R.A.E., Cheng, S., Oh, S.-E. and Logan, B.E. (2007) Power generation using different cation, anion, and ultrafiltration membranes in microbial fuel cells. *Environmental Engineering Science*, **41**, 1004–9.

[166] Zhu, X. and Logan, B.E. (2014) Microbial electrolysis desalination and chemical-production cell for CO2 sequestration. *Bioresource Technology*, **159**, 24–9.

[167] Luo, H., Jenkins, P.E. and Ren, Z. (2011) Concurrent desalination and hydrogen generation using microbial electrolysis and desalination cells. *Environmental Science & Technology*, **45**, 340–4.

[168] Kim, Y. and Logan, B.E. (2013) Microbial desalination cells for energy production and desalination. *Desalination*, **308**, 122–30.

[169] Mehanna, M., Kiely, P.D., Call, D.F. and Logan, B.E. (2010) Microbial electrodialysis cell for simultaneous water desalination and hydrogen gas production. *Environmental Science & Technology*, **44**, 9578–83.

[170] Andersen, S.J., Hennebel, T., Gildemyn, S., Coma, M., Desloover, J., Berton, J. et al. (2014) Electrolytic membrane extraction enables production of fine chemicals from biorefinery sidestreams. *Environmental Science & Technology*, **48**, 7135–42.

[171] Desloover, J., Woldeyohannis, A.A., Verstraete, W., Boon, N. and Rabaey, K. (2012) Electrochemical resource recovery from digestate to prevent ammonia toxicity during anaerobic digestion. *Environmental Science & Technology*, **46**, 12209–16.

[172] Lindstrand, V., Sundström, G. and Jönsson, A. (2000) Fouling of electrodialysis membranes by organic substances. *Desalination*, **128**, 91–102.

[173] Kimura, K., Amy, G., Drewes, J. and Watanabe, Y. (2003) Adsorption of hydrophobic compounds onto NF/RO membranes: an artifact leading to overestimation of rejection. *Journal of Membrane Science*, **221**, 89–101.

[174] Liu, J., Jiang, M., Li, G., Xu, L. and Xie, M. (2010) Miniaturized salting-out liquid-liquid extraction of sulfonamides from different matrices. *Analytica Chimica Acta*, **679**, 74–80.

[175] Mohamed, A.-M.I., Abdel-Wadood, H.M. and Mousa, H.S. (2014) Simultaneous determination of dorzolomide and timolol in aqueous humor: a novel salting out liquid-liquid microextraction combined with HPLC. *Talanta*, **130**, 495–505.

[176] Gildemyn, S., Verbeeck, K., Slabbinck, R., Andersen, S.J., Prévoteau, A. and Rabaey, K. (2015) Integrated Production, Extraction, and Concentration of Acetic Acid from CO 2 through Microbial Electrosynthesis. *Environmental Science & Technology Letters*, **2**, 325–8.

[177] Ramadan, Y., Pátzay, G. and Tamás, G. (2010) Transport of NaCl , MgSO4 , MgC2 and Na2SO4 across DL type nanofiltration membrane. *Chemical Engineering*, **2**, 81–6.

[178] Luo, J. and Wan, Y. (2013) Effects of pH and salt on nanofiltration-a critical review. *Journal of Membrane Science*, **438**, 18–28.

[179] Tansel, B., Sager, J., Rector, T., Garland, J., Strayer, R.F., Levine, L. et al. (2006) Significance of hydrated radius and hydration shells on ionic permeability during nanofiltration in dead end and cross flow modes. *Separation and Purification Technology*, **51**, 40–7.

[180] Jin, X., Huang, X. and Hoek, E.M. V. (2009) Role of specific ion interactions in seawater RO membrane fouling by alginic acid. *Environmental Science & Technology*, **43**,

3580–7.

[181] Xin, Y., Bligh, M.W., Kinsela, A.S. and Waite, T.D. (2016) Effect of iron on membrane fouling by alginate in the absence and presence of calcium. *Journal of Membrane Science*, Elsevier. **497**, 289–99. http://dx.doi.org/10.1016/j.memsci.2015.09.023

[182] Al-Juboori, R.A. and Yusaf, T. (2012) Biofouling in RO system: Mechanisms, monitoring and controlling. *Desalination*, **302**, 1–23.

[183] PUROLITE. (2006) Shallow Shell Technology Resins - Application guide.

[184] PUROLITE. (2009) Purolite(R) resins for potable and ground water treatment.

[185] BBT-kenniscentrum VITO. (2007) Lozingsnormen: concentraties of vrachten?

[186] Kurniawan, T.A., Chan, G.Y.S., Lo, W.-H. and Babel, S. (2006) Physico–chemical treatment techniques for wastewater laden with heavy metals. *Chemical Engineering Journal*, **118**, 83–98.

[187] Abu, H. and Moussab, H. (2004) Removal of heavy metals from wastewater by membrane processes : a comparative study. *Desalination*, **164**, 105–10.

[188] Fu, F. and Wang, Q. (2011) Removal of heavy metal ions from wastewaters: a review. *Journal of Environmental Management*, **92**, 407–18.

[189] Vermaas, D. a., Kunteng, D., Veerman, J., Saakes, M. and Nijmeijer, K. (2014) Periodic feedwater reversal and air sparging as antifouling strategies in reverse electrodialysis. *Environmental Science and Technology*, **48**, 3065–73.

[190] Güler, E., Elizen, R., Vermaas, D. a., Saakes, M. and Nijmeijer, K. (2013) Performance-determining membrane properties in reverse electrodialysis. *Journal of Membrane Science*, **446**, 266–76.

[191] Długołęcki, P., Dąbrowska, J., Nijmeijer, K. and Wessling, M. (2010) Ion conductive spacers for increased power generation in reverse electrodialysis. *Journal of Membrane Science*, **347**, 101–7.

[192] Vermaas, D. a., Saakes, M. and Nijmeijer, K. (2011) Power generation using profiled membranes in reverse electrodialysis. *Journal of Membrane Science*, **385-386**, 234–42.

[193] Liu, J., Geise, G.M., Luo, X., Hou, H., Zhang, F., Feng, Y. et al. (2014) Patterned ion exchange membranes for improved power production in microbial reverse-electrodialysis cells. *Journal of Power Sources*, **271**, 437–43.

[194] Güler, E., Elizen, R., Saakes, M. and Nijmeijer, K. (2014) Micro-structured membranes for electricity generation by reverse electrodialysis. *Journal of Membrane Science*, **458**, 136–48.

[195] Zhang, B., Gao, H. and Chen, Y. (2015) Enhanced Ionic Conductivity and Power Generation Using Ion-Exchange Resin Beads in a Reverse-Electrodialysis Stack. *Environmental Science and Technology*, **49**, 14717–24.

[196] Veerman, J., Saakes, M., Metz, S.J. and Harmsen, G.J. (2011) Reverse electrodialysis: A validated process model for design and optimization. *Chemical Engineering Journal*, **166**, 256–68.

[197] Teusner, A., Blandin, G. and Le-Clech, P. (2016) Augmenting water supply by combined desalination/water recycling methods: an economic assessment. *Environmental Technology*, **In press**.

[198] Vanoppen, M., Blandin, G., Derese, S., Le-Clech, P., Post, J.W. and Verliefde, A.R.D. (2016) Salinity gradient power and desalination. In: Cipollina A, and Micale G, editors. *Sustainable Energy from Salinity Gradients*, 1st ed. Woodhead Publishing-Elsevier, London. p. 281–313.

[199] Cipollina, A., Micale, G., Tamburini, A., Tedesco, M., Gurreri, L., Veerman, J. et al. (2016) Reverse electrodialysis: applications. In: Cipollina A, and Micale G, editors. *Sustainable Energy from Salinity Gradients*, 1st ed. Woodhead Publishing-Elsevier, London. p. 135–80.

[200] Stover, R.L. (2014) A new process for high-recovery, low-energy RO treatment. *Tech Talk - American Water Works Association*, 74–7.

[201] Stover, R.L. (2013) High recovery using closed circuit desalination processes for inland brackish and oil and gas applications. *The Internation Desalination Association World Congress on Desalination and Water Reuse*, Tianjin, China.

[202] Efraty, A., Barak, R.N. and Gal, Z. (2011) Closed circuit desalination - a new low energy high recovery technology without energy recovery. *Desalination and Water Treatment*, **31**, 95–101.

[203] Westerling, K. (2013) Views from the top: is this the future of RO? [Internet]. Water Online. p. http://www.wateronline.com/doc/is – this – the – future – .

[204] Verliefde, A.R.D., Van der Meeren, P. and Van der Bruggen, B. (2013) Solution-diffusion processes. In: Hoek EM V., and Tarabara V V., editors. *Encyclopedia of Membrane Science and Technology*, Wiley, Hoboken, New Jersey. p. 11–36.

[205] Mulyati, S., Takagi, R., Fujii, A., Ohmukai, Y. and Matsuyama, H. (2013) Simultaneous improvement of the monovalent anion selectivity and antifouling properties of an anion exchange membrane in an electrodialysis process, using polyelectrolyte multilayer deposition. *Journal of Membrane Science*, **431**, 113–20.

[206] White, N., Misovich, M., Alemayehu, E., Yaroshchuk, A. and Bruening, M.L. (2015) Highly selective separations of multivalent and monovalent cations in electrodialysis through Nafion membranes coated with polyelectrolyte multilayers. *Polymer*, **In Press**.

[207] Güler, E., van Baak, W., Saakes, M. and Nijmeijer, K. (2014) Monovalent-ion-selective membranes for reverse electrodialysis. *Journal of Membrane Science*, **455**, 254–70.

[208] Li, J., Zhou, M. li, Lin, J. yang, Ye, W. yuan, Xu, Y. qing, Shen, J. nan et al. (2015) Mono-valent cation selective membranes for electrodialysis by introducing polyquaternium-7 in a commercial cation exchange membrane. *Journal of Membrane Science*, **486**, 89–96.

[209] Varcoe, J.R., Atanassov, P., Dekel, D.R., Herring, A.M., Hickner, M. a., Kohl, P. a. et al. (2014) Anion-exchange membranes in electrochemical energy systems. *Energy & Environmental Science*, **7**, 3135–91.

[210] Vermaas, D. a., Guler, E., Saakes, M. and Nijmeijer, K. (2012) Theoretical power density from salinity gradients using reverse electrodialysis. *Energy Procedia*, **20**, 170–84. http://dx.doi.org/10.1016/j.egypro.2012.03.018

[211] Post, J.W., Veerman, J., Hamelers, H.V.M., Euverink, G.J.W., Metz, S.J., Nymeijer, K. et al. (2007) Salinity-gradient power: Evaluation of pressure-retarded osmosis and reverse electrodialysis. *Journal of Membrane Science*, **288**, 218–30.

[212] Schock, G. and Miquel, A. (1987) Mass transfer and pressure loss in spiral wound modules. *Desalination*, **64**, 339–52.

[213] Jerschow, A. and Müller, N. (1997) Suppression of convection artifacts in stimulated-echo diffusion experiments. Double-stimulated-echo experiments. *Journal of Magnetic Resonance*, **375**, 372–5.

[214] Connell, M. a, Bowyer, P.J., Adam Bone, P., Davis, A.L., Swanson, A.G., Nilsson, M. et al. (2009) Improving the accuracy of pulsed field gradient NMR diffusion experiments: Correction for gradient non-uniformity. *Journal of Magnetic Resonance*, **198**, 121–31.

[215] Johnson Jr., C.S. (1999) Diffusion ordered nuclear magnetic resonance spectroscopy: principles and applications. *Progress in Nuclear Magnetic Resonance Spectroscopy*, **34**, 203–56.

Appendices

1 Appendix A

1.1 Scaling removal from IEX resins during backwash

In IEX, potential scaling during the regeneration phase is removed during the back-flush stage afterwards. This was tested in the lab, by examining the resin particles under the scanning electron microscope (SEM) before and after backwash, as shown in Figure A.1. The picture before backwash shows clear deposits on the resin particles, which are completely removed after the backwash.

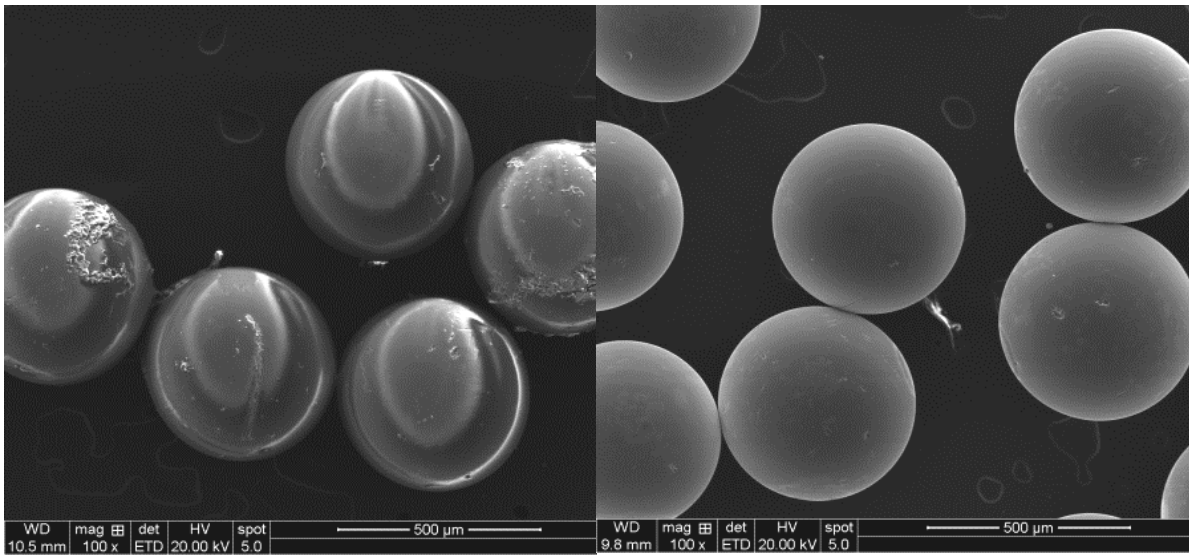

Figure A.1 SEM pictures of the resin particles before (left) and after (right) the backwash phase

The SEM analysis was performed by a FEG-SEM (Field Emission Gun-Scanning Electron Microscope) type quantaTM 450 (FEITM) (EDAX, USA).

1.2 Phosphate removal from wastewater stream

To removal of phosphate from the wastewater stream was investigated with IEX and DD. Marathon C resins and Fujifilm and PCA SA ion-exchange membranes were used respectively. The testing method was the same as the one discussed in the manuscript. For IEX, it was clear that little to no phosphate was withheld on the resin, since the effluent contained similar phosphate concentrations as the influent. Also, the resin itself showed a clear discoloration soon after starting the IEX experiment, which became darker over time (as shown in Figure A.2). This indicates the preferential interaction of the resin witch organics present in the feed stream, causing phosphate to pass through the IEX column.

Figure A.2 Discoloration of the resin (left) started soon after the start-up of the experiment with wastewater. The original color of the resin is shown on the right.

In the DD tests, similar problems rose. The phosphate in the feed stream remained the same (Figure A.3), even after switching to a different type of anion-exchange membrane. After opening the DD module, a clear discoloration of the membranes could be seen.

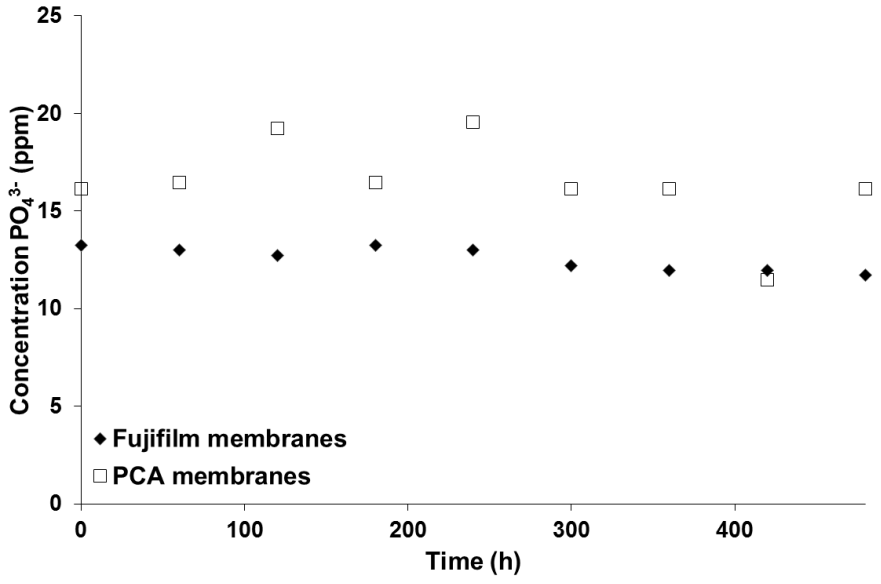

Figure A.3 Phosphate concentration over time using the Fujifilm and PCA membranes.

1.3 Saturation of scalants in RO concentrate

The saturation (%) of different salts and ions that can cause issues during RO operation is shown in Figure A.4. This saturation is based on calculations with Genesys®.

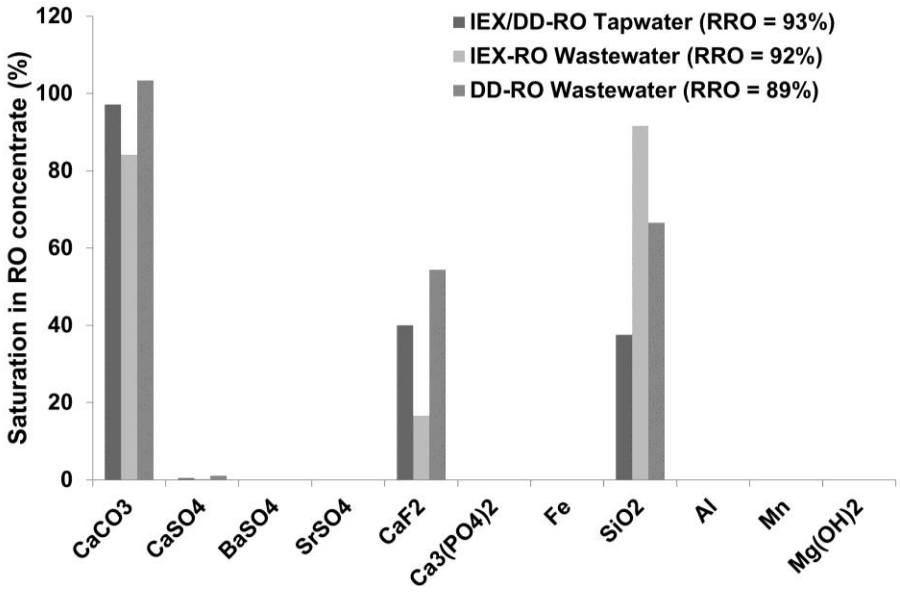

Figure A.4 Saturation of scalants in RO concentrate for the different scenarios considered.

1.4 Detailed cost overview for RO

The RO costs used in the economic analysis is based on the ROSA modelling software. The output of this software is shown in Table A.1 and Table A.2.

Table A.1 Detailed cost overview for the RO unit in the different scenarios from ROSA.

Project Identification			
Project Name	RAW	IEX-RO	DD-RO
Case #	1	1	1
Project Overview			
Unit set for economic evaluation	m^3-m^3/h-bar	m^3-m^3/h-bar	m^3-m^3/h-bar
System water production (m^3/h)	45.61	55.20	53.40
System recovery (%)	76.01	92.00	89.00
Project Economic Variables			
Project Life (years)	10	10	10
Interest rate (%)	4	4	4
Power cost ($kWh)	0.1	0.1	0.1
Pass 1			
Projection Results			
Pass 1 permeate production (m^3/h)	45.61	55.20	53.40
Pass 1 feed pressure (bar)	0.34	0.34	62.26
Pass 1 concentrate pressure (bar)	0.00	0.00	57.00
Pass 1 recovery (%)	76.00	92.00	89.00
Pass 1 energy recovery efficiency (%)	95.00%	95.00%	95.00%
Capital Expense			
Pass 1 pressure vessels	8	13	12
Pressure vessel cost ($/vessel)	500	500	500

Pass 1 capital for pressure vessels	$4000.00	$6500.00	$6000.00
Pass 1 total elements	64	78	72
Element cost ($/element)	$720.00	$720.00	$720.00
Pass 1 capital for elements ($)	$46080.00	$56160.00	$51840.00
Pass 1 capital ($)	$50080.00	$62660.00	$57840.00
Pass 1 capital($/m³)	$0.01	$0.01	$0.01
Operating Expense			
Power			
Pass 1 pumping power (kW)	0.00	0.00	216.21
Pass 1 pump specific energy (kWh/m³)	0.00	0.00	3.92
Brine energy recovery (kWh/m³)	-272.89	-331.11	-320.19
Pass 1 net energy consumption (KWh/m³)	272.89	331.11	324.11
Pass 1 net energy cost ($/year)	$654171.05	$960635.81	$909686.45
Energy expense NPV ($)	5305913.18	7791616.91	7378371.97
Pass 1 energy expense ($/m³)	$27.29	$33.11	$32.41
Membrane replacement cost			
Pass 1 replacement rate (%/year)	13	13	13
Replacement price ($/element)	$720.00	$720.00	$720.00
Pass 1 replacement cost for elements ($/year)	$5990.40	$7300.80	$6739.20
Pass 1 replacement membrane NPV ($)	$48587.51	$59216.03	$54660.95
Pass 1 membrane replacement expense ($/m³)	$0.01	$0.02	$0.01
Operating expense subtotal			
Pass 1 operating expense NPV ($)	$5354500.69	$7850832.94	$7433032.92
Pass 1 operating expense per m³	$27.30	$33.13	$32.43
Pass 1 Total			
Pass 1 cost NPV ($)	$46080.00	$56160.00	$51840.00
Life Cycle Cost ($/m³)	$0.01	$0.01	$0.01
Total System			
Capital	$50080.00	$62660.00	$57840.00
Operating expense NPV ($)	$5354500.69	$7850832.94	$7433032.92
Cost of water NPV ($/m³)	$1.35	$1.64	$1.60

Table A.2 Detailed cost overview for the RO unit in the different scenarios from ROSA

Project Identification		
Project Name	RAW	IEX/DD-RO
Case #	1	1
Project Overview		
Unit set for economic evaluation	m^3-m^3/h-bar	m^3-m^3/h-bar
System water production (m^3/h)	11.50	23.25
System recovery (%)	46.00	92.99
Project Economic Variables		
Project Life (years)	10	10
Interest rate (%)	4	4
Power cost ($kWh)	0.1	0.1
Pass 1		
Projection Results		
Pass 1 permeate production (m^3/h)	11.50	23.25
Pass 1 feed pressure (bar)	0.34	17.58
Pass 1 concentrate pressure (bar)	0.00	16.97
Pass 1 recovery (%)	46.00	93.00
Pass 1 energy recovery efficiency (%)	95.00%	95.00%
Capital Expense		
Pass 1 pressure vessels	4	6
Pressure vessel cost ($/vessel)	500	500
Pass 1 capital for pressure vessels	$2000.00	$3000.00
Pass 1 total elements	16	36
Element cost ($/element)	$720.00	$720.00
Pass 1 capital for elements ($)	$11520.00	$25920.00
Pass 1 capital ($)	$13520.00	$28920.00
Pass 1 capital($/$m^3$)	$0.01	$0.01
Operating Expense		
Power		
Pass 1 pumping power (kW)	0.00	15.26
Pass 1 pump specific energy (kWh/m^3)	0.00	0.66
Brine energy recovery (kWh/m^3)	-163.74	-334.75
Pass 1 net energy consumption (KWh/m^3)	163.74	335.41
Pass 1 net energy cost ($/year)	$98966.70	$409821.98
Energy expense NPV ($)	802708.63	3324023.33
Pass 1 energy expense ($/$m^3$)	$16.37	$33.54
Membrane replacement cost		
Pass 1 replacement rate (%/year)	13	13
Replacement price ($/element)	$720.00	$720.00
Pass 1 replacement cost for elements ($/year)	$1497.60	$3369.60
Pass 1 replacement membrane NPV ($)	$12146.88	$27330.47
Pass 1 membrane replacement expense ($/$m^3$)	$0.01	$0.02

Operating expense subtotal		
Pass 1 operating expense NPV ($)	$814855.50	$3351353.81
Pass 1 operating expense per m³	$16.39	$33.56
Pass 1 Total		
Pass 1 cost NPV ($)	$11520.00	$25920.00
Life Cycle Cost ($/m³)	$0.01	$0.01
Total System		
Capital	$13520.00	$28920.00
Operating expense NPV ($)	$814855.50	$3351353.81
Cost of water NPV ($/m³)	$0.82	$1.66

2 Appendix B

In the realistic modelling of the OD/OER-RO hybrid system, it is assumed that 90% of the applied hydraulic pressure is retained in the RO concentrate and a pressure exchanger with an efficiency of 98% is used. Pumps delivering the required pressure and flow are assumed to have a mechanistic efficiency of 95%. All other losses/inefficiencies are system specific and will be discussed below.

2.1 RED/scRED/ARED

In the modelling of the RED process, multiple modules are considered to achieve a certain recovery. These modules consist of 100 membranes with an area of 0.25m² (0.5 · 0.5 m), which all together form 50 cell pairs. The membrane characteristics are those reported for the Neosepta AMX-SB and CMX-SB membranes, with an average electrical resistance of 2.75 and 2.8 Ωm² respectively. 0.2 mm spacers were assumed to form the compartments between the membranes, resulting in a shadow factor of 0.6. A permselectivity of 98% for the membranes and a pressure drop of 1 bar per module were assumed.

The energy production (J) of one module can be calculated with the voltage (V) and current (I) through the stack, multiplied by the residence time of the water in the stack (t_{sw}):

$$E_{RED,module} = V \cdot I \cdot t_{sw} \tag{B.1}$$

This voltage is determined by the driving force, in this case the open circuit voltage (V_{OCV}), minus the losses due to non-ideality of the system:

$$V = V_{OCV} - I \cdot R_O \tag{B.2}$$

With R_O the Ohmic resistance, as stated by Vermaas et al. (2012), which takes into account the non-ideality of the membranes by introducing the permselectivity and the losses due to the spacers by introducing the shadow effect [210]. The resistance of the electrode compartments is negligible for modules this scale. Resistances due to differences in concentration between inlet and outlet were assumed to be negligible as well. V_{OCV} can be calculated from the Nerns equation:

$$V_{OCV} = \frac{2 \cdot R \cdot T}{F} \ln\left(\frac{C_{m,sw}}{C_{m,iw}}\right) \tag{B.3}$$

Due to concentration polarisation on both sides of the membranes, the concentration at the membrane surface is lowered on the seawater side and increased on the impaired water side

in respect to the bulk concentration, resulting in a decrease of the driving force and thus a decrease in V_{OCV}. This is taken into account by calculating the actual concentrations at the membrane surfaces:

$$C_{m,sw} = C_{sw} + \frac{(t_m - t_b)\cdot I\cdot \delta}{F\cdot D} \tag{B.4}$$

$$C_{m,iw} = C_{iw} - \frac{(t_m - t_b)\cdot I\cdot \delta}{F\cdot D} \tag{B.5}$$

Here, t is the transport number (-), δ the thickness of the boundary layer (m) and D the diffusion coefficient of NaCl (m^2/s). Subscripts m and b indicate the membrane and the bulk solution respectively. The transport number for cations and anions in the bulk was assumed to be 0.5, while that in the membranes was set to the permselectivity. The boundary layer thickness (δ) can be calculated by dividing the diffusion coefficient of NaCl by the mass transfer coefficient (k, m/s):

$$\delta = \frac{D}{k} \tag{B.6}$$

$$k = \frac{S_h\cdot D}{d_h} \tag{B.7}$$

This mass transfer coefficient depends on the hydraulic diameter of the module d_h (m) and the Sherwood number Sh (-). Using the compartment thickness h (m) and the width of the membranes w (m), the hydraulic diameter coefficient can be calculated:

$$d_h = \frac{2\cdot w\cdot h}{(w+h)} \tag{B.8}$$

The Sherwood number of the RED module was approximated by the Sherwood relation for a plate-and-frame system with turbulence promotors, with Sc the Schmidt number (-) and Re the Reynolds number (-):

$$S_h = 1.9\cdot Sc^{0.33}\cdot Re^{0.5}\left(\frac{h}{\Delta l}\right)^{0.5} \tag{B.9}$$

$$S_c = \frac{\eta}{\rho\cdot D} \tag{B.10}$$

$$Re = \frac{\rho\cdot u\cdot d_h}{\mu} \tag{B.11}$$

Δl is the mesh width plus the diameter of the used spacers (m), μ is the dynamic viscosity (Pa.s), ρ is the mass density of the feed water (kg/m³) and u the flow velocity in the module (m/s).

Based on the pressure drop over the different compartments and the flow rate of the different streams, the energy consumed by pumps taking into account the hydrodynamic losses can be calculated:

$$E_{pump} = \frac{Q_{sw} \cdot \Delta P_{sw} \cdot N}{\eta_p} + \frac{Q_{iw} \cdot \Delta P_{iw} \cdot N}{\eta_p} \quad \text{(B.12)}$$

Consequently, the total energy consumption (kWh/m³) of the hybrid process can be calculated by comparing the energy consumption of the RO system and the pumps with the energy production of the RED system:

$$SEC_{RED-RO} = SEC_{RO} - \left(\sum_1^N (SEC_{RED,n}) - SEC_{pump}\right) \quad \text{(B.13)}$$

Here, N is the number of modules required, n is the number of the considered module and η_p is the efficiency of the pumps.

The related processes, scRED and ARED, were modelled using the same set of equations, taking into account the differences in the external resistance. In the RED-RO models, the external resistance is assumed equal to the internal resistance for each stack, since this can be shown to result in the highest power density [211]. For scRED, the external resistance was assumed to be 0. In ARED on the other hand, the external resistance is replaced by an additional potential difference equal to $1/5^{th}$ of the initial V_{OCV} in the first module, resulting in a higher current through the system.

2.2 PRO/FO/PAO

PRO/FO/PAO was modelled using membrane modules of 4 m² (WxLxD = 4x1x0.0025 m), and the membrane properties were chosen as those reported for the CTA-W membrane (HTI, Albany, OR, USA), a well-known FO membrane with water permeability (A) of 2.2 x 10^{-12} m/(Pa.s), a structure factor (S) of 600 μm and retention for NaCl of 90%. The flow channels are spacer filled, where the channel has a specific surface of 11 600 m²/m³ and a porosity of 90%.

All membrane-related non-idealities (concentration polarisation and reverse solute diffusion) and pressure drop in the modules were incorporated. Losses due to fouling were not taken into account, due to their unpredictable nature.

Concentration profiles are believed to comply with Fick's law:

$$J = -D \cdot \frac{\partial C}{\partial x} \tag{B.14}$$

Where J is mass transfer (mol/(m².s)), D is the diffusion coefficient of the solute in water (m²/s) and $\frac{\partial C}{\partial x}$ is the concentration gradient.

When solving Fick's equation, the concentration at the membrane interface is calculated by (at the active layer, when the concentrated draw-solution is facing the active layer):

$$\frac{C_{sw,m}}{C_{sw,b}} = \exp(-\frac{J_w}{k}) \tag{B.15}$$

Where Jw is the water flux (m³/(m².s)), k is the external mass transfer coefficient (m/s) and C the concentration (mol/m³). Subscripts sw, m and b refer to seawater, membrane and bulk respectively.

At the porous layer interface, in the same configuration, for the impaired water:

$$\frac{C_{iw,m}}{C_{iw,b}} = \exp(J_w \cdot K) \tag{B.16}$$

Where K is the internal mass transfer coefficient (s/m).

The determination of the two mass transfer coefficients, k (external mass transfer coefficient) and K (internal mass transfer coefficient), differs. While at the active layer, turbulent eddies can disrupt the boundary layer, the porous support layer has a fixed laminar flow regime with reduced mass transfer speeds. Therefore, K can only be determined by determining the structure factor (which in its turn is determined empirically through flux experiments):

$$S = \frac{t \cdot \tau}{\varepsilon} \tag{B.17}$$

Where t is the thickness, τ is the tortuosity and ε is the porosity of the porous support layer. The internal mass transfer coefficient is then determined by:

$$K = \frac{S}{D} \tag{B.18}$$

The external mass transfer coefficient can be determined by calculating the Sherwood number:

$$Sh = 0.065 \cdot \ Re^{0.875} \cdot Sc^{0.25} \tag{B.19}$$

The hydraulic diameter for spacer-filled membrane channels was determined by Shock et al. [212]:

$$d_h = \frac{4 \cdot \varepsilon}{\frac{2}{h} + (1-\varepsilon) \cdot S_{V,SP}} \tag{B.20}$$

Where h is the height of the flow channel (m), and $S_{V,SP}$ is the specific surface area of the spacer (m^2/m^3). Note that the porosity in this case is the porosity of the spacer. k is then directly proportional to the Sherwood number, as stated before.

As there is a concentration gradient across the membrane, and current membranes are not perfectly selective, solute diffusing from seawater to impaired water (e.g. NaCl) causes the concentration of the impaired water near the membrane surface to rise. This further aggravates the concentration polarisation. The solute permeability through the membrane can be determined from the rejection, mass transfer coefficient and water flux:

$$B = J_w \cdot \frac{(1-R)}{R} \cdot \exp\left(-\frac{J_w}{k}\right) \tag{B.21}$$

When all effects are incorporated, water flux through the membrane can be calculated through an iterative process:

$$J_w = A \cdot \left[\frac{\pi_{sw,b} \cdot \exp\left(\frac{-J_w}{k}\right) - \pi_{iw,b} \cdot \exp(J_w K)}{1 + \frac{B}{J_w} \cdot [\exp(J_w K) - 1]} - \Delta P\right] \tag{B.22}$$

In equation B.22, π is the osmotic pressure (Pa). In every module, the concentrations of both solutions leaving the module and recuperated energy were calculated using the water flux:

$$SEC_{PRO,i} = J_{w,i} \cdot \Delta P_i \tag{B.23}$$

Where ΔP is the applied hydraulic pressure. The overall energy balance then becomes:

$$SEC_{PRO-RO} = SEC_{RO} - \sum_i^n SEC_{PRO} \tag{B.24}$$

3 Appendix C

3.1 Influence of changing diluate concentration

3.1.1 F I – 30 ml/min

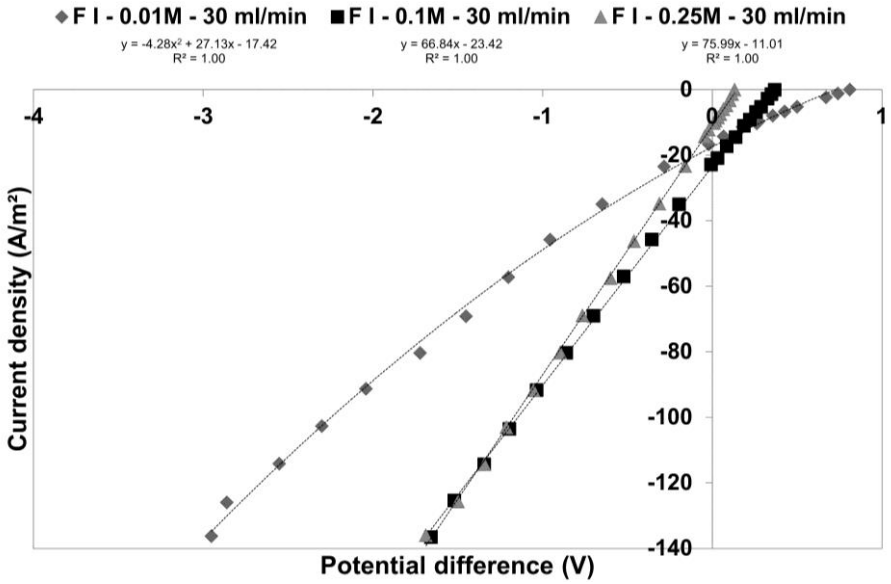

Figure C.1 Influence of different C_D concentrations on the current-voltage relation in the RED and ARED region (C_C = 0.5M, flow rate = 30 ml/min, membrane type I). Curve fitting polynomial degree is based on highest R^2 reached. Error bars are included but overall too small to be visible.

3.1.2 F I – 50 ml/min

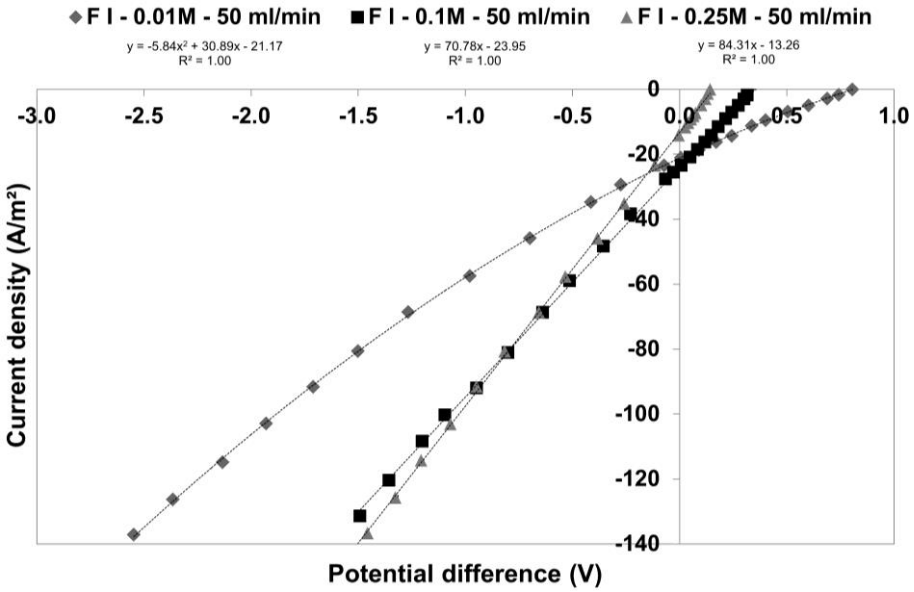

Figure C.2 Influence of different CD concentrations on the current-voltage relation in the RED and ARED region (CC = 0.5M, flow rate = 50 ml/min, membrane type I). Curve fitting polynomial degree is based on highest R^2 reached. Error bars are included but overall too small to be visible.

4 Appendix D

4.1 Resistance measurement

The clamp has platinum electrodes fitted in each leg, with a surface area of 1 cm^2. A picture of the clamp is shown in Figure C.1. When screwing both sides of the clamp together, the electrodes are exactly 1 cm apart. The electrodes were connected to a multimeter (LCR-3500, Monacor, Germany). The resistance was measured in AC mode by measuring the resistance of a 0.5M NaCl solution with and without a membrane placed between the electrodes. The membranes and resistance clamp were pre-equilibrated in the 0.5M NaCl bath at a constant temperature of 25°C for at least 30 minutes.

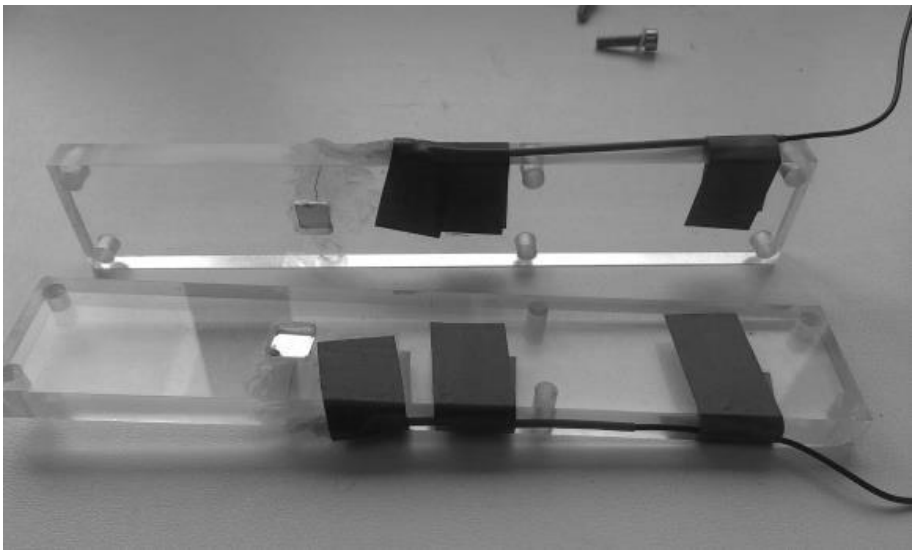

Figure D.1 Picture of the constructed resistance clamp showing the two legs and the electrodes.

4.2 UHPLC-HR-Orbitrap™-MS analysis

Prior to the TOrC analyses, a sample clean-up was required to remove all salts. An internal standard mixture, consisting of metoprolol-d_7, atrazine-d_5, diuron-d_6, paracetamol-d_4, sulfamethoxazole $^{13}C_6$ and ketoprofen-d_3 was added to all samples to ensure proper quantification.

For desalination, an SPE procedure with Oasis HLB SPE cartridges (6cc, 200 mg of sorbent, Waters Corporation, Ireland) was employed. First, the cartridges were conditioned with 2 ml LC-MS grade methanol (VWR, Belgium) and equilibrated with 2 ml ultrapure water. Next, 16 ml of sample was diluted to 50 ml with ultrapure water and loaded onto the cartridge. After this, the cartridge was washed with two times 5 ml of ultrapure water for desalination and afterwards dried by a forced airflow. This volume was shown to be effective in removing all

the salts from the adsorbent while avoiding any washing out of the adsorbed TOrCs. Finally, the TOrCs were eluted with two times 4 ml of LC-MS grade methanol, effectively doubling the concentrations in all eluted samples. To eliminate any possible effect of the sorbents, the standards used for the calibration curve underwent the same SPE treatment as the samples, which results in an automatic correction for any potential TOrC losses. Furthermore, the internal standards added ensured a further correction in case of any alterations in the concentration. All of these steps ensured a reliable results was obtained after treatment and analysis, as shown for example by the correlation coefficient of the standard curves, which was > 0.99 for all elements.

The UHPLC-HR-Orbitrap™-MS was coupled to an Accela autosampler, maintained at 15°C, an Accela degasser and an Accela 1250 pump. The solvents (0.08% HCOOH in ultrapure water (A) and MeOH (B)) and samples were pumped over a Nucleodur C_{18} pyramid (100 mm x 2.1 mm, 1.8 μm) column (Machery-nagel, USA) at a temperature of 25°C. The flow rate was set to 300 μl/min and the injection volume was equal to 10 μl. For ensuring proper chromatographic separation, gradient elution was applied. The solvent gradient applied started with 1 minute 98% solvent A and 2% solvent B, then the fraction of solvent B was increased to 90% in 3.5 minutes. In the end, the fraction of solvent B was increased to 100% in 2 minutes. After separation of the mixture on the column, the compounds were ionized with an HESI-II (Heated ElectroSpray Ionization) interface, which measured in positive and negative scan mode. The spray voltage was set to 4000 V, the capillary temperature to 250°C and the capillary voltage to 82.50 V. The sheath gas flow rate was set to 30 arbitrary units and no auxiliary gas nor sweep gas was used. The tube lens voltage and skimmer voltages were set to 120 and 20 V respectively and the vaporizer heater temperature to 350°C. Detection was performed with an Orbitrap™ HRMS from Thermo Fisher Scientific (USA) that operated in a full scan range from 100.0-700.0 m/z, measuring all precursor ions with a maximum mass deviation of 5 mg/l. A resolution of 50 000 was used, and the AGC target was set to $5E10^5$, with a maximum injection time of 500 ms. The in-source CID was disabled. Analysis of the UHPLC-HR-Oritrap™-MS output was performed with the Thermo Xcalibur 2.1.0.1140 software (Thermo-Scientific, USA).

4.3 Chemical structure of the used TOrCs.

Atrazine

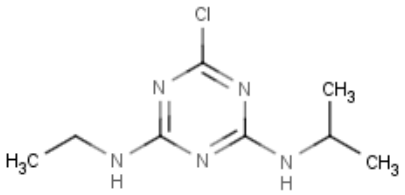

Carbamazepine

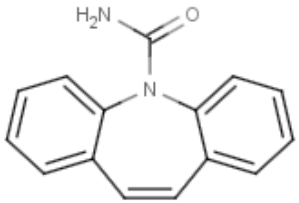

Chloridazon

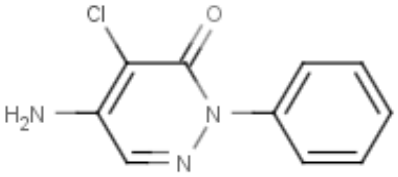

Clofibric acid

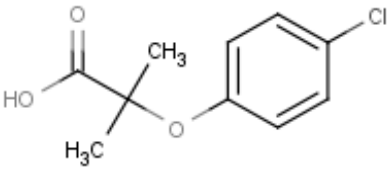

Diclofenac

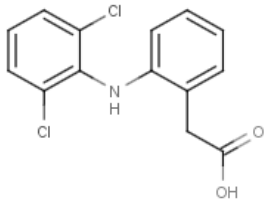

Dimethoate

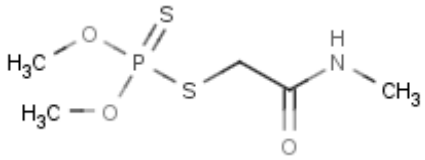

Diuron

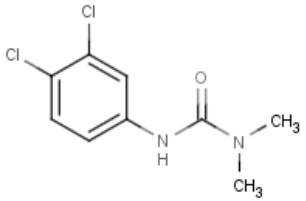

Ketoprofen

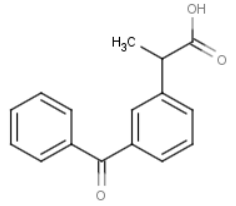

Metoprolol

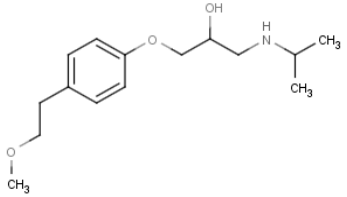

Paracetamol

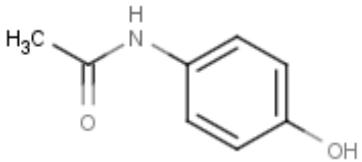

Phenazone

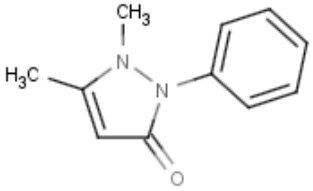

Pirimicarb

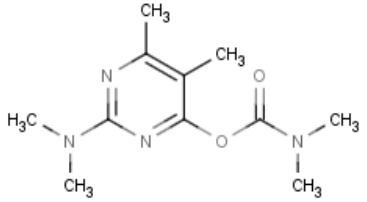

Simazine

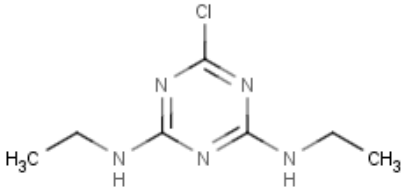

Sulfamethoxazole

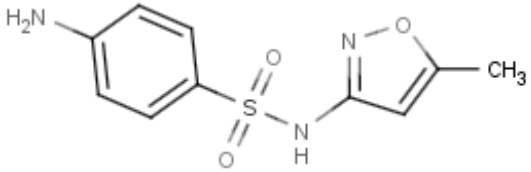

Theophylline

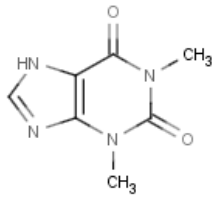

Triclopyr

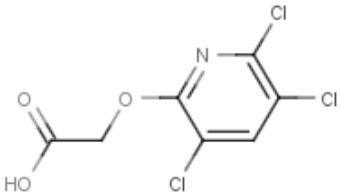

Figure D.2 Chemical structure of the used TOrCs.

4.4 Adsorption of TOrCs onto spacer material, stack and tubing.

The adsorption of TOrCs onto the ED-equipment was investigated by recirculating 5 litres of a 100 μg/l TOrC-solution with 100 g/l NaCl through the stack without membranes (but with spacers inside) for 24 hours. The total organic carbon (TOC) concentration was monitored as a substitute for the TOrC-concentration by a total organic carbon analyser (TOC-Vcpn, Shimadzu Benelux B.V., Belgium) as shown in Figure C.3.

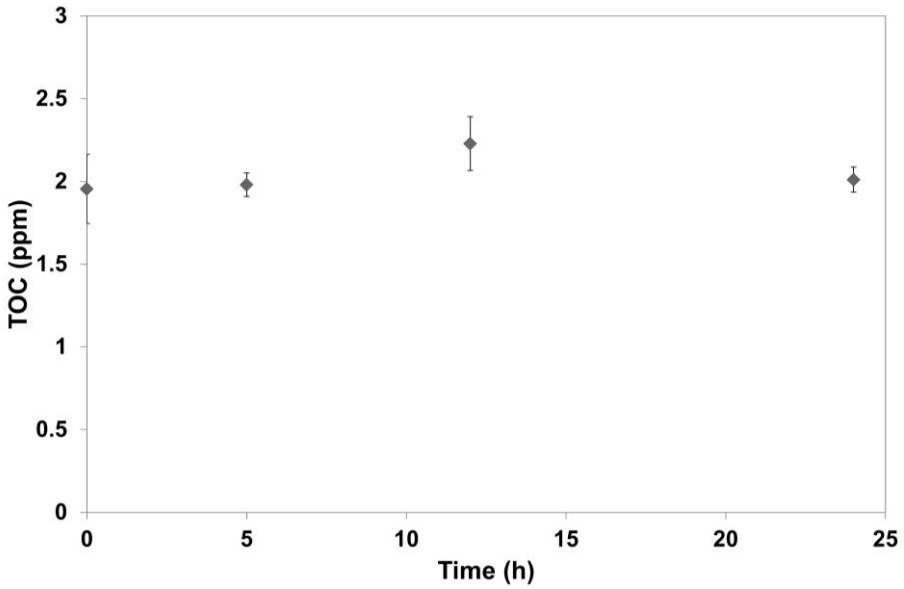

Figure D.3 TOC concentration over time.

4.5 Adsorption of TOrCs onto the membranes during adsorption experiments

The equilibrium adsorption time for TOrCs onto the membranes was determined, to determine the flushing time needed before the ED experiments. By ensuring the saturation of the membranes with TOrCs prior to the ED experiments, underestimation of the transport at the beginning of the experiments is avoided. The results for all TOrCs during the three adsorption experiments with 100 g/l NaCl in both diluate and concentrate in the concentrate is shown in. Figure C.4 and C.5 clearly show that adsorption equilibrium sets in at around 24-36 hours. In the absence of salt however, no equilibrium is reached after 48 hours, as shown in Figure C.6.

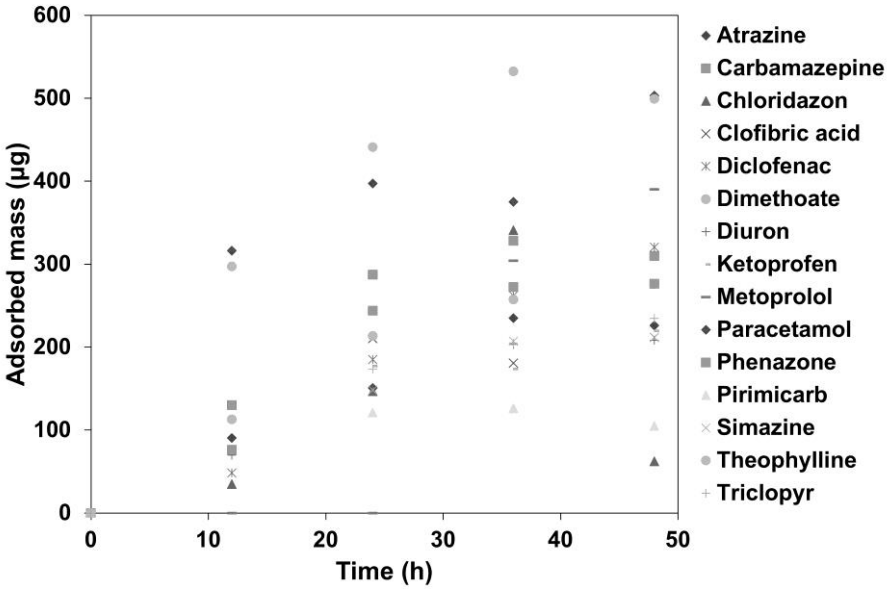

Figure D.4 Diluate TOrC concentration over time for the 100 g/l NaCl + TOrCs|10 g/l NaCl diluate|concentrate diffusion experiment.

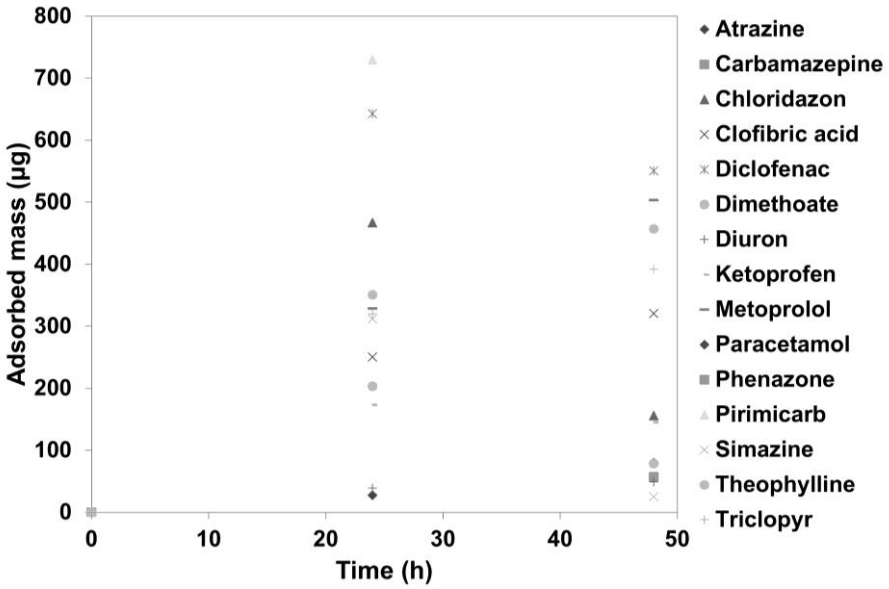

Figure D.5 Diluate TOrC concentration over time for the 100 g/l NaCl + TOrCs|100 g/l NaCl diluate|concentrate diffusion experiment.

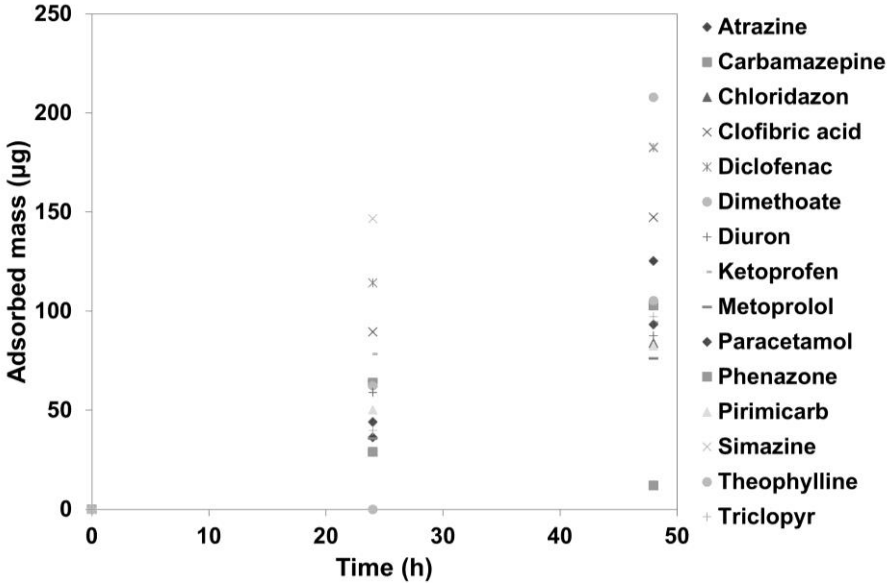

Figure D.6 Diluate TOrC concentration over time for the 0 g/l NaCl + TOrCs|0 g/l NaCl diluate|concentrate diffusion experiment.

4.6 Influence of salt concentration on TOrC diffusion coefficient.

The diffusion coefficient of atenolol was determined in the presence of different salt concentrations by PFG-NMR with a convection compensated double-stimulated-echo experiment [213] using monopolar smoothened square shaped gradient pulses and a modified phase cycle [214]. A detailed description of the PFG-NMR method and the sequences mentioned above is given by Johnson et al. [215] The measured diffusion coefficient shows a good correlation with the salt concentration (R^2 = 0.9978) as shown in Figure C.7.

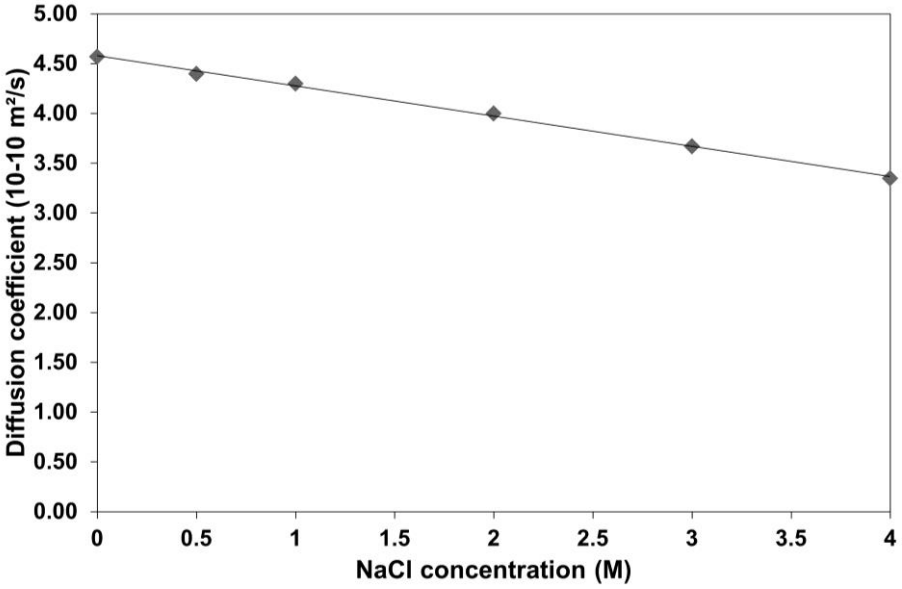

Figure D.7 Diffusion coefficient of atenolol versus NaCl concentration.

4.7 Course of the TOrC concentration over time in the electrodialysis experiments

In the figures below, the TOrC concentration over time for the three different ED experiments (100, 150 and 200 A/m²) is given. These show a linear transport when correlated to the desalination extent with an R^2 value of 0.94 ± 0.06.

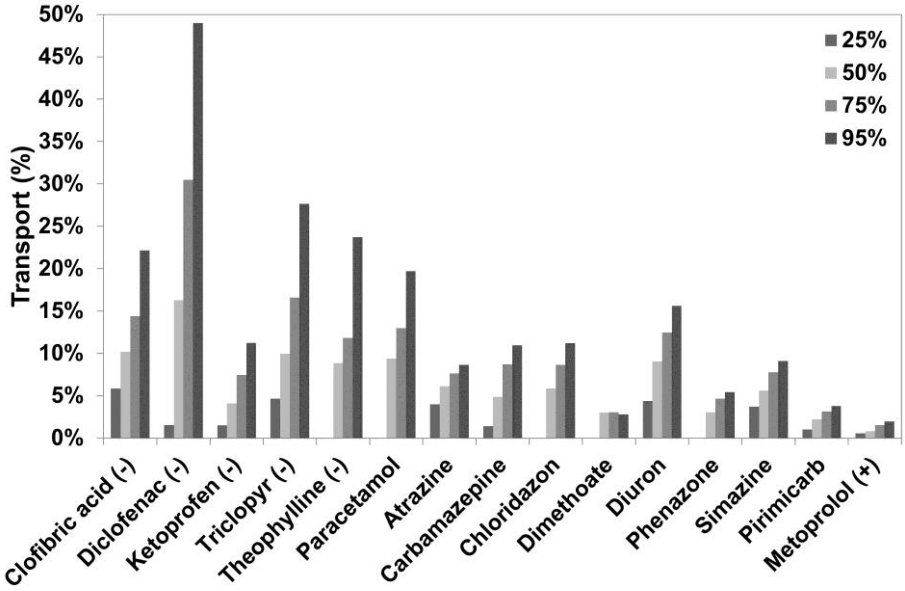

Figure D.8 TOrC concentration at different desalination extents at 100 A/m². Based on quantitative analysis with a calibration curve with an $R^2 > 0.99$.

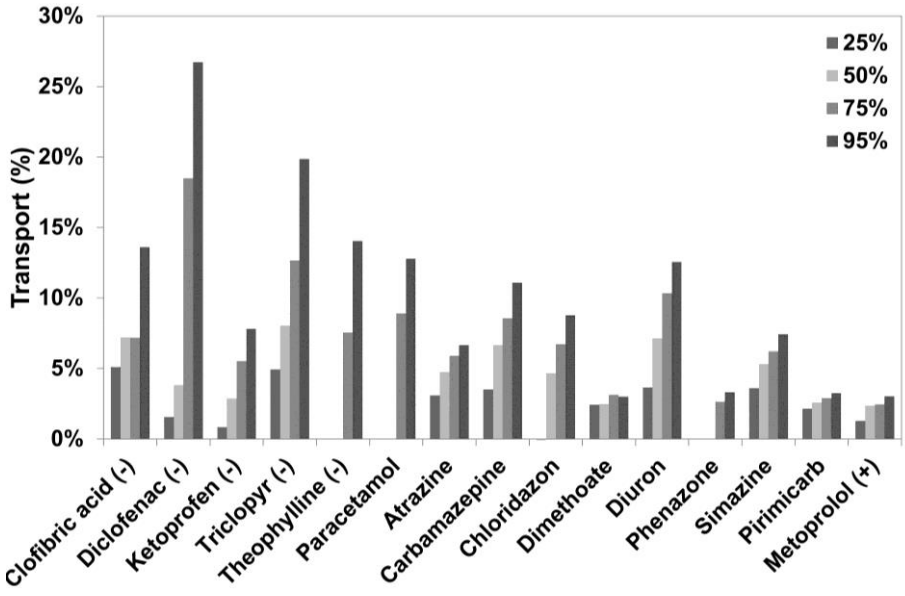

Figure D.9 TOrC concentration at different desalination extents at 150 A/m². Based on quantitative analysis with a calibration curve with an $R^2 > 0.99$.

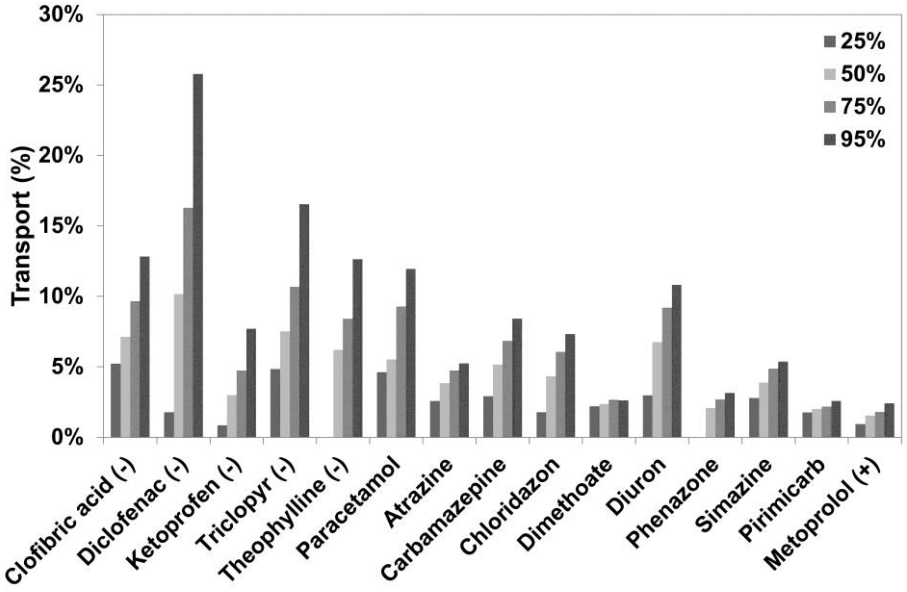

Figure D.10 TOrC concentration at different desalination extents at 200 A/m². Based on quantitative analysis with a calibration curve with an $R^2 > 0.99$.

5 Appendix E

5.1 Chemical structure of the used TOrCs

Carbamazepine

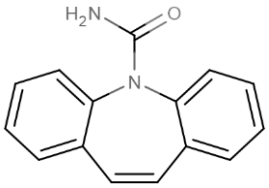

Clofibric acid

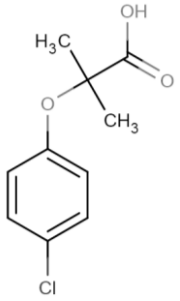

Dimethoate

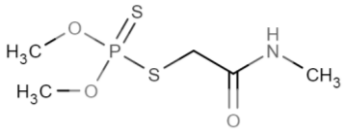

Diuron

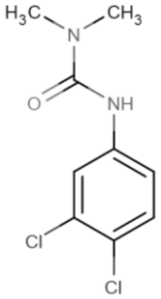

Ketoprofen

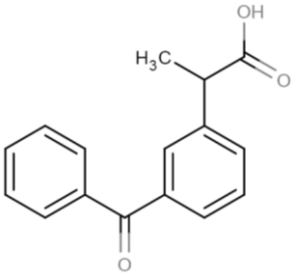

Metoprolol

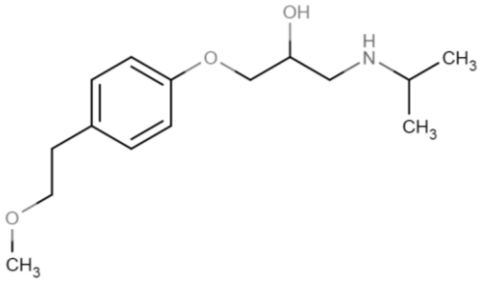

Pirimicarb

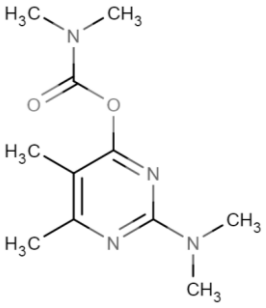

Sulfamethoxazole

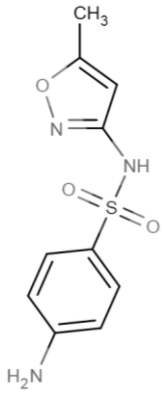

Lincomycin

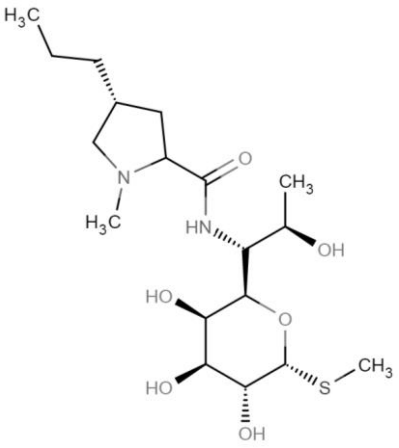

Lidocaine

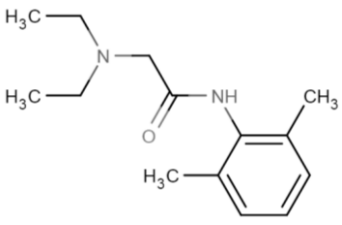

Propanolol

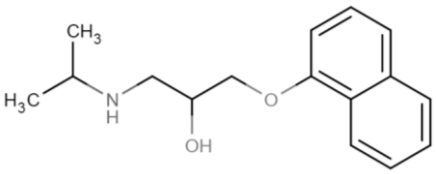

Triclopyr

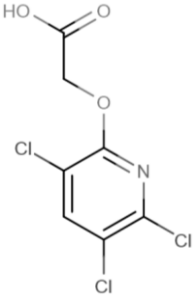

Figure E.1 Chemical structure of the used TOrCs.

5.2 Influence of salt type: results after 24h

The influence of salt type on the transport of TOrCs was tested with NaCl, $MgCl_2$ and Na_2SO_4. The results after 48 hours are presented in the study, the results after 24 hours are included here and lead to the same conclusion.

5.2.1 Diffusion

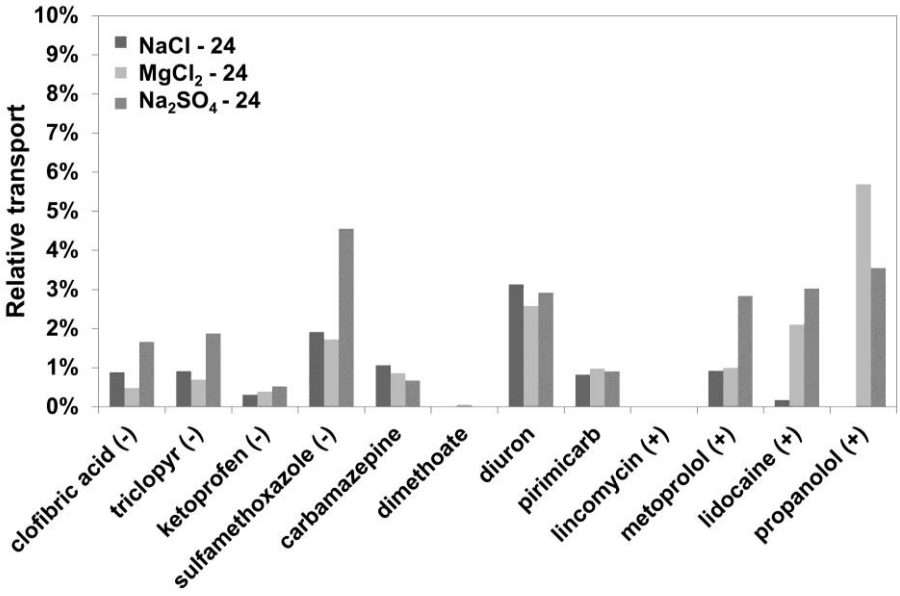

Figure E.2 Relative transport of TOrCs in the absence of an external potential difference in the presence of different salt (NaCl, $MgCl_2$ and Na_2SO_4) at 24h.

5.2.2 Electrodialysis

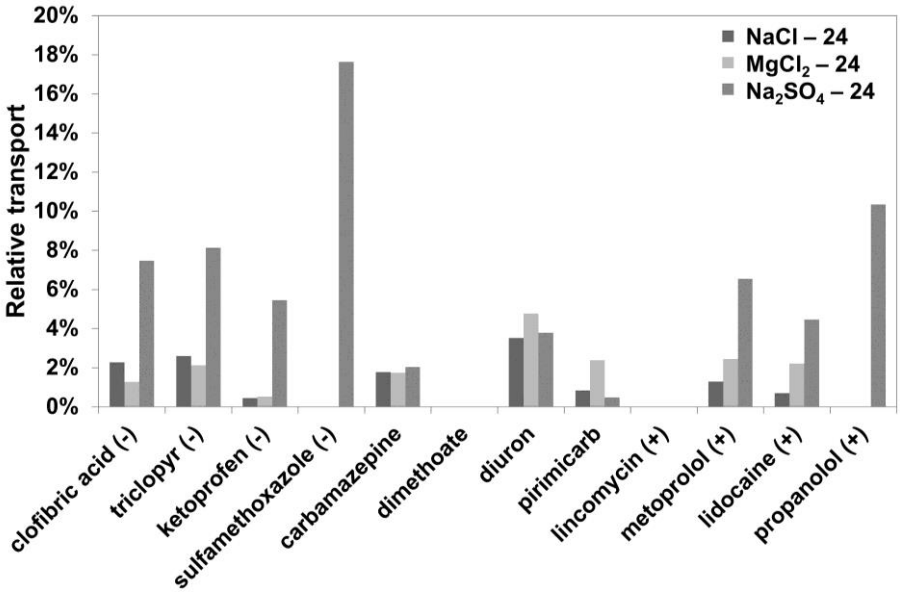

Figure E.3 Relative transport of TOrCs during electrodialysis in the presence of different salt (NaCl, $MgCl_2$ and Na_2SO_4) at 24h.

5.3 Influence of the TOrC transport direction relative to the dominant salt flux

Salt and organics are not always present in the same solution compartment and so do not always move in the same direction. Experiments with TOrCs in diluate and concentrate respectively were conducted in the presence of NaCl, $MgCl_2$ and Na_2SO_4. The results for the latter two are presented here.

5.3.1 Diffusion

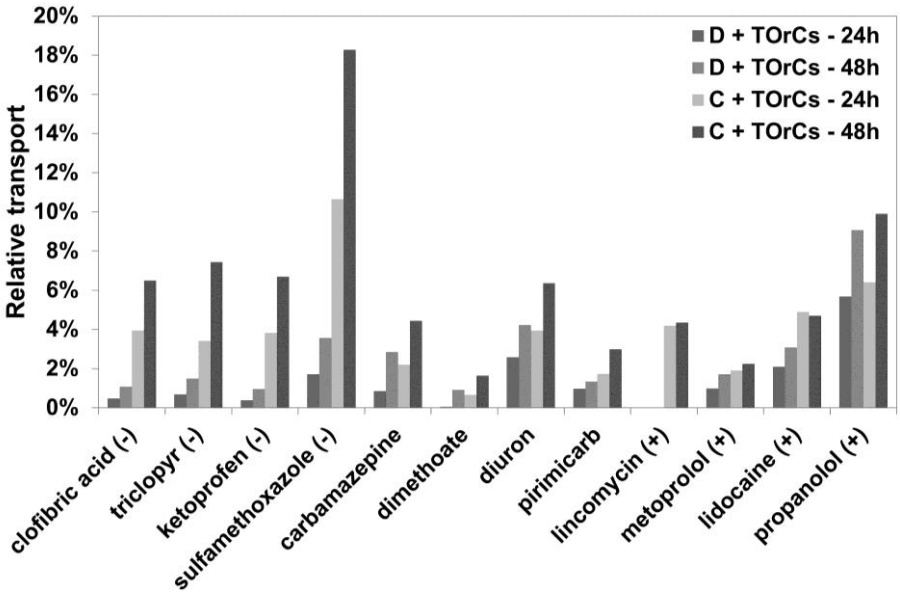

Figure E.4 Relative transport of TOrCs with $MgCl_2$ in the absence of an external potential difference with the initial dosing of the TOrCs in the concentrate (C) or diluate (D) after 24 and 48h.

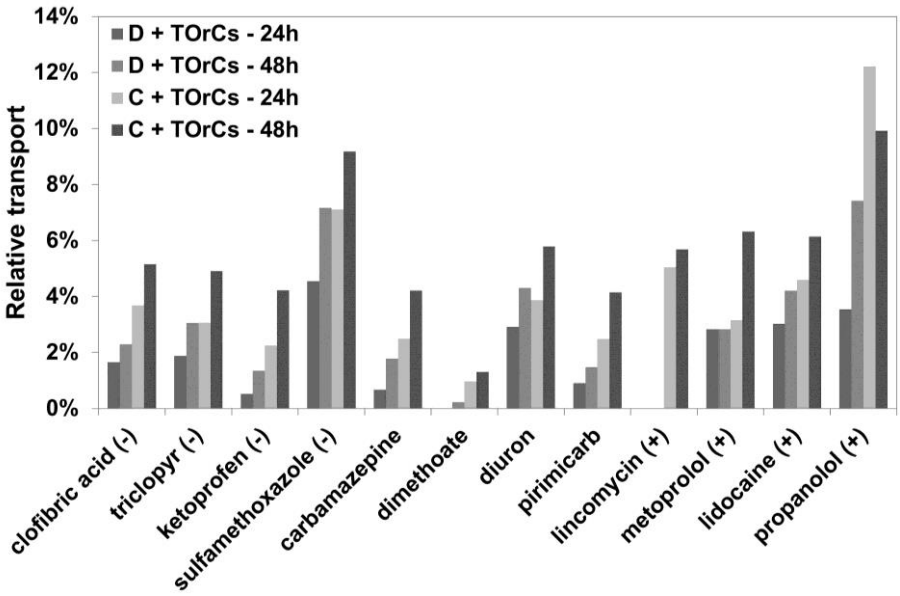

Figure E.5 Relative transport of TOrCs with Na_2SO_4 in the absence of an external potential difference with the initial dosing of the TOrCs in the concentrate (C) or diluate (D) after 24 and 48h.

5.3.2 Electrodialysis

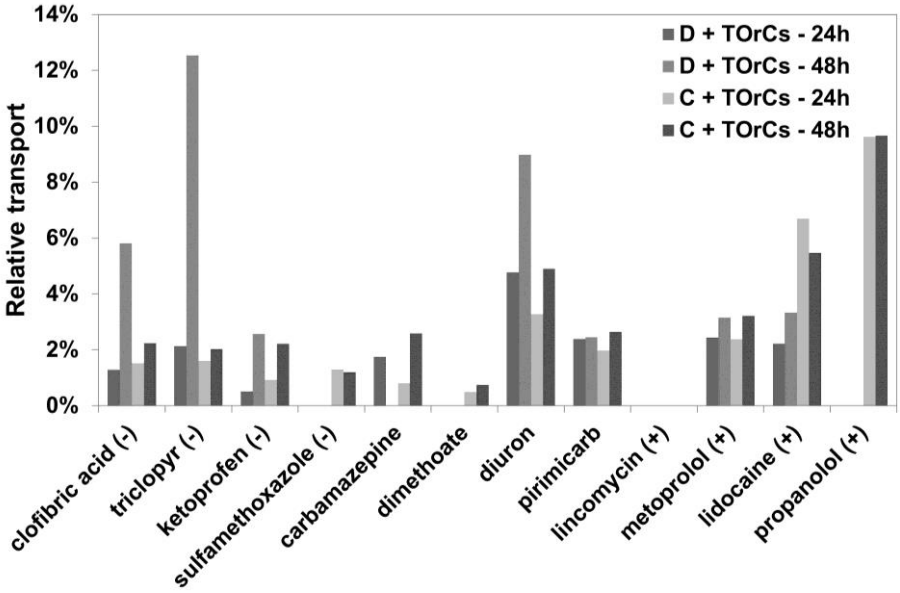

Figure E.6 Relative transport of TOrCs with $MgCl_2$ during electrodialysis with the initial dosing of the TOrCs in the concentrate (C) or diluate (D) after 24 and 48h.

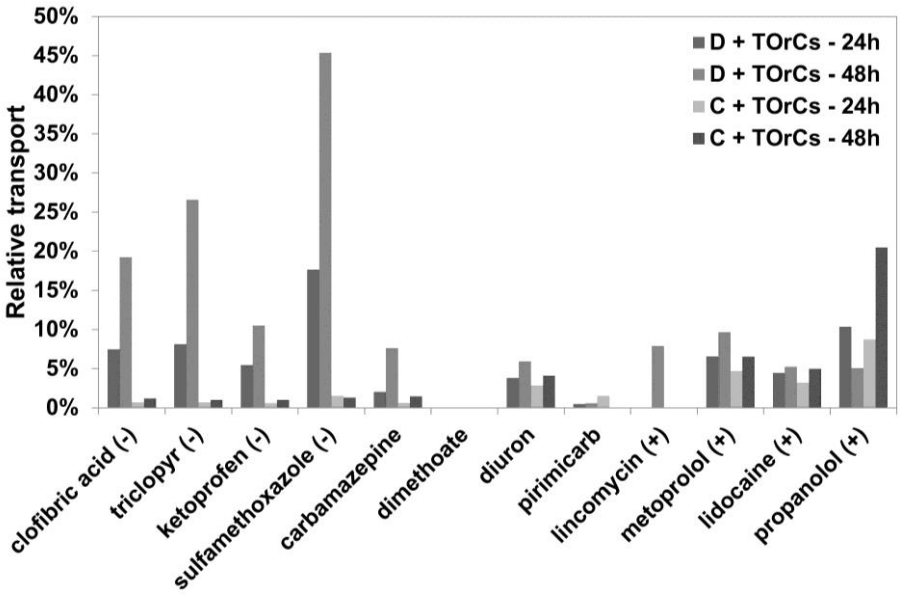

Figure E.7 Relative transport of TOrCs with Na_2SO_4 during electrodialysis with the initial dosing of the TOrCs in the concentrate (C) or diluate (D) after 24 and 48h.

Scientific achievements

1 Project participations

De Blauwe Cirkel, *Vlaams Innovatie Samenwerkingsverband*, July 2012- August 2016

Water treatment unit breadboard (WTUB), *European Space Agency*, December 2013 – December 2015

2 Published articles

Vanoppen, M., Stoffels, G., Demuytere, C., Bleyaert, W., Verliefde, A.R.D. (2015) Increasing RO efficiency by chemical-free ion-exchange and Donnan dialysis: principles and practical implications. *Water Research* 80. p. 59-70.

Vanoppen, M., Bakelants, A., Gaublomme, D., Schoutteten, K., Vanden Bussche, J., Vanhaecke, L., Verliefde, A.R.D. (2015) Properties governing the transport of trace organic contaminants through ion-exchange membranes. *Environmental Science & Technology*, 49. p. 489-497.

Vanoppen, M., Stoffels, G., Buffel, J., De Gusseme, B., Verliefde, A.R.D. (2016) A hybrid IEX-RO process with brine recycling for increased RO recovery without chemical addition: a pilot-scale study. *Desalination*, 394. p. 185-194.

3 Published bookchapters

Vanoppen, M., Blandin, G., Derese, S., Le Clech, P., Post, J., Verliefde, A.R.D. (2016) Salinity gradient power and desalination. In: Cipollina, A. & Micale, G. (eds.) *Sustainable energy from salinity gradients.* Londen: Woodhead publishing, Elsevier.

4 Submitted articles

Vanoppen, M., Stoffels, G., Ma, L., De Meyer, E., Schoutteten, K.V.K.M., Vanden Bussche, J., Vanhaecke, L., Verliefde, A.R.D. Organics transport in ion-exchange membranes: influence of solution matrix and organic properties. Submitted (May 2016) to Environmental Science and Technology.

5 Articles in preparation

Vanoppen, M., Criel, E., Walpot, G., Andersen, S., Prévoteau, A., Verliefde, A.R.D. Assisted reverse electrodialysis: a novel technique to decrease reverse osmosis energy demand. In preparation for Energy and Environmental Science.

6 Conference contributions

Vanoppen, M., Stoffels, G., Buffel, J., De Gusseme, B., Verliefde, A.R.D. (2016) Increasing RO recovery without anti-scalants – a pilot study. Poster presentation at the *E4Water final conference: integrated industrial water managements: solutions for practice*, Brussels, Belgium.

Vanoppen, M., Criel, E., Andersen, S., Prévoteau, A., Verliefde, A.R.D. (2016) Assisted reverse electrodialysis: a novel technique to decrease reverse osmosis energy demand. Oral presentation at the *AMTA/AWWA 2016 Membrane Technology Conference & Exposition*, San Antonio, TX, USA.

Vanoppen, M., Stoffels, G., Demuytere, C., Bleyaert, W., De Gusseme, B., Verliefde, A.R.D. (2015) Increased RO recovery without chemical addition by the recycling of RO brine to an IEX or Donnan dialysis pre-treatment step. Poster presented at the *1st IWA Resource Recovery Conference*, Ghent Belgium an at the *4th IWA Benelux Regional Young Water Professionals Conference*, Leeuwarden, the Netherlands.

Vanoppen, M., Gaublomme, D., Schoutteten, K., Vanhaecke, L., Vanden Bussche, J., Verliefde, A.R.D. (2015) Properties governing the transport of organic pollutants through ion-exchange membranes using desalination of complex waste streams in ED. Oral presentation at the *AMTA/AWWA 2015 Membrane Technology Conference & Exposition*, Orlando, FL, USA and invited presentation at the *AMTA/AWWA 2016 Membrane Technology, Conference & Exposition*, San Antonio, TX, USA.

Vanoppen, M., Derese, S., Bakelants, A., Verliefde, A.R.D. (2014) Reduction of specific energy demand of seawater RO by osmotic dilution/osmotic energy recovery: a realistic modelling approach. Oral presentation at the *Desalination for the Environment: Clean Water and Energy Conference*, Limassol, Cyprus.

Vanoppen, M., Bakelants, A., Derese, S., Verliefde, A.R.D. (2013) Influence of osmotic energy recovery/osmotic dilution on seawater desalination energy demand. Oral presentation to the *3rd IWA Benelux Regional Young Water Professionals Conference*, Belval, GD Luxembourg.

7 Grants and awards

"Best student paper presentation award", AMTA/AWWA Membrane Technology Conference & Exposition. Orlando, FL, USA, March 2015.

Finalizing PhD grant. BOF, special research fund, UGent. September 2015 – July 2016

Grant for participation in an international conference, FWO, Flanders. December 2012 for the *AMTA/AWWA 2016 Membrane Technology Conference & Exposition*, San Antonio, TX, USA.

"Best student paper presentation award", AMTA/AWWA Membrane Technology Conference & Exposition. San Antonio, TX, USA, February 2016.

8 Guided master-theses

Mahieu, A. (2012-2013) Terugwinning van zoutrijke stromen uit de industrie met elektrodialyse.

Bakelants, A. (2012-2013) A novel method for energy-efficient seawater desalination by predilution with impaired water.

Moens, N. (2012-2013) Recovering phosphorus through electrodialysis.

Gaublomme, D. (2013-2014) Het gedrag van organische componenten bij elektrodialyse van complexe stromen.

Criel, E. (2014-2015) Energy-efficient seawater desalination: a comparison between reverse electrodialysis and assisted reverse electrodialysis as pre-treatment for reverse osmosis.

Stoffels, G. (2014-2015) Electro-separation processes for resource recovery in industrial applications.

Walpot, G. (2015-2016) Mass transfer in assisted reverse electrodialysis as a novel pre-treatment for reverse osmosis.

De Paepe, J. (2015-2016) Water recycling in space: from urine to hygienic water.

Dieltjens, S. (2015-2016) Removal of fluorine from E-glass production plant wastewater.

De Pryck, L. (2016) Waterzuivering in de ruimte: van urine tot drinkbaar water.

9 Teaching experience

Supervising practical exercises, *Environmental Technology: water – part physico-chemistry*, 2012-2016

Supervising practical exercises, *Analysis and Abatement of Water pollution – part technology*, 2012-2016

Theory class 'Hybridisation for water treatment and recovery', *Membrane Technology*, 2015

Curriculum vitae

Marjolein Vanoppen was born in Lier, Belgium on June 26th of 1989. She finished her secondary school at the Sint-Ursula Lyceum in Lier in 2007, after which she started her studies to become a bio-science engineer. She finished her bachelor at the University of Antwerp in 2010 and graduated as a bio-science engineer in environmental technology at Ghent University in 2012. She started her PhD research on hybrid water treatment systems with ion-exchange processes soon after, at the Particle and Interfacial Technology group at Ghent University, under the guidance of prof. dr. ir. Arne R. D. Verliefde.

"The most important thing is that you have fun."

A.R.D. Verliefde